Development of potent and selective antagonists at $P2Y_{11}$ receptors: Symmetrical and asymmetrical derivatives of NF340

Inaugural-Dissertation

zur

Erlangung des Doktorgrades

der Mathematisch-Naturwissenschaftlichen Fakultät

der Heinrich-Heine-Universität Düsseldorf

vorgelegt von

DARUNEE HONGWISET

aus Trat, Thailand

Düsseldorf 2008

Aus dem Institut für Pharmazie
der Heinrich-Heine-Universität Düsseldorf

„Gedruckt mit Unterstützung des Deutschen Akademischen Austauschdienstes“

Gedruckt mit Genehmigung der
Mathematisch-Naturwissenschaftlichen Fakultät der
Heinrich-Heine-Universität Düsseldorf

Referent: Prof. Dr. M. U. Kassack
Koreferent: Prof. Dr. T. Kurz
Tag der mündlichen Prüfung: 29.10.2008

Erklärung

Hiermit erkläre ich ehrenwörtlich, dass ich die vorliegende Dissertation mit dem Titel „Development of potent and selective antagonists at $P2Y_{11}$ receptors: Symmetrical and asymmetrical derivatives of NF340" selbst angefertigt habe. Außer den angegebenen Quellen und Hilfsmitteln wurden keine weiteren verwendet. Diese Dissertation wurde weder in gleicher noch in abgewandelter Form in einem anderen Prüfungsverfahren vorgelegt.

Düsseldorf, den 04.08.2008

Darunee Hongwiset

Acknowledgements

First of all, I would like to thank my thesis advisor, Prof. Dr. Matthias U Kassack, for accepting me as a doctoral candidate and giving me a chance to pursue my Ph.D. study first at University of Bonn and then at the University of Düsseldorf, Germany. I am sincerely grateful for his valuable advices, suggestions to approach the research problems, patience, kindness and sympathy through my Ph.D study.

I am also very thankful to Prof. Dr. Thomas Kurz, for his willingness to be a second referee.

My sincere thanks are expressed to Prof. Dr. Michael Wiese for his hospitality and for providing all facilities during working at the University of Bonn.

For the best friend and best colleague, I am deeply thankful to Mr. Heiko Ullmann for his help, understanding and friendship. These thanks go also to Dr. Alexandra Hamacher and Dr. Sabine Meis. Special thanks go to Mr. Heiko Ullmann and Dr. Alexandra Hamacher for their helps in correcting this manuscript.

I would like to thank all colleagues at the pharmaceutical chemistry department, University of Bonn and Düsseldorf, for their helpful cooperation and a nice working atmosphere.

My deepest thanks go to Dr Busaban and Dr Jakkapan Sirithanyalug to encourage me to come to study in Germany.

I owe a heavy debt of gratefulness to Dr. Chuleekorn (Sirisangtrakul) Kummeich for her friendship along the time of study. My thanks go also to all of my friends in Bonn and Cologne for very nice experiences in Germany.

My special thanks go to German Academic Exchange Service (DAAD) for granting financial support.

My deepest gratitude goes to my beloved parents, my sisters and brother for their support, encouragement and inspiration in all times of my study.

For my family

Für meine Familie

สำหรับครอบครัวของฉัน

Contents

1 Introduction

1.1 P2 receptors

Purinergic (P2) receptors are cell surface receptors for endogenous nucleotides such as adenosine 5'-triphosphate (ATP) or adenosine 5'-diphosphate (ADP) which act as extracellular signalling molecules.[1] In 1985, P2 receptors were divided according to their molecular structures and signal transduction pathways into two classes, namely P2X and P2Y (Figure 1.1).[1-3]

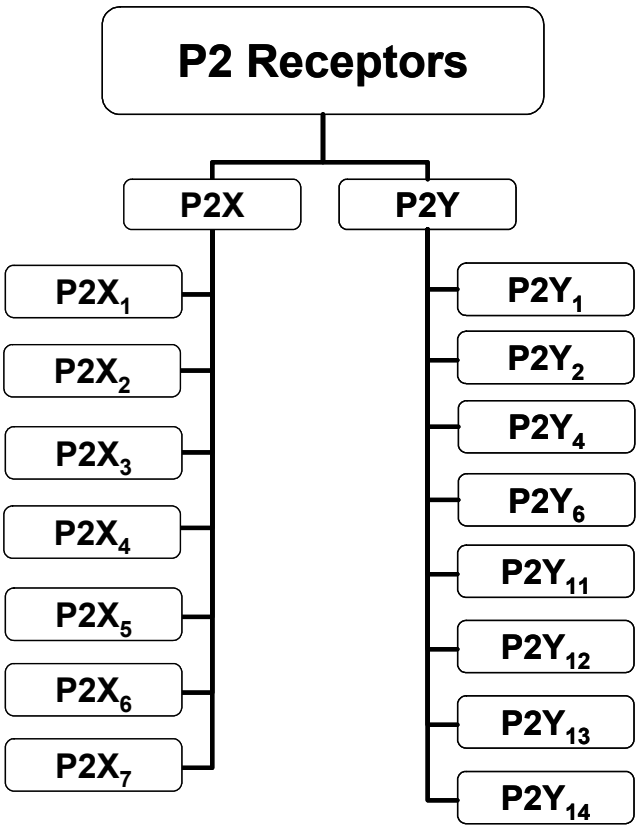

Figure 1.1. Classification of human P2 receptors.

1.1.1 P2X receptors

P2X receptors are ligand-gated ion channels. They are subdivided into 7 subtypes: $P2X_{1-7}$ (Figure 1.1).[4,5] Like other ion channel receptors, P2X receptors are oligomeric proteins composed of more than one subunit per functional receptor. The main structure features of P2X receptors are two transmembrane domains separated by an extracellular N-glycosylated loop segment and intracellular N- and C-termini (Figure 1.2).[6,7]

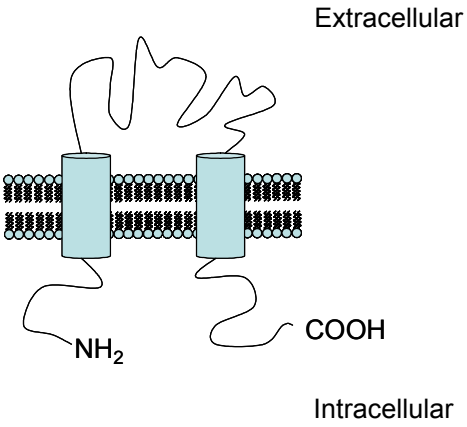

Figure 1.2. P2X ion channel receptor monomer, containing two transmembrane spanning domains, intracellular amino and carboxy termini and a large extracellular ligand-binding loop.

All P2X receptors are cation selective channels with equal permeability for Na^+ and K^+, and significant permeability for Ca^{2+}.[8] P2X receptors are widely expressed in the central nervous system and in the body periphery. They play important roles in various biological functions, such as smooth muscle contraction, modulation of the cardiovascular and respiratory system, immunomodulation, inflammation and cell death, generation and transmission of nociceptive signals and modulation of transmitter release and neuronal excitability.[9-11]

1.1.2 P2Y receptors

P2Y receptors belong to the superfamily of G protein-coupled receptors and can be subdivided into 8 subtypes: $P2Y_{1,2,4,6,11-14}$ (see Figure 1.1).[12-15] The proteins of the human P2Y receptors compose of 328 – 377 amino acids corresponding to a predicted molecular mass of 41-53 kDa of the glycosylated proteins.[16]

P2Y receptors show the typical features of G protein-coupled receptors (Figure 1.3):

- seven predicted hydrophobic transmembrane regions connected by three extracellular loops and three intracellular loops,
- an intracellular C-terminus,
- and an extracellular N-terminus.

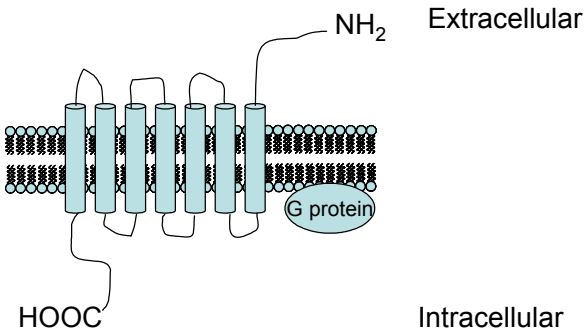

Figure 1.3. G-Protein coupled receptor, containing seven transmembrane spanning domains, an extracellular amino terminus and intracellular carboxy terminus.

The different P2Y receptor subtypes couple with different G proteins and show therefore different effects after ligand stimulation. The main tissue distribution and G protein coupling of P2Y receptors are presented in Table 1.1.

Table 1.1. Tissue distribution and G protein coupling of P2Y receptors.[16]

Receptor Subtype	Tissue distribution	G protein coupling
$P2Y_1$	epithelial and endothelial cells, platelets, immune cells, osteoblasts	$G_{q/11}$: PLCβ activation
$P2Y_2$	immune cells, epithelial and endothelial cells, kidney tubules, osteoblasts	$G_{q/11}$: PLCβ activation and possibly G_i
$P2Y_4$	endothelial cells	$G_{q/11}$: PLCβ activation and possibly G_i
$P2Y_6$	some epithelial cells, placenta, T cells, thymus	$G_{q/11}$: PLCβ activation
$P2Y_{11}$	spleen, intestine, granulocytes, cardiomyocytes	$G_{q/11}$: PLCβ activation and G_s: increase cAMP
$P2Y_{12}$	platelets, glial cells	$G_{i/o}$: inhibition of adenylate cyclase
$P2Y_{13}$	spleen, brain, lymphnodes, bone marrow	$G_{i/o}$: inhibition of adenylate cyclase
$P2Y_{14}$	placenta, adipose tissue, stomach, intestine	$G_{i/o}$: inhibition of adenylate cyclase

1.2 P2Y receptors and their roles as potential therapeutic targets

P2Y receptors play important physiological and pathophysiological roles in a variety of biological processes. For example, $P2Y_1$ and $P2Y_{12}$ receptors are involved in platelet aggregation and formation of a thrombus[17,18], whereas $P2Y_2$ receptors mediate increased secretion of salt, water and mucus. However, the understanding of the physiological roles of all P2Y subtype receptors is unclear because of the lack of specific agonists and antagonists.[19] Some examples of agonists and antagonists at P2Y receptors are shown in Table 1.2.

Table 1.2. Agonists and antagonists of P2Y receptors. [16,20]

Receptor Subtype	Agonist	Antagonist
$P2Y_1$	MRS2365, 2-MeSADP, ADP, ADPβS	MRS2179, MRS2279, MRS2500
$P2Y_2$	UTP, ATP, Diquafosol, Denufosol, Ap4A	suramin
$P2Y_4$	UTP, UTPγS	RB2
$P2Y_6$	UDP, 5-Br-UDP	MRS2567
$P2Y_{11}$	AR-C67085, ATPγS, BzATP, ATP	NF157 , suramin , RB2
$P2Y_{12}$	2-MeSADP, ADP	Metabolite of Ticlopidine, Clopidogrel and Prasugrel; Cangrelor, AZD6140
$P2Y_{13}$	2-MeSADP, ADP	MRS2211
$P2Y_{14}$	UDP-glucose, UDP-galactose	UDP

The development of P2Y-selective ligands may lead to the identification of species differences in the P2Y receptor pharmacology and it is also important for the process of drug discovery. So far, two $P2Y_{12}$ antagonists, ticlopidine and clopidogrel (Figure 1.4), are approved by the FDA as anti-platelet agents.[21]

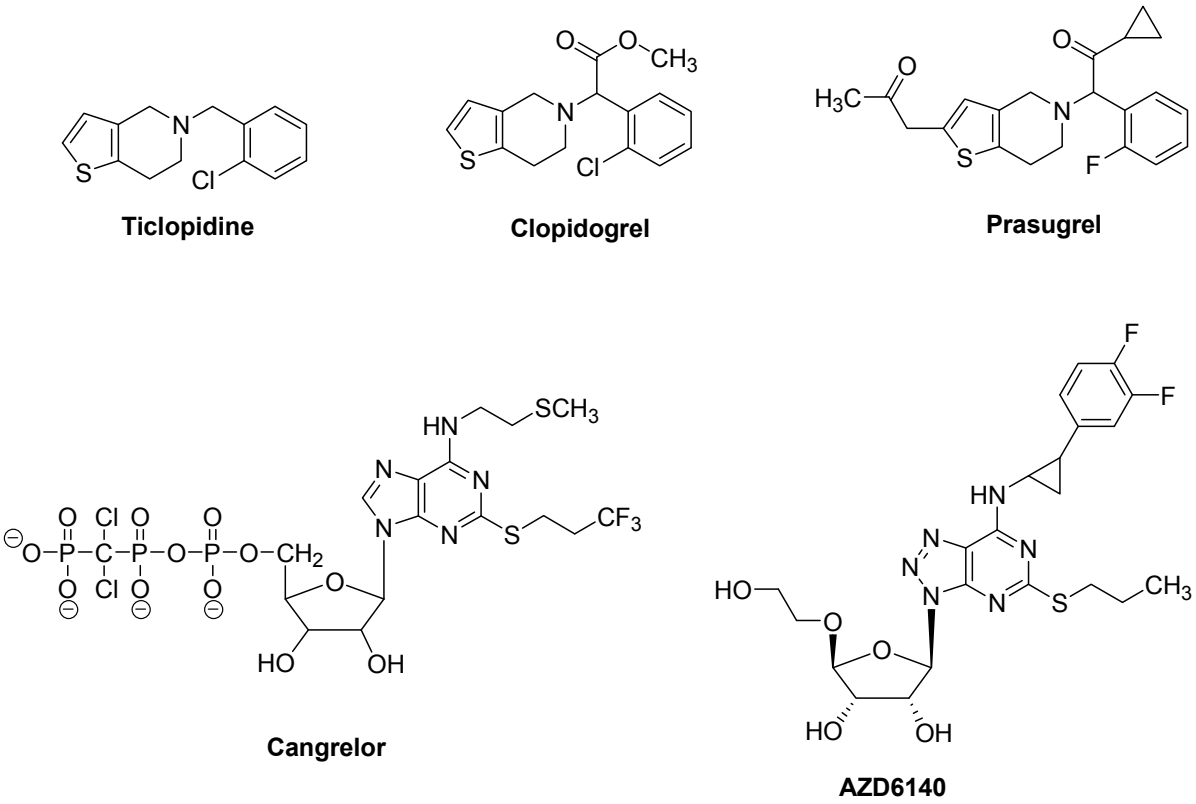

Figure 1.4. $P2Y_{12}$ receptor antagonists: Thienopyridines (Ticlopidine, Clopidrogrel and Prasugrel) and ATP analogues (Cangrelor and AZD6140).

Ticlopidine and clopidogrel are thienopyridine prodrugs which are metabolized through cytochrome P450 in the liver. A new thienopyridine prodrug, prasugrel, is also under clinical investigation as novel orally-administered platelet inhibitor. [22-24] Some selective P2Y ligands, e.g. cangrelor, AZD6140, diquafosol and denufosol, are also under clinical investigation.[17] Cangrelor (AR-C69931MX) is a competitive $P2Y_{12}$ antagonist which is in phase II clinical trial as an antithrombotic drug. AZD6140, a first orally available reversible ADP receptor antagonist, is currently in a large phase III clinical trial for the treatment of acute coronary syndromes.[25-27] Diquafosol and denufosol (Figure 1.5) are $P2Y_2$ receptor agonists, which are currently undergoing clinical evaluation for the symptomatic treatment of cystic fibrosis and dry eye syndrome, respectively.[28-30]

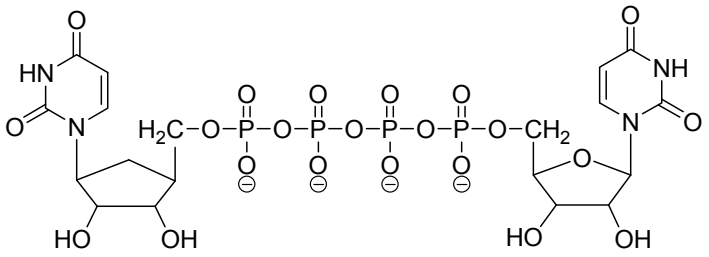

Diquafosol

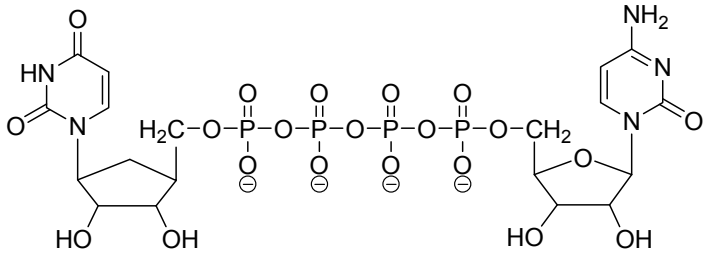

Denufosol

Figure 1.5. $P2Y_2$ receptor agonists: Diquafosol and Denufosol.

1.3 $P2Y_{11}$ receptors

$P2Y_{11}$ receptors are found to be expressed in the spleen, small intestine and HL-60 cells, a human promyelocytic leukemia cell line.[31,32] Moreover, $P2Y_{11}$ receptors have also been found in human monocyte-derived dendritic cells, macrophages, Jurkat T cells and LB23 melanoma cells.[33] The study of pharmacological functions of $P2Y_{11}$ receptors led to some proposals of new therapy approaches for immune system and cardiovascular system. The study of the ability of ATP to down-regulate the pro-inflammatory cytokine TNF-α via an activation of $P2Y_{11}$ receptors led to propose a new approach for the treatment of chronic inflammatory diseases by altering the balance among pro- and anti-inflammatory cytokines.[34] Wilkin et al. showed that ATP and ATP derivatives such as ATPγS induced the maturation of human monocyte-derived dendritic cell via an increase in cAMP and they concluded that $P2Y_{11}$ receptors may play an immunomodulatory role by activating dendritic cells.[35] The effect of ATP in the regulation of the trafficking of specific dendritic cell population was studied by Schurr and co-workers and they suggested that $P2Y_{11}$ receptor inhibition may represent a new strategy to improve the migration of antigen-loaded dendritic cells from the vaccination site to lymph nodes.[36] Moreover, $P2Y_{11}$ receptors showed some involvement in cardiovascular diseases. Balogh showed that the $P2Y_{11}$-like receptors in mouse cardiomyocytes were involved in controlling cardiomyocyte contractility.[37] Therefore, it is possible

that $P2Y_{11}$ receptor agonists could be used to improve cardiac output in patients with circulatory shock and $P2Y_{11}$ receptor antagonists could be beneficial in patients with congestive heart failure (CHF). Erlinge and co-workers found that the common Ala-87-Thr polymorphism of the $P2Y_{11}$ receptor was associated with an increased risk for acute myocardial infarction (AMI) and then suggested that the $P2Y_{11}$ receptor may be a promising new drug target in the prevention of AMI.[38] Furthermore, $P2Y_{11}$ receptors are also involved in the apoptosis of neutrophils and were proposed to be a key factor during inflammation.[39]

1.3.1 $P2Y_{11}$ receptor agonists

Agonists at $P2Y_{11}$ receptors are ATP and its analogues (Figure 1.6). In $P2Y_{11}$ receptor expressing 1321N1 astrocytoma cells or CHO-K1 cells, ATP and its analogues showed the following potency: AR-C67085MX > ATPγS = 2' or 3'-O-(4-benzoylbenzoyl)-ATP > ATP > 2-MeSATP > ADP. Extracellular NAD^+ showed also agonistic activity at $P2Y_{11}$ receptors.[40,41]

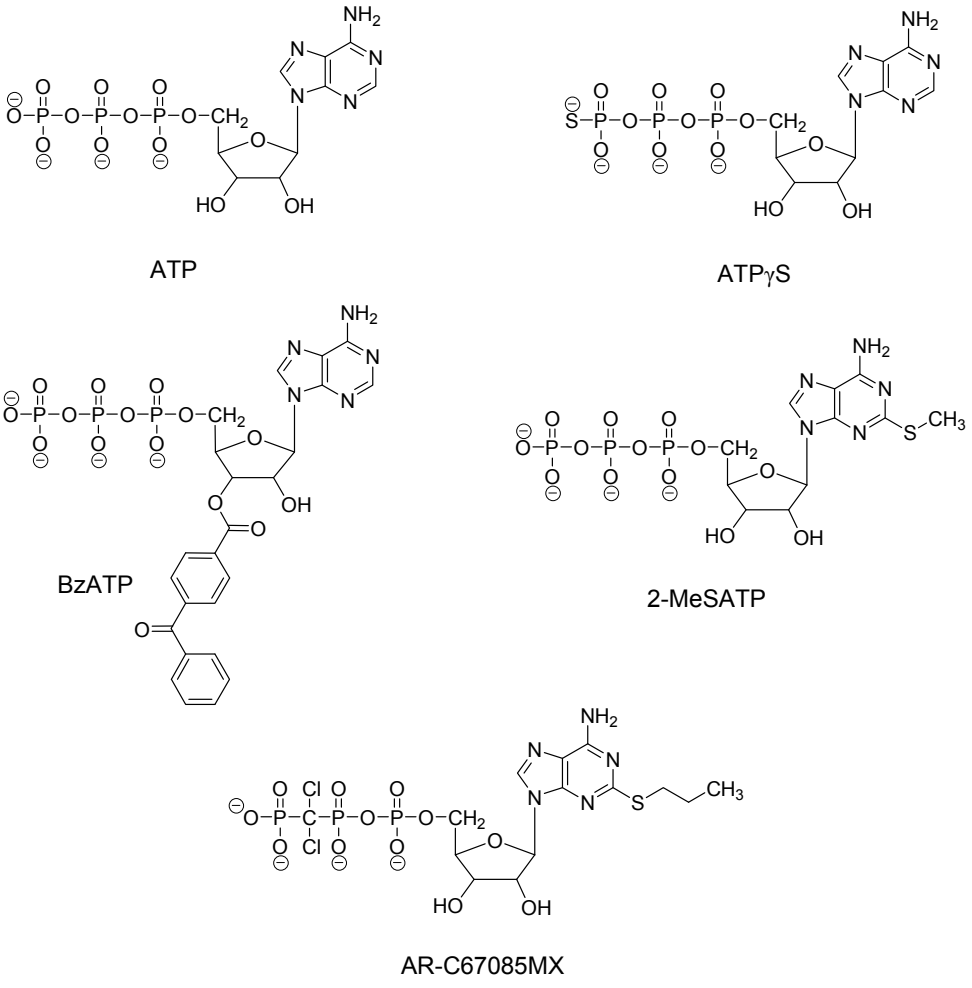

Figure 1.6. ATP and analogues as $P2Y_{11}$ receptor agonists.

Recently, Greve et al. reported new $P2Y_{11}$ receptor agonists which were extracted from the marine sponge *Ianthella quadrangulata*.[42] From the study of the biological activity at $P2Y_{11}$ receptors recombinantly expressed in 1321N1 cells, iso-iantheran A and its carboxyl derivative showed an EC_{50} of 1.92 µM and 0.48 µM, respectively.

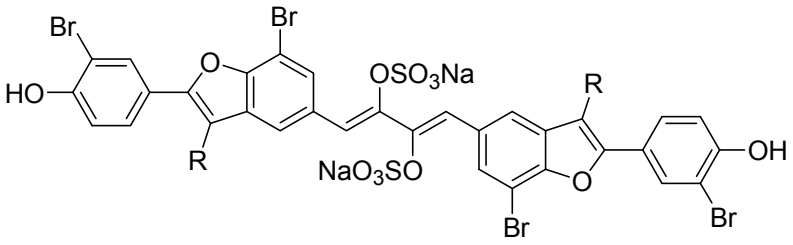

Iso-iantheran A R = H

8-Carboxy-iso-iantheran A R = COOH

Figure 1.7. Iso-iantheran A and carboxy derivative , new $P2Y_{11}$ receptor agonists.

1.3.2 $P2Y_{11}$ receptor antagonists

The known antagonists at human $P2Y_{11}$ receptors are suramin and reactive blue 2 (Figure 1.8).[43,44] However, both substances are weakly potent and non-selective antagonists.

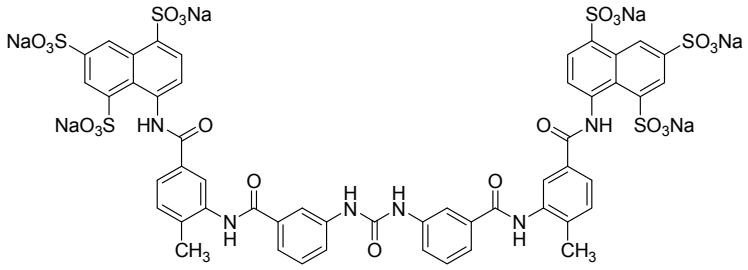

Suramin

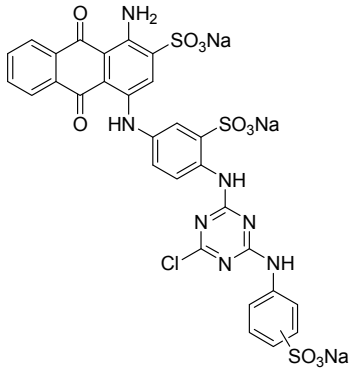

Reactive blue 2

Figure 1.8. $P2Y_{11}$ receptor antagonists: suramin and reactive blue 2 (RB2).

1.4 Suramin and suramin derivatives as P2 receptor ligands

Suramin is a polysulfonic acid substituted naphthalene urea, which was developed by Bayer in 1920 as antitrypanosomal agent. Nowadays, suramin is used primarily for the treatment of African trypanosomiasis, but it is inactive against American trypanosomiasis.[45] Suramin also exhibited a potent inhibitory effect on the retroviral reverse transcriptase *in vitro*, but it is not effective against HIV infection.[45-47] Other therapeutic effects, for example antineoplastic and angiostatic effects, were also found.[48-52] However, the clinical application of suramin is restricted because of the high polarity and toxicity of the molecule. Structure modifications of suramin were intensively performed in the group of Prof. Nickel.[53-57] These works resulted in a compound library (NF-compounds).

The activity of suramin at P2 receptors was firstly reported by Dunn and Blakeley in 1988. They showed the antagonistic effects of suramin against the response of α,β-meATP at P2 receptors of the mouse vas deferens.[58] Suramin was further studied and is known as a non-selective antagonist at both P2X and P2Y receptors with relatively low potency (approximately pA_2 values of 5 – 6). Modifications of the suramin structure led to the discovery of more selective and more potent antagonists at various P2 receptors. For example, NF023, a truncated urea analogue, was reported as a $P2X_1$ antagonist.[59] NF279 showed $P2X_1$ antagonistic activity too.[60-62] NF449 is, so far, the most potent and selective $P2X_1$ receptor antagonist[63], whereas its benzene monosulfonic acid substituted analogue, NF110, was reported as $P2X_3$ antagonist (Figure 1.9).[64]

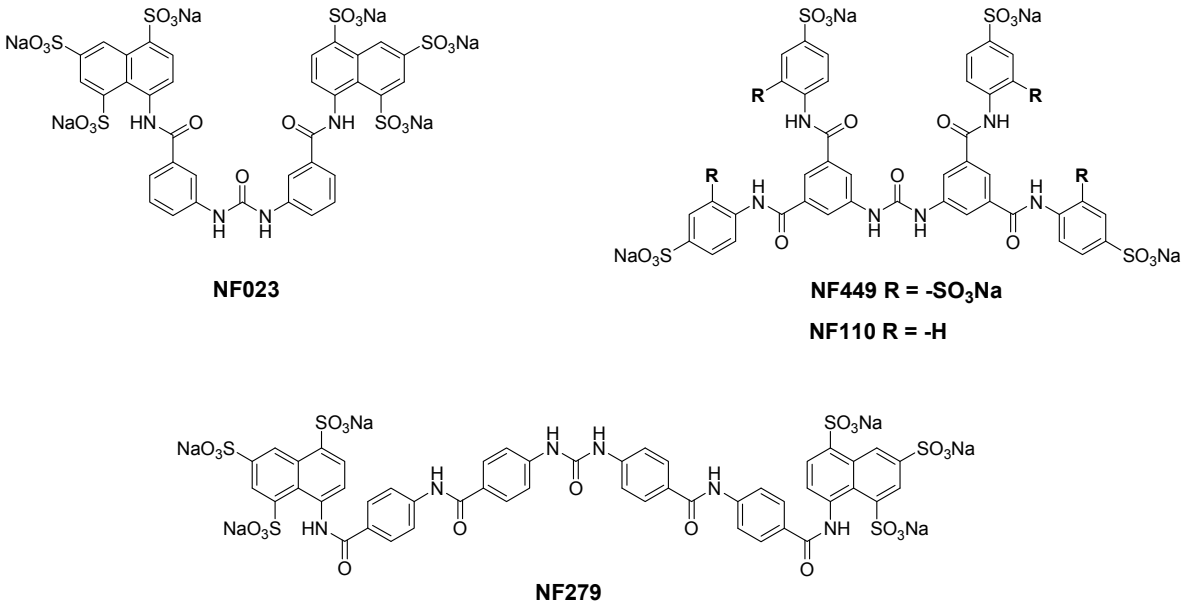

Figure 1.9. Structure formula of suramin derivatives: NF023, NF279, NF449 and NF110.

In 2005, Ullmann et al. studied the activities of suramin and its analogues at P2Y receptors.[65] In this study, analogues of suramin with the variation of substitution at the position R (Figure 1.10), small urea derivatives, and their amino- and nitro-precursors were investigated for their activity at $P2Y_1$, $P2Y_2$ and $P2Y_{11}$ receptors.

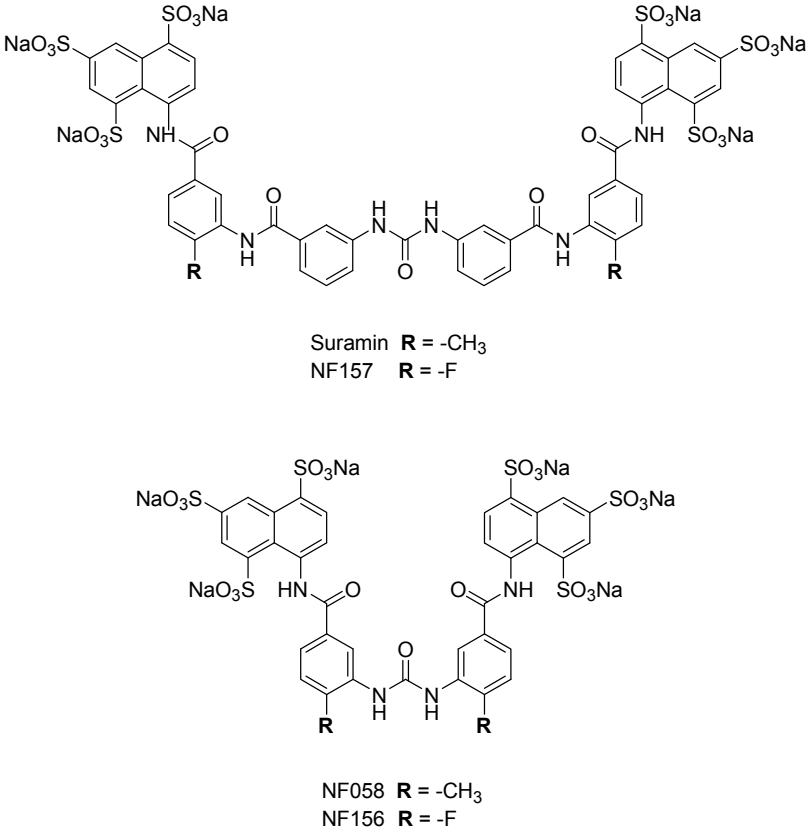

Figure 1.10. Suramin derivatives studied by Ullmann et al. [65]

It was found that NF157 (Figure 1.10), a fluorinated suramin analogue, showed the highest antagonistic potency at $P2Y_{11}$ receptors with an apparent pK_i of 7.35 ± 0.06.
Moreover, NF157 showed a high selectivity for $P2Y_{11}$ receptors over $P2Y_1$ and $P2Y_2$ receptors, but no selectivity over $P2X_1$ receptors. The small urea derivatives showed lower activity at $P2Y_{11}$ receptors in comparison to suramin, whereas the nitro- and amino- precursors showed no effect at $P2Y_{11}$ receptors.

Shortly after the discovery of the activity of NF157, S. Meis reported NF340 as a slightly more potent $P2Y_{11}$ antagonist than NF157.[66] NF340 is a small urea derivative with two sulfonic acid substituents at each naphthalene ring (Figure 1.11).

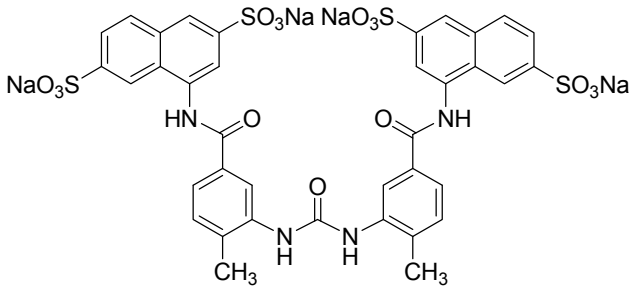

Figure 1.11. NF340, the so far most potent $P2Y_{11}$ receptor antagonist.

NF340 showed an apparent pK_i of 7.71 ± 0.04 in the calcium assay and showed a pA_2 of 8.02 ± 0.06 in the Schild plot analysis.[79] Moreover, NF340 showed high selectivity at $P2Y_{11}$ receptors over $P2Y_1$, $P2Y_2$, $P2Y_4$, $P2Y_6$ and $P2Y_{12}$ receptors.
However, the information of the structural requirement of NF340 for $P2Y_{11}$ receptor activity so far is limited.

1.5 Study of P2Y activity of compounds by measurement of ligand-induced changes in the intracellular calcium concentration

Stimulation of G protein-coupled receptors results in various responses (Figure 1.12). Activation of G_q-coupled receptors stimulates phospholipase C (PLC), causing the formation of inositol-1,4,5-triphosphate (IP_3) and mobilization of intracellular Ca^{2+} from endoplasmic reticulum. Stimulation of G_s-couple receptor

increase cAMP, while stimulation of G_i proteins inhibits adenylate cylcase. Therefore, there are different pharmacological tools to study effects of ligands at GPCRs such as measuring of IP_3, ligand-induced changes in the intracellular Ca^{2+} concentration, or cAMP for example.[67-70]

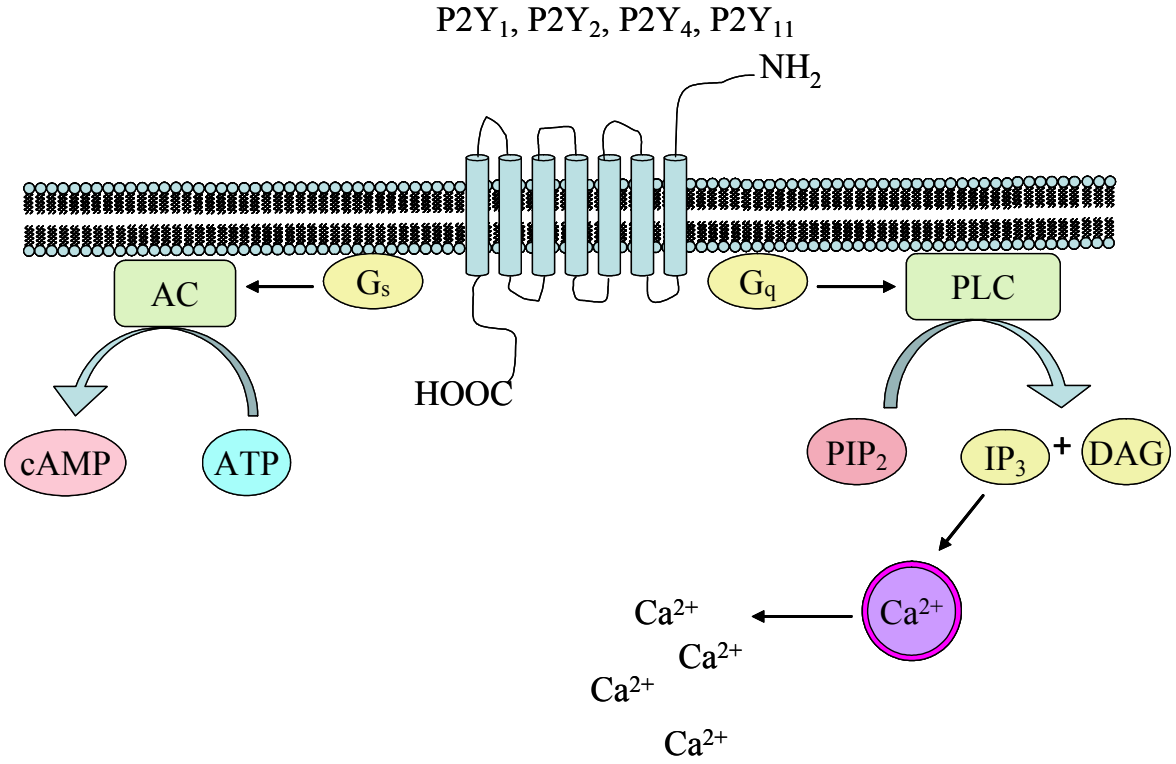

Figure 1.12. Activation of $P2Y_1$, $P2Y_2$, $P2Y_4$ and $P2Y_{11}$ receptors promotes G_q-mediated activation of phospholipase C, which in turn hydrolyzes membrane PIP_2 to yield IP_3 and DAG. IP_3 consequently promotes the release of Ca^{2+} from intracellular stores. $P2Y_{11}$ receptors are also coupled to G_s-mediated activation of AC. Therefore, stimulation of the $P2Y_{11}$ receptors results in increasing concentrations of intracellular cyclic AMP.

In 2002, M. U. Kassack used the measurement of changes in the intracellular Ca^{2+} concentration as a method to yield information about the agonistic or antagonistic character of test compounds which act at GPCRs as targets.[71,72] In combination with radioligand binding experiments, the calcium assay study could be used to comprehensively identify the characteristics of novel GPCR ligands.

Thus, measurement of the intracellular calcium was used to assess the activity of compounds at $P2Y_{11}$ receptors.

2 Aim of the project

$P2Y_{11}$ receptors seem to play roles in the immune system and may be involved in an increased risk for myocardial infarction. However, full comprehension of the physiological and pharmacological functions of $P2Y_{11}$ receptors is not available. Although NF157 and NF340 were reported as potent antagonists at $P2Y_{11}$ receptors, both compounds are polysulfonated urea derivatives which can not penetrate the cell membrane because of their highly hydrophilic character. *In vivo* investigation of both compounds is therefore limited. New $P2Y_{11}$ receptor ligands are still required. Moreover, so far there is no information about structural requirements of NF340 for $P2Y_{11}$ receptor activity. To allow a rational design of $P2Y_{11}$ receptor ligands, basic information about structure-activity relationships of NF340 are needed.

This project aimed to develop new potent and selective $P2Y_{11}$ receptor ligands, using NF340 as a template for structural modification. Symmetrical and asymmetrical urea derivatives of NF340 were designed, synthesized and studied for their pharmacological activities.

The project was divided in 2 parts: synthesis and biological evaluation.

2.1 Synthesis of NF340 and derivatives

NF340 was planned to be resynthesized and used as standard antagonist. Although NF340 was formerly synthesized by the group of Prof. Nickel, analytical data of NF340 are not available until now. Therefore, the synthesis method and analytical data of NF340 are mentioned here. Variations of NF340 derivatives were planned to be synthesized. Structure modifications could be summarized as shown in Figure 2.1.

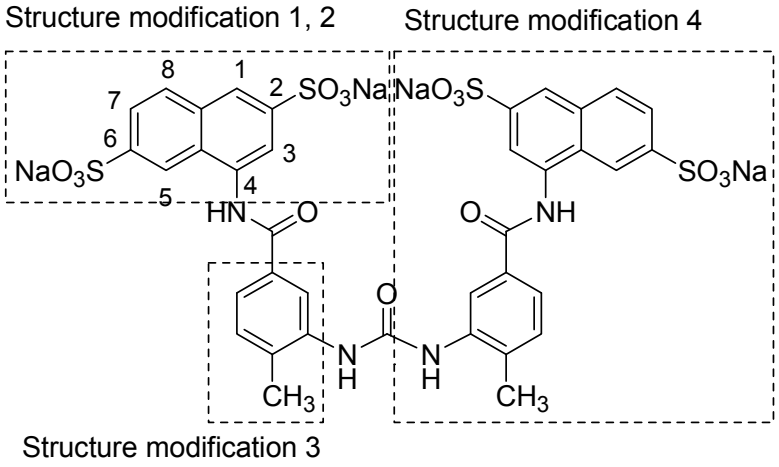

Figure 2.1. Structure modifications of NF340.

Modification 1: variation of the numbers and positions of the sulfonic acid moieties of the naphthalene ring. Symmetrical urea analogues with monosulfonic acid substitution at position 2, 6, or 1 on each naphthalene ring were planned to be synthesized in order to study which of the sulfonic acid moieties were essential for the high $P2Y_{11}$ receptor inhibitory potency of NF340. In addition, synthesis of other di- and tri-sulfonic acid substitutions of the naphthalene than in NF340 was planned.

Modification 2: reduction of the ring size: substitution of the naphthalene by a benzene ring. Symmetrical benzene sulfonic acid derivatives were planned to be synthesized to investigate if the naphthalene ring is required for activity.

Modification 3: variation of the phenylene-linker. Symmetrical benzene sulfonic acid urea derivatives with para-phenylene-linker were planned to be synthesized to investigate the effects of the phenylene-linker.

Modification 4: synthesis of asymmetrical urea derivatives. In order to investigate whether the symmetrical structure is required for $P2Y_{11}$ receptor activity, asymmetrical urea derivatives of NF340 were planned to be synthesized.

2.2 Biological evaluation of the synthesized compounds

The synthesized compounds and compounds from the NF-library of Prof. Nickel, Bonn, which were structurally related to the synthesized compounds, should be evaluated for agonistic and antagonistic activities at $P2Y_{11}$ receptors recombinantly expressed in 1321N1 astrocytoma cells by measuring ligand induced changes in the intracellular calcium concentration. Structure-activity relationships should be analysed from all obtained biological results. Moreover, all test compounds were tested for their activities at $P2Y_1$, $P2Y_2$ and $P2Y_4$ receptor for selectivity reasons.

3 Chemistry

3.1 Synthesis pathway of NF340

NF340 or 4,4'- (carbonylbis (imino-3,1- (4-methylphenylene) carbonylimino)) bis- (naphthalene-2,6-disulfonic acid) tetrasodium salt was first synthesized in 1986 by the group of Prof. Nickel, using 1-amino-2,6-naphthalene disulfonic acid as a precursor. However, the synthesis method and analytical data were not yet published.[73] Nowadays, 1-amino-2,6-naphthalene disulfonic acid is not available. Therefore, naphthalene-2,6-disulfonic acid was used in this work as a precursor instead. The synthesis pathway of NF340 is shown in Figure 3.1.

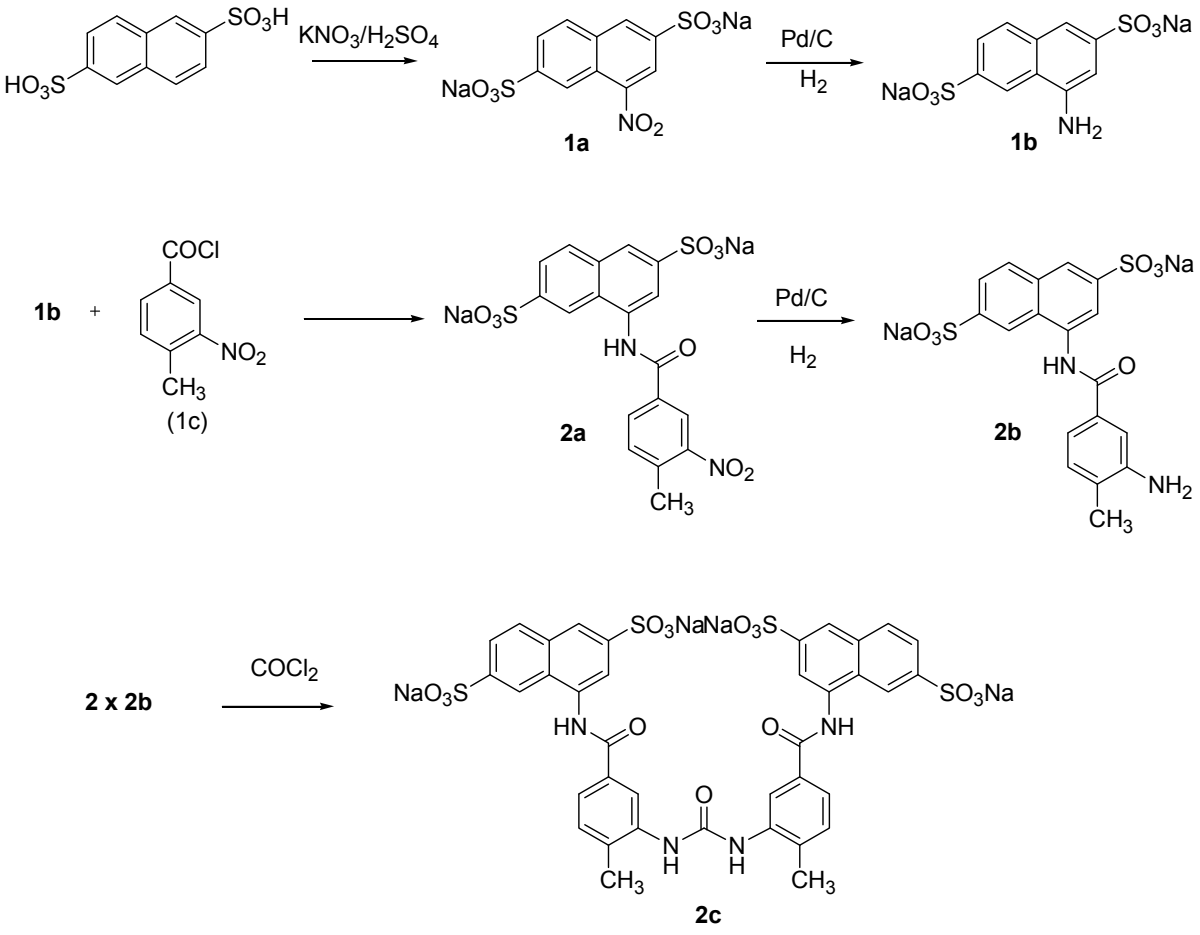

Figure 3.1. Synthesis pathway of NF340 (2c).

First, naphthalene-2,6-disulfonic acid was nitrated with potassium nitrate in conc. sulphuric acid. Then, the nitro group of the product (1a) was reduced to the amino group (1b), using 10 % palladium/carbon as catalyst. Next, acylation of compound

1b dissolved in water with 4-methyl-3-nitrobenzoyl chloride (1c), dissolved in toluene, was done at a constant pH of 4.0 to obtain compound 2a. Afterwards, the nitro group of compound 2a was catalytically hydrogenated again using 10 % palladium/carbon. Finally, NF340 (2c) was obtained by addition of a solution of phosgene in toluene (20 %) to compound 2b in aqueous solution at a constant pH of 3.7.

3.1.1 Synthesis of 4-nitronaphthalene-2,6-disulfonic acid disodium salt

In 1958, Farbenfabriken Bayer AG patented the method to synthesize 4-nitronaphthalene-2,6-disulfonic acid by the sulfonation of 8-nitronaphthalene-2-sulfonic acid at position 6 (Figure 3.2).[74]

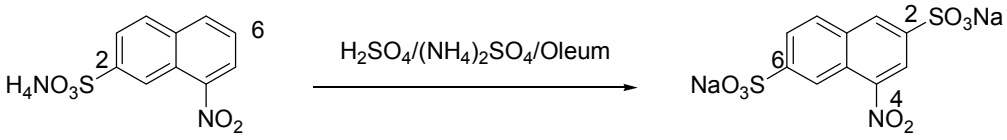

Figure 3.2. Sulfonation of 8-nitronaphthalene-2-sulfonic acid ammonium salt.

4-Nitronaphthalene-2,6-disulfonic acid could however easier be synthesized by nitration of naphthalene-2,6-disulfonic acid. Dinitration at position 4 and 8 of the naphthalene ring could have occurred when using the mixture of conc. sulphuric acid and conc. nitric acid as a nitrating agent. To minimize the dinitration side product, potassium nitrate in sulphuric acid was used as a nitrating agent (Figure 3.3). This reaction gave about 88 % mononitration and about 6 % dinitration.

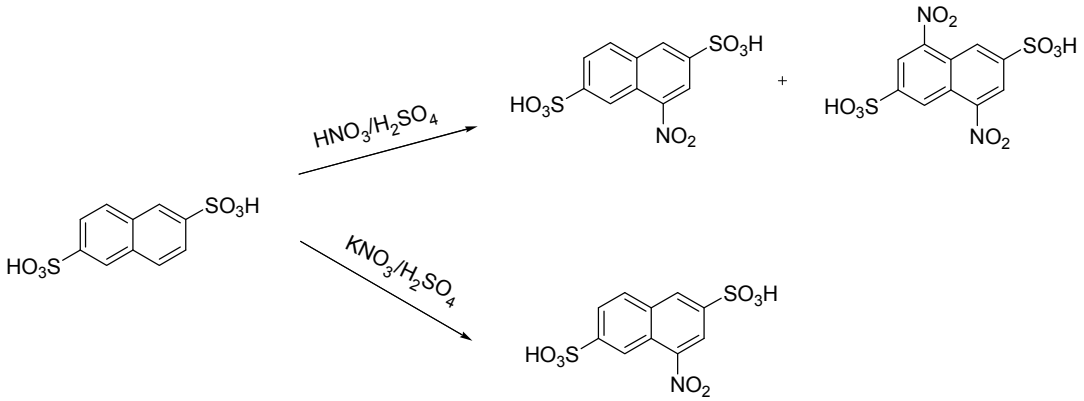

Figure 3.3. Nitration of naphthalene-2,6-disulfonic acid.

Because of the poor solubility of naphthalene-2,6-disulfonic acid in conc. sulphuric acid, the nitration was done in suspension. Potassium nitrate, dissolved in conc.

sulphuric acid, was slowly dropped to the suspension of naphthalene-2,6-disulfonic acid in conc. sulphuric acid at a temperature of 0°C. The completion of the reaction was indicated by obtaining a clear solution. A cooled solution of 20 % sodium chloride was very slowly dropped into the clear solution and the mixture was stirred until the yellow product precipitated. The product was filtered and washed with cooled NaCl solution and methanol.

Although only one spot was detected in TLC, the HPLC result showed one major peak and two minor peaks (chromatogram no shown). The major peak showed an area under curve of 88.4 % and could be interpreted by the NMR spectrum (see Figure 3.4) as mononitrosubstituted product. One of the small peaks was defined as the naphthalene-2,6-disulfonic acid precursor by comparison with the reference peak. The other small peak could be identified with the ^{1}H NMR signals as 4,8-dinitro-substituted side product. Compound 2a was further purified by stirring with methanol/water.

So far there is no published analytical data, especially NMR spectrum, of compound 1a. Therefore, the structure confirmation of compound 1a is explained here.

Structure confirmation

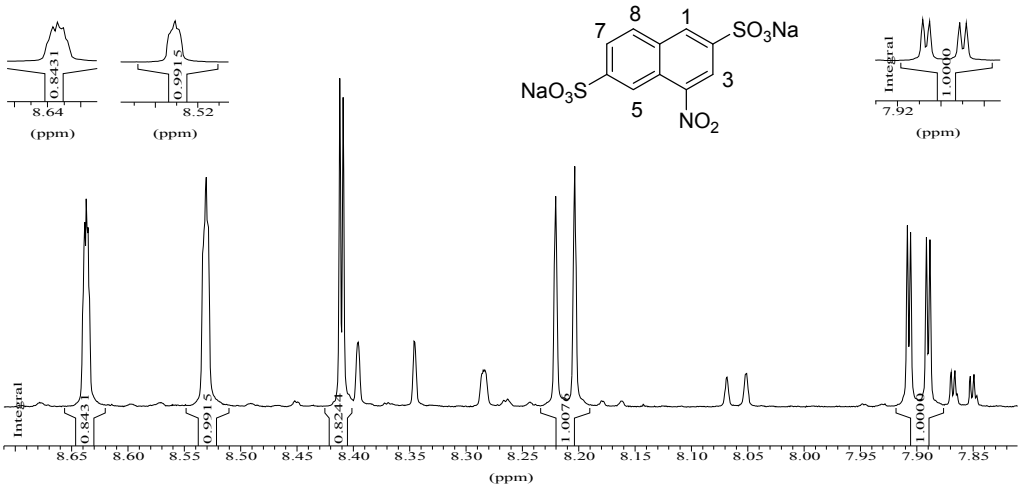

Figure 3.4. 500 MHz ^{1}H NMR spectrum of compound 1a in DMSO-d_6 with integrated intensities shown below. The multiplets are shown in the expanded peaks. The small peaks (without integration) could be interpreted as impurities (dinitro-substituted side product and naphthalene-2,6-disulfonic acid precursor).

Figure 3.4 shows the ^{1}H NMR spectrum of compound 1a with five resonance signals. Their integration represented five protons. From the splitting patterns and

H,H-COSY (Correlation Spectroscopy) spectrum, this spectrum could confirm the structure of compound 1a as described in the following:

The signals of proton H7 and H8 could be easily interpreted by the coupling patterns. A doublet of doublet at 7.90 ppm was identified as the signal of the proton H7 which was coupled to H8 with an ortho-coupling (^3J = 8.5 Hz) and also coupled to H5 with a meta-coupling (^4J = 1.6 Hz). With the same ortho-coupling constant, the signal of the proton H8 appeared as a doublet at 8.21 ppm. Theoretically, the signal of the proton H3 should appear in the lowest field of the spectrum because of the –I and –M effect of the $–NO_2$ and $–SO_3^-$ groups. Figure 3.5 shows the result from an H,H-COSY experiment.

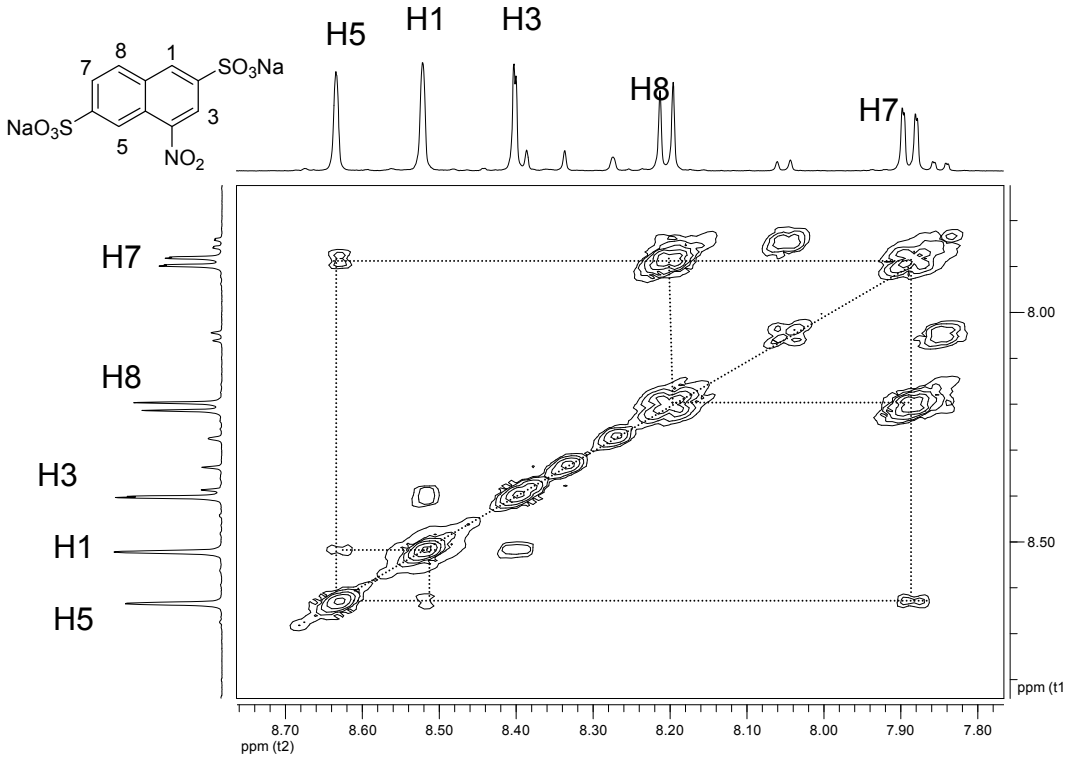

Figure 3.5. 500 MHz H,H-COSY-90 spectrum of compound 1a shown as a contour plot. At the top and the left-hand edge is the one-dimensional ^{1}H NMR spectrum with partial assignments. The diagonal peak and cross peaks of the proton H7 forms a corner of two squares, as this proton was coupled both to the proton H8 and H5.

The cross peaks (dotted lines) in the spectrum showed the coupling of the protons H7 (δ 7.90 ppm) to H8 (δ 8.21 ppm) and H5 (δ 8.64 ppm). The pseudotriplet signal of H5 showed the coupling not only to the proton H7 but also to the proton H1. Normally, coupling through five or more bonds can rarely be observed, except couplings through "zig-zag bond" systems in unsaturated compounds.[75,76] In this case, the protons H1 and H5 could also couple through the zig-zag bond system (Figure 3.6) and the coupling constant was measured as ^5J = 0.8 Hz.

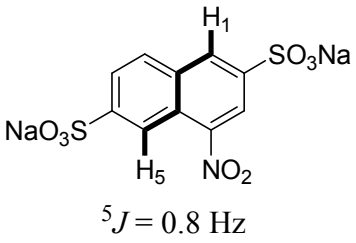

Figure 3.6. A „zig-zag bond" between the proton H1 and H5 showed the ^5J coupling constant of 0.8 Hz.

This coupling character was confirmed by the correlation of H5 and H1 signals at 8.64 ppm and 8.53 ppm in the H,H-COSY spectrum. Signals at 8.53 ppm and 8.41 ppm represented the proton H1 and H3, respectively. The proton H1 coupled to H3 and H5. The splitting pattern of this signal showed a pseudotriplet, however the coupling constant could not be measured. The proton H3 coupled only to H1 and appeared as a doublet with ^4J = 1.6 Hz.

Figure 3.7 shows the ^{13}C NMR spectrum of compound 1a.

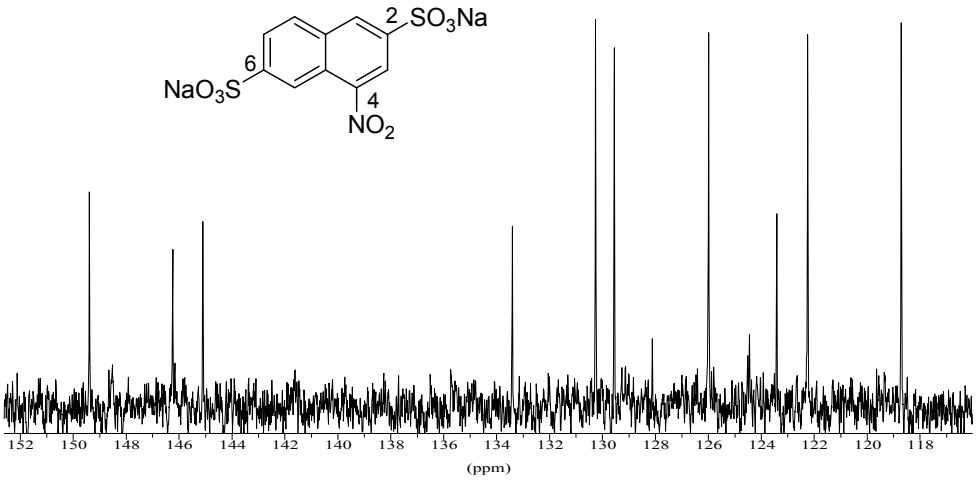

Figure 3.7. 125 MHz ^{13}C NMR spectrum of compound 1a in DMSO-d_6.

Using substituent increment calculation, HSQC (Heteronuclear single quantum correlation, Figure 3.8) spectrum and HMBC (Heteronuclear multiple bond correlation) spectrum (spectrum not shown), the signals of ^{13}C NMR could be interpreted as follows:

The signal of the sulfonic acid substituted carbon (C6) appeared at the lowest field of the spectrum (149.4 ppm), while the signal of the other sulfonic acid substituted carbon (C2) appeared in a slightly higher field at 145.1 ppm. The signal at 146.2 ppm was interpreted and confirmed by HMBC spectrum as the nitro-substituted carbon (C4).

Due to the -I and –M effects of the nitro group, the signals of the carbon C8a and C4a were found at 133.4 ppm and 123.4 ppm, respectively.

The signal in the upfield of the spectrum (118.7 ppm) represented the carbon C5. This interpretation was confirmed by the HSQC spectrum, which showed a correlation between the signals at 8.64 ppm and 118.7 ppm (Figure 3.8).

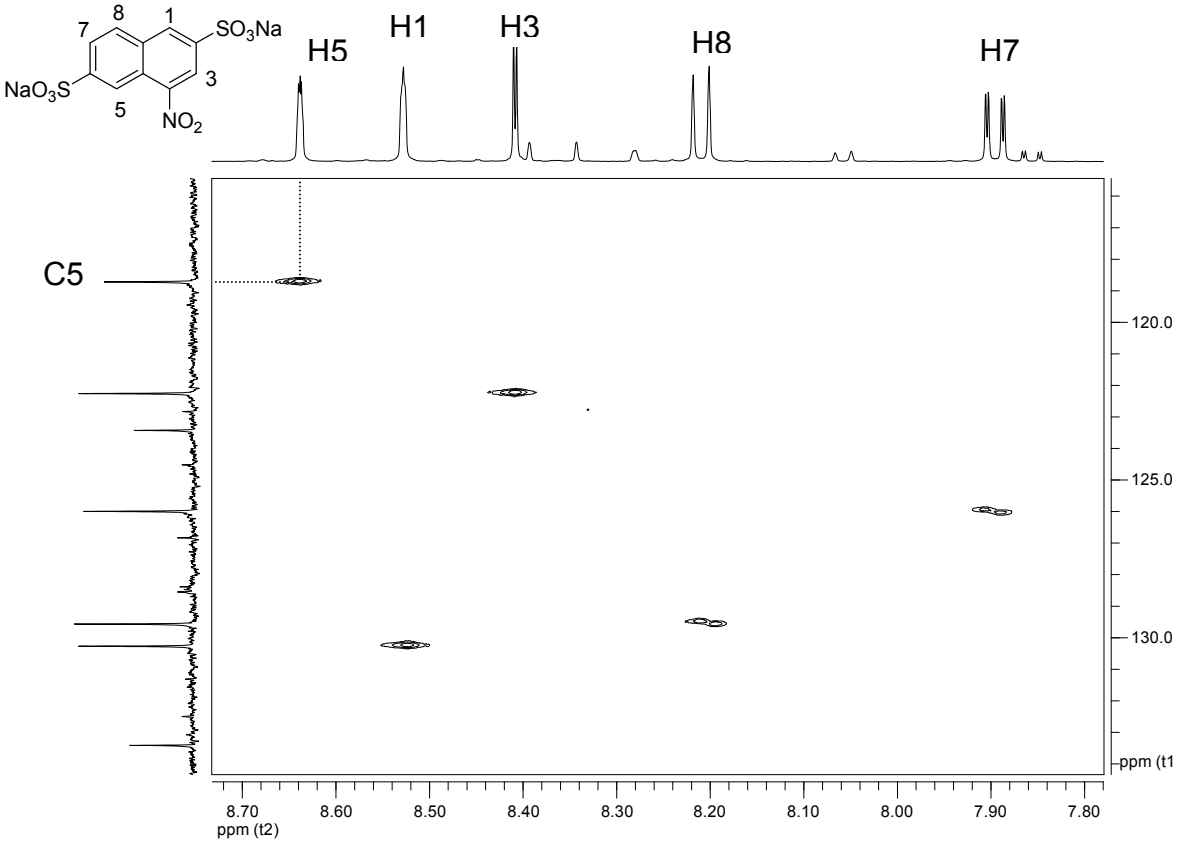

Figure 3.8. HSQC spectrum of compound 1a in DMSO-d_6. The one-dimensional 500 MHz ^1H NMR spectrum with assignments is shown at the top edge, while at the left-hand edge is the one-dimensional 125 MHz ^{13}C NMR. The dotted construction lines show the analysis of H5-C5 as an example.

From the HSQC spectrum, the signals at 122.2 ppm, 125.9 ppm, 129.6 ppm and 130.3 ppm were further assigned as the carbons C3, C7, C8 and C1, respectively.
The IR spectrum showed the nitro group as two signals: a -NO_2 stretching (asym) vibration at 1522 cm^{-1} and a -NO_2 stretching (sym) vibration at 1348 cm^{-1}. In addition, there was an aromatic C=C stretching vibration at 1628 cm^{-1}.
In the ESI-MS measurement, 1a showed a signal at m/z 354.3 which could be interpreted as $[M-Na]^-$, compared to m/z 353.9 from the calculated value. The other major peak found at m/z 731.2 could be interpreted as $[2M-Na]^-$.

3.1.2 Hydrogenation of 4-nitronaphthalene-2,6-disulfonic acid disodium salt

A nitro group can be reduced to the corresponding amino group by various methods. In our laboratory, catalytic hydrogenation with palladium/carbon was performed. Compound 1a was dissolved in water and hydrogenated under pressure, using 10% palladium/carbon as a catalyst.

Structure confirmation

The ^1H NMR spectrum of compound 1b (Figure 3.9 a)) showed a singlet at 5.66 ppm with an integration of two protons. This signal disappeared in the D_2O exchange spectrum (Figure 3.9 b)) and therefore was characterized as the signal of the $–NH_2$ group. Because of the +M effect of the $–NH_2$ group, the signals of the naphthalene ring of compound 1b appeared at the higher field (7.0 – 8.3 ppm) in comparison with the signals of the precursor 1a (7.9 – 8.6 ppm). The signal of the proton H3 appeared as a doublet at 6.98 ppm with the meta-coupling (^4J = 1.6 Hz) to H1. The signal of the proton H1 appeared as a pseudotriplet at 7.31 ppm. The signals of proton H8 and H7 were found as a doublet (^3J = 8.5 Hz) and a doublet of doublet (^3J = 8.2 Hz and ^4J = 1.6 Hz) at 7.67 ppm and 7.60 ppm, respectively. The signal in the lowest field (8.26 ppm) represented the proton H5 which appeared as a pseudotriplet with the meta-coupling (^4J = 1.6 Hz) to H7 and the zig-zag bond coupling (^5J = 0.8 Hz) to H1.
Figure 3.9 c) shows the ^{13}C NMR spectrum of compound 1b.

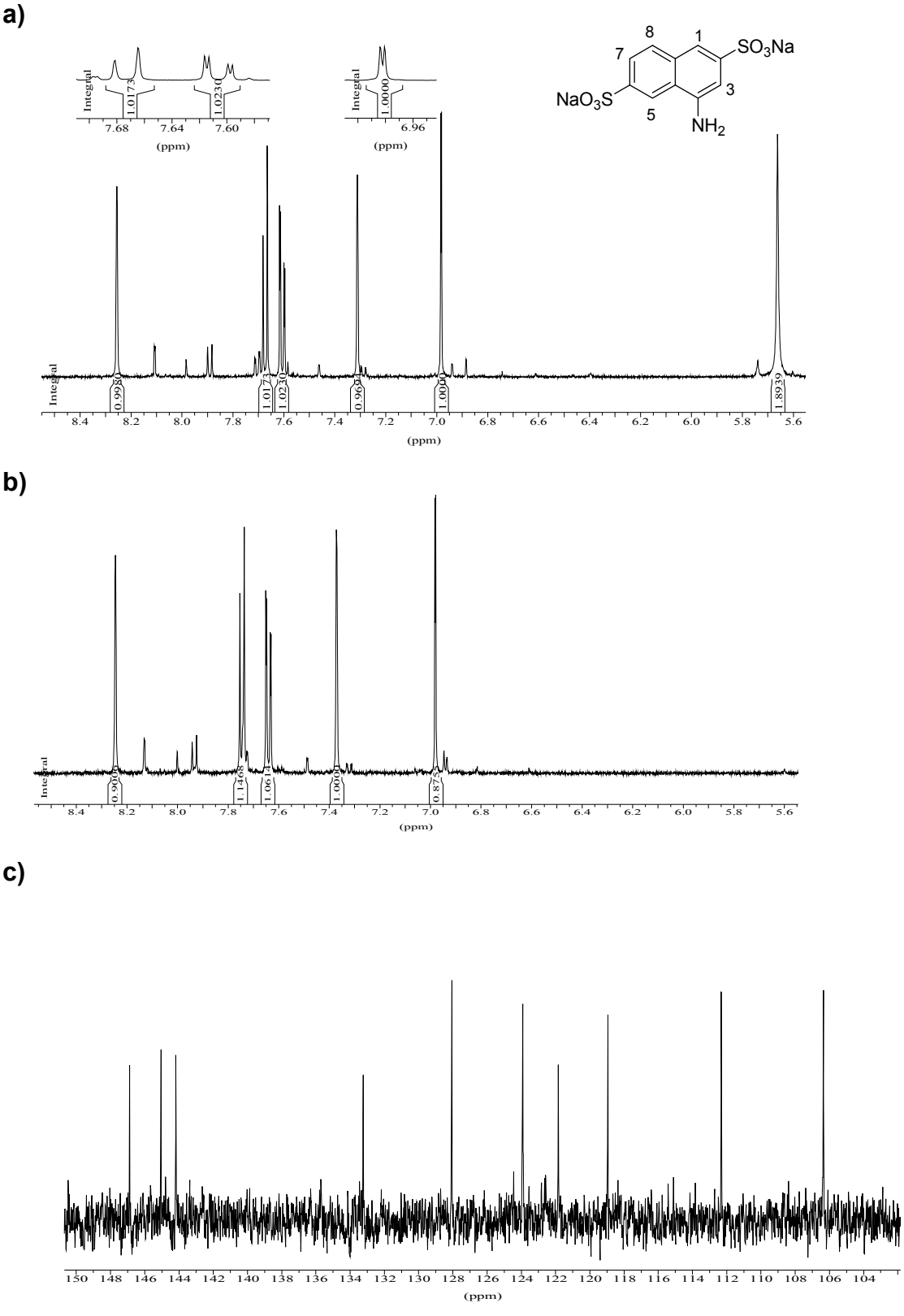

Figure 3.9. 500 MHz ^{1}H and 125 MHz ^{13}C NMR spectra of compound 1b in DMSO-d_6.
a) Whole ^{1}H NMR spectrum with expanded peaks.
b) D_2O exchange spectrum.
c) ^{13}C NMR spectrum

The interpretation of signals was performed by comparison of the found signals with the estimated signals from the software ChemDraw Ultra 7.0. Table 3.1 shows the interpretation of carbon signals of compound 1b.

Table 3.1. Comparison of the calculated and found ^{13}C NMR chemical shift δ (ppm) of compound 1b.

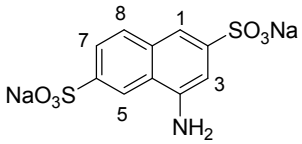

Position	δ calculated (ppm)	δ found (ppm)
C1	115.3	112.3
C2	144.0	146.9
C3	107.4	106.3
C4	143.3	144.2
C4a	122.6	121.8
C5	117.3	118.9
C6	142.4	145.0
C7	123.6	123.9
C8	129.6	128.0
C8a	133.4	133.2

The MALDI-MS in the positive mode showed the signal of $[M+H]^+$ at m/z 347.7. Another major peak found at m/z 304.0 could be interpreted as $[M-2Na+3H]^+$. The measurement of MALDI-MS in the negative mode found two major peaks at m/z 692.8 and m/z 714.8, which could be interpreted as $[2M-H]^-$ and $[2M+Na-2H]^-$, respectively.

3.1.3 Synthesis of 4-methyl-3-nitrobenzoyl chloride

Thionyl chloride is the most common reagent to prepare acid chlorides. In this experiment, 4-methyl-3-nitrobenzoic acid was suspended in toluene and reacted with thionyl chloride (Figure 3.10), using DMF as the catalyst.[77] SO_2 and HCl were trapped by 5 M NaOH during the reaction and the excess of $SOCl_2$ was distilled off after the reaction was completed.

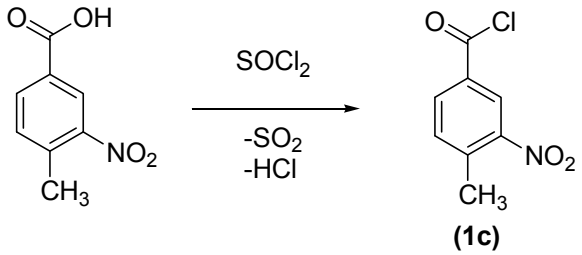

Figure 3.10. Formation of 4-methyl-3-nitrobenzoyl chloride (1c).

3.1.4 Acylation of 4-aminonaphthalene-2,6-disulfonic acid disodium salt

Acylation was performed to synthesize compound 2a. 4-Aminonaphthalene-2,6-disulfonic acid (1b) was dissolved in water and acylated with acid chloride (1c), dissolved in toluene. The pH of the reaction had to be controlled during this reaction because the acid chloride (1c) could be hydrolysed to the corresponding acid at a high pH value and the amino group could be protonated at a low pH. Continuous titration with 2 M Na_2CO_3 was performed to keep the pH at a constant value of 4.0. After the reaction was completed, the reaction mixture was extracted with diethyl ether to remove the nitrobenzoic acid side product.

Structure confirmation

Figure 3.11 shows the ^{1}H NMR spectrum of compound 2a.

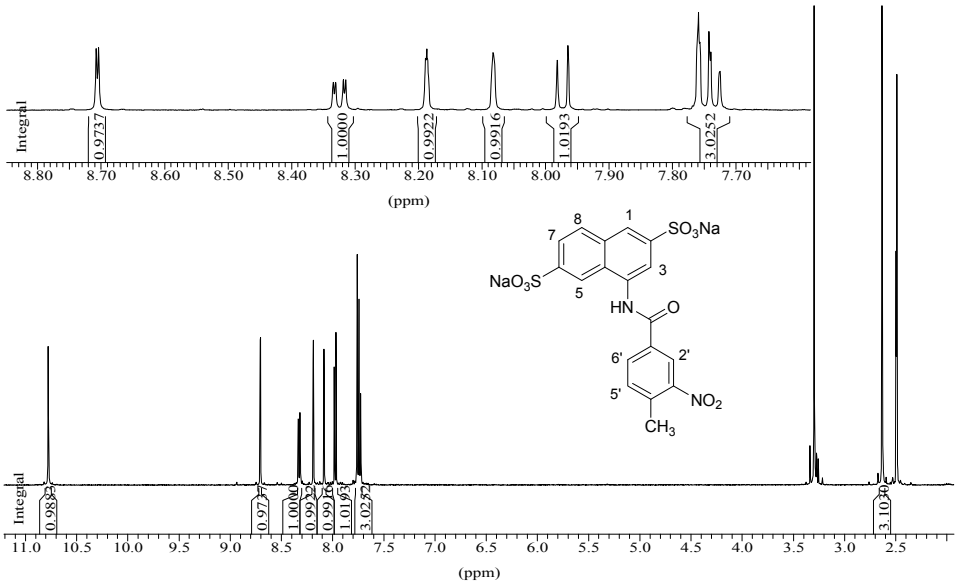

Figure 3.11. 500 MHz ^{1}H NMR spectrum of compound 2a in DMSO-d_6.

The signal in the lowest field of the spectrum (10.79 ppm) showed a singlet which disappeared upon the addition of D_2O. This signal represented the amide proton which indicated the success of the reaction.

The signals of the naphthalene protons formed an ABX-A'X'-system as the nitro- and amino- precursors did (1a and 1b). The signal of the proton H3 (A') appeared as a doublet at 7.76 ppm with the meta-coupling (^4J = 1.6 ppm) to H1, whereas the signal of the proton H1 (X') appeared as a broad singlet at 8.08 ppm. The signal of the proton H5 (X) appeared as a pseudotriplet at 8.19 ppm with the meta-coupling to H7 and the “zig-zag bond” coupling to H1. The signal of the protons H8 (B) and H7 (A) were found as a doublet and a doublet of doublet at 7.97 ppm and 7.75 ppm, respectively.

The three protons of the benzamido residue formed an ABX-system. Because of the –I and –M effects of the $–NO_2$ group, the signal of the proton H2' (X) appeared in the downfield (8.70 ppm) as a doublet with the meta-coupling (^4J = 1.7 Hz) to H6'. The signal of the proton H6' (B) appeared in the higher field (8.32 ppm). The signal showed the splitting pattern as a doublet of doublet which could be interpreted as the ortho-coupling (^3J = 8.0 Hz) to H5' and the meta-coupling (^4J = 1.7 Hz) to H2'. The signal of the proton H5' (A) appeared as a doublet at 7.73 ppm with ^3J = 8.0 Hz.

The three protons of the methyl group showed a singlet signal at 2.63 ppm with an integration of three protons.

Figure 3.12 shows the ^{13}C NMR spectrum of compound 2a.

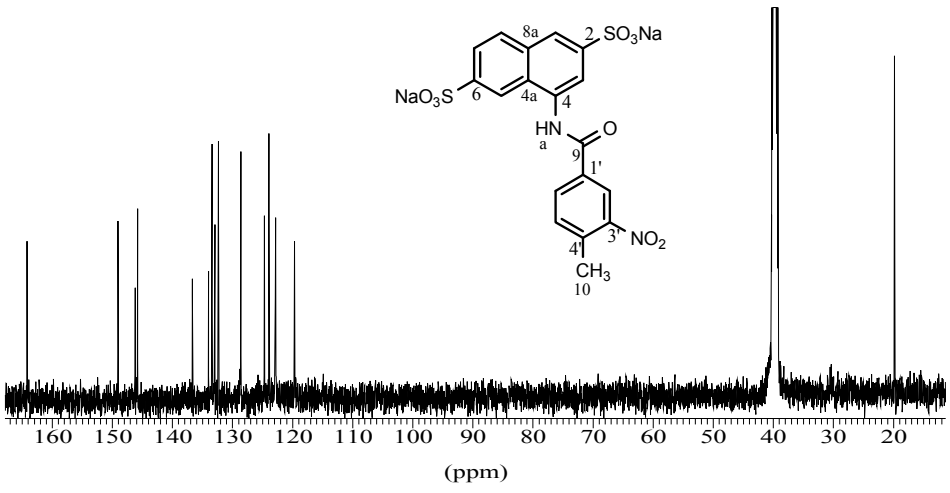

Figure 3.12. 125 MHz ^{13}C NMR spectrum of compound 2a in DMSO-d_6.

The signal in the lowest field of the spectrum (164.2 ppm) represented the carbonyl carbon (C9), whereas the signal at the upfield (19.8 ppm) represented the methyl carbon (C10).

The signals of sulfonic acid substituted naphthalene ring were interpreted by comparison with the calculated signals from ChemDraw Ultra 7.0 and comparison with the carbon signals of amino (2b, see details in section 3.1.5) and urea compounds (2c, see details in section 3.1.6). Table 3.2 shows the comparison of ^{13}C signals at the naphthalene ring between 2a -2c.

Table 3.2. Comparison of δ-values of ^{13}C NMR signals of naphthalene ring between nitro (2a), amino (2b) and urea (2c) derivatives.

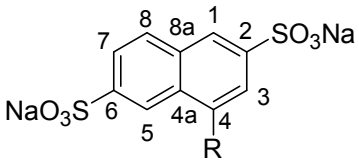

Position	Signals of nitro 2a (δ/ppm)	Signals of amino 2b* (δ/ppm)	Signals of urea 2c (δ/ppm)
C1	122.8	122.3	122.5
C2	146.2	145.9	145.9
C3	122.8	122.7	122.8
C4	134.0	134.9	134.8
C4a	128.6	128.9	128.9
C5	119.7	119.9	120.0
C6	145.8	145.7	145. 6
C7	124.7	124.5	124.6
C8	128.6	128.4	128.5
C8a	133.4	133.1	132.9

*Tertiary carbons of amino derivative 2b were confirmed by HSQC spectrum (see Figure 3.15)

The six ^{13}C NMR signals of the benzamido residue were interpreted by comparison with the calculated signals from ChemDraw Ultra 7.0. Table 3.3 shows the comparison of calculated signals and found signals.

Table 3.3. Interpretation of the ^{13}C NMR signals of benzamido residue of compound 1b in comparison with the calculated signals.

Position	δ calculated (ppm)	δ found (ppm)
C1'	131.4	132.9
C2'	122.3	123.9
C3'	149.2	149.0
C4'	136.2	136.7
C5'	130.3	132.3
C6'	133.3	133.4

The IR spectrum confirmed the presence of the amide functional group with the characteristic bands of the C=O stretching vibration at 1653 cm^{-1} and the N-H bending vibration at 1528 cm^{-1}.

The ESI-MS in the negative mode showed the peaks of $[M-H]^-$ at m/z 509.4, $[M-Na]^-$ at m/z 487.5, $[M-2Na+H]^-$ at m/z 465.5 and $[2M-Na]^-$ at m/z 997.5.

3.1.5 Hydrogenation of 4-(3-nitro-4-methylbenzamido naphthalene-2,6-disulfonic acid disodium salt

The nitro group of compound 2a could be reduced to the corresponding amino group by catalytic hydrogenation, using 10% Pd/C as the catalyst.

Structure confirmation of 4-(3-amino-4-methylbenzamido)naphthalene-2,6-disulfonic acid disodium salt (2b)

Figure 3.13 shows the ^1H NMR spectrum of compound 2b.

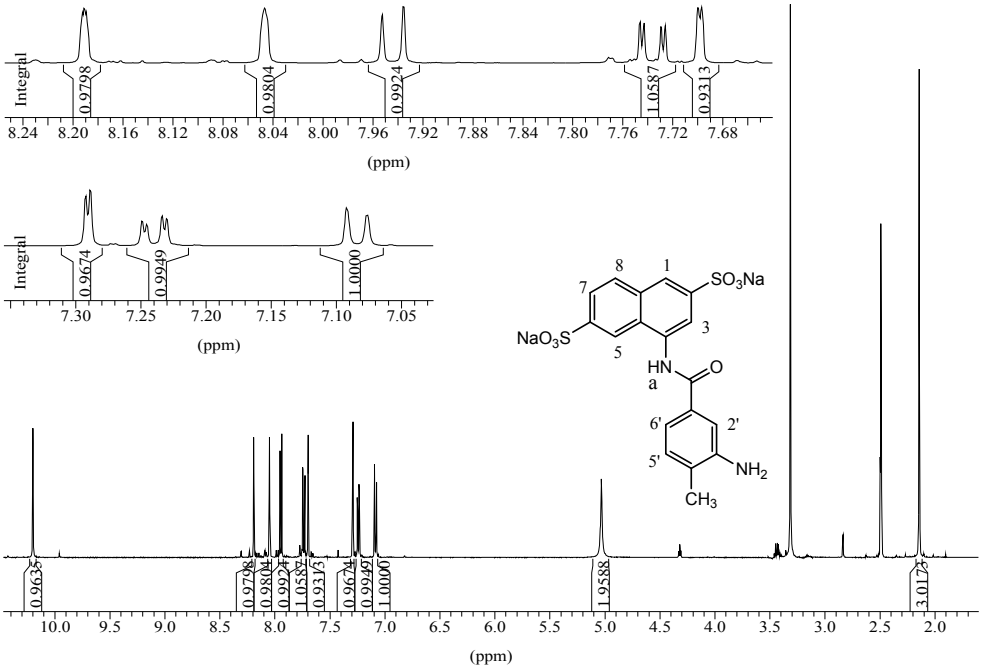

Figure 3.13. 500 MHz ^{1}H NMR spectrum of compound 2b in DMSO-d_6.

The D_2O exchangeable singlet at 5.03 ppm with an integration of two protons was characterized as the signal of the $–NH_2$ protons. The amide proton appeared as a singlet at 10.20 ppm which disappeared in the D_2O exchange spectrum as well. The signals of the five protons of the naphthalene ring appeared in nearly the same positions as the signals of the nitro precursor (2a), but the signals of the three protons of the benzamido residue were shifted to the higher field because of the +M effect of the amino group. The signal of proton H2' appeared as a doublet at 7.29 ppm. The doublet of doublet signal of H6' was shifted to 7.24 ppm, whereas the signal of H5' appeared as a doublet at 7.08 ppm. The signal of three protons of the methyl group was found as a singlet at 2.14 ppm.

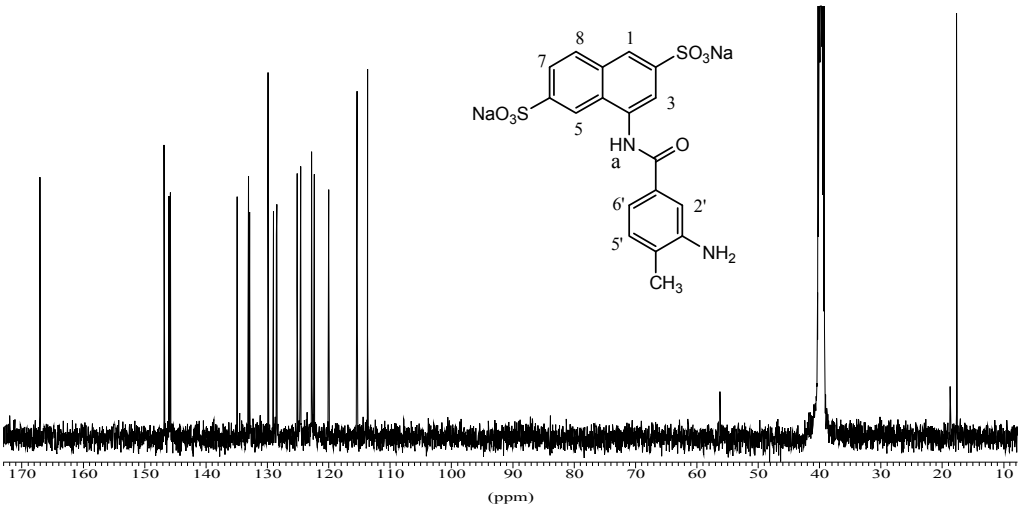

Figure 3.14. ^{13}C NMR spectrum of compound 2b in DMSO-d_6.

For further structure confirmation of compound 2b, ^{13}C NMR (Figure 3.14) and HSQC (Figure 3.15) were performed. The correlation of the protons and the carbons from the HSQC spectrum is presented in Table 3.4.

Table 3.4. Correlations between ^{1}H and ^{13}C NMR from the HSQC spectrum and the assignment of compound 2b.

^{1}H (δ/ppm)	^{13}C (δ/ppm)	Position assignment
8.19	119.9	5
8.05	122.3	1
7.94	128.4	8
7.73	124.5	7
7.70	122.7	3
7.29	113.6	2'
7.24	115.3	6'
7.08	129.8	5'
2.14	17.6	-CH_3

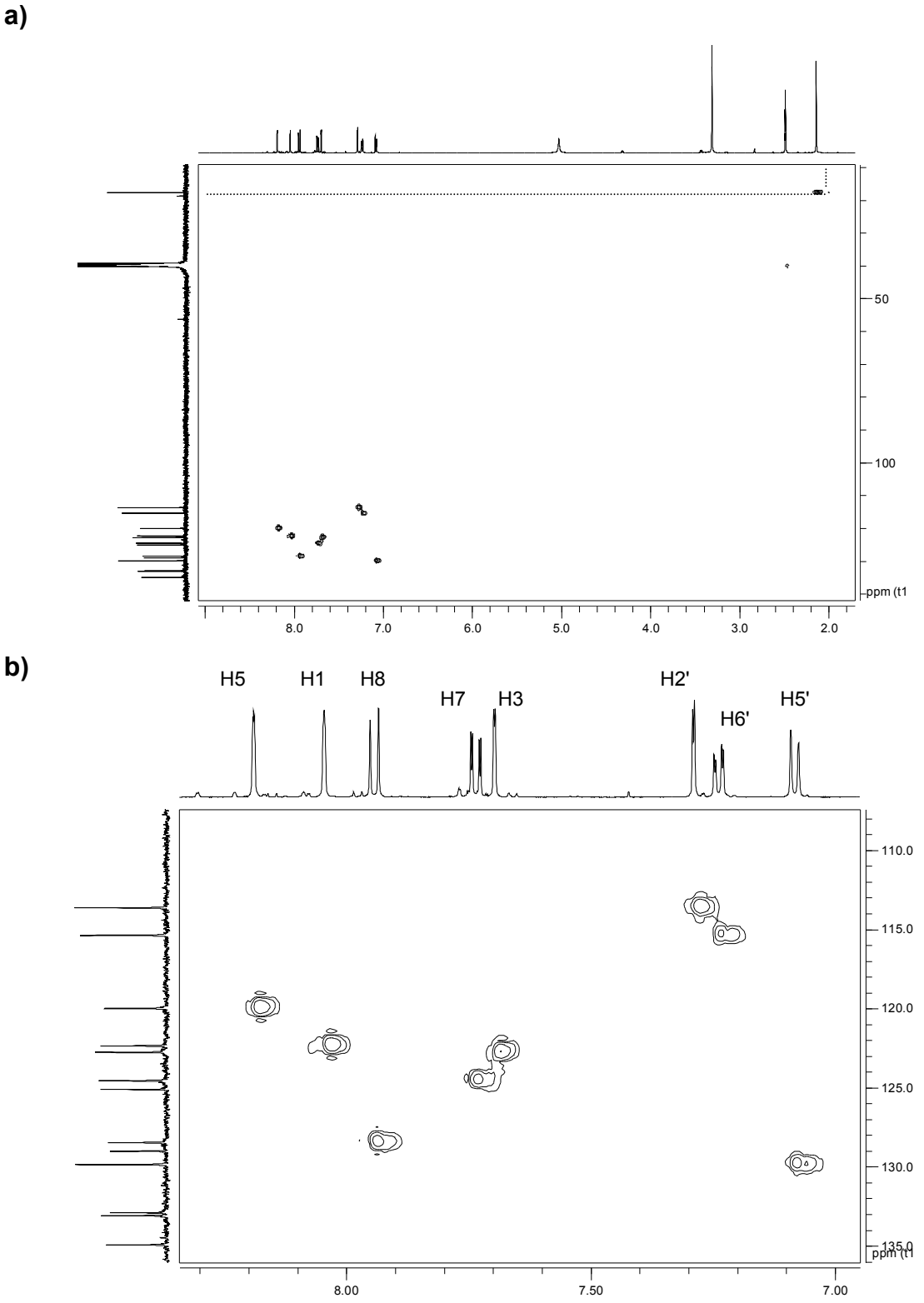

Figure 3.15. HSQC spectrum of compound 2b in DMSO-d_6. The one-dimensional 500 MHz ^{1}H NMR spectrum is shown at the top edge, while at the left-hand edge the one-dimensional 125 MHz ^{13}C NMR spectrum is shown.
a) The whole HSQC spectrum shows the correlation (dotted lines) of the signal of ^{1}H at 2.14 ppm and ^{13}C at 17.6 ppm of the methyl group (C10).
b) HSQC expanded signals in the aromatic region.

The signal of the carbonyl carbon C9 appeared in the lowest field (167.0 ppm).
The signals of the naphthalene carbons appeared in the relatively same range as in the nitro precursor (2a). Due to the +M effect of the $–NH_2$ group, the signals of the benzamido residue were shifted to the higher field. The amino-substituted carbon C3' was detected as a signal at 146.8 ppm, whereas the signal of C4' was shifted to 132.9 ppm. The signal of the carbonyl-substituted carbon C1' appeared at 125.1 ppm. The interpretation of the three tertiary carbons C5', C6' and C2' was confirmed by the HSQC spectrum as the signals at 129.8 ppm, 115.3 ppm and 113.6 ppm, respectively.
The signal of the methyl carbon (C10) appeared at 17.6 ppm. This signal showed a correlation with the methyl proton at 2.14 ppm in the HSQC spectrum.
The results from HPLC showed a purity of 90.95 % with a peak at a retention time of 1.11 min, compared with a retention time of the more lipophilic nitro precursor at 2.01 min. (The dead time for this system was 0.96 min).
The measurement of ESI-MS in the negative mode showed a signal of $[M-H]^-$ at m/z 479.3, compared with m/z 479.0 from the calculation. The signals at m/z 457.3, m/z 435.3 and m/z 937.3 represented to $[M-Na]^-$, $[M-2Na+H]^-$ and $[2M-Na]^-$, respectively (calculated m/z: 457.0, 435.0 and 937.0, respectively).

3.1.6 Phosgenation of 4-(3-amino-4-methylbenzamido) naphthalene-2,6-disulfonic acid disodium salt

Phosgenation of the compound 2b was performed in aqueous solution. Therefore, the pH of the reaction had to be controlled to 3.7.[78]
4,4'-(Carbonylbis(imino-3,1-(4-methylphenylene)carbonylimino))bis-(naphthalene-2,6-disulfonic acid) tetrasodium salt (2c or NF340) was obtained as a pale pink powder.

Structure confirmation of compound 2c (NF340)

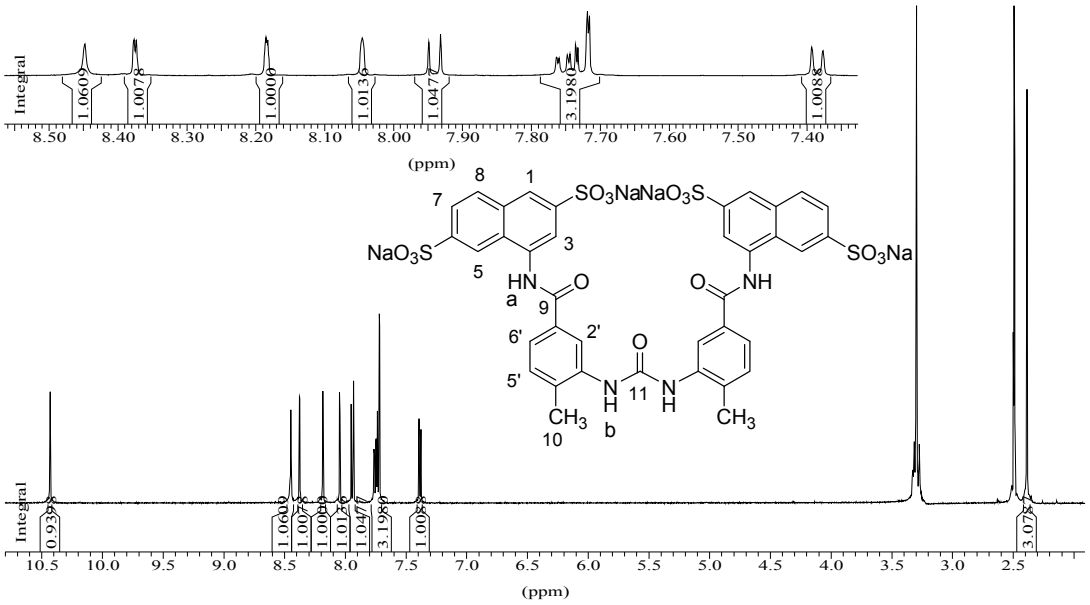

Figure 3.16. 500 MHz ^{1}H NMR spectrum of compound 2c (NF340) in DMSO-d_6.

Figure 3.16 shows the ^{1}H NMR spectrum of 2c (NF340). Comparing with the D_2O exchange spectrum (spectrum not shown), two D_2O exchangeable signals were detected at 10.45 and 8.59 ppm. The singlet at 10.45 ppm was interpreted as the signal of the amide proton (NHa), whereas the singlet at 8.59 ppm represented the signal of the urea proton (NHb). The five protons of the naphthalene ring showed signals and splitting patterns comparable to the amine precursor (2b, see Figure 3.13).

The signals of three protons of the benzamido residue appeared in the lower field region compared to the amino precursor. Table 3.5 shows the comparison of the chemical shifts of the benzamido residue of the nitro- and amino-precursors (2a, 2b) and the urea (2c, NF340).

Table 3.5. Comparison of ^{1}H NMR signals (DMSO-d_6) and splitting patterns of protons at benzamido residues between 2a-2c.

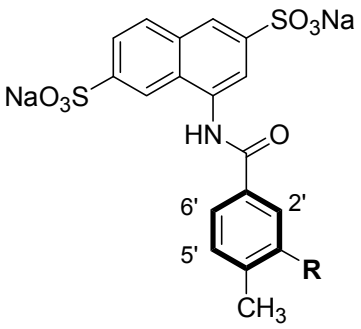

2a R = -NO_2

2b R = -NH_2

2c R = -NHCONH-

	2a		2b		2c (NF340)	
	δ (ppm)	Coupling pattern	δ (ppm)	Coupling pattern	δ (ppm)	Coupling pattern
H2'	8.70	d: *J* = 1.7 Hz	7.29	d: *J* = 1.7 Hz	8.42	d: *J* = 1.4 Hz
H5'	7.73	d: *J* = 8.0 Hz	7.08	d: *J* = 8.0 Hz	7.40	d: *J* = 7.6 Hz
H6'	8.32	dd: *J* = 8.0 Hz *J* = 1.7 Hz	7.24	dd: *J* = 8.0 Hz *J* = 1.7 Hz	7.75	dd: *J* = 7.6 Hz *J* = 1.4 Hz

The signal of the methyl group of 2c (NF340) appeared as a singlet at 2.41 ppm.

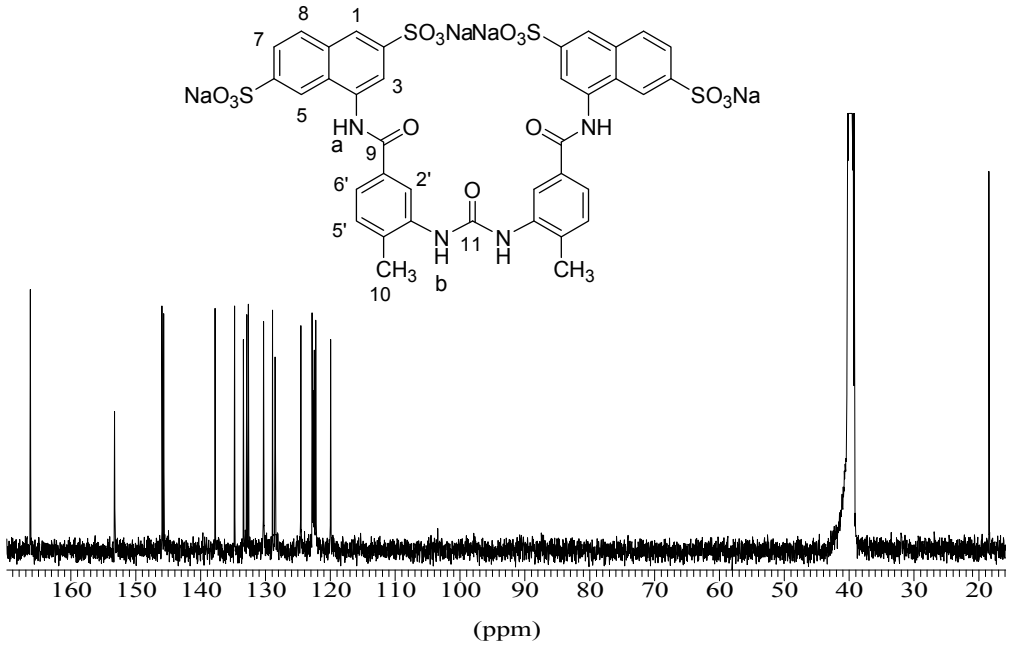

Figure 3.17. 125 MHz ^{13}C NMR spectrum of compound 2c (NF340) in DMSO-d_6.

The ^{13}C NMR spectrum of 2c (Figure 3.17) showed the characteristic carbonyl urea carbon at 153.2 ppm. The signal of the carbonyl carbons of the amide group (C9) appeared at 166.2 ppm. The signals of the naphthalene carbons appeared in a similar region as the precursor (2b, see Table 3.2).

The signals of benzamido carbons were shifted to lower field region in comparison with the amino precursors, except the signal C3'. The interpretation of the carbon signal was performed by comparison with the calculated signals. Table 3.6 shows the assignment of the carbon signals on benzamido residue in nitro- and amino-precursors and the urea 2c (NF340).

Table 3.6. δ-Values of ^{13}C NMR signals at benzamido residues of 2a-2c and the calculated signals of 2c.

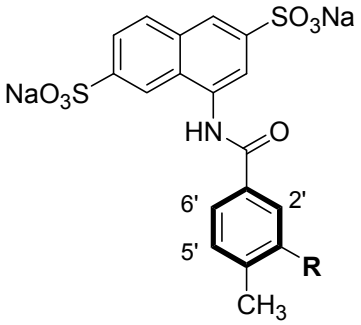

2a R = -NO_2

2b R = -NH_2

2c R = -NHCONH-

Position	Found signals			Calcd signals
	2a	2b	2c (NF340)	of 2c
C1'	132.9	125.1	132.7	130.7
C2'	123.9	113.6	122.3	119.1
C3'	149.0	146.8	137.8	139.0
C4'	136.7	132.9	133.4	133.0
C5'	132.3	129.8	130.3	129.5
C6'	133.4	115.3	122.6	122.8

The signal at 18.4 ppm represented the methyl group.

The MALDI-MS (positive mode) of 2c (Figure 3.18) confirmed the correct molecular mass.

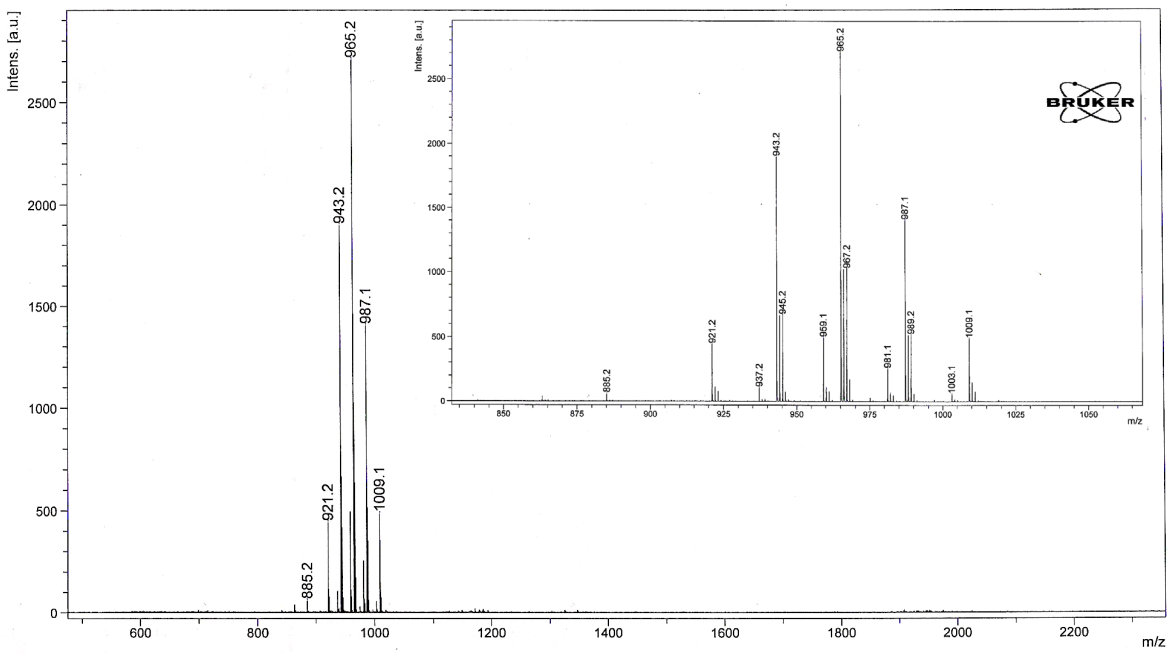

Figure 3.18. Positive-ion MALDI spectrum of compound 2c with expanded signals.

The interpretation of MALDI-MS was done by comparison with the calculated m/z and is summarized in Table 3.7.

Table 3.7. MALDI-MS results in positive mode of 2c (NF340) in comparison with the calculated m/z.

Ions	Calcd m/z	Found m/z
$[M+Na]^+$	1009.0	1009.1
$[M+H]^+$	987.0	987.1
$[M-Na+2H]^+$	965.0	965.2
$[M-2Na+3H]^+$	943.0	943.2
$[M-3Na+4H]^+$	921.0	921.2

3.2 Synthesis of symmetrical derivatives of NF340 with variations of numbers and positions of sulfonic acid groups

To allow the analysis of structure-activity relationships of NF340 and derivatives at $P2Y_{11}$ receptors, variations of the NF340 molecule are required. Monosulfonic acid substituted (4c - 6c), disulfonic acid substituted (3c) and trisulfonic acid substituted (7c) naphthalene analogues were synthesized according to the same method as 2c (NF340). An overview of the synthetic variations is shown in Figure 3.19.

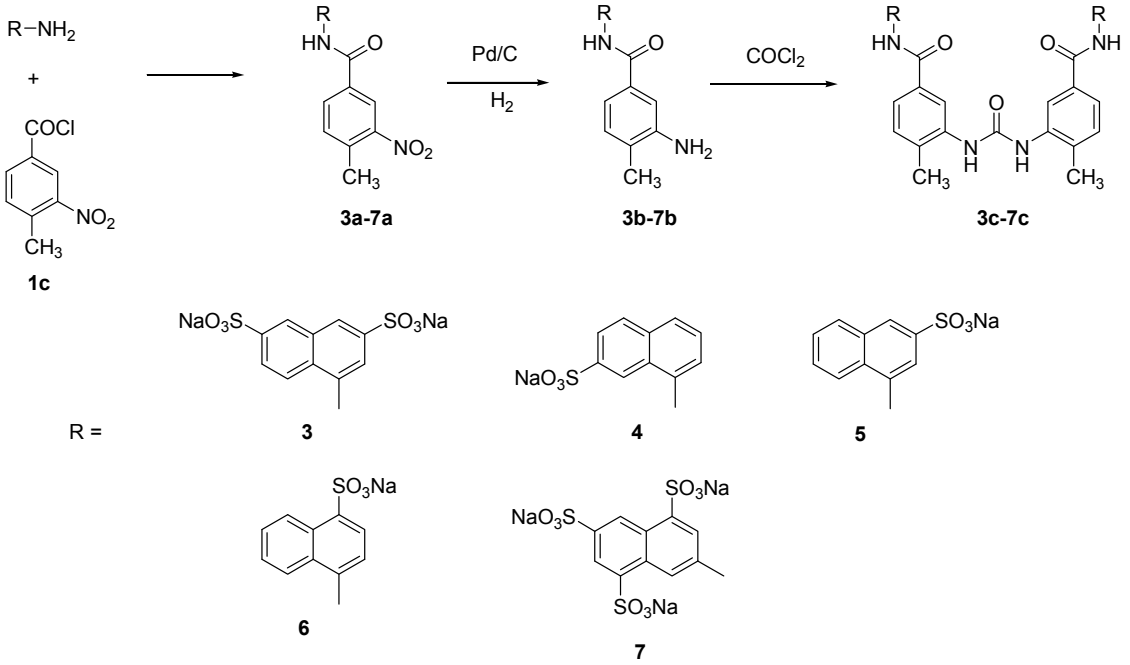

Figure 3.19. Synthetic variations of symmetrical naphthalene sulfonic acid ureas (3c-7c).

3.2.1 4,4'-(Carbonylbis(imino-3,1-(4-methylphenylene)-carbonylimino)) bis-(naphthalene-2,7-disulfonic acid) tetrasodium salt (3c) and precursors

Because NF340 showed high antagonistic activity at $P2Y_{11}$ receptors[79], other disulfonic acid substituted naphthalene derivatives were also interesting to be studied for the $P2Y_{11}$ receptors activity. In the NF-library from Prof. Nickel, there are some disulfonic acid substituted naphthalene derivatives such as NF290, NF294 and NF298 (Appendix B3). However, a structure confirmation of these compounds was not reported. Hence, the structure confirmation of these compounds was done in this work. Moreover, nitro- and amino- precursors which were not available anymore in the NF-library were also resynthesized and named

as ‘’MK-compounds’’ (Appendix B2). However, the analytical data of resynthesized compounds (MK-compounds) and also the analytical data of NF-compounds are not presented here. One new disulfonic acid substituted naphthalene derivative (3c) was synthesized. Compound 3c was synthesized starting from 4-aminonaphthalene-2,7-disulfonic acid .

Structure confirmation of 3a-3c

Figure 3.20 shows the ^{1}H NMR spectrum of compound 3c.

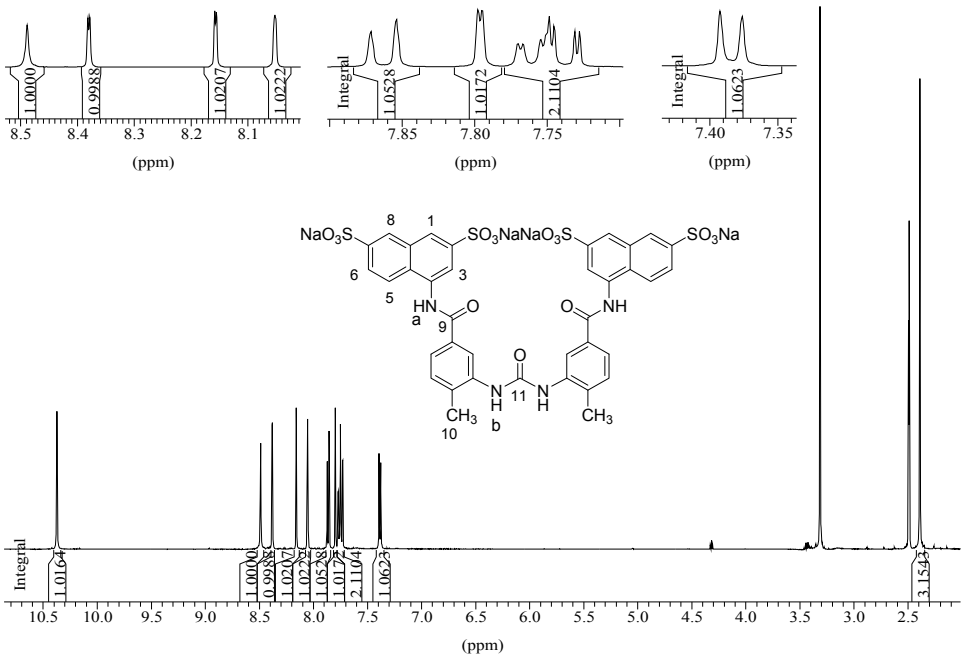

Figure 3.20. 500 MHz ^{1}H NMR spectrum of compound 3c in DMSO-d_6.

The ^{1}H NMR spectrum of 3c showed two singlets which disappeared upon addition of D_2O. The signal at 10.37 ppm was assigned as the amide proton (NHa) which was compared to the amide proton of the nitro precursor (3a) at 10.76 ppm and the proton of the amino precursor (3b) at 10.18 ppm. The signal of the urea proton caused the other D_2O exchangeable peak at 8.49 ppm.

The five protons of the naphthalene ring formed an ABX-A'X' system. Table 3.8 shows the comparison of the δ-values of the naphthalene ring protons of the urea (3c) and its precursors (3a and 3b).

Table 3.8. Comparison of δ-values of the naphthalene ring protons of nitro- (3a), amino- (3b) and urea-derivatives (3c).

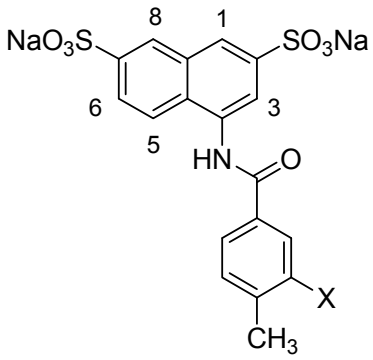

Compound	X	δ (ppm)				
		H1	H3	H5	H6	H8
3a	-NO_2	8.08	7.81	7.81	7.75	8.18
3b	-NH_2	8.04	7.79	7.85	7.72	8.15
3c	-NH-CO-NH-	8.05	7.79	7.86	7.74	8.15

The splitting pattern of the signals of the urea derivative (3c) could be explained as follows: The signal of the proton H8 (X) appeared as a doublet at 8.15 ppm with a meta-coupling (^4J = 1.6 Hz) to H6. The proton H6 (B) was coupled to the proton H8 and H5, thus the signal of this proton appeared as a doublet of doublet at 7.74 ppm with ^3J = 8.8 Hz and ^4J = 1.6 Hz. Theoretically, the signal of proton H5 (A) should appear as a doublet of doublet because of the coupling of H5 to H6 and H1, but the meta-coupling could not be detected in this experiment. Therefore, the signal of H5 appeared as a doublet at 7.86 ppm with an ortho-coupling (^3J = 8.8 Hz). Due to the coupling with proton H1, the signal of proton H3 (A') was found as a doublet at 7.79 ppm with ^4J = 1.3 Hz. The signal of the proton H1 (X') was coupled to H3 and H5, therefore the splitting pattern showed a pseudotriplet at 8.05 ppm. However, the coupling constant of H1 could not be measured because of poor resolution.

The three protons of the benzamido residue formed an ABX-system. The positions of the protons of 3c and its precursors (3a and 3b) showed signals in relatively similar regions as the signals of 2c and its precursors (2a and 2b). Table 3.9

shows the comparison of the NMR signals of the benzamido residues of compounds 2a-2c and 3a-3c.

Table 3.9. Comparison of δ-values of protons at benzamido residues between 2a-2c and 3a-3c.

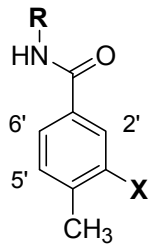

2 R =

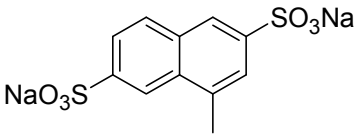

3 R =

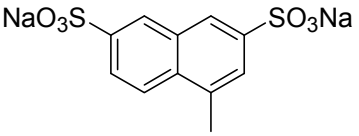

Cpd	X	δ (ppm)					
		H2'		H5'		H6'	
		2	3	2	3	2	3
a	$-NO_2$	8.70	8.68	7.73	7.71	8.32	8.34
b	$-NH_2$	7.29	7.29	7.08	7.07	7.24	7.23
c	-NH-CO-NH-	8.42	8.38	7.40	7.38	7.75	7.76

The splitting pattern of the proton H2' showed a doublet with a meta-coupling (^4J = 1.6 Hz). Coupled to H2' and H5', the signal of proton H6' appeared as a doublet of doublet (^3J = 8.0 Hz and ^4J = 1.6 Hz). The signal of the proton H5' formed a doublet with an ortho-coupling (^3J = 8.0 Hz).

The methyl group of the nitro-derivative (3a) appeared as a singlet signal with the integration of three protons at 2.62 ppm, whereas the methyl signals of the amino- (3b) and the urea-derivative (3c) were found at 2.13 ppm and 2.39 ppm, respectively.

The ^{13}C NMR spectrum of compound 3c is shown in Figure 3.21.

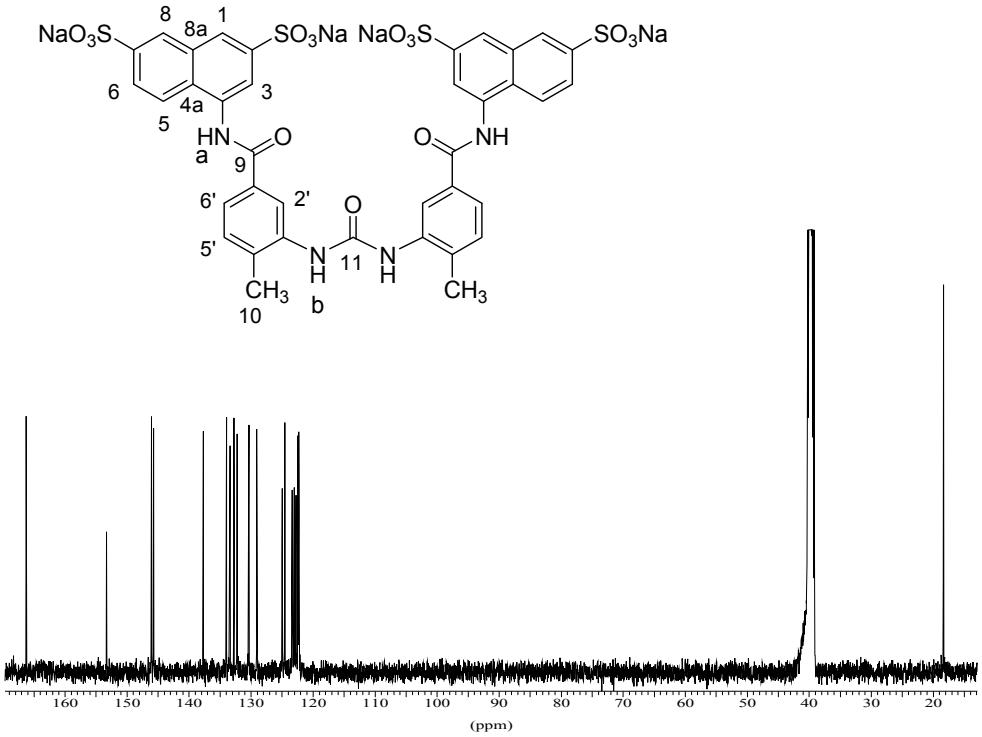

Figure 3.21. 125 MHz ^{13}C NMR spectrum of compound 3c in DMSO-d_6.

The signal of the urea carbon (C11) appeared at 153.3 ppm, whereas the signal of the amide carbon (C9) shifted to the lowest field, 166.2 ppm. Due to the effect of the sulfonic acid groups, the signals of the carbon C2 and C7 were found at 146.1 and 145.7 ppm, respectively. The signal of the carbon C4 appeared at 133.9 ppm, while the signals of the carbon C4a and C8a appeared at 132.3 ppm and 129.1 ppm, respectively.

The tertiary carbons from the aromatic ring system were interpreted and confirmed by the HSQC spectrum (Figure 3.22).

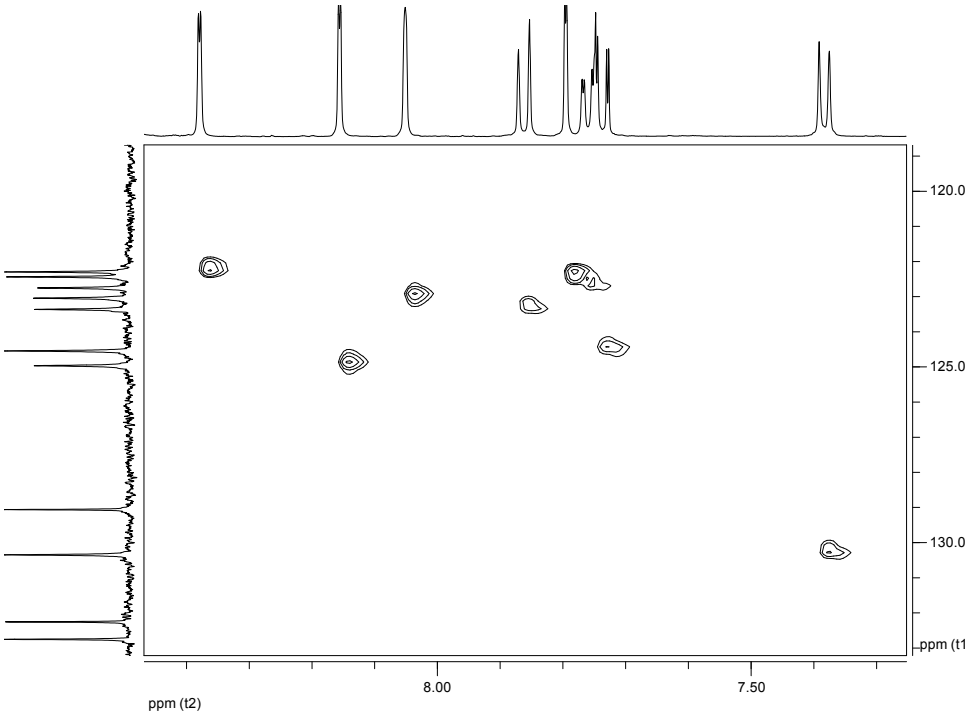

Figure 3.22. HSQC spectrum of compound 3c in DMSO-d_6. Only signals in the aromatic region are shown here. The one-dimensional 500 MHz ^{1}H NMR spectrum is shown at the top edge, while at the left-hand edge the one-dimensional 125 MHz ^{13}C NMR is shown.

The correlation between ^{1}H and ^{13}C was summarized and the positions of carbons were assigned as shown in Table 3.10.

Table 3.10. Correlation between ^{1}H and ^{13}C NMR from the HSQC spectrum and the assignment of compound 3c.

^{1}H (δ/ppm)	^{13}C (δ/ppm)	Position assignment
8.38	122.3	2'
8.15	124.9	8
8.05	123.0	1
7.86	123.4	5
7.79	122.4	3
7.75	122.7	6'
7.73	124.5	6
7.38	130.3	5'
2.39	18.3	-CH_3*

* Signal in HSQC not shown here

The MALDI spectrum confirmed the molecular mass of the urea (3c). The positive ions found in the MALDI spectrum could be analyzed as shown in Table 3.11.

Table 3.11. MALDI-MS results in positive mode of 2c (NF340) in comparison with the calculated m/z.

Ions	Calculated m/z	m/z detected from experiment
$[M+Na]^+$	1009.0	1009.1
$[M+H]^+$	987.0	987.1
$[M+2H-Na]^+$	965.0	965.1
$[M+3H-2Na]^+$	943.0	943.1
$[M+4H-3Na]^+$	921.0	921.2

3.2.2 Naphthalene monosulfonic acid derivatives

The disulfonic acid derivative NF340 showed higher antagonistic potency at $P2Y_{11}$ receptors than the trisulfonic acid analogue NF058 (see section 4.4.4). It was thus interesting to study a further reduction in the numbers of sulfonic acid group. Moreover, to study which of the sulfonic acid moieties of NF340 was essential for the high $P2Y_{11}$ receptor inhibitory potency, monosulfonic acid urea analogues of NF340 (4c and 5c) were synthesized. Furthermore, 6c, a monosulfonic acid substitution in position 4 was also synthesized to compare the activity. Compounds 4c-6c (Figure 3.23) were synthesized, using the same methods as for the synthesis of NF340,

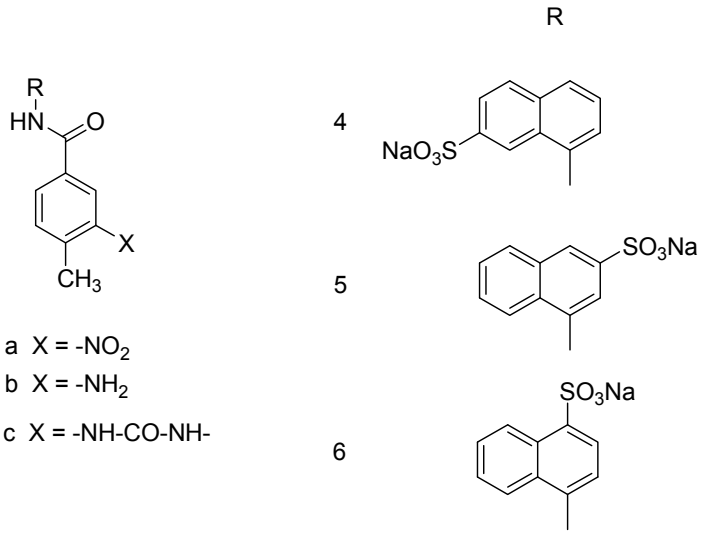

Figure 3.23. Structural formula of symmetrical naphthalene monosulfonic derivatives (4a-c – 6a-c).

Acylation of aminonaphthalene monosulfonic acid was performed under a constant pH of 4.5. Because of the poor water solubility of the nitro naphthalene monosulfonic acid derivatives (4a, 5a and 6a, Figure 3.23), a mixture of water and methanol was used as a solvent during hydrogenation.

Analytical data of 4a-c - 6a-c are presented in the Monographs section. Here, the structure confirmation of compound 6c was explained as an example for monosulfonic acid derivatives.

Structure confirmation of compound 6c

Figure 3.24 shows the ^{1}H NMR spectrum of compound 6c.

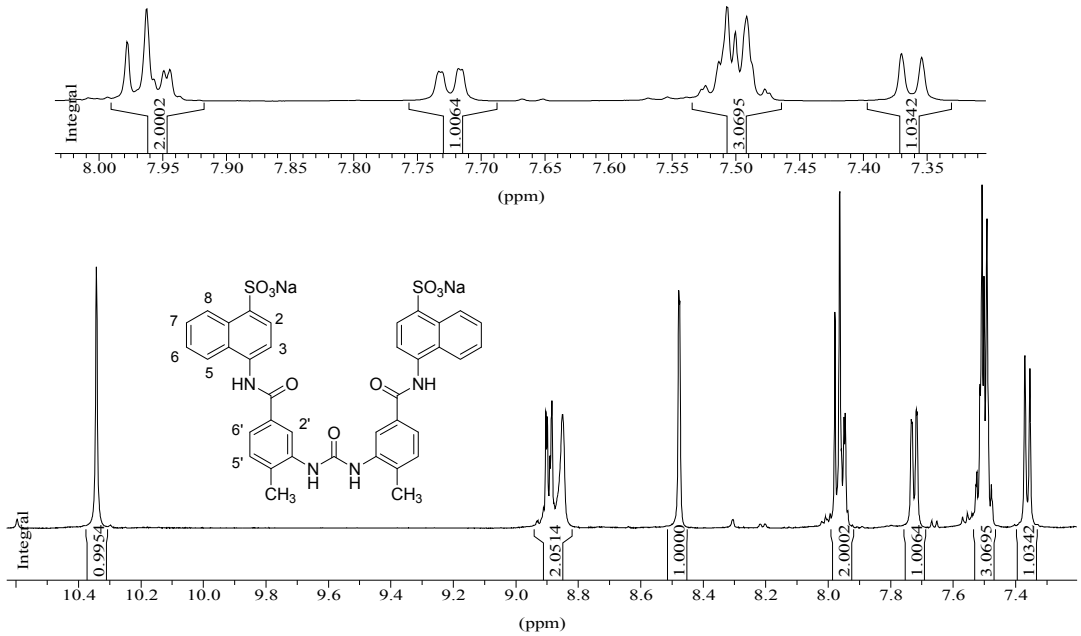

Figure 3.24. 500 MHz ^{1}H NMR spectrum of compound 6c in the range of δ 7.20 – 10.60 ppm.

The signal in the lowest field (10.34 ppm), which disappeared in the D_2O exchange spectrum, represented the amide proton. The signal of the urea proton appeared as a broad D_2O exchangeable singlet at 8.85 ppm. The signal of the methyl protons appeared as a singlet at 2.41 ppm. The six protons of the naphthalene sulfonic acid ring formed an ABXY-A'B'-system. Due to the effect of the sulfonic acid neighbouring group, the signal of the proton H8 was shifted to 8.90 ppm. This proton coupled to H7 with an ortho-coupling (^3J = 8.8 Hz) and to H6 with a meta-coupling (^4J = 2.5 Hz), therefore the splitting pattern appeared as a

doublet of doublet. Due to the effect of the amide neighbouring group, the signal of proton H5 was shifted to 7.95 ppm and appeared as a doublet of doublet with the ortho-coupling to proton H6 (^3J = 6.3 Hz) and the meta-coupling to proton H7 (^4J = 2.2 Hz). The protons H6, H7 and H2 of compound 6c showed signals in a similar region (δ 7.47 – 7.53 ppm with the integration of three protons); therefore the splitting patterns and the coupling constants of these protons could not be properly identified. Nevertheless, the signals of these three protons of the nitro- and amino-precursors (6a and 6b) were slightly shifted and splitting patterns could be partially interpreted.

The signal of the proton H7 (B) of 6b (spectrum not shown) appeared as a multiplet at 7.52 ppm. This proton (H7) was ortho-coupled to H6 (^3J = 6.6 Hz) and ortho-coupled to H8 with a different coupling constant (^3J = 7.6 Hz). Moreover, it was meta-coupled to H5 (^4J = 1.6 Hz). The scheme of coupling pattern for the proton H7 (B) of 6b is shown in Figure 3.25.

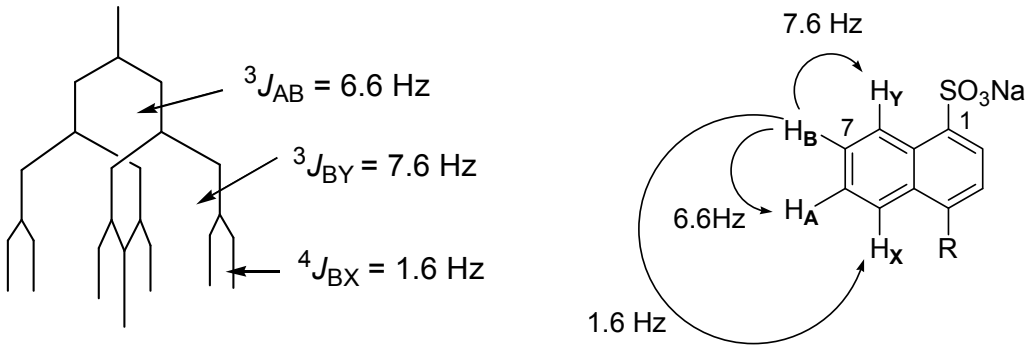

Figure 3.25. Scheme of the splitting pattern of proton H7 of compound 6b (see text).

Theoretically, the signal of H6 should show the same splitting pattern as H7. But because of the interference from the signal of the proton H2, only a doublet of doublet at 7.48 ppm was found in this experiment. The signals of the protons H2 and H3 coupled and showed two doublets with the coupling constant of 7.9 Hz at 7.50 and 7.97 ppm.

The signals of the benzamido residue of 6a-6c were assigned according to the assignment of the benzamido residue of NF340 and precursors (section 3.1.6).

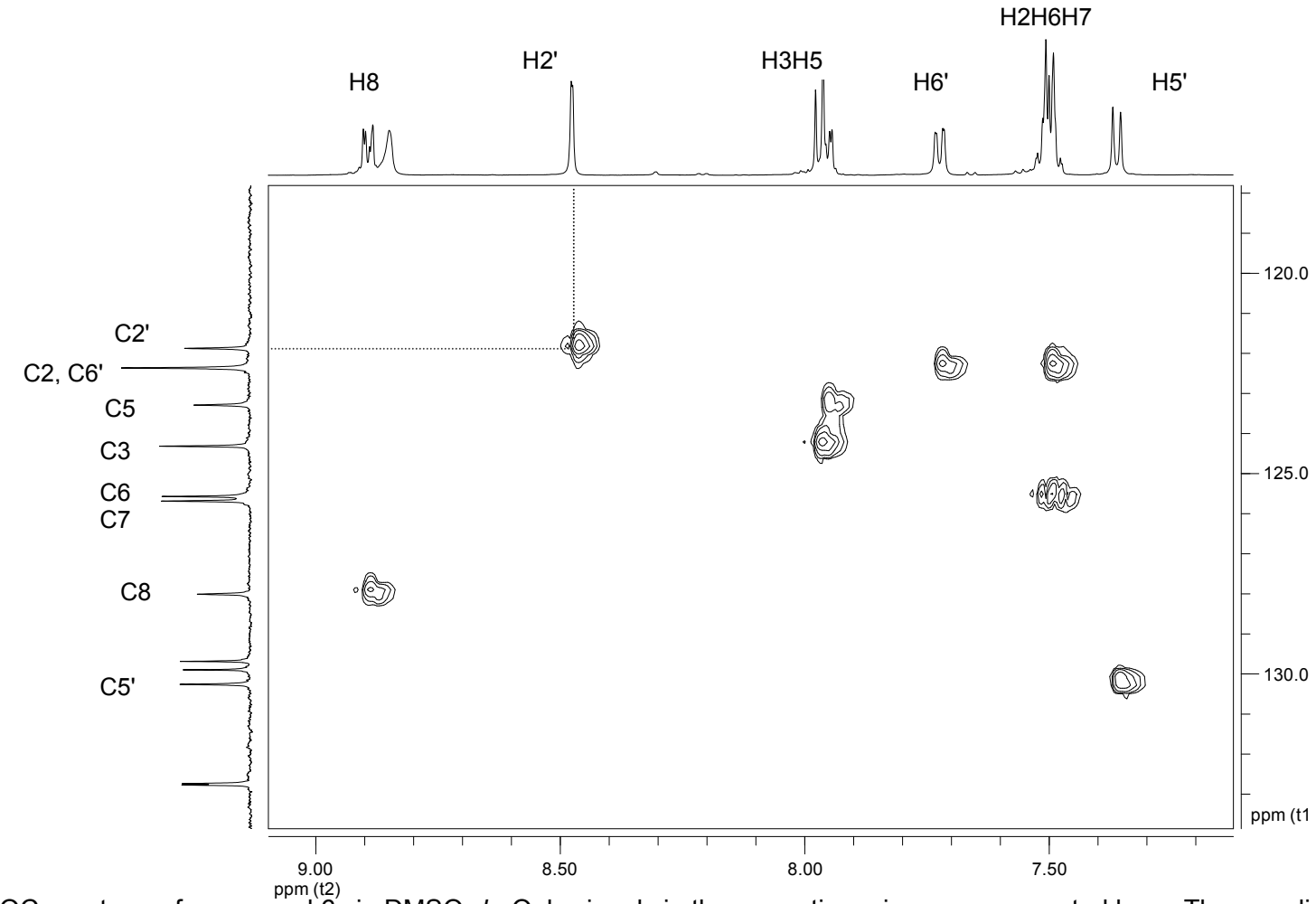

Figure 3.26. HSQC spectrum of compound 6c in DMSO-d_6. Only signals in the aromatic region were presented here. The one-dimensional 500 MHz ^{1}H NMR spectrum is shown at the top edge, while at the left-hand edge the one-dimensional 125 MHz ^{13}C NMR is presented.

In the ^{13}C NMR spectrum (spectrum not shown), the signal of the urea carbonyl was detected at 153.4 ppm, while the signal of the amide carbonyl appeared at 166.7 ppm. The signal at 142.3 ppm was assigned as the sulfonic acid substituted carbon (C1), whereas the signal at 135.2 ppm represented the carbon C4. Due to the effect of the sulfonic acid and amide neighbouring groups, the signals of C4a and C8a appeared in the similar resonance (C4a at 129.7 ppm and C8a at 129.9 ppm). By means of the HSQC method, the signals at 122.4 ppm, 124.3 ppm, 123.3 ppm, 125.6 ppm, 125.7 ppm and 128.0 ppm were interpreted as the signals of the carbons C2, C3, C5, C6, C7 and C8, respectively (see Figure 3.26).

The MALDI mass spectrum in positive mode of compound 6c (Figure 3.27) showed peaks of $[M+H]^+$, $[M+Na]^+$ and $[M-Na+2H]^+$ at m/z 783.1, m/z 805.1 and m/z 761.1, respectively. Moreover, the peaks of the dimer $[2M+Na]^+$ and the trimer $[3M+Na]^+$ were detected in this spectrum at m/z 1587.3 and m/z 2369.4.

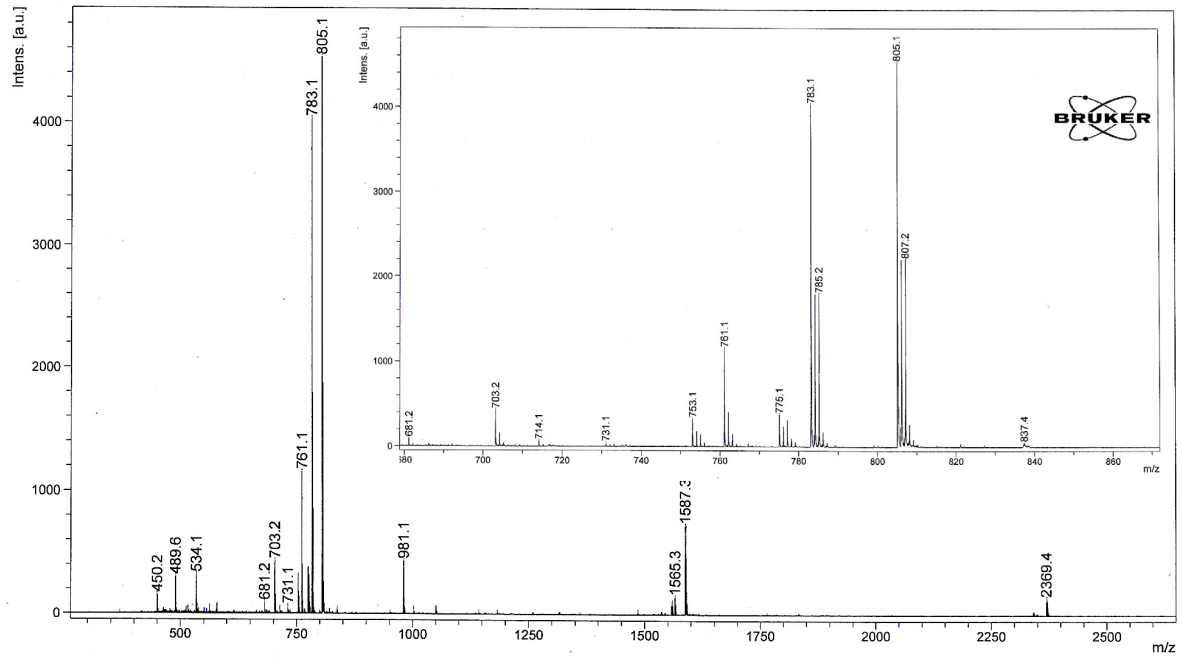

Figure 3.27. MALDI mass spectrum in positive mode of compound 6c.

3.2.3 7,7'-(Carbonylbis(imino-3,1-(4-methylphenylene)carbonylimino)) bis-(naphthalene-1,3,5-trisulfonic acid) hexasodium salt (7c)

Due to the high $P2Y_{11}$ receptor antagonistic activity of NF294 reported by Meis[79] (see Table 4.7 in section 4.4.4), 2-aminonaphthalene sulfonic acid derivatives were interesting to be studied. Thus, the trisulfonic acid substituted urea derivative 7c (structure shown in Figure 3.28), using 7-aminonaphthalene-1,3,5-trisulfonic acid as a precursor, was synthesized. Because of the good water solubility of the substance, all reactions were done in aqueous solution. The acylation and phosgenation were done under a controlled pH of 4.0.

Structure confirmation of compound 7c

The four protons of the trisulfonic acid substituted naphthalene ring of 7a, 7b and 7c showed two doublets and two doublets of doublets. Figure 3.28 shows the ^{1}H NMR spectrum of compound 7c.

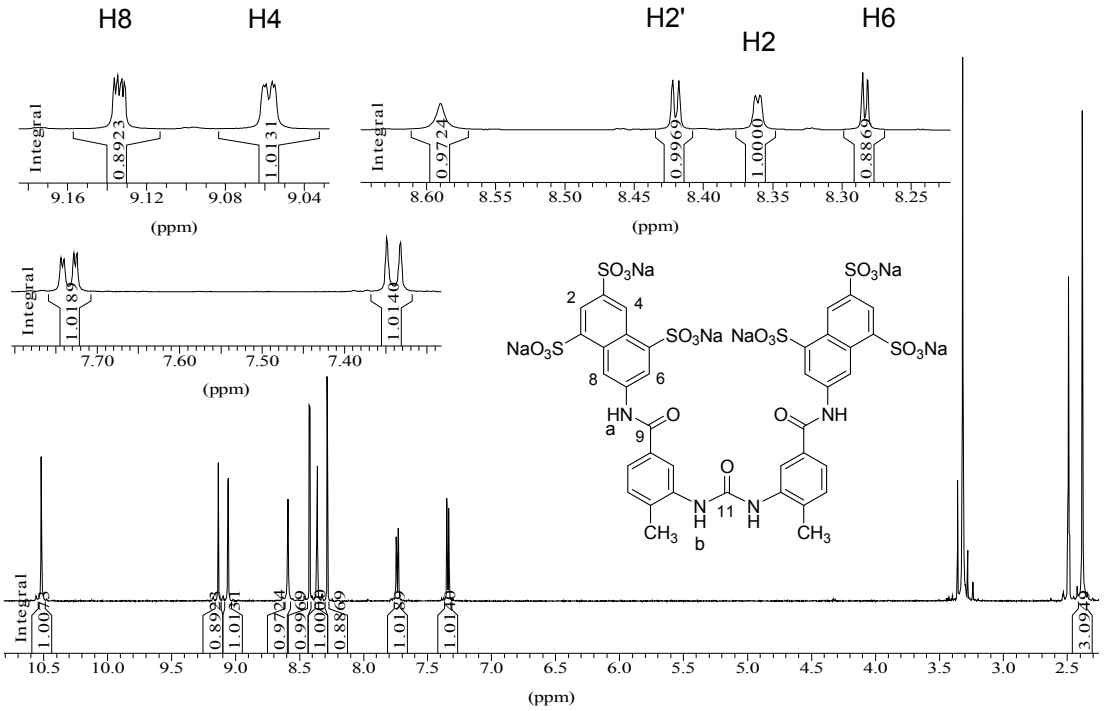

Figure 3.28. 500 MHz ^{1}H NMR spectrum of compound 7c in DMSO-d_6 with assignment of the naphthalene protons.

The protons H2 and H6 of compound 7c showed two doublets at 8.36 ppm (^4J = 1.6 Hz) and 8.28 ppm (^4J = 2.0 Hz), respectively. The signals of the protons H8

appeared as a doublet of doublet at 9.13 ppm with one meta-coupling (^4J = 2.0 Hz) and a zig-zag bond coupling (^5J = 0.6 Hz). With the same coupling pattern as H4, the signal of H4 appears also as a doublet of doublet at 9.06 ppm (^4J = 1.6 Hz and ^5J = 0.6 Hz). The protons of the benzamido residue, NH amide and NH urea showed signals in a similar range as previously shown for 2c (NF340) and precursors.

The measurement of the ESI-mass spectrum in the negative mode showed a $[M\text{-}Na]^-$ signal at m/z 1167.4 which was in accordance to the calculated m/z of 1166.9. The measurement of mass in the positive mode showed the peaks of $[M\text{-}Na+2H]^+$ and $[M\text{-}4Na+5H]^+$ at m/z 1169.6 and m/z 1103.0 (calculated values: m/z 1168.9 and m/z 1102.9, respectively).

3.3 Synthesis of asymmetrical NF340 derivatives

The results from Ullmann et al. showed that only symmetrical urea derivatives owned antagonistic activity at $P2Y_{11}$ receptors, whereas the nitro- and amino-precursors were inactive.(65) The symmetrical structure seems thus important for the antagonistic activity. However, in this work, some nitro- and amino-precursors such as 2a and 2b showed a significant inhibitory effect at $P2Y_{11}$ receptors with 7-fold and 4-fold lower potency than suramin, respectively (for details see section 4.4.3). Although the potency of the nitro- and amino-precursors was low (app. pK_i 5.93 and 5.67), it led to the hypothesis that a symmetrical urea is not required for $P2Y_{11}$ antagonist activity. To confirm this hypothesis and to investigate the structure requirements for high $P2Y_{11}$ receptor activity, asymmetrical ureas of NF340 were planned to synthesize. The *N*-monosubstituted urea of NF340 and various *N,N'*-disubstituted ureas were synthesized (Figure 3.29), using 2b as precursor.

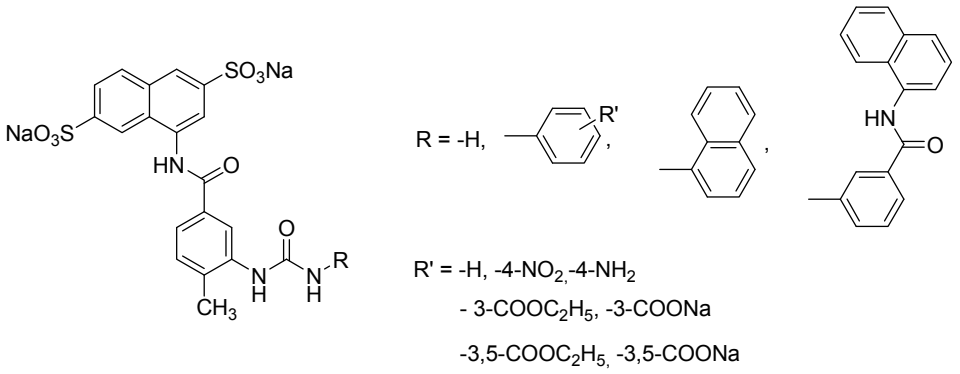

Figure 3.29. Structure formulas of the synthesized asymmetrical urea derivatives.

3.3.1 4-(4-Methyl-3-ureidobenzamido)naphthalene-2,6-disulfonic acid disodium salt

The classical synthesis of *N*-arylureas is the reaction of salts of primary amines and alkali metal cyanates.[80] The reaction is most conveniently carried out by warming the amine in aqueous solution with an equivalent amount of alkali cyanate and an excess of acetic acid or by heating the amine hydrochloride in aqueous solution with urea.[81]

To synthesize 4-(4-methyl-3-ureidobenzamido)naphthalene-2,6-disulfonic acid disodium salt (2d), potassium cyanate was added in small portions to the amine (2b) which was soluble in water and acetic acid (Figure 3.30). The mixture was stirred at room temperature until finish. This method was modified from Müller.[54]

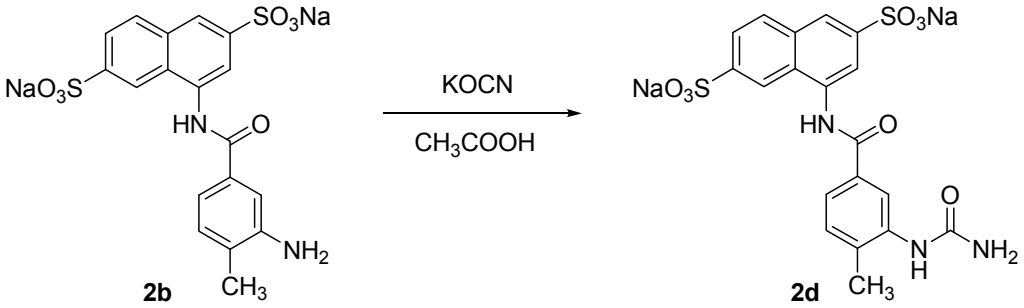

Figure 3.30. Synthesis of compound 2d.

Structure confirmation

The success of the reaction was confirmed by the ^{1}H NMR spectroscopy (Figure 3.31). The singlet at 6.10 ppm which disappeared in the D_2O exchange spectrum and showed the integration of two protons represented the signal of the -NH_2 protons. The signals of the urea proton (NHb) and amide proton (NHa) showed D_2O exchangeable singlets at 7.96 and 10.37 ppm.

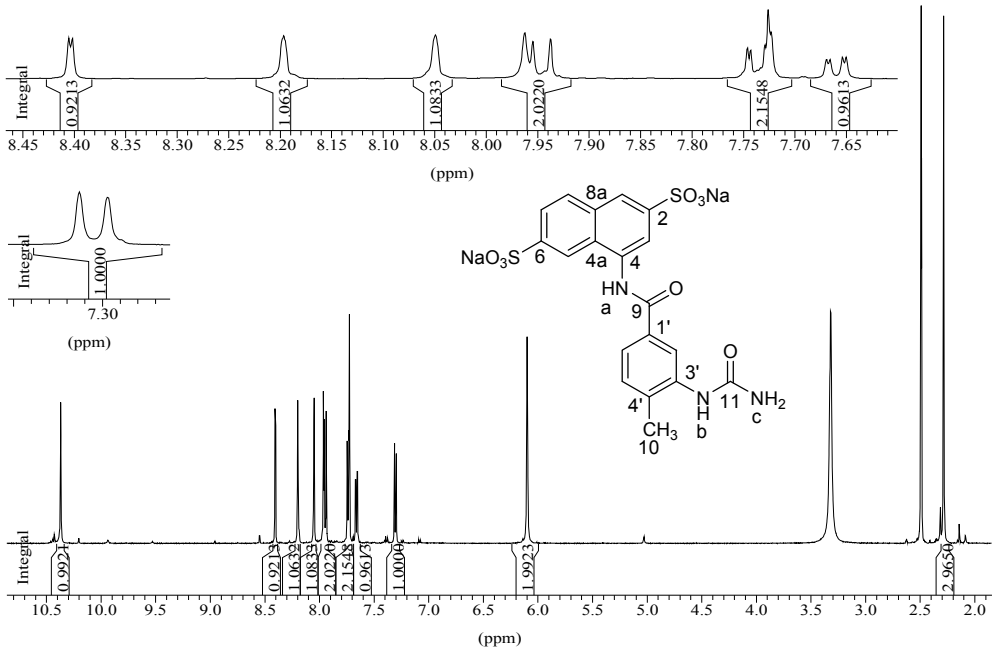

Figure 3.31. 500 MHz ^{1}H NMR spectrum of compound 2d in DMSO-d_6.

The ^{13}C NMR signal of the urea carbon (C11) appeared at 156.4 ppm (spectrum not shown). Other signals of 2d in proton and carbon NMR spectra could be interpreted according to 2c (NF340) (Table 3.12).

Table 3.12. Interpretation of ^{13}C NMR signals of 2d in aromatic rings by comparison with the signals of 2c (NF340).

Position	2d (δ/ppm)	2c (NF340) (δ/ppm)	Position	2d (δ/ppm)	2c (NF340) (δ/ppm)
C1	122.4	122.5	C1'	132.0	132.7
C2	146.0	145.9	C2'	121.5	122.3
C3	122.7	122.8	C3'	138.5	137.8
C4	134.7	134.8	C4'	132.6	133.4
C4a	128.8	128.9	C5'	130.0	130.3
C5	119.9	120.0	C6'	121.6	122.6
C6	145.8	145.6			
C7	124.5	124.6			
C8	128.5	128.5			
C8a	132.9	132.9			

The MALDI mass spectrum confirmed the molecular mass of compound 2d by the peak of $[M+H]^+$ at m/z 523.9 (calculated m/z of 524.0). Another major signal was detected at m/z 545.9 which represented $[M+Na]^+$ and was in agreement with the calculated m/z of 546.0.

3.3.2 4-(4-Methyl-3-(3-phenylureido)benzamido)naphthalene-2,6-disulfonic acid disodium salt and its thiourea analogue

The *N*-monosubstituted urea 2d showed similar potency as the nitro- and amino-precursors 2a and 2b, but it was less potent than the *N,N'*-disubstituted urea 2c (NF340, see Figure 4.7). Variation of the structure of 2d was interesting to be further studied. The asymmetrical urea 2e in which the *N'*-position was substituted with a phenyl group was synthesized. Moreover, its bioisostere thiourea analogue was also synthesized.

The general procedure for the synthesis of *N,N'*-asymmetrical ureas or thioureas involved the nucleophilic addition reaction of primary amines with isocyanates or isothiocyanates, respectively.

The asymmetrical urea 2e was synthesized by the addition of phenyl isocyanate to the amine 2b, using triethylamine as a catalyst (Figure 3.32). The thiourea analogue (2f) was synthesized accordingly by using phenyl isothiocyanate.

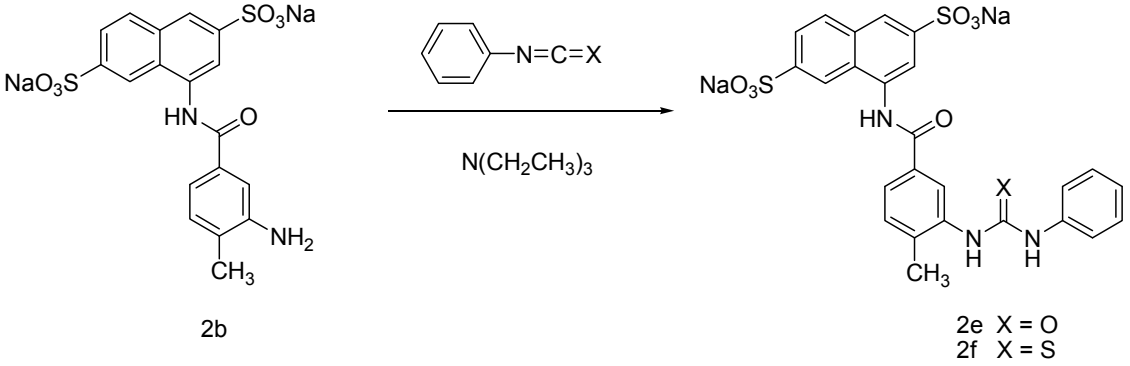

2b

2e X = O
2f X = S

Figure 3.32. Synthesis pathway of 2e and 2f.

N,N'-diphenylurea was found as a side product from the hydrolysis of phenyl isocyanate and subsequent reaction with phenyl isocyanate (Figure 3.33).

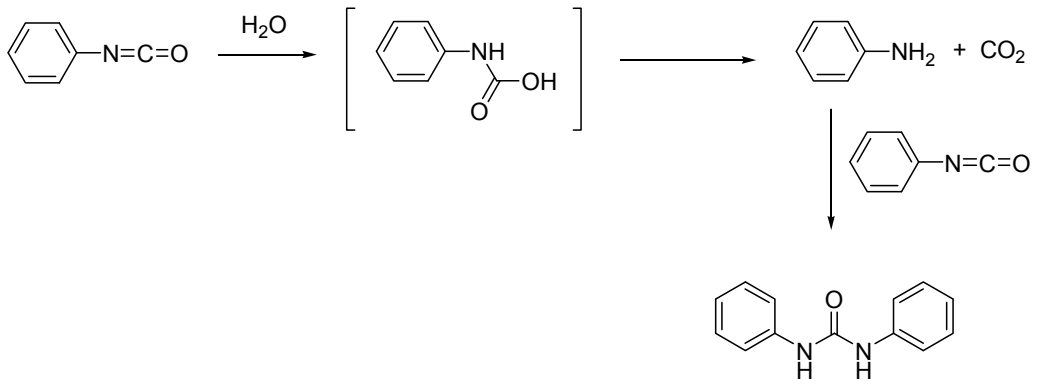

Figure 3.33. Formation of the *N,N′*-diphenylurea side product.

N,N′-Diphenylthiourea was also found as a side product when utilizing phenyl isothiocyanate. However, these side products could easily be separated by extraction with diethyl ether.

Structure confirmation of the urea derivative 2e

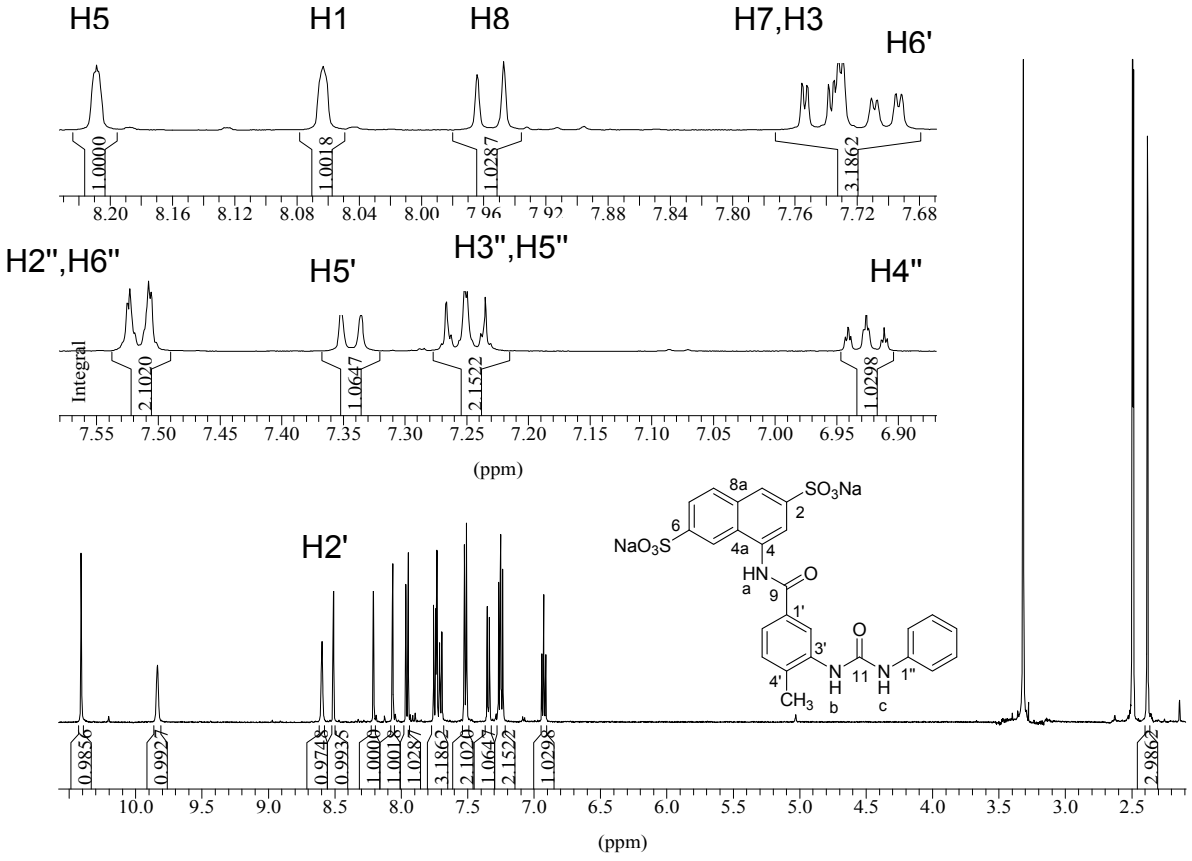

Figure 3.34. 500 MHz ^{1}H NMR spectrum of compound 2e in DMSO-d_6 with assignment.

The structure of compound 2e was confirmed by the ^{1}H NMR spectrum (Figure 3.34). The three D_2O exchangeable singlets at 10.41 ppm, 9.83 ppm and 8.59 ppm were interpreted as the signals of the -NHa, -NHc and –NHb, respectively. The protons of the naphthyl and the benzamido residues were interpreted as described in section 3.1.6.

The five protons of the *N'*-phenyl residue formed an AA'XX'Y-system. The doublet of doublet at 7.52 ppm represented the signals of the chemical equivalent protons H2'' and H6'' (AA') with the ortho-coupling (^{3}J = 8.0 Hz) to H3''H5'' and the meta-coupling (^{4}J = 1.3 Hz) to H4''. The signals of the chemical equivalent protons H3'' and H5'' (XX') appeared as a multiplet at 7.25 ppm. These protons were ortho-coupled to H2''H6'' with ^{3}J = 8.0 Hz and ortho-coupled to H4'' with ^{3}J = 7.3 Hz. Moreover, the signal of H3'' was also coupled to H5'' with ^{4}J = 1.3 Hz. The signal of the proton H4'' (Y) was found as a triplet of triplet at 6.93 ppm with an integration of one proton. This proton was coupled to H3''H5'' with ^{3}J = 7.3 Hz and coupled to H2''H6'' with ^{4}J = 1.3 Hz.

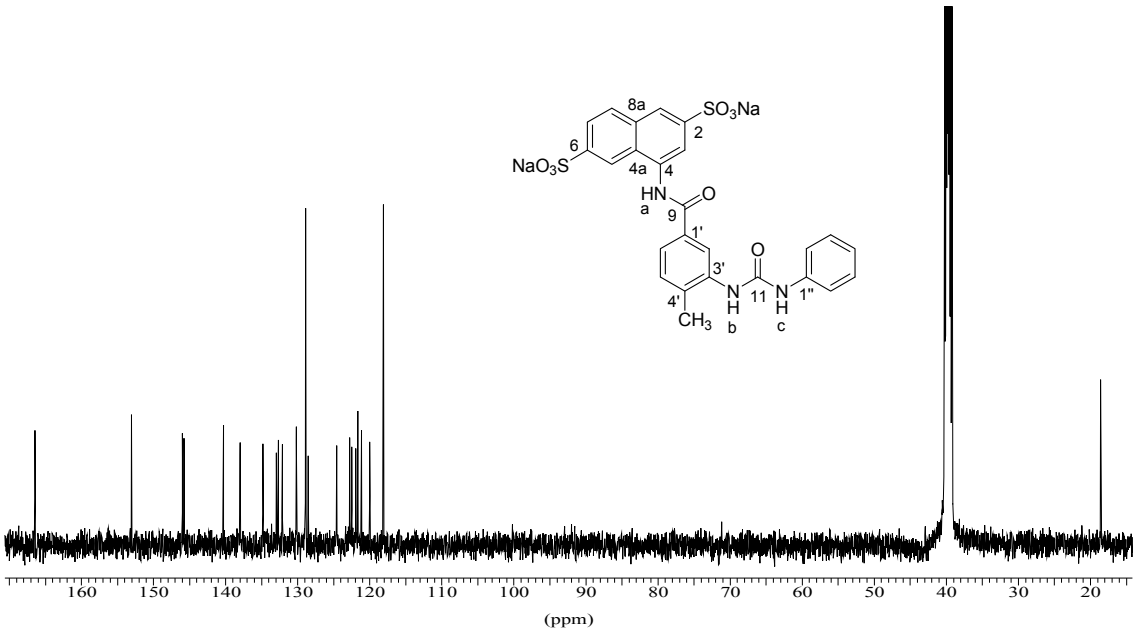

Figure 3.35. 125 MHz ^{13}C NMR spectrum of compound 2e in DMSO-d_6.

The ^{13}C NMR spectrum of compound 2e is presented in Figure 3.35. The two remarkable signals with very high intensity at 128.8 ppm and 118.1 ppm represented the equivalent carbons C3''C5'' and C2''C6'', respectively. Due to the effect of the urea-bridge, the signal of the carbon C1'' appeared at 140.3 ppm. The

signal of C4'' was shifted to 121.9 ppm. The signal of the amide carbon appeared in the lowest field of the spectrum (166.4 ppm), whereas the signal of the urea carbon appeared at 153.0 ppm. The signals of the carbons of the naphthyl and benzamido residues were interpreted as mentioned in section 3.3.1.

The MALDI mass spectrum confirmed the molecular mass of 2e with the signals measured in both positive mode and negative mode as shown in Table 3.13 and Table 3.14.

Table 3.13. MALDI-MS results of 2e in the positive mode in comparison with the calculated m/z.

Ions	Calculated m/z	m/z detected from experiment
$[M+H]^+$,	600.0	600.0
$[M+Na]^+$	622.0	622.0
$[M-Na+2H]^+$	578.1	578.0
$[M-2Na+3H]^+$	556.1	556.1

Table 3.14. MALDI-MS results of 2e in the negative mode in comparison with the calculated m/z.

Ions	Calculated m/z	m/z detected from experiment
$[M-Na]^-$,	576.1	575.9
$[M-2Na+H]^-$	554.1	554.0

Structure confirmation of the thiourea analogue 2f

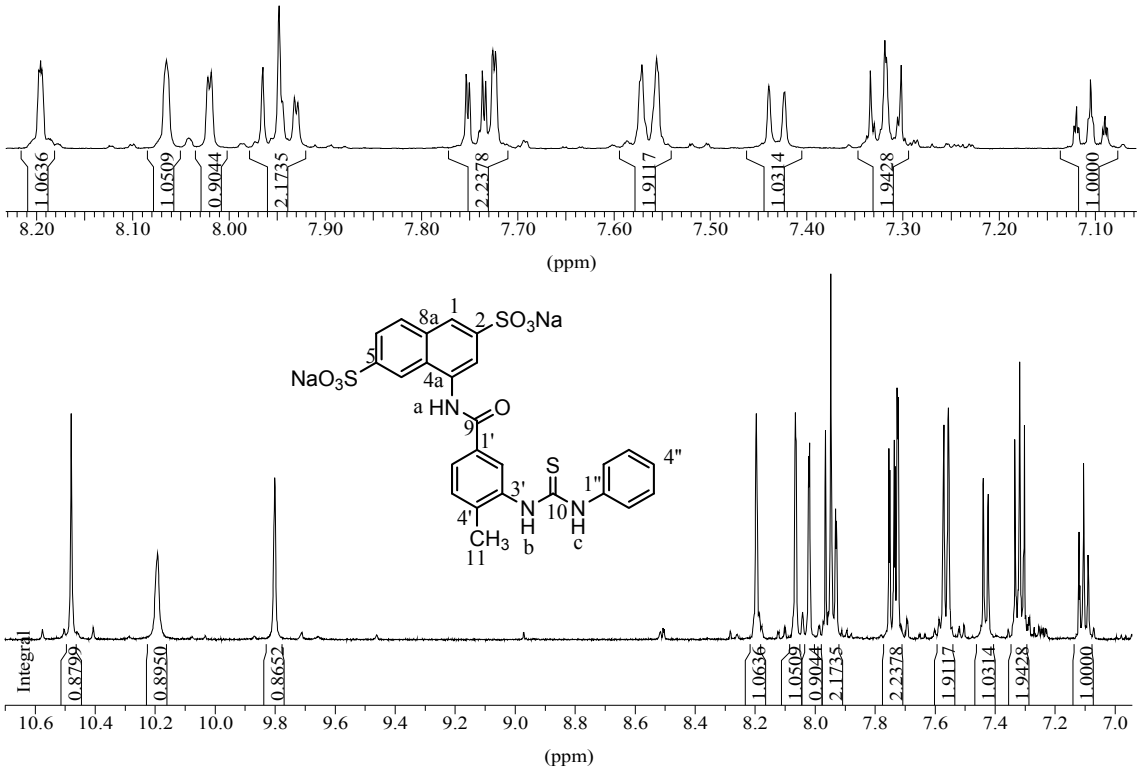

Figure 3.36. 500 MHz ^{1}H NMR spectrum of compound 2f in the range of δ 7.0 - 10.6 ppm.

The NMR spectrum of the thiourea analogue (2f, Figure 3.36) showed the same splitting pattern as the proton NMR spectrum of the urea (2e). Due to the effect of the sulfur atom, the signals of the NH of thiourea 2f were more deshielded to the lower field.[82] Therefore, the signal of NHb and NHc appeared at 9.80 ppm and 10.19 ppm, respectively. The D_2O exchangeable signal of the amide proton (NHa) appeared in the similar position as the signal of the urea derivative (10.48 ppm). The signals of the aromatic protons were assigned equivalent to the signals of the urea analogue (2e).

Figure 3.37 shows the ^{13}C NMR spectrum of 2f.

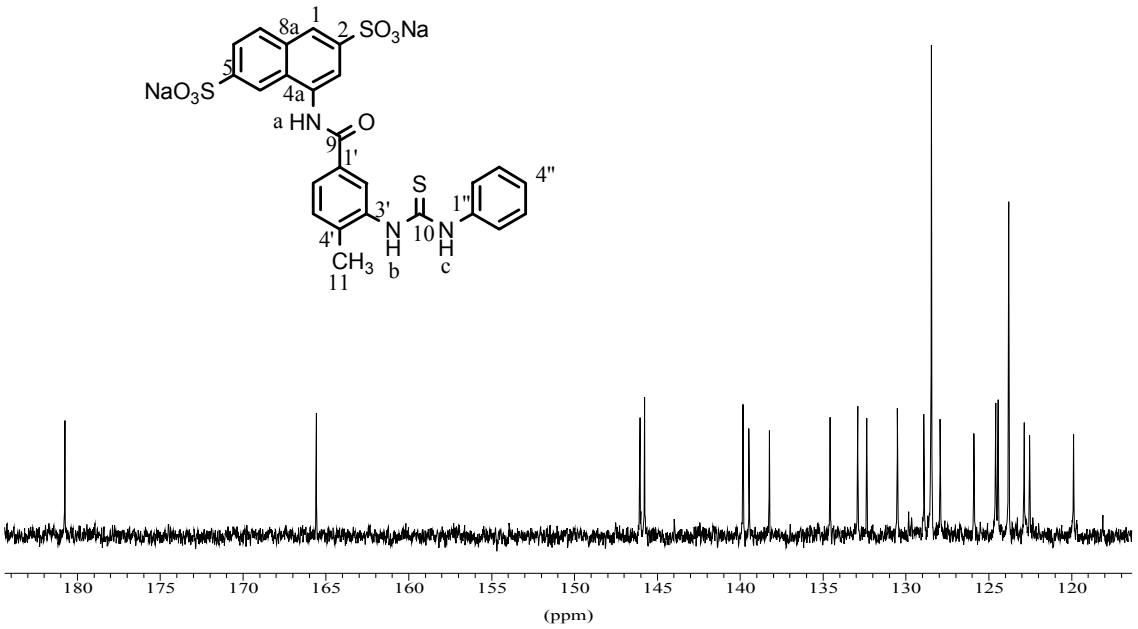

Figure 3.37. 125 MHz ^{13}C NMR spectrum of compound 2f in the range of δ 115 – 185 ppm.

The thiocarbonyl carbon resonated at much lower field than the comparable carbonyl group (δ C=S of 2f: 180.8 ppm; δ C=O of 2e: 153.0 ppm).[83,84] Other signals of 2f were interpreted similarly to the signals of compound 2e.

The MALDI mass spectra confirmed the molecular mass of 2f with peaks found in both positive and negative modes of measurement as shown in Table 3.15 and Table 3.16.

Table 3.15. MALDI-MS results of 2f in the positive mode in comparison with the calculated m/z.

Ions	Calculated m/z	m/z detected from experiment
$[M+Na]^+$	638.0	638.0
$[M+H]^+$	616.0	616.0
$[M-Na+2H]^+$	594.0	594.0
$[M-2Na+3H]^+$	572.1	572.0

Table 3.16. MALDI-MS results of 2f in the negative mode in comparison with the calculated m/z.

Ions	Calculated m/z	m/z detected from experiment
$[M-H]^-$	614.0	613.9
$[M-Na]^-$	592.0	591.9
$[M-2Na+H]^-$	570.0	569.9

3.3.3 4-(4-Methyl-3-(3-(4-nitrophenyl)ureido)benzoylamino) naphthalene- 2,6-disulfonic acid disodium salt and its corresponding amino-derivative

The higher potency of *N'*-phenyl urea 2e than of the *N'*-non-substituted urea (2d) (see detail in section 4.8) led to the further study of other phenyl derivatives. The nitro- and amino- substituted phenyl derivatives (2g and 2h, Figure 3.39) were synthesized based on the found activity of the nitro- and amino-precursors 2a, 2b, 7a and 7c.

Compound 2g was synthesized by addition of 4-nitrophenyl isocyanate to the amine (2b) in the presence of triethylamine (Figure 3.38). Catalytical reduction of 3g obtained the corresponding amine 2h.

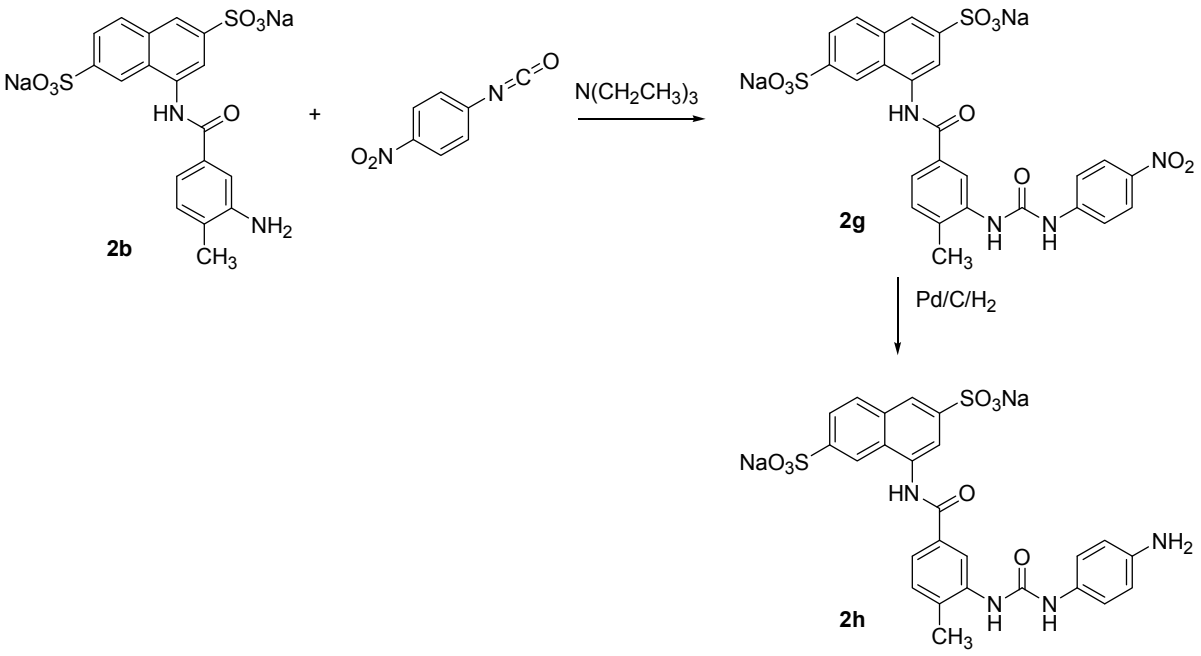

Figure 3.38. Synthesis pathway of nitro- and amino derivatives 2g and 2h.

Structure confirmation of 2g and 2h

Figure 3.39 shows the ^{1}H NMR spectra of 2g and 2h.

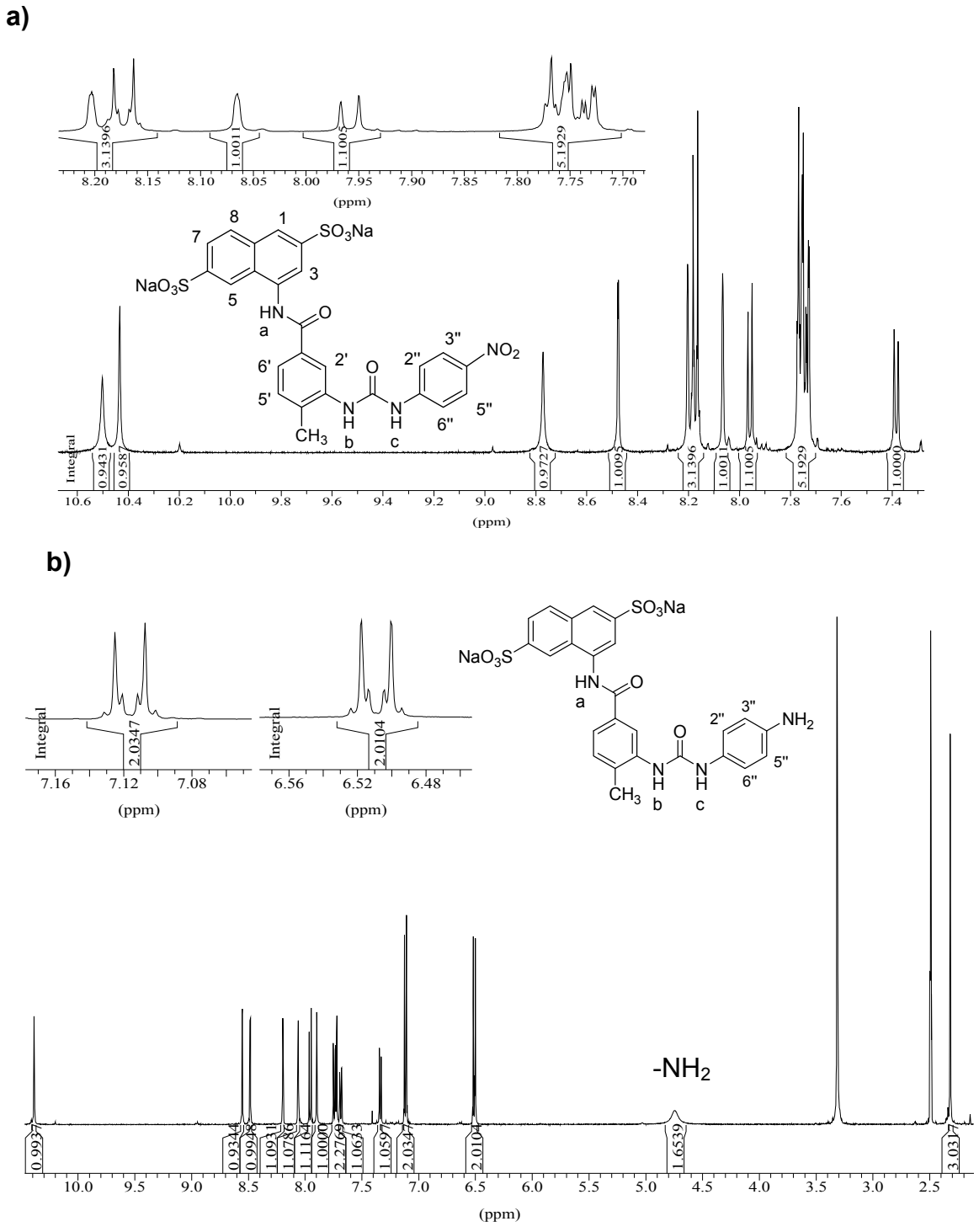

Figure 3.39. 500 MHz ^{1}H NMR spectra of nitro derivative 2g (a) and the corresponding amino derivative 2h (b) in DMSO-d_6 .

The three D_2O exchangeable singlets at 10.50 ppm, 10.43 ppm and 8.77 ppm were interpreted as the signals of protons NHa, NHc and NHb, respectively. The protons of the naphthalene ring and benzamido residue were interpreted as mentioned for 2c (NF340) (section 3.1.6).

The four protons of the *N′*-nitrophenyl residue formed an AA'BB'-system. Because of the –M and –I effects of the nitro group, protons H3'' and H5'' which were chemically equivalent but magnetically non-equivalent were deshielded and formed BB' with a multiplet at 8.17 ppm.[(75)] The proton H3'' was ortho-coupled to H2'' (^3J = 9.5 Hz) and meta-coupled to H5'' (^4J = 2.8 Hz). The proton H2'' and H6'' were less deshielded and formed AA' at 7.75 ppm. Theoretically, signals of AA' should show the same splitting pattern as BB', but in this spectrum the coupling constants of AA' signals could not be calculated because the signals of AA' appeared in the same region as the signals of H3, H7 and H6'.

The four protons of the *N′*-aminophenyl residue also formed an AA'BB'-system. The signal of the aminophenyl residue was however shifted to the upper field in comparison with the spectrum of 2g because of the +M effect of the $–NH_2$ group. The coupling constants of AA' were ^3J = 8.6 Hz and ^4J = 3.1 Hz, whereas of BB' were ^3J = 8.6 Hz and ^4J = 2.2 Hz. Table 3.17 shows the δ of the protons of the *N′*-phenyl substitution.

Table 3.17. ^1H NMR signals of the *N′*-nitro or amino-phenyl ring of 2g and 2h in comparison with calculated δ.

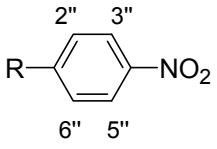

2g

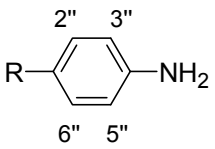

2h

	2g (δ/ppm)		2h (δ/ppm)	
	Found	Calcd	Found	Calcd
H2'', H6''	7.75	7.90	7.11	7.39
H3'', H5''	8.17	8.17	6.51	6.44

The D_2O exchangeable singlet at 4.75 ppm with an integration of two protons in the ^1H NMR spectrum of 2H represented the signal of the $–NH_2$ group.

Figure 3.40 shows the ^{13}C NMR spectrum of compound 2g.

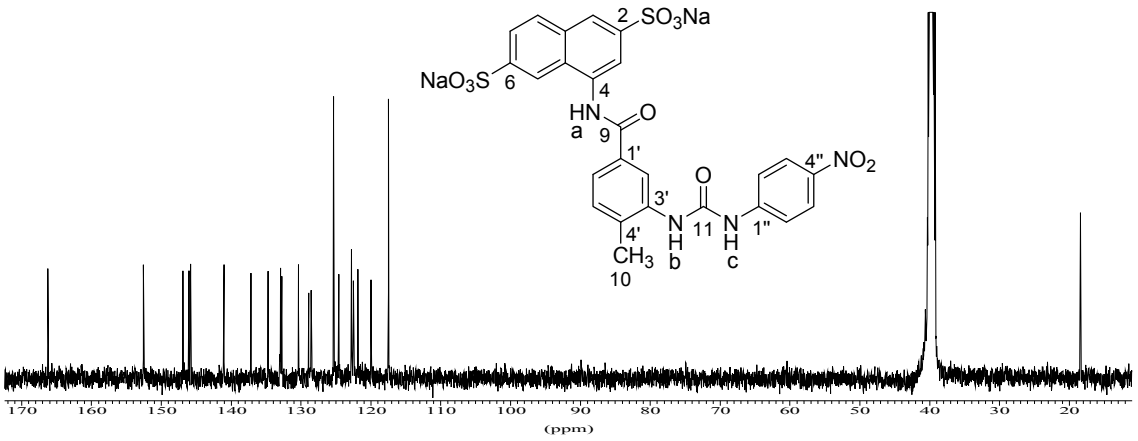

Figure 3.40. 125 MHz ^{13}C NMR spectrum of urea derivative 2g in DMSO-d_6.

The signals of the *N′*-nitro- or aminophenyl ring of 2g or 2h were interpreted by comparison with the calculated signals as shown in Table 3.18.

Table 3.18. ^{13}C NMR signals of the *N′*-nitro or amino-phenyl ring of 2g and 2h in comparison with calculated δ.

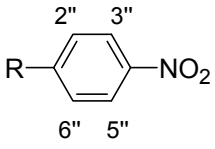

2g

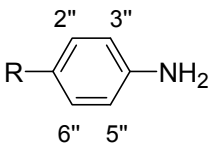

2h

	2g (δ/ppm)		2h (δ/ppm)	
	Calcd	Found	Calcd	Found
C1"	144.3	146.9	128.2	128.5
C2" C6"	121.3	117.4	121.2	120.7
C3" C5"	123.8	125.3	115.3	114.7
C4"	144.0	141.0	142.3	144.1

Other signals were interpreted according to the carbon signals of 2c (NF340) in section 3.1.6.

The molecular mass of 2g was confirmed by ESI-mass spectrometry. The main signal in the ESI-MS was found in the negative mode at m/z 643.3 which could be interpreted as $[M-H]^-$ (calculated m/z 643.0).
The MALDI mass spectrum measured in the positive mode confirmed the molecular mass of compound 2h with the signal of $[M+H]^+$ at m/z 615.0 (calculated m/z of 615.1). Another major peak was found at m/z 637.0 which represented the $[M+Na]^+$. This signal was equal to the calculated m/z of 637.0. The monosodium salt of 2h showed the signal of $[M-Na]^-$ at m/z 591.0 in the negative mode and the signal of $[M-Na+2H]^+$ at m/z 593.0 in the positive mode.

3.3.4 4-(3-(3-(3-(Ethoxycarbonyl)phenyl)ureido)-4-methylbenzamido) naphthalene-2,6-disulfonic acid disodium salt and its hydrolyzed product 2j

Derivatives of 2d containing an ester or a carboxylic acid substitution on the phenyl ring were further synthesized in order to investigate their effects at $P2Y_{11}$ receptors.
Like other asymmetrical urea derivatives, 2i (Figure 3.43) could be obtained from the nucleophilic addition reaction of amine 2b with ethyl 3-isocyanatobenzoate.
There are more than 25 methods for the preparation of isocyanates.[85] One of the most important is the phosgenation of an amine or its salt form. The classical method is passing the bubbling phosgene gas through a solution of amine at an elevated temperature. A variety of methods or reagents were developed to improve the preparation of isocyanates such as using a reaction of amines with phosgene in the presence of a base or using phosgene substitutes such as diphosgene or triphosgene (Figure 3.41).[86,87]

Diphosgene Triphosgene

Figure 3.41. Diphosgene and triphosgene.

Triphosgene (bis(trichloromethyl)carbonate or BTC) is a crystalline solid with a melting point of 80-81 ^{0}C. Therefore, it is easier to handle than phosgene. [88] In the past decade, numerous applications of triphosgene were published to prepare

carbamoyl chlorides, isocyanates, carbamates, symmetrical ureas and asymmetrical ureas.[89-94]

Triphosgene can react with aryl amines or their salts to yield trichloromethyl carbamates which can readily form isocyanates. To synthesize ethyl 3-isocyanatobenzoate, ethyl 3-aminobenzoate was dissolved in dichloroethane and reacted with triphosgene in the presence of triethylamine (Figure 3.42).[95]

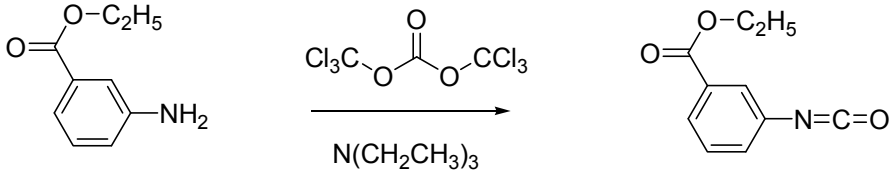

Figure 3.42. Synthesis pathway of ethyl 3-isocyanatobenzoate.

Ethyl 3-isocyanatobenzoate could be characterized by a very strong stretching vibration at 2200 cm^{-1} in its IR spectrum. The ethyl 3-isocyanatobenzoate was further used without purification to react with 2b (Figure 3.43).

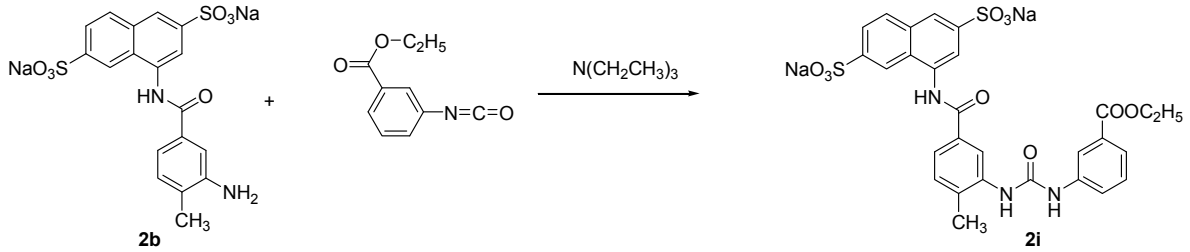

Figure 3.43. Synthesis pathway of 2i.

Structure confirmation

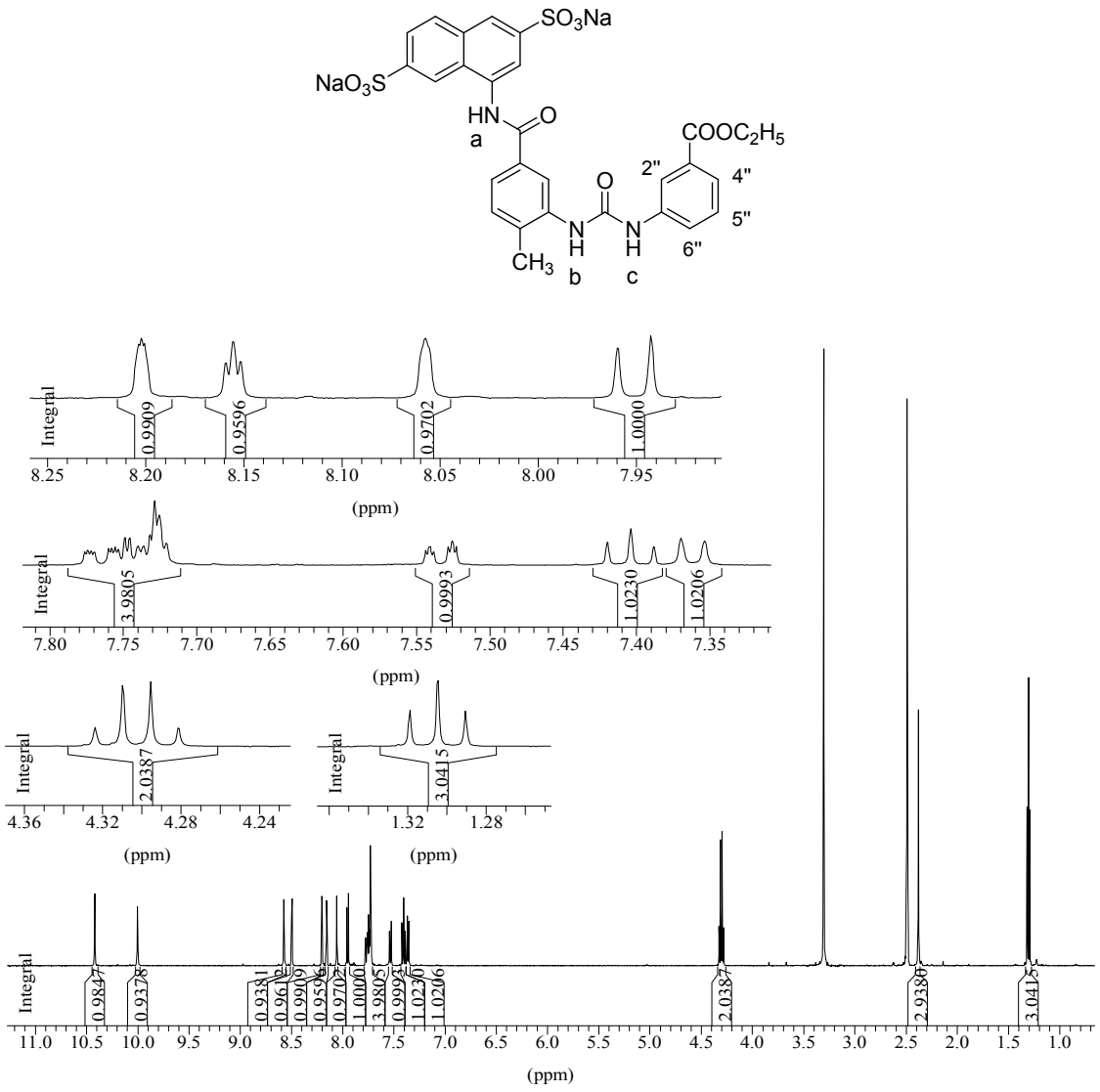

Figure 3.44. 500 MHz ^{1}H NMR spectrum of compound 2i in DMSO-d_6.

The structure of compound 2i was confirmed by the ^{1}H NMR spectrum shown in Figure 3.44. The signals of the ethyl ester were detected at 4.30 ppm and 1.30 ppm and formed an A_3M_2-system. The three chemically and magnetically equivalent methyl protons formed a triplet with the intensity of 1:2:1 and ^{3}J = 7.1 Hz. The methylene group formed a quartet with the intensity of 1:3:3:1 and ^{3}J = 7.1 Hz.

Three singlets at 10.42 ppm, 10.00 ppm and 8.57 ppm, which disappeared in the D_2O exchange spectrum, were interpreted as the signals of protons NHa, NHc and NHb, respectively. The protons of the naphthalene ring and benzamido residue were interpreted as described in section 3.1.6.

The four protons of the 3-(ethoxycarbonyl)phenyl moiety formed an ABCX-system. Because of the –I effect of the ethoxycarbonyl group and the urea neighbouring group, the signal of the proton H2'' (X) was deshielded to 8.15 ppm. It coupled to H4'' (^4J = 1.6 Hz) and H6'' (^4J = 2.2 Hz). The signal of the proton H5'' (B) appeared as a pseudotriplet at 7.40 ppm. H5'' coupled to H4'' with an ortho-coupling (^3J = 7.6 Hz) and coupled to H6'' with an ortho-coupling (^3J = 8.2 Hz). The signal of the proton H6'' was shifted to 7.76 ppm. With one ortho-coupling (^3J = 8.2 Hz) to H5'' and two meta-couplings (^4J = 1.3 Hz to H4'' and ^4J = 2.2 Hz to H2''), the signal of H6'' was found as a ddd. The signal of the proton H4'' appeared as a doublet of triplet at 7.53 ppm (^3J = 7.6 Hz, ^4J = 1.6 Hz and ^4J = 1.3 Hz).

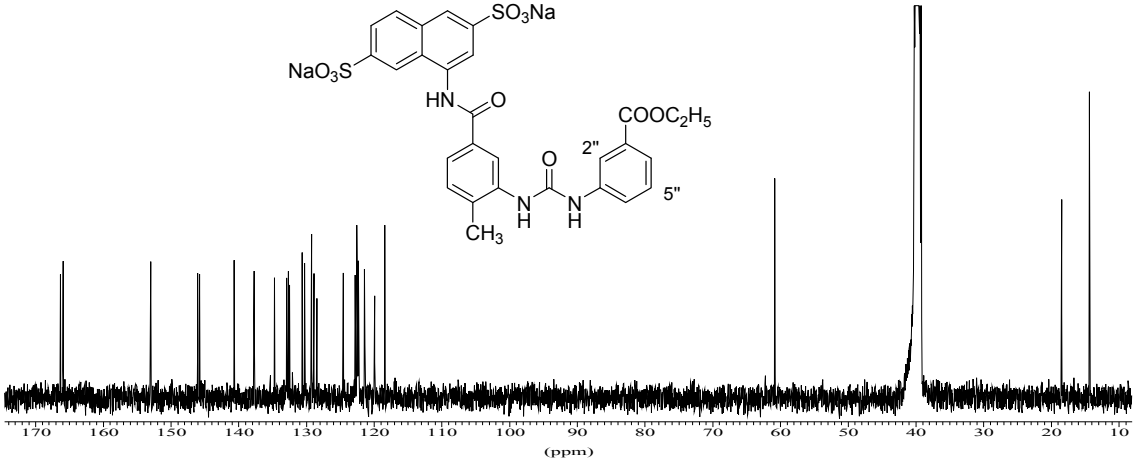

Figure 3.45. 125 MHz ^{13}C NMR spectrum of compound 2i in DMSO-d_6.

The ethoxy moiety of compound 2i was identified from the ^{13}C NMR spectrum (Figure 3.45) with the signal of -O***CH$_2$***CH$_3$ at 60.8 ppm and of -OCH$_2$***CH$_3$*** at 14.3 ppm. The signal of the ester carbonyl appeared at 166.3 ppm, while the signal of amide carbonyl appeared at 165.9 ppm. The signal of urea was found at 152.9 ppm. The signals of *N'*-ethoxycarbonylphenyl ring could be interpreted by comparison with the calculated signals as shown in Table 3.19. Other signals of ^{13}C NMR were interpreted as described in section 3.1.6.

Table 3.19. ^{13}C NMR signals of *N'*- ethoxycarbonylphenyl ring of 2i in comparison with calculated δ (ppm).

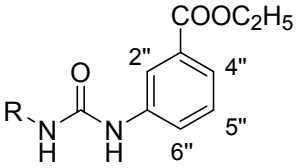

	δ calcd (ppm)	δ found (ppm)
C1''	138.1	140.6
C2''	121.6	118.4
C3''	130.7	130.7
C4''	125.3	122.4
C5''	128.6	129.3
C6''	124.7	122.3

The IR spectrum of 2i showed the stretching vibration of the carbonyl ester at 1713 cm^{-1}.

Measurement of MALDI-MS in the positive mode confirmed the molecular mass of 2i with a signal of $[M+H]^+$ at m/z 672.0 which was comparable to the calculated m/z of 672.1. The peak at m/z 694.0 and m/z 650.0 were interpreted as $[M+Na]^+$ and $[M-Na+2H]^+$, respectively (calculated m/z of 694.1 and 650.1). Measurement in the negative mode showed the signals of $[M-Na]^-$ and $[M-2Na+H]^-$ at m/z 648.1 and m/z 626.0, which were comparable to the calculated m/z of 648.1 and 626.1, respectively.

The ester group of compound 2i was hydrolyzed by 0.1 M NaOH (Figure 3.46).

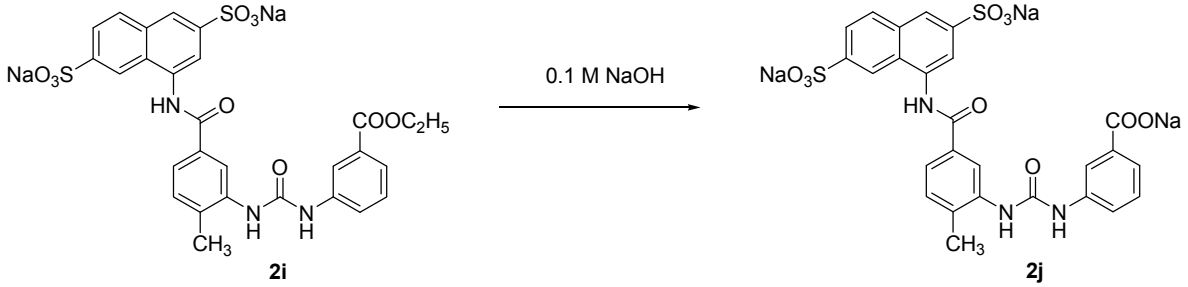

Figure 3.46. Hydrolysis of 2i with 0.1 M NaOH resulting in 2j.

The retention time in the HPLC chromatogram shifted from 4.78 min of the ester (2i) to 2.25 min of the hydrolysed product (2j). The signals at 4.30 ppm and 1.30 ppm in the ^{1}H NMR spectrum disappeared and this indicated the completion of hydrolysis. The molecular mass of compound 2j was confirmed again by measurement of a mass spectrum. The peak at m/z 644.0 in the MALDI-MS could be interpreted as $[M+H]^{+}$. Other major peaks were found at m/z 666.0 which represented $[M+Na]^{+}$ and at m/z 688.0 which could be assigned as $[M+2Na-H]^{+}$. Mass spectrum in the negative mode also confirmed the molecular mass of compound 2j with signals at m/z 641.9 as $[M-H]^{-}$, at m/z 620.0 as $[M-Na]^{-}$ and the peak at m/z 598.0 as $[M-2Na+H]^{-}$.

3.3.5 4-(3-(3-(3,5-Bis(ethoxycarbonyl)phenyl)ureido)-4-methyl benzamido)naphthalene-2,6-disulfonate disodium salt (2k) and its hydrolyzed product 2l

Because of the higher antagonistic activity at $P2Y_{11}$ receptors of the carboxylic acid derivative (2j) compared with the parent phenyl derivative (2e) (see section 4.9), dicarboxylic acid substitution on the phenyl ring was further investigated. The isophthalic acid derivative 2l was synthesized and studied for activity. Diethyl 5-isocyanatoisophthalate was prepared from the reaction of diethyl 5-aminoisophthalate and triphosgene, using dichloromethane as a solvent. The synthesized isocyanate was directly further reacted with amine 2b in the presence of triethylamine to obtain the diethyl ester derivative 2k. Compound 2k could be hydrolyzed with 0.1 M NaOH to the corresponding acid 2l (Figure 3.47).

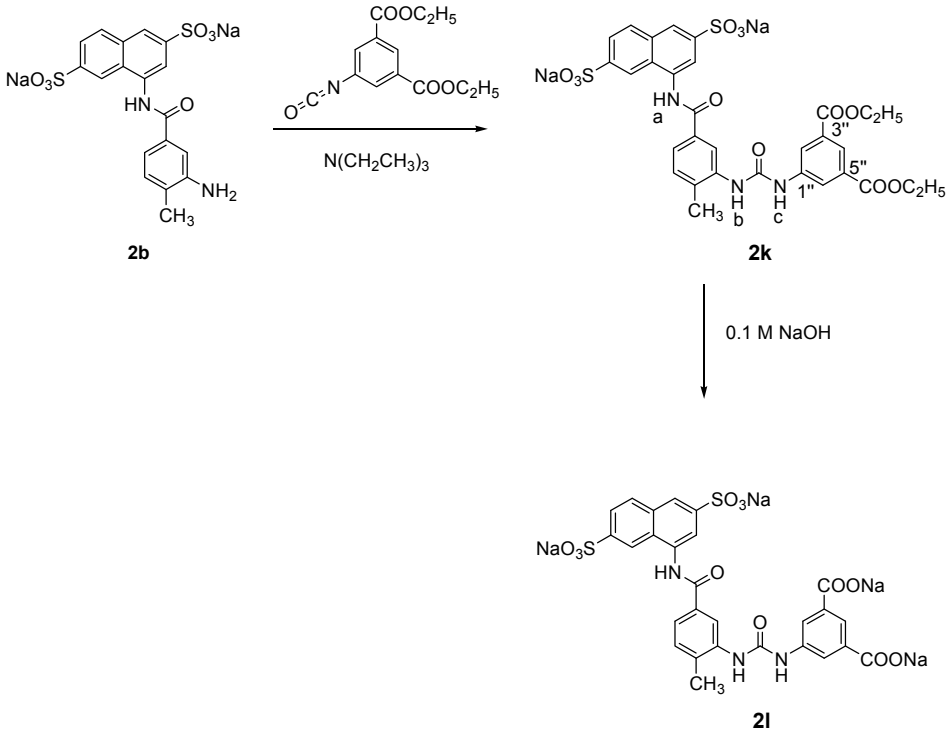

Figure 3.47. Synthesis pathway of compound 2k and 2l.

Structure confirmation

Figure 3.48 shows the ^{1}H NMR spectrum of compound 2k.

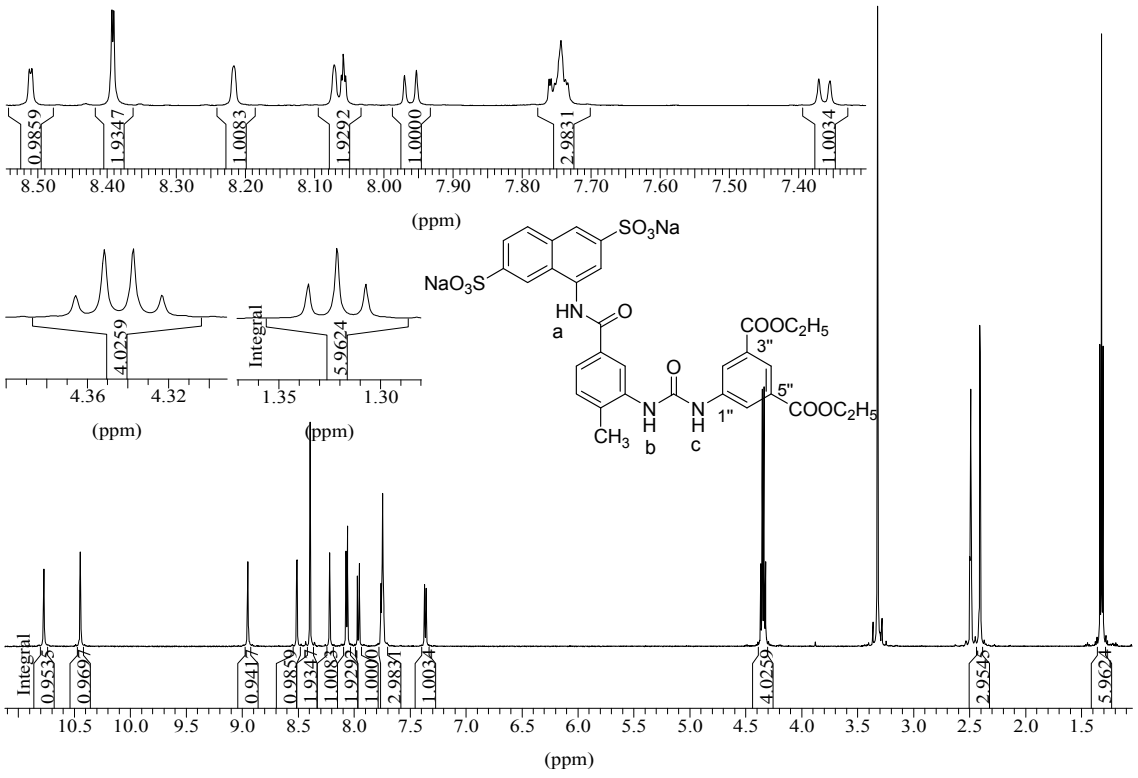

Figure 3.48. 500 MHz ^{1}H NMR spectrum of compound 2k in DMSO-d_6.

The signals of the ethyl group of 2k formed a typical A_3M_2-system at 4.34 ppm and 1.32 ppm. The integrations showed four and six protons, respectively. The three chemically and magnetically equivalent protons of the methyl groups formed a triplet with ^3J = 7.1 Hz, whereas the methylene protons formed a quartet with the same coupling constant (^3J = 7.1 Hz).

Three singlets at 10.77 ppm, 10.45 ppm and 8.94 ppm, which disappeared by the addition of D_2O, could be interpreted as the protons of NHa, NHc and NHb, respectively. The protons of the naphthalene ring and benzamido residue were interpreted as mentioned in section 3.1.6.

The signals of the 3,5-diethoxycarbonylphenyl residue formed an AB_2-system. The signal at 8.39 ppm with the integration of two protons represented the H2'' and H6'' (B_2). Both protons coupled to the proton H4'', therefore the splitting pattern appeared as a doublet with ^4J = 1.3 Hz. The signal of H4'' (A) appeared as a triplet at 8.05 ppm with the meta-coupling to H2''and H6'' (^4J = 1.3 Hz).

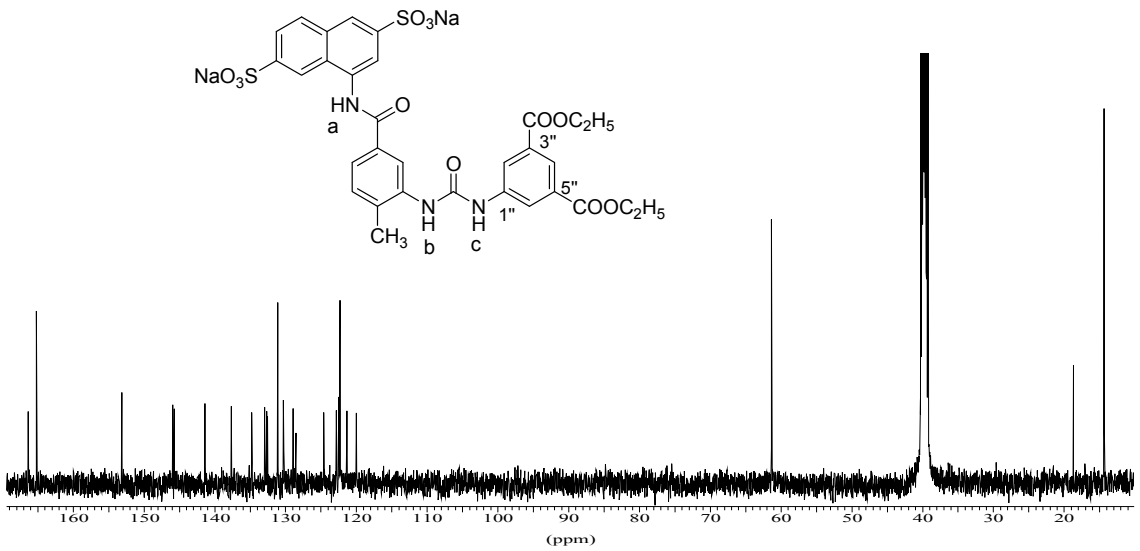

Figure 3.49. 125 MHz ^{13}C NMR spectrum of compound 2k in DMSO-d_6.

The signal of the amide carbonyl carbon appeared at 166.3 ppm in the ^{13}C NMR spectrum (Figure 3.49). The signal of the carbonyl carbon nuclei of the esters was shifted slightly to the higher field (165.2 ppm). The signal at 153.1 ppm represented the carbonyl urea, whereas the signal of C1'' appeared at 141.4 ppm. Due to the effect of the carbonyl neighbouring group, the signal of C4'' appeared at 122.5 ppm, whereas the carbons C2'' and C6'' appeared as an intensive signal at 122.3 ppm. The signals of C3'' and C5'' were deshielded to 131.1 ppm. Other signals of the

naphthalene ring and benzamido residue were interpreted as mentioned in section 3.1.6.

In the IR spectrum, the strong signal at 1712 cm^{-1} represented the C=O stretching vibration of the ester functional groups and the signal at 1672 cm^{-1} represented the C=O stretching vibration of the amide functional group.

The ESI-MS performed in the negative mode showed a signal at m/z 720.1 which could be interpreted as $[M-Na]^-$ which was equal to the calculated m/z of 720.1.

After hydrolysis of 2k with 0.1 M NaOH, the retention time of the hydrolyzed product 2l was shifted to 1.14 min in the HPLC spectrum, while the retention time of the more lipophilic ester (2k) was detected at 6.48 min.

The structure of 2l was confirmed by NMR spectra (^1H and ^{13}C). In the ^1H NMR spectrum of 2l, two signals at 4.34 ppm and 1.32 ppm disappeared, whereas in the ^{13}C NMR spectrum, the signals at 61.3 ppm and 14.3 ppm disappeared.

The molecular mass of the hydrolyzed product 2l was confirmed by ESI-MS as shown in Table 3.20 and Table 3.21.

Table 3.20. ESI-MS signals in the positive mode of the dicarboxylic acid derivative 2l in comparison with the calculated m/z.

Ions	Calculated m/z	m/z detected from experiment
$[M+Na]^+$	754.0	754.2
$[M-2Na+3H]^+$	688.0	688.4

Table 3.21. ESI-MS signals in the negative mode of the dicarboxylic acid derivative 2l in comparison with the calculated m/z.

Ions	Calculated m/z	m/z detected from experiment
$[M-H]^-$	730.0	730.2
$[M-Na]^-$	708.0	708.2
$[M-2Na+H]^-$	686.0	686.2
$[M-3Na+2H]^-$	664.0	664.2
$[M-4Na+3H]^-$	642.0	642.2
$[M-3Na+H]^{2-}$	331.5	331.6

3.3.6 4-(4-Methyl-3-(3-naphthalen-1-ylureido)benzamido)naphthalene-2,6-disulfonic acid disodium salt (2m)

The *N′*-naphthalene derivative 2m was synthesized to study the effect of a large aromatic group upon $P2Y_{11}$ receptor activity. 1-Naphthalene isocyanate was synthesized from the reaction of 1-aminonaphthalene and 20 % phosgene solution.[96] The IR spectrum showed the characteristic peak of isocyanate at 2300 cm^{-1}. 1-Naphthalene isocyanate was further reacted with amine 2b to obtain compound 2m.

Structure confirmation

Figure 3.50 shows the ^{1}H NMR spectrum of compound 2m.

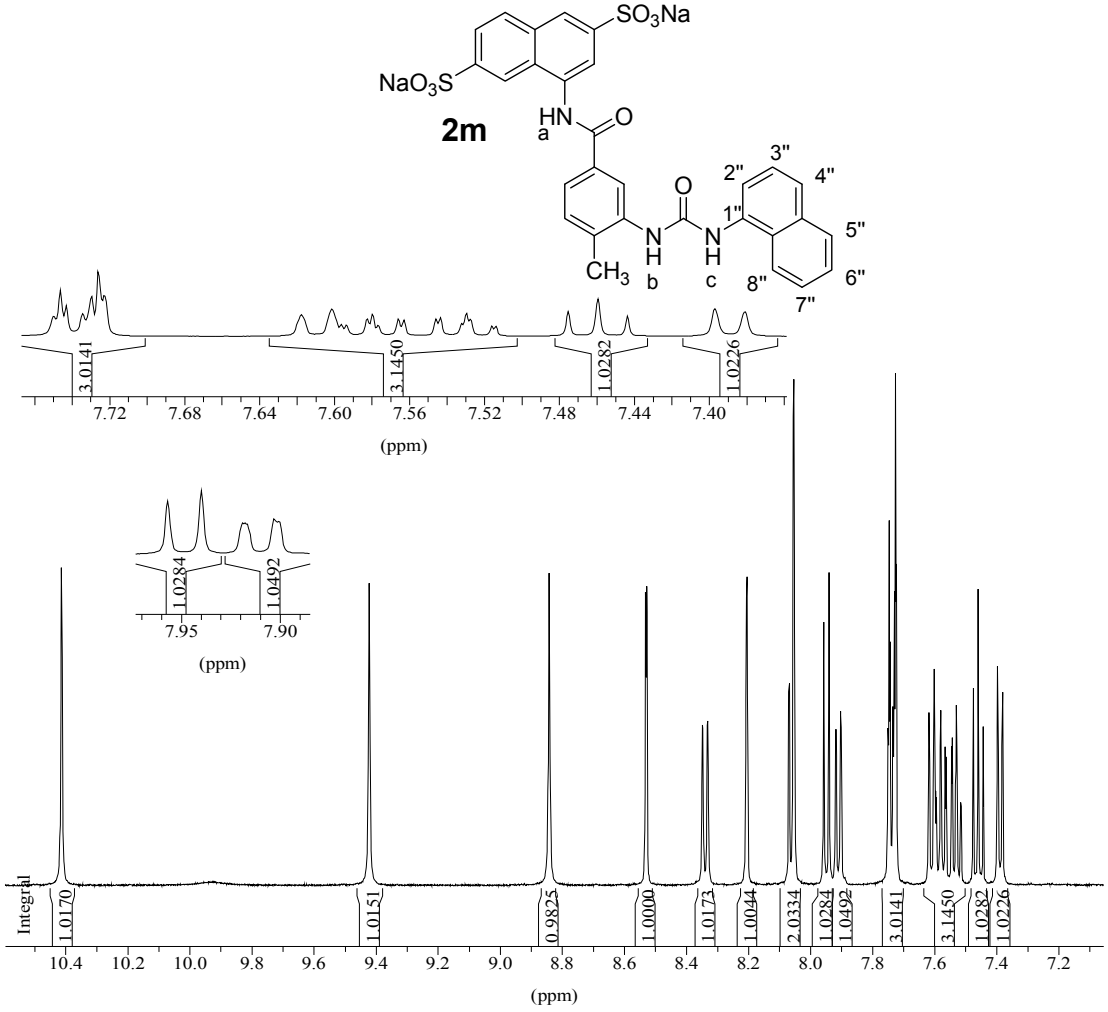

Figure 3.50. 500 MHz ^{1}H NMR spectrum (DMSO-d_6) of compound 2m in the range of δ 7.2 –10.6 ppm.

The signal of the amide NHa was found as a D_2O exchangeable singlet at 10.41 ppm. The signals of the urea protons (NHc and NHb) appeared at 9.42 ppm and 8.84 ppm, respectively.

The seven protons of the *N'*-naphthyl moiety formed a multiple-spin system. The signal of the proton H3'' was coupled to proton H2'' and H4'', therefore this signal appeared as a triplet (^3J = 8.1 Hz) at 7.46 ppm. Theoretically, the signal of H2'' should appear as a doublet of doublet, but with the poor resolution in this experiment, the coupling of H2'' and H4'' could not be detected. The signal of H2'' was coupled to H3'' and appeared as a doublet (^3J = 8.1 Hz) at 7.61 ppm. The signal of H4'' was coupled to both H3'' (^3J = 8.1 Hz) and H2'' (^4J = 1.3 Hz), hence the splitting pattern appeared as a doublet of doublet at 7.91 ppm. The signal of the proton H8'' was found as a doublet at 8.34 (^3J = 8.0 Hz), whereas the coupling constant between H8'' and H6'' could not be measured because of the poor resolution of the spectrum. Comparing with the coupling pattern of H8'', the signal of H5'' appeared as a doublet of doublet from the coupling with H6'' (^3J = 8.0 Hz) and H7'' (^4J = 1.1 Hz) at 8.07 ppm. The signals of H7'' and H6'' showed a similar coupling pattern as two multiplets at 7.58 ppm and 7.53 ppm, respectively. The coupling patterns of protons H7'' and H6'' could be explained as mentioned in section 3.2.2 (the coupling pattern of proton H7 of compound 6b, see Figure 3.25).

The signals of the naphthalene sulfonic acid and benzamido residues were interpreted as described in section 3.1.6.

Figure 3.51 shows the ^{13}C NMR spectrum of 2m.

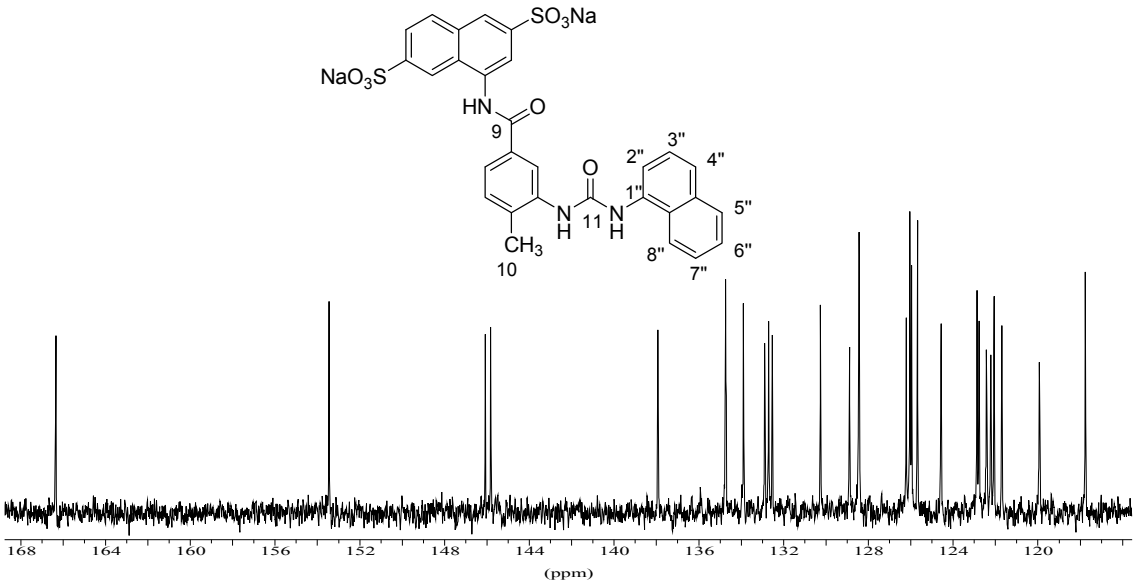

Figure 3.51. 125 MHz ^{13}C NMR spectrum (DMSO-d_6) of compound 2m in the range of δ 116 – 168 ppm.

The signal of the urea carbonyl appeared at 153.4 ppm, whereas the signal of the amide carbonyl was found at the lowest field of this spectrum (166.3 ppm). The signal of the methyl group appeared at 18.5 ppm.

The signals of the *N'*-naphthalene protons were interpreted were interpreted by comparison with the increment calculation and could be explained as follows: Due to the urea-bridge, the signal of C1" appeared at 134.7 ppm. As the neighbouring carbons, the signals of C2" and C8" were shifted to 117.7 ppm and 122.9 ppm, respectively. The signal of C4" appeared at 122.2 ppm. The signals of C5", C6", C7" and C3" were found at 128.4 ppm, 126.0 ppm, 125.9 ppm and 126.2 ppm, respectively. The signal of C8a" appeared at 125.7 ppm, whereas the carbon C4a" was shifted to 133.9 ppm.

The MALDI-MS in the positive mode confirmed the molecular mass of the compound 2m with a peak $[M+H]^+$ at m/z 650.1 (calculated m/z of 650.1). The other major peak shown at m/z 628.1 represented $[M-Na+2H]^+$, which is equal to calculated m/z of 628.1. The measurement of MALDI-MS in the negative mode showed the peak of $[M-Na]^-$ at m/z 626.0 and the peak of $[M-2Na+H]^-$ at m/z 604.0.

3.3.7 4-(4-Methyl-3-(3-(3-(naphthalen-1-ylcarbamoyl)phenyl) ureido) benzamido)naphthalene-2,6-disulfonic acid disodium salt (2n)

To study whether sulfonic acid substitutions on both naphthalene rings are necessary for the $P2Y_{11}$ receptor activity, compound 2n was synthesized and studied for its activity. 2n was synthesized from reaction of 3-isocyanato-*N*-naphthalen-1-yl-benzamide and amine 2b. Therefore, *N*-naphthalen-1-yl-3-nitro-benzamide was first synthesized by acylation of 1-aminonaphthalene with 3-nitrobenzoyl chloride. Because of the lipophilic property of the precursor, this acylation was done in toluene. Hydrogenation was performed in methanol, using 10 % Pd/C as catalyst. The synthesis method of *N*-naphthalen-1-yl-3-nitro-benzamide and 3-amino-*N*-naphthalen-1-yl-benzamide was performed according to Wehner and structure confirmation was in accordance with Wehner.[55] Therefore, synthetic details and analytical data are not presented here.

3-Isocyanato-*N*-naphthalen-1-yl-benzamide was synthesized from the reaction of amine with triphosgene in the presence of triethylamine (Figure 3.52). The isocyanate product was confirmed by the IR spectrum with the characteristic band of the N=C=O stretching vibration at 2280 cm^{-1}.

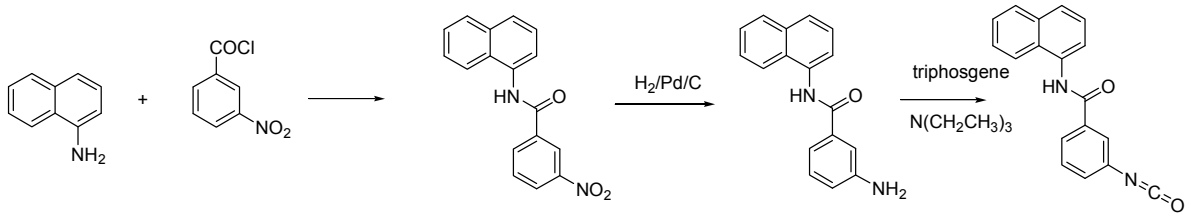

Figure 3.52. Synthesis pathway of 3-isocyanato-*N*-naphthalen-1-yl-benzamide.

Structure confirmation

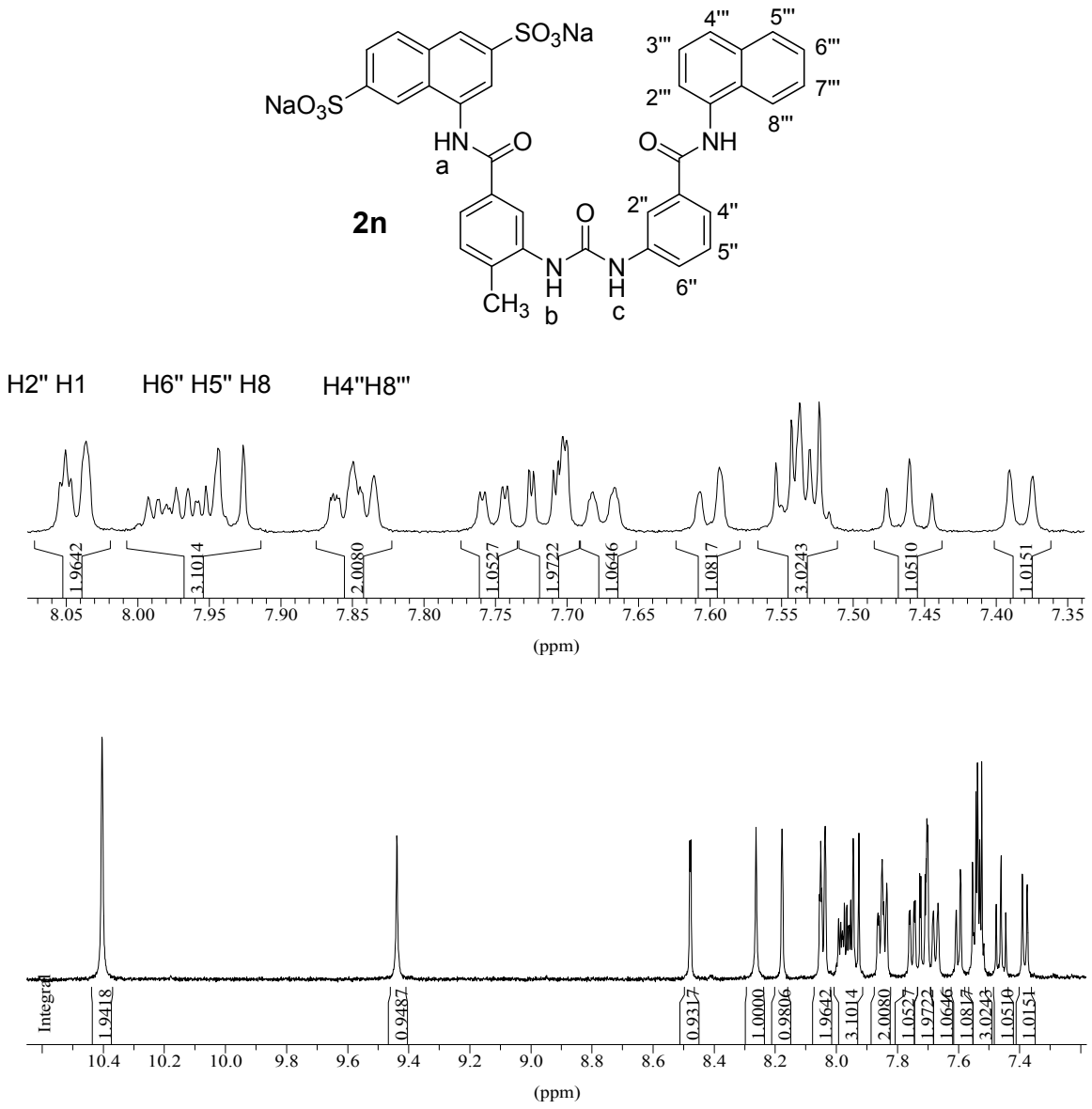

Figure 3.53. 500 MHz ^{1}H NMR spectrum of compound 2n in the range of δ 7.20 – 10.60 ppm.

Figure 3.53 shows the ^{1}H NMR spectrum of compound 2n in the range of δ 7.20 – 10.60 ppm. The signals of the amide protons (NHa and NHd) appeared at the same resonance (10.40 ppm), therefore, a D_2O exchangeable singlet with an integration of two protons was found. The signals of the urea protons (NHc and NHb) appeared at 9.44 and 8.26 ppm, respectively. The singlet at 2.36 ppm represented the signal of the methyl group (signal not shown).

The seven protons of the naphthalene ring formed a multiple-spin system similar to the naphthalene ring of compound 2m (see section 3.3.6).

The four protons of the *N'*-benzamido moiety formed an ABCX-system. Due to the effect of the amide and urea-bridge, the signal of the proton H2'' (X) was deshielded and appeared as a triplet at 8.05 ppm with ^4J = 1.9 Hz. The signals of proton H4'' (A) appeared as a multiplet at 7.85 ppm. Because this signal appeared in nearly the same region as the signal of H8''', the coupling pattern could only partially be identified. This proton (H4'') was ortho-coupled to H5'' (^3J = 8.2 Hz), meta-coupled to H2'' (^4J = 1.6 Hz) and also meta-coupled to H6'' (^4J = 1.6 Hz). A multiplet at 7.92 – 8.00 ppm with the integration of three protons was assigned as the signal of the protons H5'', H6'' and H8.

The molecular mass of 2n was confirmed by MALDI-MS measuring in the positive and negative modes (see Table 3.22 and 3.23).

Table 3.22. MALDI-MS signals of compound 2n in the positive mode in comparison with the calculated m/z.

Ions	Calculated m/z	m/z detected from experiment
$[M+H]^+$	769.1	769.1
$[M+Na]^+$	791.1	791.1
$[M-Na+2H]^+$	747.1	747.1
$[M-2Na+3H]^+$	725.1	725.2

Table 3.23 MALDI-MS signals of compound 2n in the negative mode in comparison with the calculated m/z.

Ions	Calculated m/z	m/z detected from experiment
$[M-Na]^-$	745.1	745.1
$[M-2Na+H]^-$	723.1	723.1

3.4 Benzene sulfonic acid derivatives of 2c (NF340)

To investigate if the naphthalene ring is required for $P2Y_{11}$ activity, symmetrical benzene sulfonic acid urea derivatives were synthesized and studied for their activity at $P2Y_{11}$ receptors. Six benzene sulfonic acid urea analogues of NF340 (Figure 3.54) were synthesized according to the same methods as for 2c (NF340) analogues, using various aminobenzene sulfonic acids and 4-methyl-3-nitrobenzoyl chloride as precursors.

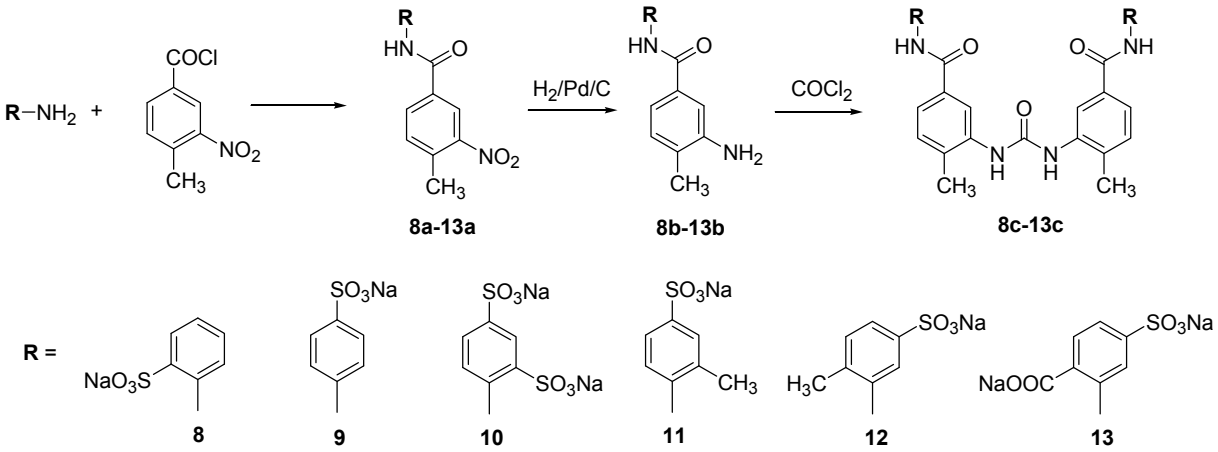

Figure 3.54. Synthetic variations and structural formulas of benzene sulfonic acid urea analogues of 2c (NF340).

NF250 and NF251 (Figure 3.55) were synthesized by the group of Prof. Nickel. [73] However, the nitro- and amino-precursors were not available. Therefore, the nitro- and amino-precursors of these two compounds were resynthesized, but the analytical data were not presented here.

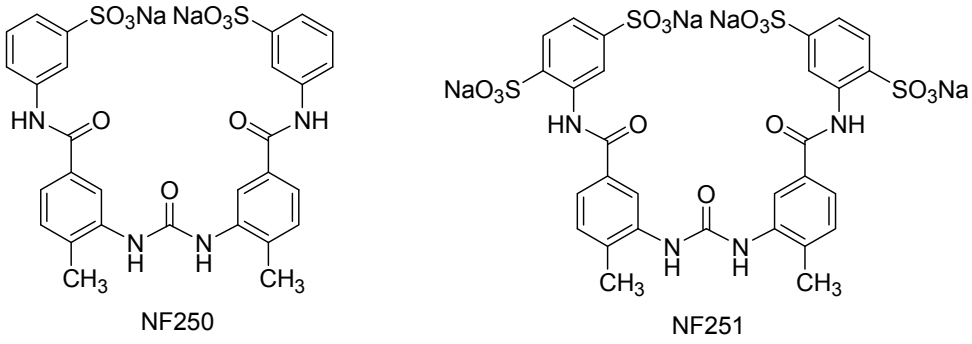

Figure 3.55. Structural formulas of NF250 and NF251.

The synthetic details and analytical data of compounds 8a – 13c are presented in the Monographs section. Here, the structure confirmation of compound 13c, the most potent $P2Y_{11}$ antagonist of this series, is discussed as an example.

Structure confirmation of 2,2'-(carbonylbis(imino-3,1-(4-methylphenylene) carbonylimino))bis-(4-sulfonatobenzoate) tetrasodium salt (13c)

Figure 3.56 shows the ^{1}H NMR spectrum of compound 13c.

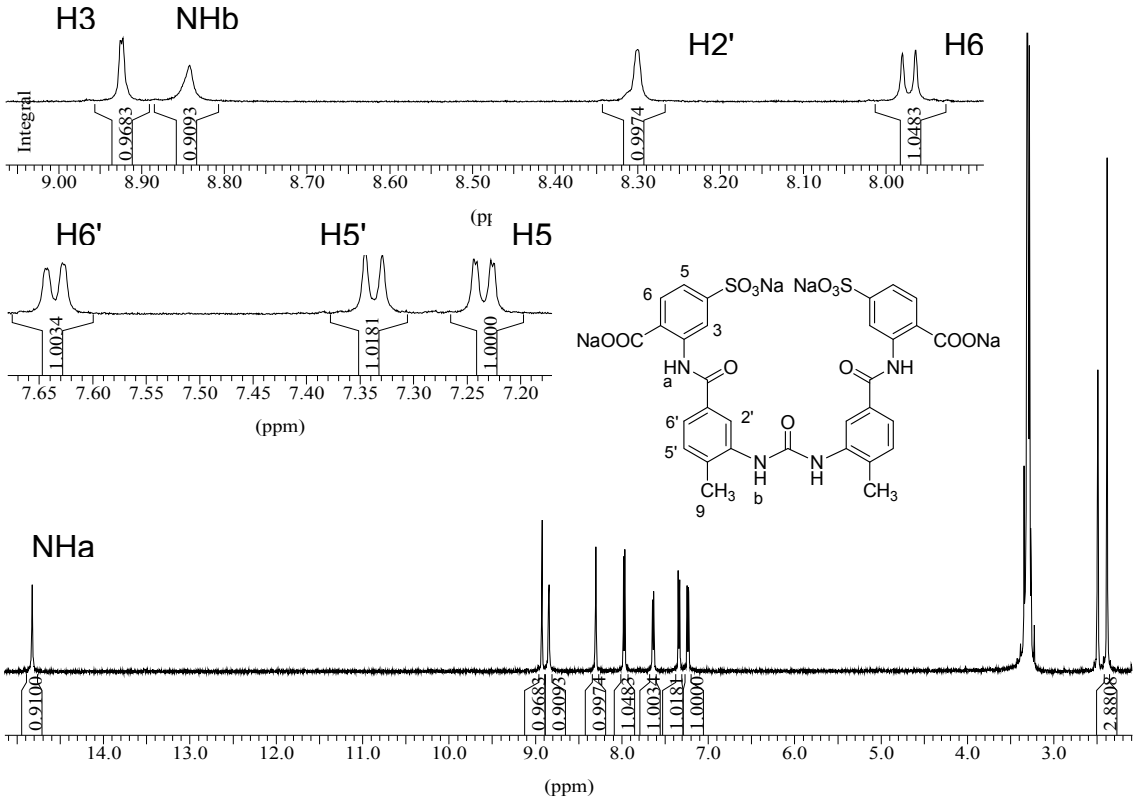

Figure 3.56. 500 MHz ^{1}H NMR spectrum of compound 13c in DMSO-d_6.

Because of the intramolecular H-bond, the D_2O exchangeable signals of the amide protons of 13c were more deshielded to the very low downfield (14.82 ppm), compared with the signals of other amide compounds such as 8c (11.32 ppm) or 9c (10.20 ppm). The signal of the urea proton appeared as a D_2O exchangeable singlet in the normal range as other ureas did (8.84 ppm).

The three protons of the sulfonic acid substituted benzene ring formed an ABX-system. The signal of proton H3 (X) was found as a doublet at 8.92 ppm with the meta-coupling (^4J = 1.3 Hz) to H5. The signal of the proton H5 (A) appeared as a doublet of doublet at 7.23 ppm with the ortho-coupling (^3J = 8.0 Hz) to H6 and the

meta-coupling (^4J = 1.3 Hz) to H3. Due to the -I effect of the carboxyl group, the signal of the proton H6 (B) was deshielded to 7.97 ppm and showed a doublet with the ortho-coupling (^3J = 8.0 Hz) to H5.

The three protons of the benzamido residue also formed another ABX-system and were interpreted by comparison with the benzamido residue of 2c (NF340, see section 3.1.6).

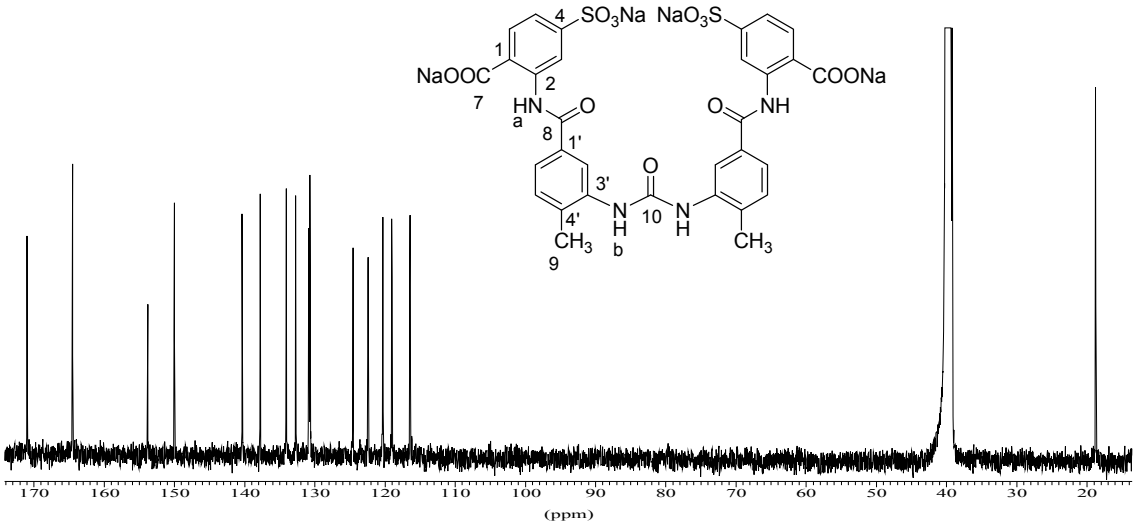

Figure 3.57. 125 MHz ^{13}C NMR spectrum of compound 13c in DMSO-d_6.

In Figure 3.57, the ^{13}C NMR spectrum shows a signal of the urea carbonyl carbon at 153.8 ppm, while the signal of the amide carbonyl appeared at 164.5 ppm. The signal of the carboxyl carbon appeared at very low downfield (170.9 ppm). The signals of carbons of the sufonato-4-benzoate moiety were interpreted according to the substituent increment calculation. The signal of the carbon C1 appeared at 130.0 ppm, whereas the signal of the sulfonic acid substituted carbon (C4) appeared at 149.9 ppm. A signal at 140.3 ppm was assigned to the carbon C2. The signal of C3 was shifted to 116.4 ppm. The signals of C5 and C6 were found at 118.9 ppm and 124.5 ppm, respectively. The carbon signals of the benzamido residue and the methyl group were interpreted as described in section 3.1.6.

The ESI-MS confirmed the molecular mass of 13c with the signals of $[M\text{-}Na]^-$ and $[M\text{-}H]^-$ at m/z 791.1 and m/z 813.2, which were in agreement with the calculated m/z of 791.0 and 813.0, respectively.

3.5 Benzene sulfonic acid derivatives with para-phenylene linker

The benzene sulfonic acid derivative 13c showed a high antagonistic activity at $P2Y_{11}$ receptors (see section 4.4.6); therefore other benzene sulfonic acid derivatives were synthesized and studied for their activity. Variation of the meta-phenylene linker to the para-phenylene liker was done to investigate the effect of phenylene-linker position.

Using p-nitrobenzoyl chloride instead of 4-methyl-3-nitrobenzoyl chloride, five benzene sulfonic acid urea derivatives (14c-18c, Figure 3.58) were synthesized as p-phenylene derivatives of 2c (NF340).

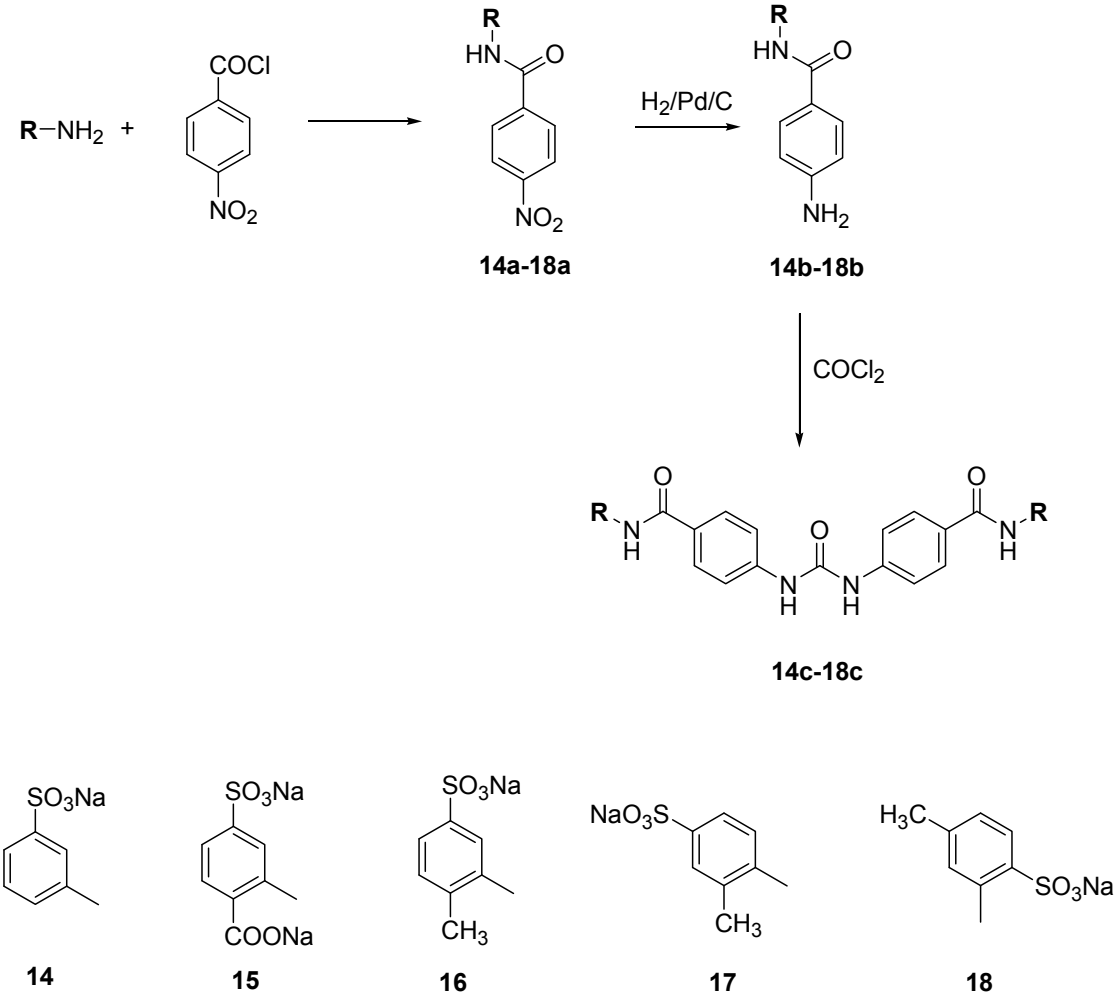

Figure 3.58. Synthetic variations and structural formulas of benzene sulfonic acid derivatives with p-phenylene linker.

The analytical data of all compounds are presented in the Monographs section. Here, analytical data of compound 14c, the most potent $P2Y_{11}$ antagonist in this series, is discussed as an example.

Structure confirmation of 3,3'-(carbonylbis(imino-4,1-phenylenecarbonyl imino))bis-(benzene sulfonic acid) disodium salt (14c)

Figure 3.59 shows the ^{1}H NMR spectrum of compound 14c.

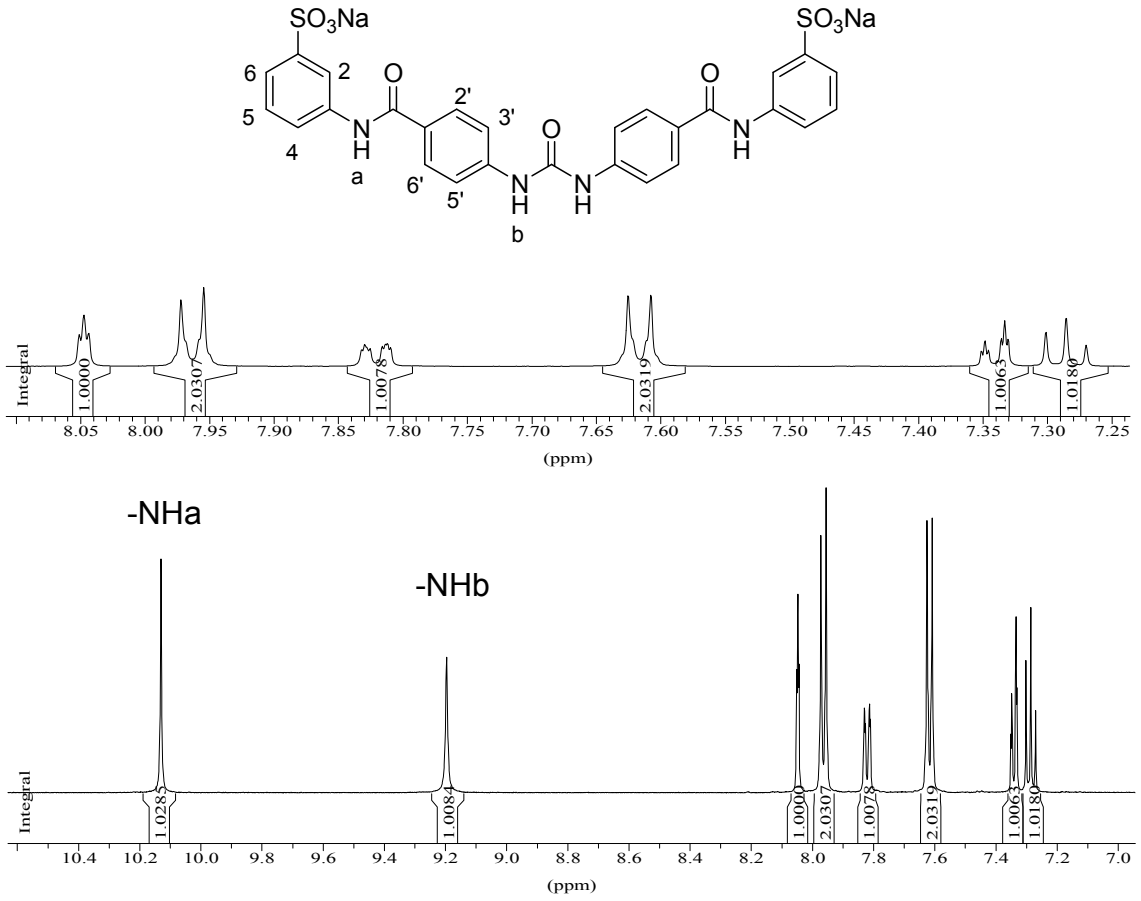

Figure 3.59. 500 MHz ^{1}H NMR spectrum of compound 14c in DMSO-d_6.

Two D_2O exchangeable signals at 9.20 ppm and 10.13 ppm represented the signals of urea and amide protons, respectively.

The four protons of the benzene sulfonic acid formed an ABCX system. Because of the effect of the sulfonic acid and amide groups, the signal of the proton H2 (X) was deshielded to 8.05 ppm. This proton was coupled to proton H4 and H6 with the same coupling constants (^{4}J = 1.9 Hz) and therefore the splitting pattern was detected as a pseudotriplet. The proton H5 (B) was coupled to proton H4 and H6 with ^{3}J = 7.9 Hz and showed the signal at 7.28 ppm as a triplet. Due to the effect of the sulfonic acid group, the signal of proton H6 (A) appeared at 7.34 ppm. This proton was coupled to H5 with ^{3}J = 7.9 Hz, to H4 with ^{4}J = 1.3 Hz and to H2 with ^{4}J = 2.2 Hz, therefore the splitting pattern appeared as a doublet of triplet. The signal

of the proton H4 (C) appeared as a doublet of triplet at 7.82 ppm with the ortho-coupling to H5 (^3J = 7.9 Hz), meta-coupling to H2 (^4J = 2.2 Hz) and meta-coupling to H6 (^4J = 1.3 Hz). The four protons of the phenylene-bridge formed an AA'BB'-system. Table 3.22 shows the signals of the AA'BB'-system of compounds 14a – 14c. The signals of 14a were deshielded to 8.22 – 8.35 ppm because of the –I and –M effects of the nitro group, whereas the +M effect of the amino group shielded the signal of 14b to an upper field.

Table 3.24. Comparison of ^{1}H NMR signals of protons in p-benzamido residues of compounds 14a-14c.

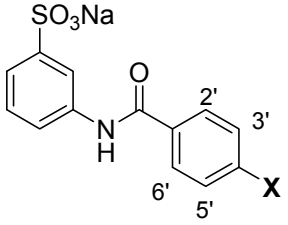

Cpd	X	C2'C6'	C3'C5'
		δ (ppm)	δ (ppm)
14a	-NO_2	8.22	8.35
14b	-NH_2	7.73	6.58
14c	-NHCONH-	7.96	7.62

The splitting pattern could be explained as mentioned in section 3.3.4. Similar splitting patterns were also found for other p-benzamido derivatives (15a - 18c).

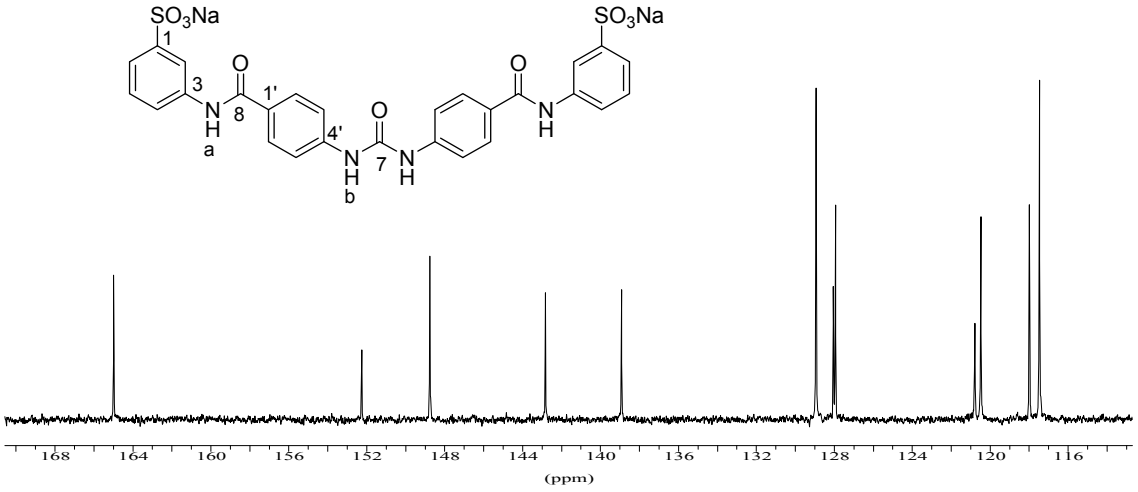

Figure 3.60. 125 MHz ^{13}C NMR spectrum of compound 14c in DMSO-d_6.

In the ^{13}C NMR spectrum of compound 14c (Figure 3.60), the signal of the urea carbonyl carbon appeared at 152.2 ppm, whereas the signal at 164.9 ppm represented the amide carbonyl carbon. The interpretation of other signals was performed by comparison of the found signals with the estimated signals from the software ChemDraw Ultra 7.0. The signal of the sulfonic acid substituted carbon C1 appeared at 148.7 ppm, while the signal of C1' was found at 127.9 ppm. The signals of NH-substituted carbons C3 and C4' appeared at 138.9 ppm and 142.8 ppm, respectively. The chemically equivalent carbons C2'C6' and C3'C5' appeared as the high intensity signals at 117.5 ppm and 128.9 ppm, respectively. The signal of C4 was shifted to 120.8 ppm, while the signals of C5 and C6 appeared at 128.0 ppm and 120.5 ppm, respectively. The signal of C2 appeared at 118.0 ppm.

Measurement of ESI-MS in the negative mode gave the peaks of $[M-Na]^-$ and $[M-H]^-$ at m/z 631.2 and m/z 653.0, respectively (calculated m/z of 631.1 and 653.0, respectively).

4 Pharmacology

4.1 Measurement of ligand-induced changes in the intracellular calcium concentration

The $P2Y_1$, $P2Y_2$, $P2Y_4$ and $P2Y_{11}$ receptors recombinantly expressed in 1321N1 astrocytoma cells, respectively, were established by S. Meis and used as functional test systems by measuring intracellular Ca^{2+}.[79]

After injection of buffer or standard agonist such as ATP to $P2Y_{11}$ receptor expressing 1321N1 cells, the fluorescence intensity was measured. Figure 4.1 shows an example of the resulting fluorescence intensity over time after the injection of buffer or increasing concentrations of ATP.

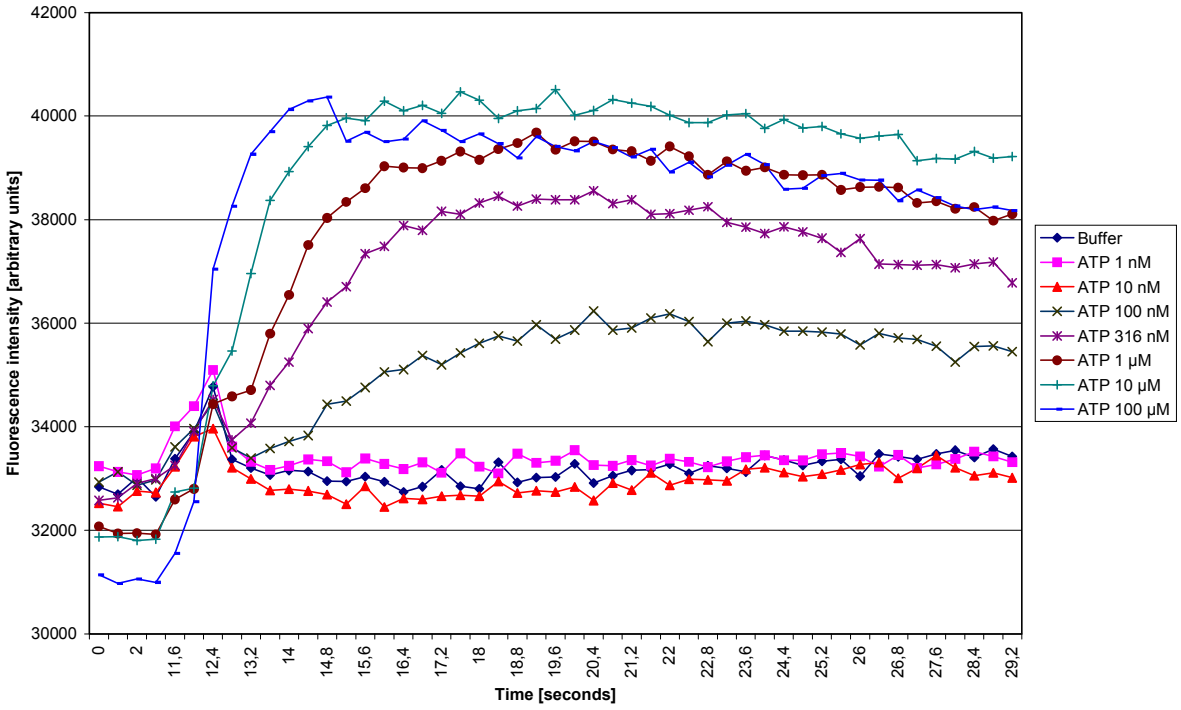

Figure 4.1. Fluorescence intensity-time curves after the injection of buffer or increasing concentrations of ATP to $P2Y_{11}$ receptor expressing 1321N1 cells.

The change of fluorescence intensity before and after injection of control (buffer) or compounds was estimated and used for the construction of concentration-response curves as shown in Figure 4.2 (for details see experimental part).

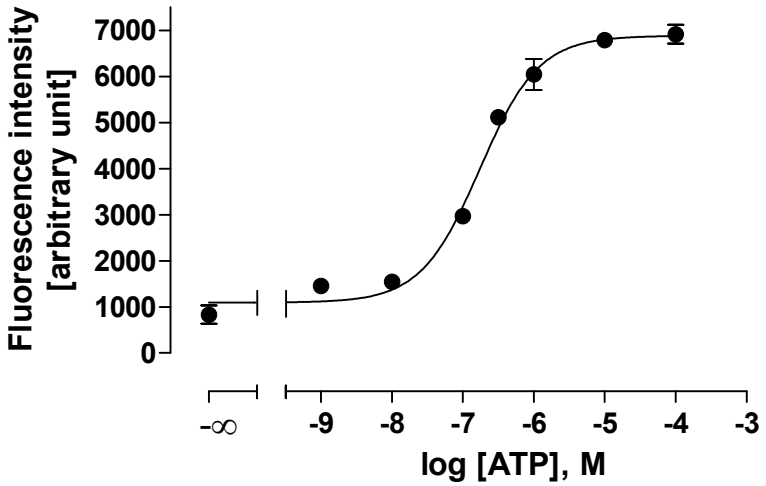

Figure 4.2. Example of a concentration-response curve derived from the data of Figure 4.1 (3 replicates).
EC_{50} = 173 nM (Hill slope = 1.047 ± 0.214).

4.2 Pharmacological responses of standard agonists at $P2Y_1$, $P2Y_2$, $P2Y_4$ and $P2Y_{11}$ receptors

To study if the receptor recombinantly expressed in 1321N1 cells responded to the respective standard nucleotide agonist in the calcium assay, intracellular calcium was measured upon the injection of standard agonists at $P2Y_1$, $P2Y_2$, $P2Y_4$ and $P2Y_{11}$ receptors. The obtained EC_{50} values of standard agonists were compared with the EC_{50} values reported in the literature as presented in Table 4.1.

Table 4.1. Comparison of the EC_{50} values estimated in this work and reported EC_{50} values from literature.

Receptors	Standard agonist	EC_{50} estimated in this work (nM)	EC_{50} reported in Literature (nM)
$P2Y_1$	2-MeSADP	2.82	1.7 ± 0.2 [97]
			3.5 [79]
$P2Y_2$	UTP	200	139 [79]
$P2Y_4$	UTP	21.9	20 [79]
$P2Y_{11}$	ATP	207	214 [79]
			2370 [98]

2-MeSADP was used as standard agonist at $P2Y_1$ receptors. 2-MeSADP at $P2Y_1$ receptors gained a pEC_{50} value of 8.55 ± 0.08 (n = 6, EC_{50}: 2.82 nM). This result was about 1.7-fold higher than the EC_{50} value reported by Niebauer et al. (EC_{50}: 1.7 ± 0.2 nM) and similar to the EC_{50} value reported by Meis.[79] Therefore, 2-MeSADP was used as standard agonist for $P2Y_1$ receptors at a concentration of 31.6 nM (about 11-fold above EC_{50}).

UTP was used as a standard agonist at $P2Y_2$ and $P2Y_4$ receptors. At $P2Y_2$ receptors, UTP gained a pEC_{50} value of 6.70 ± 0.05 (n = 5, EC_{50}: 200 nM).The result was in approximate agreement with the EC_{50} found by Meis (139 nM). The pEC_{50} value of UTP at $P2Y_4$ was 7.66 ± 0.07 (n = 9, EC_{50}: 21.9 nM). This result is equal to the EC_{50} reported by Meis.[79] 1 µM and 100 nM UTP (4-5 fold above EC_{50}) were used as standard agonist concentrations for $P2Y_2$ and $P2Y_4$ receptors, respectively.

ATP was used as standard agonist at $P2Y_{11}$ receptors. The obtained concentration-response curve for ATP is presented in Figure 4.3.

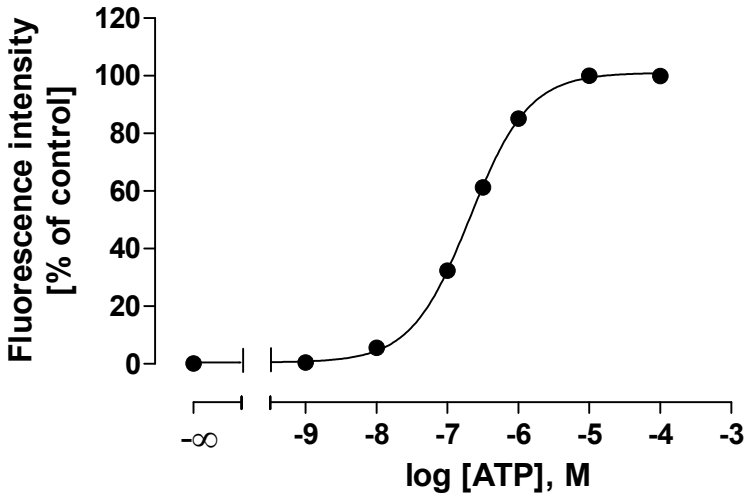

Figure 4.3. Concentration-response curve of ATP at $P2Y_{11}$ receptors recombinantly expressed in 1321N1 cells. 1 µM ATP was used as standard agonist.

pEC_{50} [ATP] = 6.68 ± 0.04, n = 7. Slope was not significantly different from unity.

The pEC_{50} value of ATP in the test system was 6.68 ± 0.04 (n = 7, EC_{50}: 207 nM) which was in agreement with results reported by Meis (EC_{50}: 214 nM).[79] 1 µM ATP (about 5-fold above EC_{50}) was used as the standard agonist concentration for $P2Y_{11}$ receptors.

4.3 Investigation of NF157 as standard antagonist at $P2Y_{11}$ receptors

NF157 was used as standard antagonist. Compounds were tested for their antagonistic effect by testing their ability to inhibit a calcium response elicited by the injection of 1 µM ATP (≈ 5-fold over EC_{50}) to $P2Y_{11}$ receptors stably expressed in 1321N1 cells. The concentration-inhibition curve of NF157 is shown in Figure 4.4.

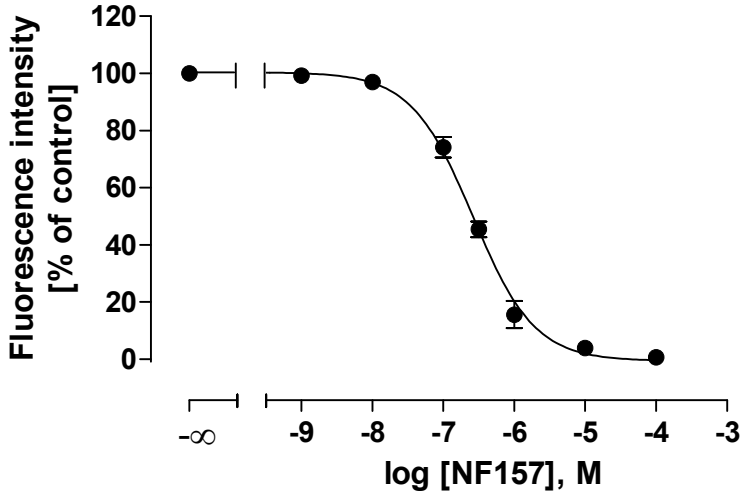

Figure 4.4. Concentration-inhibition curve of NF157 at $P2Y_{11}$ receptors recombinantly expressed in 1321N1 cells. 1 µM ATP was used as standard agonist.

pIC_{50} [NF157] = 6.58 ± 0.05, n = 4. Slope was not significantly different from unity.

The app. pK_i value of NF157 was calculated as 7.33 ± 0.12 which was similar to the app. pK_i value of 7.35 reported in the literature.[65]

4.4 Pharmacological results of test compounds

4.4.1 General consideration

105 Compounds were investigated for their activities at $P2Y_1$, $P2Y_2$, $P2Y_4$ and $P2Y_{11}$ receptors. The test compounds included:

- Compounds 3a – 18c and 2d – 2n, which are new compounds (structures shown in Appendix B1) synthesized in this thesis,

- 31 NF-compounds (Appendix B3), which are structurally related to NF340 and were synthesized by the group of Prof. Nickel, University of Bonn,[53,73] and MK-compounds (Appendix B2). The latter are compounds which are not novel but were formerly synthesized by the group of Prof. Nickel. However, they were not available anymore. Thus, they were resynthesized and their structures and purities were confirmed by ^{1}H- and ^{13}C-NMR, CHN and MS. These data were in accordance with data from Prof. Nickel and thus not presented in this work.

Pharmacological results were then analyzed for structure-activity relationships.

4.4.2 Agonist screening at $P2Y_{11}$ receptors

All test compounds were screened at $P2Y_{11}$ receptors for agonistic activity. None of them showed more than 40 % response of the standard agonist 1 µM ATP at a concentration of 100 µM (Appendix A1-A4). It could be concluded that no potent agonists at $P2Y_{11}$ receptors were found in this work.

4.4.3 Nitro- and amino-naphthalene derivatives and their antagonistic activities at $P2Y_{11}$ receptors

22 Nitro- and 16 amino-naphthalene derivatives were tested at $P2Y_{11}$ receptors. Most of the nitro- and amino-derivatives showed no ability to block the agonistic signal induced by 1 µM ATP at $P2Y_{11}$ receptors (Figure 4.5, for details see Appendix A1 - A2).

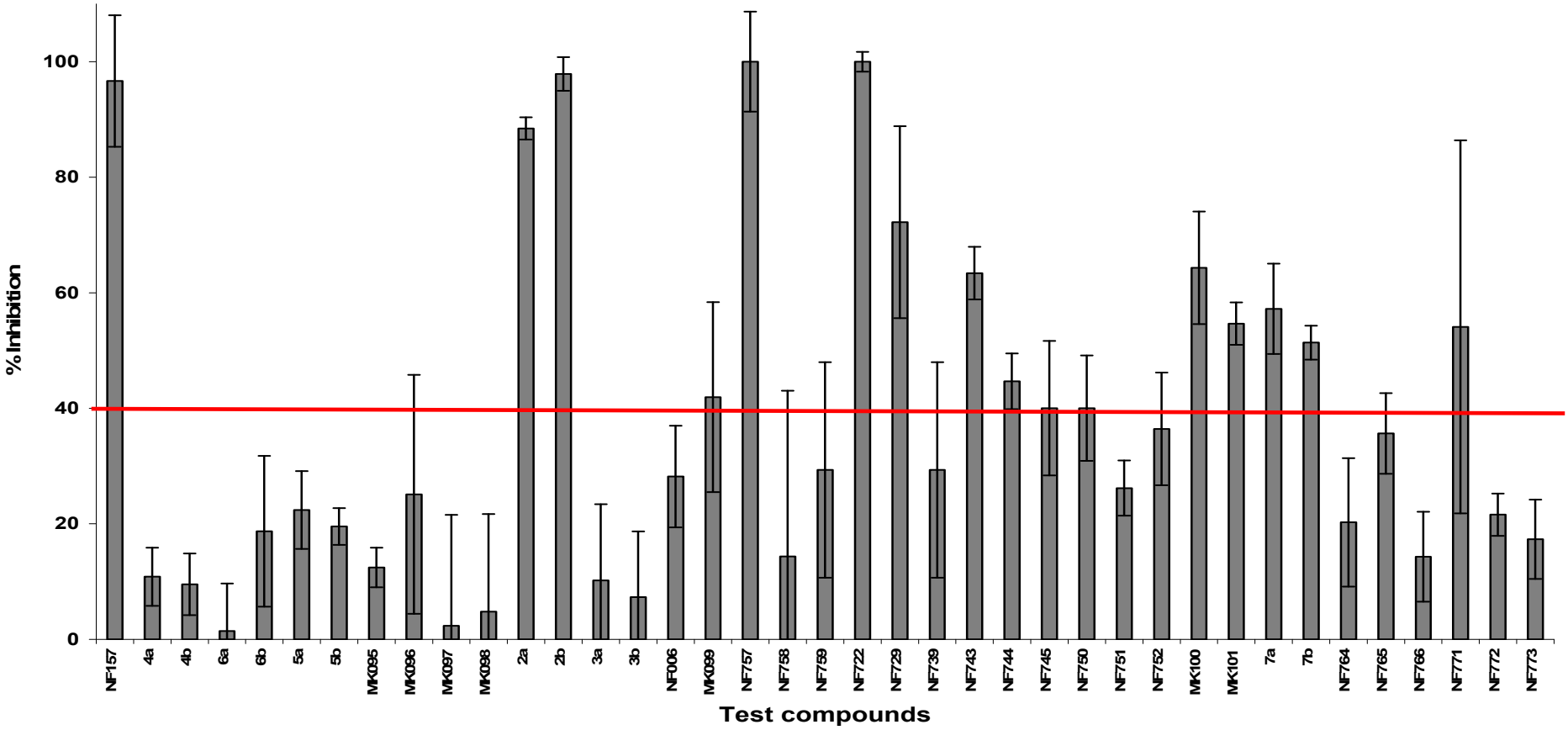

Figure 4.5. Primary screening for the antagonistic effect (% inhibition) by 100 μM nitro- and amino- derivatives of 1 μM ATP induced calcium mobilization at $P2Y_{11}$ receptors recombinantly expressed in 1321N1 astrocytoma cells.

Ten nitro- and five amino-derivatives showed more than 40 % inhibition of the 1 µM ATP signal and were further investigated to obtain their app. pK_i values. Figure 4.6 shows an example of concentration-inhibition curves of NF722 and NF729.

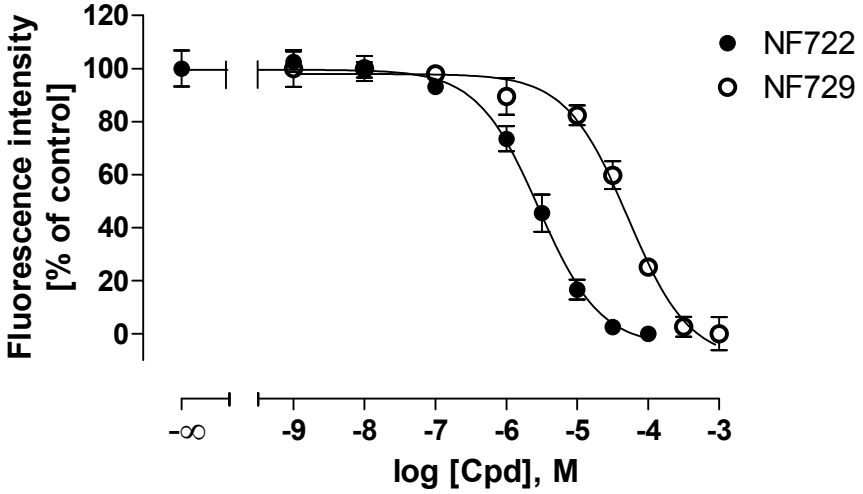

Figure 4.6. Concentration-inhibion curves of NF722 and NF729 at $P2Y_{11}$ receptors recombinantly expressed in 1321N1 cells. 1 µM ATP was used as standard agonist.

pIC_{50} [NF722] = 5.55 ± 0.07. pIC_{50} [NF729] = 4.29 ± 0.10. Slopes were not significantly different from unity.

NF722 is a hydroxy substituted naphthalene sulfonic acid derivative, whereas NF729 is the corresponding methoxy analogue (see structure in Table 4.2). The methoxy derivative NF729 showed 15-fold lower potency than the hydroxy derivative.

The decrease in potency upon substitution of hydroxy group by a methoxy group was also observed in NF757, NF743, NF750 and NF771 as shown in Table 4.2.

Table 4.2. Comparison of app. pK_i values and corresponding K_i values of hydroxy and methoxy derivatives at $P2Y_{11}$ receptors recombinantly expressed in 1321N1 cells. 1 µM ATP was used as standard agonist.

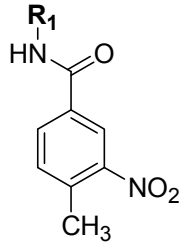

R_1	R_2	Cpd	App. pK_i	Corresponding K_i (µM)
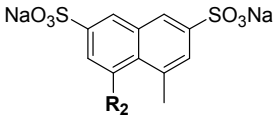	**-OH**	**NF722**	**6.24 ± 0.08**	**0.57**
	$-OCH_3$	NF729	5.06 ± 0.21	8.71
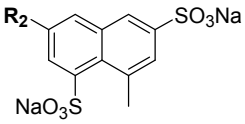	-OH	NF757	5.71 ± 0.10	1.95
	$-OCH_3$	NF758	< 4	> 100
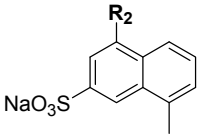	-OH	NF743	4.51 ± 0.17	30.9
	$-OCH_3$	NF744	4.43 ± 0.24	37.1
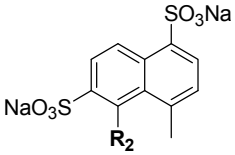	-OH	NF750	4.35 ± 0.06	44.7
	OCH_3	NF751	< 4	> 100
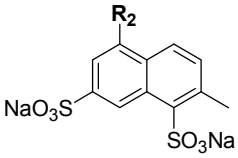	-OH	NF771	4.75 ± 0.14	17.8
	$-OCH_3$	NF772	< 4	> 100
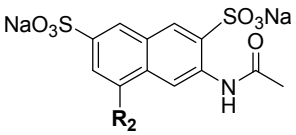	-OH	NF764	< 4	> 100
	$-OCH_3$	NF765	< 4	> 100

The hydroxy derivatives exhibited weak antagonistic activities with app. pK_i values in the range from 4.35 – 6.24, except NF764 which showed only 20 % inhibition. Among all examined nitro- and amino- derivatives, NF722 was the most potent compound with an app. pK_i value of 6.24.

Two disulfonic acid nitro compounds (2a and MK100, Table 4.3) showed up to 9-fold higher potency than the trisulfonic acid analogue 7a, whereas other nitro compounds showed no appreciable antagonistic effect (see Figure 4.5 and for details see Appendix A1 and A2).

Table 4.3. Structural formulas and app. pK_i values of active nitro disulfonic acid and trisulfonic acid derivatives at $P2Y_{11}$ receptors recombinantly expressed in 1321N1 cells. 1 µM ATP was used as standard agonist.

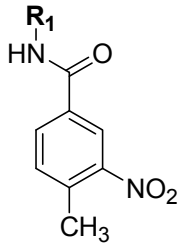

R_1	Cpd	App. pK_i	Corresponding K_i (µM)
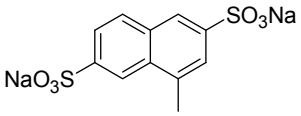	2a	5.93 ± 0.25	1.17
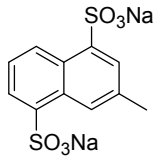	MK100	5.45 ± 0.08	3.55
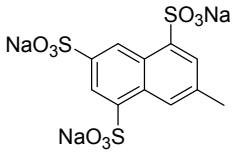	7a	4.98 ± 0.08	10.5

Because amino derivatives of the hydroxy compounds are unavailable in the NF-library, only amino derivatives of the methoxy compounds were evaluated for their activity. The results of 16 test compounds are presented as % inhibition of 1 µM ATP as shown in Table 4.4.

Table 4.4. % Inhibition by 100 μM amino-derivatives of 1 μM ATP induced calcium mobilization at $P2Y_{11}$ receptors recombinantly expressed in 1321N1 astrocytoma cells.

Group of compound	Compound	% Inhibition
Monosulfonic acid substitution	4b	9.5 ± 5.3
	5b	19.5 ± 3.2
	6b	18.7 ± 13.0
Disulfonic acid substitution	**2b**	**97.9 ± 2.9**
	3b	7.3 ± 11.3
	MK096	25.1 ± 20.7
	MK098	4.8 ± 16.9
	MK101	**54.7 ± 3.7**
Trisulfonic acid substitution	**7b**	**51.4 ± 2.9**
	MK099	**41.9 ± 16.4**
Monosulfonic acid and methoxy substitution	**NF745**	**40.0 ± 11.6**
Disulfonic acid and methoxy substitution	NF730	35.1 ± 21.2
	NF752	36.4 ± 9.7
	NF759	29.3 ± 18.7
	NF766	14.3 ± 7.8
	NF773	17.3 ± 6.9

The monosulfonic acid substituted amino compounds (4b – 6b) did not inhibit the response of 1 μM ATP. The disulfonic acid substituted derivatives 3b, MK096 and MK098 showed less than 40 % inhibition, whereas 2b and MK101 showed 97.9 and 54.7 % inhibition, respectively. The trisulfonic acid MK099 and 7b showed 40-50 % inhibition. It is interesting that NF745, which is a monosulfonic acid and methoxy substituted derivative showed 40 % inhibition, while other methoxy amino derivatives showed less than 40 % inhibition. Five amino derivatives were further investigated for app. pK_i. The structural formulas and their app. pK_i values are presented in Table 4.5.

Table 4.5. Structural formulas and app. pK_i values of active amino derivatives at $P2Y_{11}$ receptors recombinantly expressed in 1321N1 cells.

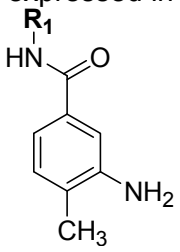

R_1	Cpd	App. pK_i	Corresponding K_i (µM)
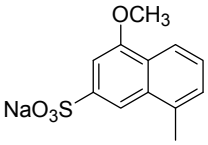	NF745	4.41 ± 0.06	38.9
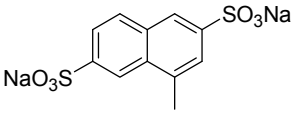	2b	5.67 ± 0.14	2.14
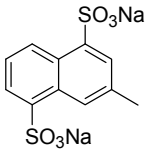	MK101	5.16 ± 0.21	6.92
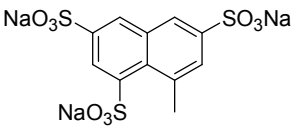	MK099	4.57 ± 0.06	26.9
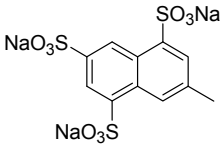	7b	4.89 ± 0.24	12.9

All the active amino compounds showed app. pK_i values in the range of 4.41 – 5.67. The amino disulfonic acid derivatives (2b and MK101) showed higher potency than trisulfonic acid (MK099 and 7b) and monosulfonic acid derivatives (NF745), respectively.

Among analogues containing the same naphthalene sulfonic acid residue, the nitro- and amino- derivatives showed almost equal potencies such as 2a and 2b, 7a and 7b, or NF744 and NF745. Figure 4.7 shows as an example of the concentration-inhibition curves of the nitro- (2a) and amino- (2b) precursors in comparison to the urea 2c (NF340).

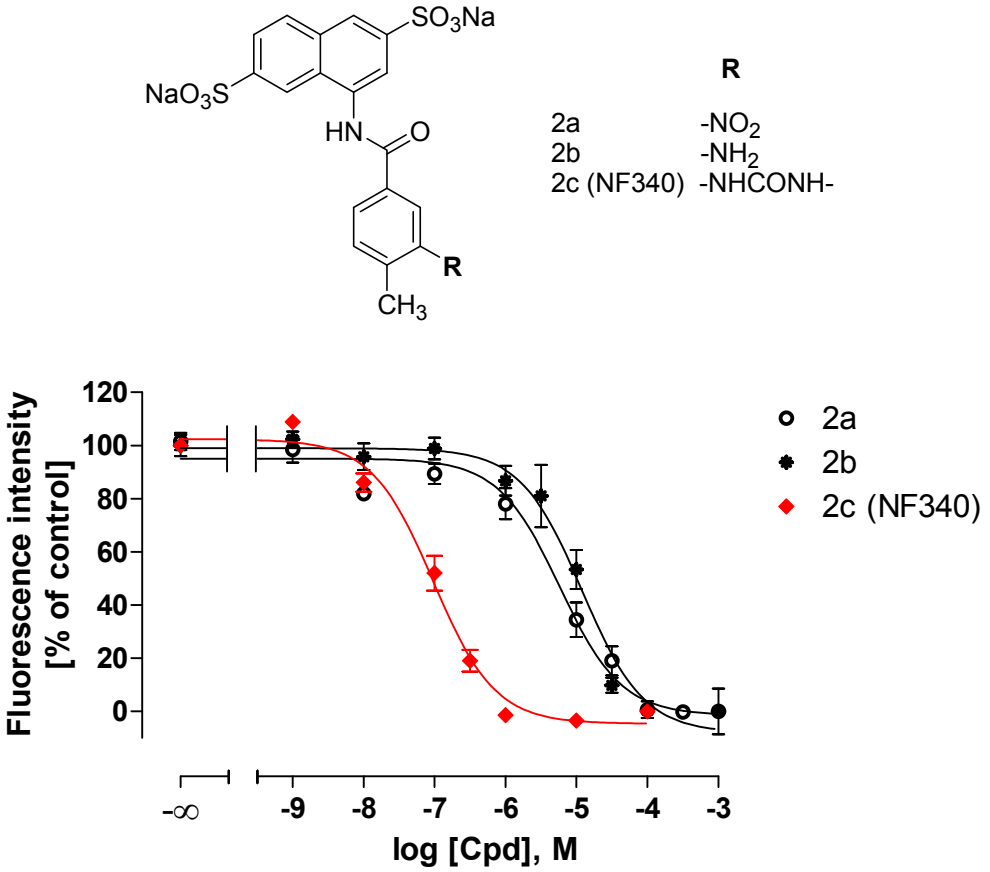

Figure 4.7. Concentration-inhibition curves of 2a and 2b in comparison with 2c (NF340) at $P2Y_{11}$ receptors recombinantly expressed in 1321N1 cells. 1 µM ATP was used as standard agonist.
pIC_{50} [2a] = 5.23 ± 0.10. pIC_{50} [2b] = 4.92 ± 0.09. pIC_{50} [2c, NF340] = 7.02 ± 0.06. Slopes were not significantly different from unity.

The study of the activity of suramin derivatives from Ullmann et al. showed that only symmetrical ureas displayed antagonistic activity at $P2Y_{11}$ receptors, whereas the examined nitro- and amino- derivatives exhibited no activity.[65] The discovery of activity of nitro- and amino- derivatives in this work implied that the symmetrical structure may not be required for antagonistic activity. Therefore, besides the symmetrical ureas, **asymmetrical ureas** were synthesized and tested for their activity (see details in section 4.4.5). However, first the results from the **symmetrical ureas** will be presented.

4.4.4 Symmetrical urea derivatives and their antagonistic activities at $P2Y_{11}$ receptors

The study of the pharmacological activity of symmetrical ureas was started with the evaluation of the potency of 2c (NF340). The concentration-inhibition curve of 2c (NF340) is shown in Figure 4.8.

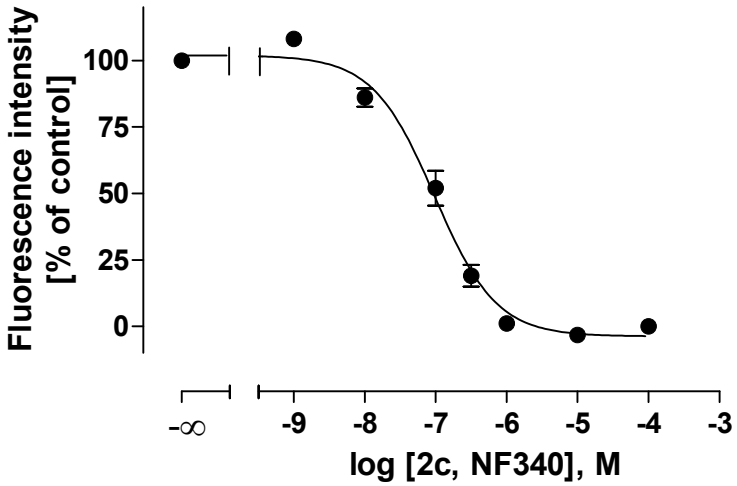

Figure 4.8. Concentration-inhibition curve of 2c (NF340) at $P2Y_{11}$ receptors recombinantly expressed in 1321N1 cells. 1 µM ATP was used as standard agonist.
pIC_{50} [2c] = 7.02 ± 0.06. Slope was not significantly different from unity.

In this study, an app. pK_i value of 7.80 ± 0.15 was calculated for 2c (NF340), which was in accordance with the app. pK_i value reported by Meis (7.71 ± 0.04, calcium assay).[79] This result confirmed that NF340 was about 3-fold more potent than the standard antagonist NF157.[65]

Other symmetrical urea derivatives with variations in the numbers and/or positions of sulfonic acid moieties at the naphthalene ring were tested for their inhibitory effect. All of the test compounds showed more than 70 % inhibition of the standard agonist (1 µM ATP) response, except 6c and NF298, which showed 35.5 and 50.7 % inhibition, respectively (Figure 4.9). All urea derivatives were further investigated to determine app. pK_i values. The results are presented in Table 4.6.

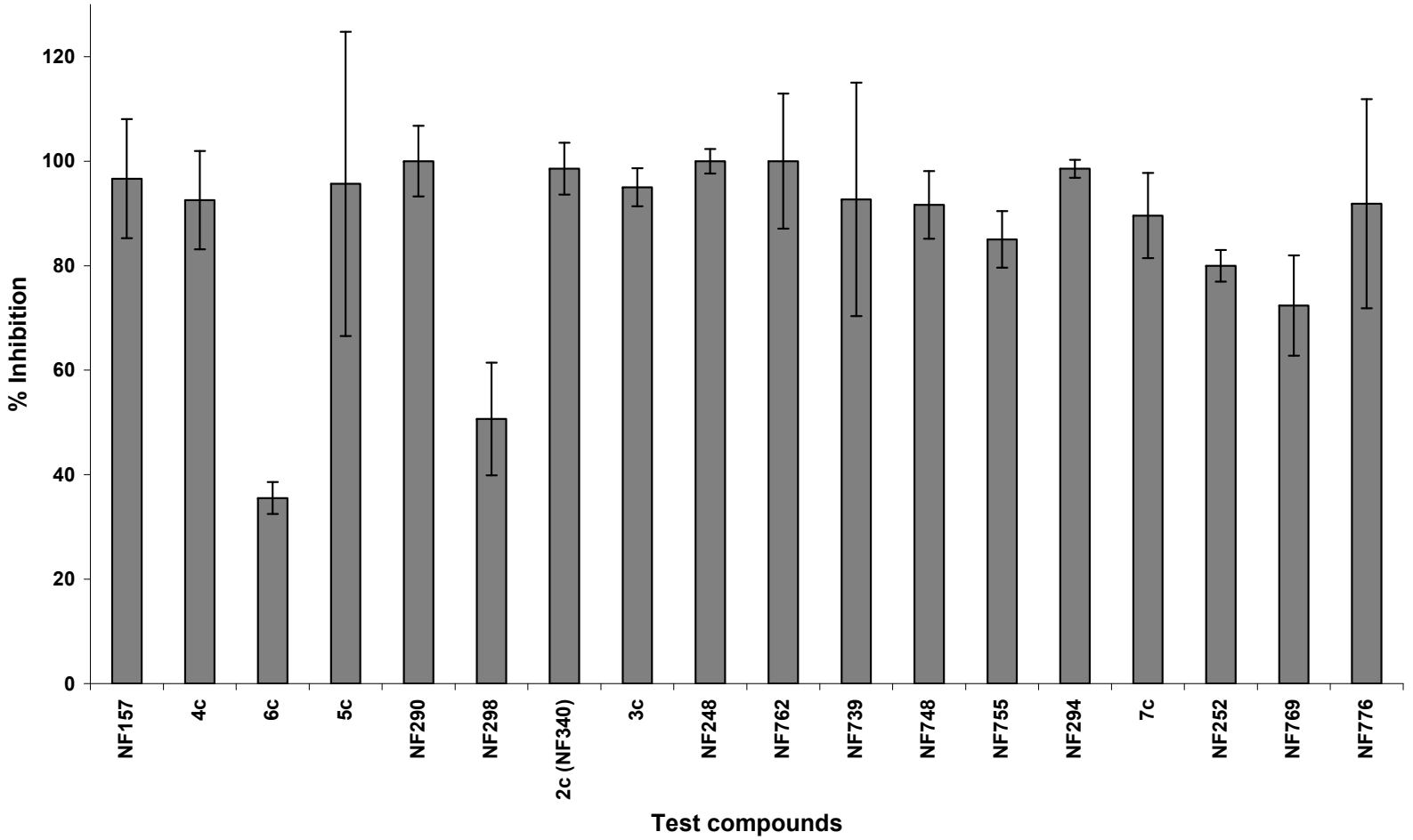

Figure 4.9. Primary screening for the antagonistic effect (% inhibition) by 100 µM symmetrical ureas of 1 µM ATP induced calcium mobilization at $P2Y_{11}$ receptors recombinantly expressed in 1321N1 astrocytoma cells. NF157 was used as standard antagonist. 1 µM ATP was used as agonist.

Table 4.6. Structural formulas and functional inhibitory activity of 1-naphthalene symmetrical urea derivatives at $P2Y_{11}$ receptors determined with the calcium assay.

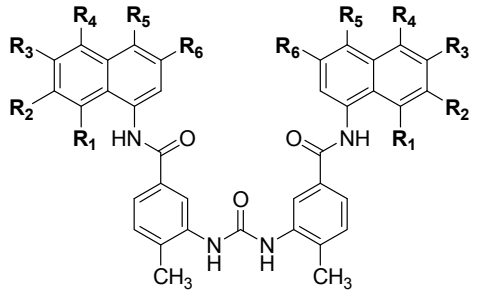

Cpd	R_1	R_2	R_3	R_4	R_5	R_6	app.pK_i	K_i (nM)
4c	-H	-SO_3Na	-H	-H	-H	-H	6.13 ± 0.01	714
5c	-H	-H	-H	-H	-H	-SO_3Na	5.74 ± 0.10	1820
6c	-H	-H	-H	-H	-SO_3Na	-H	4.57 ± 0.14	26915
NF290*	-SO_3Na	-H	-H	-H	-SO_3Na	-H	5.68 ± 0.33	2089
NF298*	-H	-H	-SO_3Na	-H	-SO_3Na	-H	4.89 ± 0.11	12882
2c (NF340)	**-H**	**-SO_3Na**	**-H**	**-H**	**-H**	**-SO_3Na**	**7.80 ± 0.15**	**15.8**
3c	-H	-H	-SO_3Na	-H	-H	-SO_3Na	6.09 ± 0.09	812
NF058*	-SO_3Na	-H	-SO_3Na	-H	-SO_3Na	-H	5.12 ± 0.13	7586
NF248*	-SO_3Na	-H	-SO_3Na	-H	-H	-SO_3Na	6.47 ± 0.08	339
NF762	-SO_3Na	-H	-OCH_3	-H	-H	-SO_3Na	6.32 ± 0.01	479
NF739	-OCH_3	-H	-SO_3Na	-H	-H	-SO_3Na	5.61 ± 0.09	2455
NF748	-H	-SO_3Na	-H	-OCH_3	-H	-H	6.40 ± 0.04	398
NF755	-OCH_3	-SO_3Na	-H	-H	-SO_3Na	-H	5.49 ± 0.05	3236

* Compounds were characterized by Meis[79]

Shift of the sulfonic acid in 2c (NF340) from the R_2 to the R_3 position in 13c led to a 51-fold reduction in potency.

Two other disulfonic acid derivatives (NF290 and NF298) also showed low potency with app. pK_i values of 5.68 and 4.89, respectively.[79] This result implied that the position of sulfonic acid groups is very important for antagonistic activity.

To investigate which positions of the sulfonic acid group are more relevant for the antagonistic activity, the monosulfonic acid derivatives 4c and 5c (Figure 4.10) were synthesized and investigated for inhibitory activity.

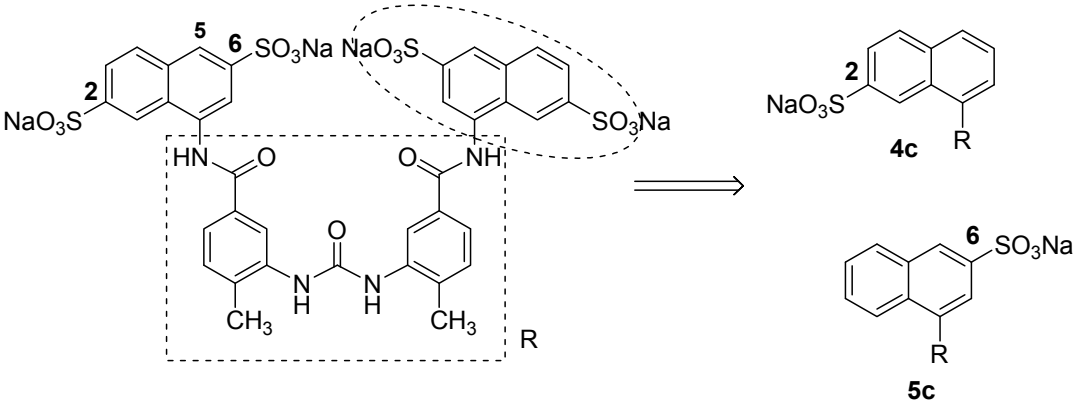

Figure 4.10. Design of the monosulfonic acid derivatives 4c and 5c in order to investigate which sulfonic acid is more important for the antagonistic activity of 2c (NF340).

Figure 4.11 shows the concentration-inhibition curves of 4c – 6c in comparison with 2c (NF340).

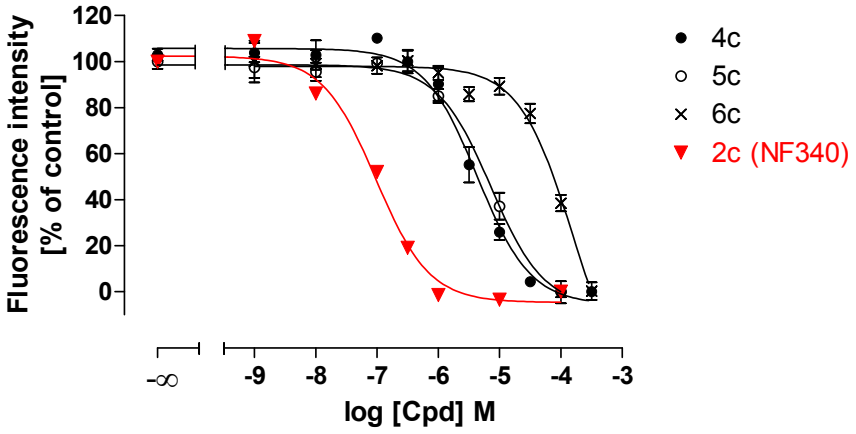

Figure 4.11. Concentration-inhibition curves of 4c, 5c and 6c at $P2Y_{11}$ receptors recombinantly expressed in 1321N1 cells in comparison to 2c (NF340). 1 µM ATP was used as standard agonist.
pIC_{50} [2c, NF340] = 7.02 ± 0.06. pIC_{50} [4c] = 5.36 ± 0.08.
piC_{50} [5c] = 5.15 ± 0.09. pIC_{50} [6c] = 3.81 ± 0.10.
Slopes were not significantly different from unity.

Although compounds 4c and 5c showed antagonistic activity at $P2Y_{11}$ receptors (app. pK_i [4c]: 6.13; app. pK_i [5c]: 5.74), they were much less potent (45-fold and 115-fold) than the disulfonic acid substituted compound 2c (NF340). Therefore, it was concluded that the combination of both sulfonic acid groups in position R_2 and R_6 is important for a high antagonistic potency. Shifting the sulfonic acid group from the R_2 or R_6 into the R_5 position gave the lowest potency among the examined monosulfonic acid derivatives.

The similar tendency was also found in the trisulfonic acid analogues. Shifting of sulfonic acid group from R_6 (NF248) to R_5 position (NF058) showed 22-fold reduction of the potency (app. pK_i [NF248]: 6.47; app. pK_i [NF058]: 5.12).[79] None of the trisulfonic acid analogues exhibited higher potency than the disulfonic acid urea derivative 2c (NF340).

The exchange of a sulfonic acid moiety by a methoxy group or the addition of a methoxy group to sulfonic acid urea derivatives was investigated in compounds NF762, NF739, NF748 and NF755 (Table 4.6). The result showed that the exchange of the sulfonic acid group of NF248 in position R_3 by a methoxy group (NF762) exhibited similar potency (app. pK_i [NF248]: 6.47; app. pK_i [NF762]: 6.32). The equivalent exchange in the R_1 position (NF739) led however to 7-fold reduction of the potency in comparison with NF248.

The addition of one methoxy group in R_4 position (NF748) exhibited a similar potency as the monosulfonic acid 4c. The addition of a methoxy group in R_1 position and a sulfonic group in R_5 position of compound 4c (NF755) showed 4.5-fold lower potency than the monosulfonic acid 4c.

Among the 1-aminonaphthalene derivatives, a large similarity for change of potency upon shift of sulfonic acid groups was observed. No compound was more active than the previously reported 2c (NF340). 2c (NF340) was at least 21-fold better than all of the examined mono-, di-, or trisulfonic acid derivatives.

A further interesting result was found when the 1-aminonaphthalene was substituted by the 2-aminonaphthalene residue. Figure 4.12 shows the concentration-inhibition curves of all 2-aminonaphthalene urea derivatives.

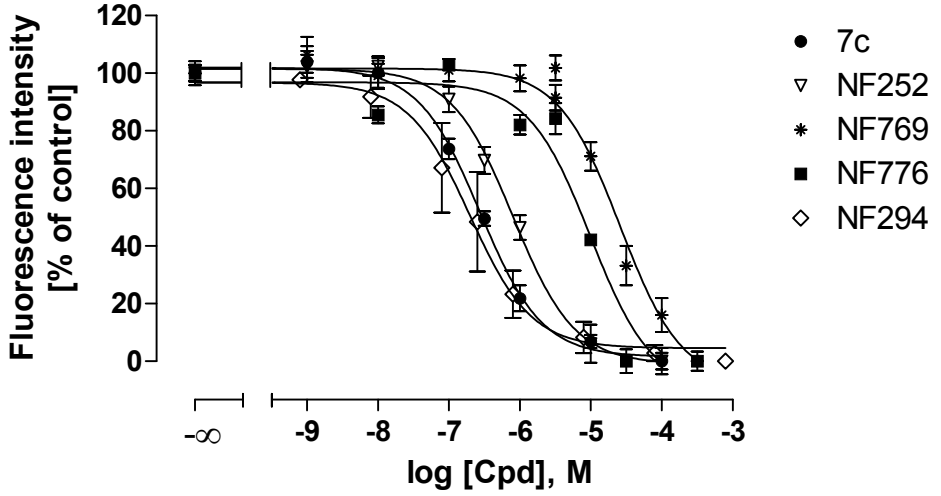

Figure 4.12. Concentration-inhibition curves of 7c, NF252, NF769, NF776 and NF294 at $P2Y_{11}$ receptors recombinantly expressed in 1321N1 cells. 1 µM ATP was used as agonist, expect for NF294.
pIC_{50} [7c] = 6.56 ± 0.06. pIC_{50} [NF252] = 6.10 ± 0.08.
pIC_{50} [NF769] = 4.57 ± 0.10. pIC_{50} [NF776] = 5.01 ± 0.13.
1 µM ATPγS as agonist was used as agonist for NF294.
pIC_{50} [NF294] = 6.71 ± 0.17.[79]
Slopes were not significantly different from unity.

The calculated app. pK_i values of the 2-aminonaphthalene urea derivatives are shown in Table 4.7.

Table 4.7. Structural formulas and functional inhibitory activity of 2-aminonaphthalene derivatives at recombinantly expressed $P2Y_{11}$ receptors determined with calcium assay.

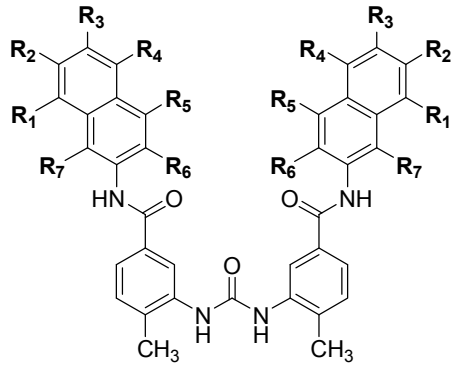

Cpd	R_1	R_2	R_3	R_4	R_5	R_6	R_7	app.pK_i	K_i (nM)
NF294*	**-SO_3Na**	**-H**	**-H**	**-H**	**-SO_3Na**	**-H**	**-H**	**7.42 ± 0.11**	**38.0**
7c	**-SO_3Na**	**H**	**-SO_3Na**	**H**	**-SO_3Na**	**-H**	**-H**	**7.14 ± 0.06**	**72.4**
NF252	-SO_3Na	-H	-SO_3Na	-H	-H	-SO_3Na	-H	6.70 ± 0.22	199
NF769	-OCH_3	-H	-SO_3Na	-H	-H	-SO_3Na	-H	5.03 ± 0.09	9332
NF776	-H	-SO_3Na	-H	-OCH_3	-H	-H	-SO_3Na	5.55 ± 0.31	2818

* Compound was characterized by Meis[79]

The most potent antagonist in this group was NF294 which was the 2-amino-naphthalene analogue of NF290. NF294 was 55-fold more potent at $P2Y_{11}$ receptors than the 1-aminonaphthalene analogue NF290. The increase in potency of the 2-aminonaphthalene analogue was also observed in 7c which was 105-fold more potent than NF058. NF252 showed 2-fold higher potency than NF248. In contrast, the methoxy derivative NF769 showed 4-fold less potency than NF739.

It was noticed that the most potent antagonists at $P2Y_{11}$ receptors were found in a group of compounds which had a sulfonic acid substitution in meta-position to the amido-linkage group, e.g. 2c (NF340), NF294 and 7c (Figure 4.13). This observation may also explain why the potency of NF769 was lower than NF739.

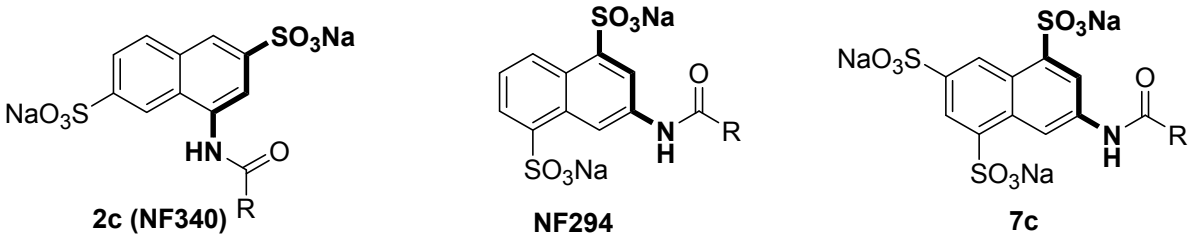

Figure 4.13. Partial structures of 2c (NF340), NF294 and 7c show meta-substitution of a sulfonic acid group and the amido linker. These compounds showed high antagonistic potency at recombinantly expressed $P2Y_{11}$ receptors with app. pKi values > 7.

At last, exchange of the methyl group of 2c (NF340) against fluorine was studied, because the fluorinated derivative NF156 was previously found to have a higher potency than the methyl derivative NF058[99] and the fluorinated derivative NF157 was also more potent than methyl derivative suramin.[65] Surprisingly, the biological activity of the fluorinated compound (MK196) was reduced by 23-fold compared to 2c (NF340) (Table 4.8).

Table 4.8. Structural formulas and app. pK_i of methyl and fluorinated derivatives of di- and tri-sulfonic acid substituted ureas at $P2Y_{11}$ receptors determined with the functional calcium assay.

	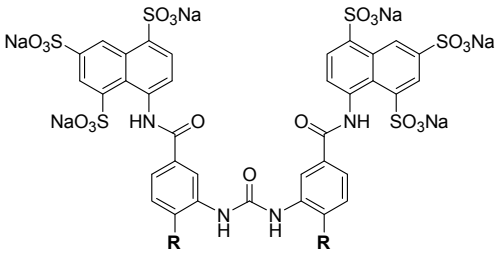		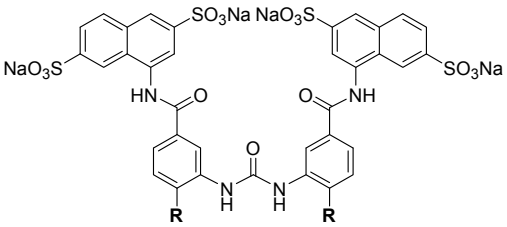	
R	$-CH_3$	-F	$-CH_3$	F
	(NF058)	(NF156)	(2c, NF340)	(MK196)
App. pK_i	5.12 ± 0.13	5.63 ± 0.18 [99]	7.80 ± 0.15	6.43 ± 0.16
K_i	7.59 µM	2.36 µM	15.8 nM	371 nM

Therefore, it could be concluded that exchange of the methyl group by a fluorine atom provides a higher potency at $P2Y_{11}$ receptors in the trisulfonic acid derivative but not in the disulfonic acid derivative.

4.4.5 Asymmetrical urea derivatives and their antagonistic activities at $P2Y_{11}$ receptors

As mentioned in section 4.4.3, the discovery of the antagonistic activity of nitro- and amino- derivatives triggered the further investigation of asymmetrical ureas. The *N*-monosubstituted urea derivative 2d of 2c (NF340) was synthesized and showed 56-fold less potency (app.pK_i: 6.05) than the *N,N'*-disubstituted symmetrical urea 2c (NF340).Compound 2d exhibited similar potency as the nitro precursor (2a). Figure 4.14 shows the structure of 2d and the concentration-inhibition curves of 2c and 2d at $P2Y_{11}$ receptors.

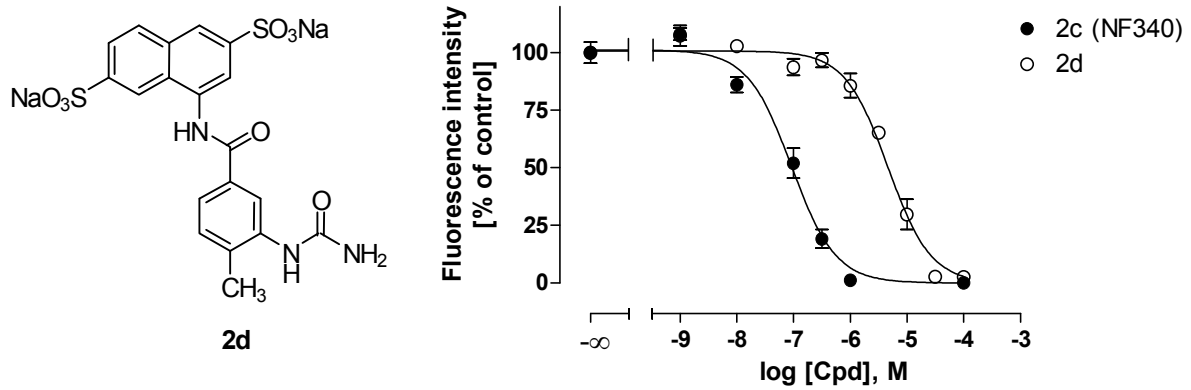

Figure 4.14. Characterization of the *N*-monosubstituted urea derivative 2d. Concentration-response curves of 2c (NF340) and 2d at $P2Y_{11}$ receptors are shown. 1 µM ATP was used as agonist.
pIC_{50} [2c, NF340] = 7.03 ± 0.06. pIC_{50} [2d] = 5.34 ± 0.07. Slopes were not significantly different from unity.

Ten asymmetrical urea derivatives were screened at a concentration of 100 µM and showed 81.1 – 99.7 % inhibition of the standard agonist (1 µM ATP) response at $P2Y_{11}$ receptors (Figure 4.15). All compounds were further investigated to estimate app.pK_i values.

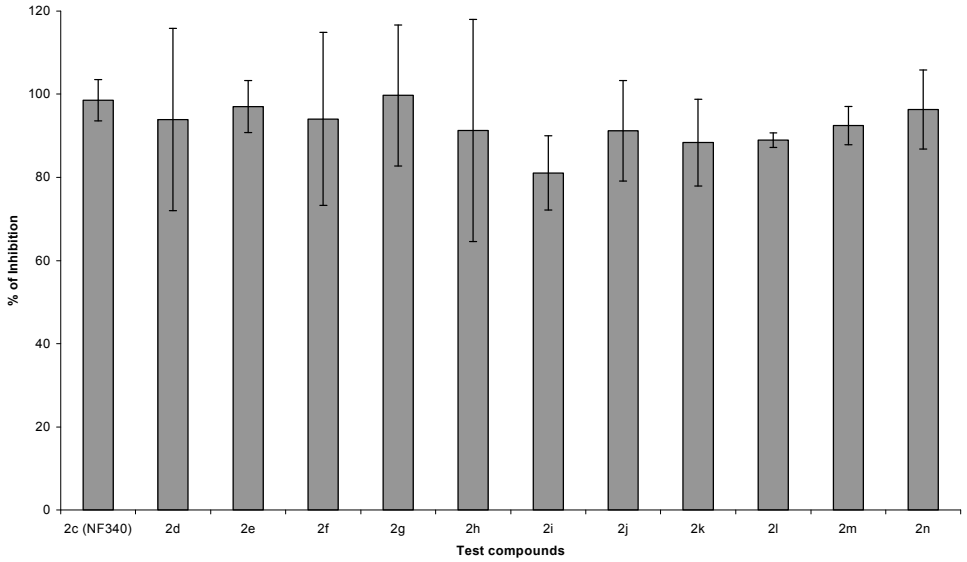

Figure 4.15. Primary screening for the antagonistic effect (% inhibition) by 100 µM of NF340 or asymmetrical urea derivatives of 1 µM ATP induced calcium mobilization at $P2Y_{11}$ receptors recombinantly expressed in 1321N1 astrocytoma cells.

The obtained app. pK_i values are shown in Table 4.9.

Table 4.9. Structural formulas and functional inhibitory activity of asymmetrical urea derivatives of NF340 at $P2Y_{11}$ receptors recombinantly expressed in 1321N1 cells.

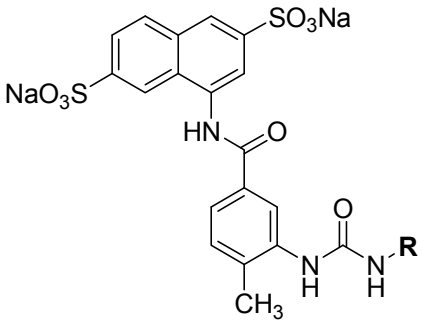

Cpd	R	app.pK_i	K_i (nM)	Cpd	R	app.pK_i	K_i (nM)
2d	H	6.05 ± 0.05	891	**2f * (thio-urea)**	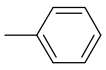	**6.89 ± 0.26**	**129**
2e	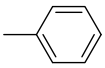	6.36 ± 0.25	436				
2g	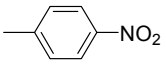	6.62 ± 0.04	240	2h	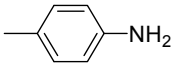	6.53 ± 0.14	295
2i	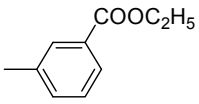	6.23 ± 0.18	589	2j	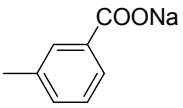	6.79 ± 0.29	162
2k	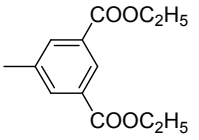	5.98 ± 0.29	1047	2l	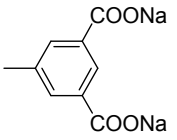	6.30 ± 0.14	501
2m	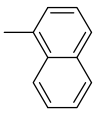	6.13 ± 0.36	741	2n	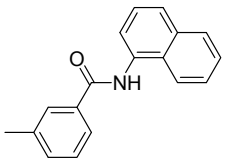	6.16 ± 0.30	692

To evaluate an extension of the structure of 2d, the *N'*-phenyl derivative 2e, was synthesized and tested for activity. Compound 2e showed 2-fold higher potency than the parent compound 2d, but was 28-fold less potent than the symmetrical urea 2c (NF340). Because nitro- and amino-precursors of 2c (NF340) were found as active $P2Y_{11}$ receptor antagonists (see Table 4.3 and Table 4.5), the nitro- and amino-derivatives of 2e (2g and 2h) were synthesized and tested. Compound 2g and 2h showed similarly potency and were slightly more potent than the non-substituted phenyl compound 2e.

Extension of compound 2d with naphthalene or 2e with naphthalene amido moiety resulting in 2m or 2n, respectively, did not result in a major change of the potency.
Variation of the phenyl-substitution with an ethyl ester group in meta-position (2i) gave a slight decrease in potency. However, the corresponding carboxylic acid derivative 2j was about 4-fold more potent than its ester. Dicarboxylic acid substitution on the phenyl ring was further investigated in 2k and 2l. The potency of 2l was approximately 3-fold lower than the mono-carboxylic acid derivative 2j. It was noticed that the carboxylic acid derivatives showed higher activity than the ester substitution. It was concluded that a large hydrophobic group is not well tolerated. This is in agreement with the result of the substitution with a bulky naphthalene group (2m).
Although all asymmetrical urea derivatives were less potent than the symmetrical urea 2c (NF340) with app. pK_i values in the range of 5.98 – 6.89, the carboxylic acid derivative 2j showed a slightly higher potency than suramin (app. pK_i: 6.52). Therefore, it can be concluded that the symmetrical structure is not a requirement for $P2Y_{11}$ receptor antagonistic activity, but negatively charged groups at both ends of naphthalene structures were preferred for high potency. This result was in agreement with the result of Bst101, which was studied by R. Bültmann and co-worker in 1996.[100] Bst101 (Figure 4.16) was tested at P_{2Y} receptors in the rat vas deferens and guinea-pig taenia coli and showed low antagonistic activity. The authors concluded that the symmetrical nature of the suramin structure was not a requirement for the activity.

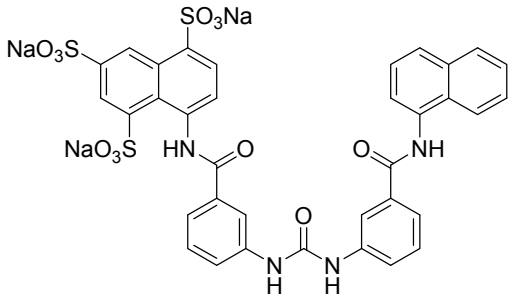

BSt101

Figure 4.16. BSt101, an asymmetrical urea derivative.

However, not all asymmetrical urea derivatives of suramin showed activity: Kassack and co-workers showed that the asymmetrical urea NF815 (Figure 4.17) was inactive at $P2Y_{11}$ receptors.[101]

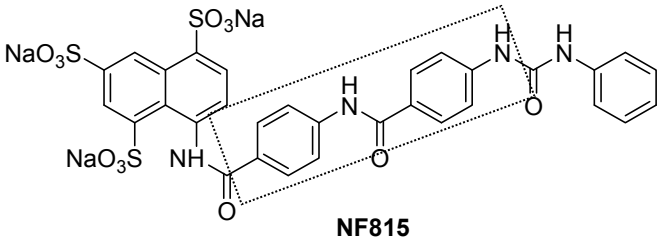

Figure 4.17. NF815, an asymmetrical urea derivative with 2 para-phenylene linkers, which is inactive at $P2Y_{11}$ receptors.

Thus, besides symmetry or asymmetry of ureas, a certain linker is required for $P2Y_{11}$ activity.

Another interesting result was found for the thiourea derivative 2f (see Table 4.9). Although the thiourea 2f was 8-fold less potent than NF340, it showed 3-fold higher potency than the corresponding urea analogue 2e. Therefore, thiourea derivatives were suggested as an interesting structure for further development of $P2Y_{11}$ receptor ligands.

4.4.6 Antagonistic activities of benzene sulfonic acid derivatives with meta phenylene-linker at $P2Y_{11}$ receptors

The next aim of this study was to investigate whether the naphthalene ring is required for $P2Y_{11}$ receptor antagonistic activity. Therefore, the size reduction from naphthalene to benzene was performed. Six new symmetrical benzene derivatives were synthesized for this purpose. These six benzene derivatives (8c – 13c) and two NF-compounds (NF250 and NF251), including their precursors (nitro- and amino- derivatives), were investigated for their activity at $P2Y_{11}$ receptors. The % inhibition of response of 1 µM ATP of all benzene derivatives, tested at a concentration of 100 µM, is presented in Figure 4.18.

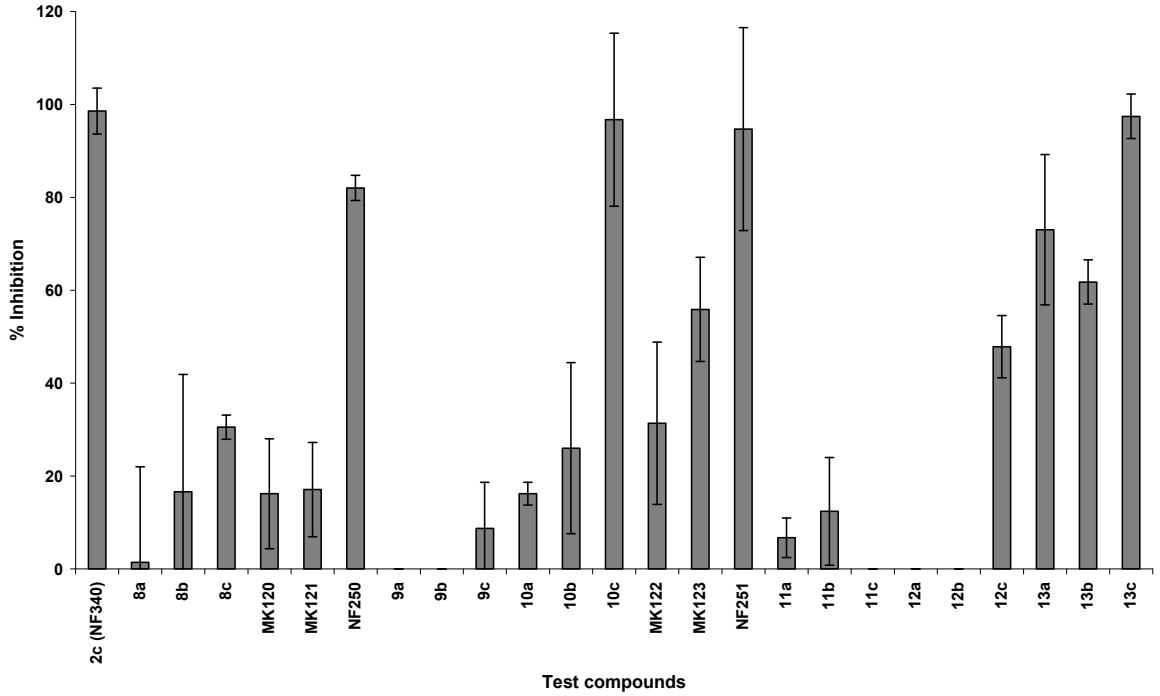

Figure 4.18. Primary screening of the antagonistic effect (% inhibition) by 100 µM of benzene sulfonic acid derivatives of 1 µM ATP induced calcium mobilization at $P2Y_{11}$ receptors recombinantly expressed in 1321N1 astrocytoma cells.

Most of the nitro- and amino-derivatives did not inhibit the effect of 1 µM ATP at $P2Y_{11}$ receptors, except one nitro compound (13a) and two amino derivatives (MK123 and 13b), which inhibited the response of 1 µM ATP by 73.0, 55.8 and 61.8 %, respectively. Compounds 13a and 13b were further selected to estimate their app. pK_i values. The result showed an equal potency of 13a and 13b (app. pK_i [13a]: 5.30; app. pK_i [13b]: 5.38). Both nitro- (13a) and amino- (13b) derivatives showed app. pK_i values in the same range as nitro- and amino-precursors of NF294 (MK100 and MK101) and slightly lower than the app. pK_i values of the precursors of 2c (NF340) (2a and 2b, Figure 4.7). The structures and app. pK_i values of 13a and 13b, in comparison with a selective of related compounds (precursors and ureas), are shown in Table 4.10.

Table 4.10. Comparison of app. pK_i values of nitro-, amino- and urea derivatives of selected series at $P2Y_{11}$ receptors recombinantly expressed in 1321N1 cells.

R	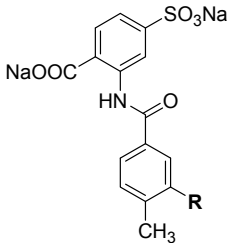	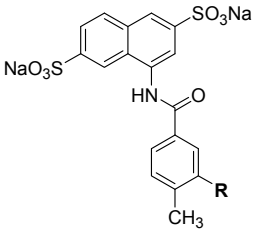	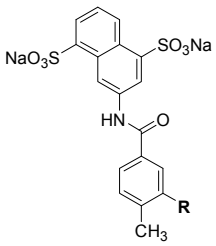	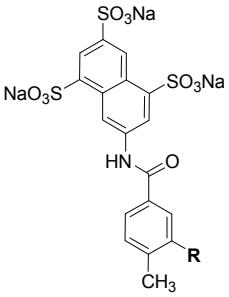
-NO_2	5.30 ± 0.11 (13a)	5.93 ± 0.25 (2a)	5.45 ± 0.08 (MK100)	4.98 ± 0.08 (7a)
-NH_2	5.38 ± 0.11 (13b)	5.67 ± 0.14 (2b)	5.16 ± 0.21 (MK101)	4.89 ± 0.24 (7b)
-NHCONH-	7.42 ± 0.14 (13c)	7.80 ± 0.15 (2c, NF340)	7.42 ± 0.11 (NF294)	7.14 ± 0.06 (7c)

The urea derivatives of benzene sulfonic acid were further investigated. Figure 4.19 shows the concentration-inhibition curves of 13c, the most potent benzene derivative and NF251, the disulfonic acid urea derivative, in comparison with 2c (NF340) at $P2Y_{11}$ receptors.

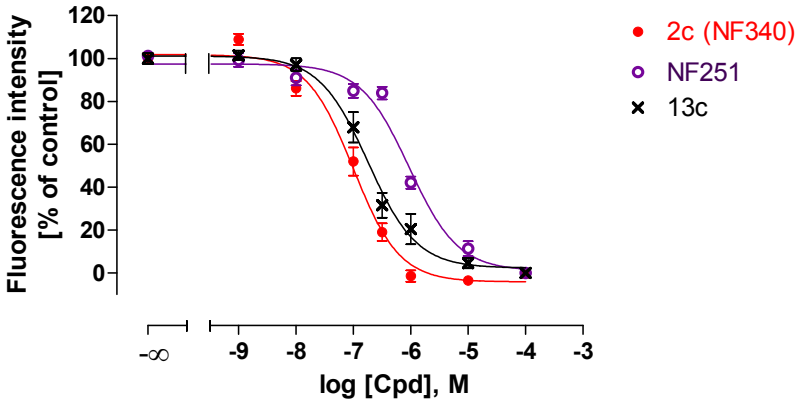

Figure 4.19. Concentration-inhibition curves of 2c (NF340), NF251 and 13c at $P2Y_{11}$ receptors recombinantly expressed in 1321N1 cells. 1 µM ATP was used as agonist.
pIC_{50} [NF251] = 6.03 ± 0.07. pIC_{50} [13c] = 6.75 ± 0.07. Slopes were not significantly different from unity.

The obtained app. pK_i values of the benzene sulfonic acid ureas are presented in Table 4.11.

Table 4.11. Structural formulas and functional inhibitory activity of benzene sulfonic acid derivatives with meta-phenylene linker at $P2Y_{11}$ receptors recombinantly expressed in 1321N1 cells.

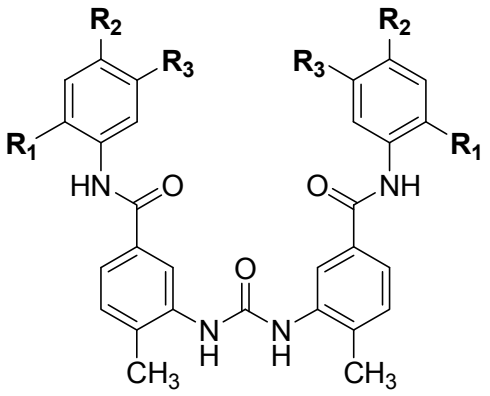

Cpd	R_1	R_2	R_3	app.pK_i	K_i (nM)
8c	-SO_3Na	-H	-H	< 4	> 100000
NF250	-H	-H	-SO_3Na	4.98 ± 0.39	10471
9c	-H	-SO_3Na	-H	< 4	> 100000
10c	-SO_3Na	-SO_3Na	-H	6.34 ± 0.01	457
NF251	-SO_3Na	-H	-SO_3Na	6.74 ± 0.11	182
11c	-CH_3	-SO_3Na	-H	< 4	> 100000
12c	-CH_3	-H	-SO_3Na	4.56 ± 0.14	27542
13c	**-COONa**	**-H**	**-SO_3Na**	**7.42 ± 0.14**	**38.0**

Two disulfonic acid substituted benzene derivatives (10c and NF251) showed a moderate potency with app. pK_i values of 6.34 and 6.74, respectively. The difference between the two compounds is the substitution in R_2 and R_3 position. A meta-position of the sulfonic acid moiety and the amido-linkage group seems more favourable. Deletion of one sulfonic acid moiety (NF250, 8c and 9c) or exchange of one sulfonic acid group by a methyl group (11c and 12c) resulted in a decrease or loss of potency. This result was in agreement with the result found in the deletion of one sulfonic acid moiety in the naphthalene derivative 2c (NF340).

An interesting result was observed in the exchange of the sulfonic acid moiety in the R_1 position with a carboxylic acid group. Compound 13c was found as the most potent benzene sulfonic acid derivative with an app. pK_i value of 7.42, which was as potent as NF294 (see Table 4.10), slightly more potent than the standard antagonist

NF157 and only 2-fold less active than 2c (NF340) (see Table 4.10, relative potency: NF157 < 13c = NF294 < NF340).

This result suggested that carboxylic acid derivatives are also interesting compounds for further study of activity at $P2Y_{11}$ receptors.

4.4.7 Benzene sulfonic acid derivatives with para-phenylene linker and their antagonistic activities at $P2Y_{11}$ receptors

Because 13c showed a high antagonistic potency at $P2Y_{11}$ receptors, structural modification of benzene sulfonic acid derivatives was also interesting to be studied. Here, changing of the substitution from meta-phenylene linker to a para-phenylene linker (Figure 4.20) was investigated.

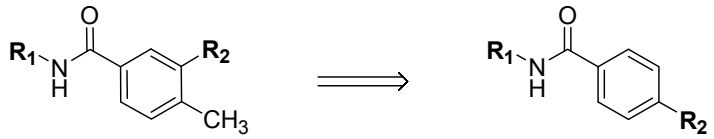

R_1 = benzene sulfonic acid moiety

R_2 = -NO_2, NH_2, -NHCONH-

Figure 4.20 Substitution of the meta-phenylene linker to a para-phenylene linker in benzene sulfonic acid derivatives.

Five new ureas (14c – 18c) were synthesized and tested for their activity. Figure 4.21 shows the % inhibition of the response of 1 µM ATP by benzene sulfonic acid ureas, including nitro- and amino-precursors, which were tested at a concentration of 100 µM.

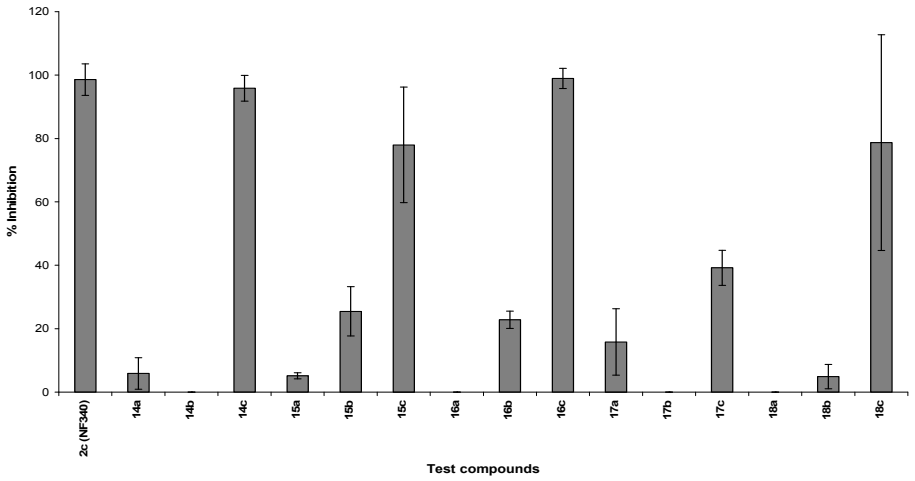

Figure 4.21. Primary screening of antagonistic effect (% inhibition) by 100 µM benzene sulfonic acid derivatives with para-phenylene linker of 1 µM ATP induced calcium mobilization at $P2Y_{11}$ receptors recombinantly expressed in 1321N1 astrocytoma cells.

Neither nitro- nor amino- derivatives showed a significant inhibitory potency at $P2Y_{11}$ receptors (less than 30 % inhibition). The urea derivatives 14c - 18c were however further investigated for their app. pK_i values and the results are shown in Table 4.12.

Table 4.12. Structural formulas and functional inhibition activity of benzene sulfonic acid urea derivatives with para-phenylene linker at $P2Y_{11}$ receptors recombinantly expressed in 1321N1 cells.

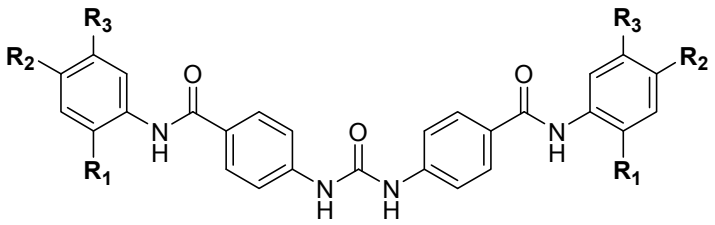

Cpd	R_1	R_2	R_3	app.pK_i	K_i (nM)
14c	**-H**	**-H**	**-SO_3Na**	**7.24 ± 0.14**	**57.5**
15c	-COONa	-H	-SO_3Na	5.42 ± 0.21	3802
16c	-CH_3	-H	-SO_3Na	6.98 ± 0.14	105
17c	-CH_3	-SO_3Na	-H	< 4	> 100000
18c	-SO_3Na	-CH_3	-H	6.29 ± 0.05	513

Compound 15c showed an astonishing result: 15c, the para-substitution analogue of 13c, was 100-fold less potent than the meta-phenylene linker analogue 13c (see Table 4.11). Replacement of the carboxylic group at R_1 of 15c by a methyl group (16c) showed a 36-fold increase in potency. This methyl analogue (16c) showed 262-fold higher potency than the corresponding meta-analogue (12c). Substitution of the carboxylic acid group at R_1 position of 15c by hydrogen (14c) showed another surprising result: 14c showed an app. pK_i value of 7.24 ± 0.14. This compound showed 66-fold higher potency than the carboxylic acid analogue (15c) and 182-fold higher potency than the corresponding meta-analogue NF250. The order of potency of 14c-16c in comparison to the meta analogues is summarized in Figure 4.22.

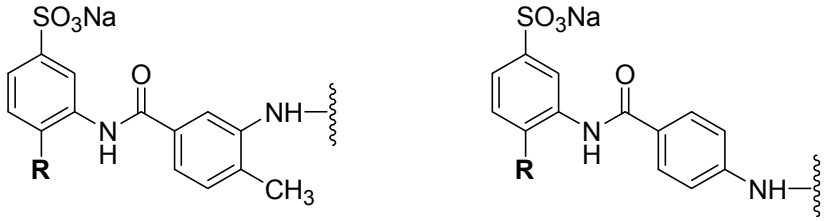

R = -COONa >> -H > -CH_3

(13c >> NF250 > 12c)

R = -H > -CH_3 >> -COONa

(14c > 16c >> 15c)

Figure 4.22. Partial structures of benzene sulfonic acid derivatives with variations of the R group and meta-phenylene or para-phenylene linker and differences in the order of potency as $P2Y_{11}$ receptor antagonist.

Variation of the position of sulfonic acid groups (17c and 18c) showed a decrease in potency in comparison to 16c (see Table 4.12) It was concluded that the antagonist activity of the benzene sulfonic acid derivatives with para-phenylene linker increased when shifting the sulfonic acid moiety in the following order: para (R_2) < ortho (R_1) < meta (R_3).

The most potent $P2Y_{11}$ receptor antagonist of the para-phenylene linkage derivatives was 14c with an app. pK_i of 7.24 which was 3.6-fold less potent than NF340 but nearly similar potent as NF157. Concentration-inhibition curves of 14c and 16c are shown in Figure 4.23.

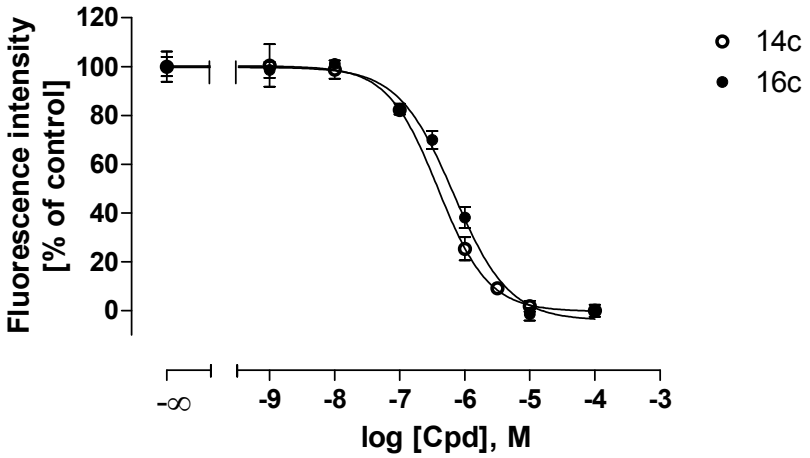

Figure 4.23. Concentration-inhibition curves of 14c and 16c at $P2Y_{11}$ receptors recombinantly expressed in 1321N1 cells. 1 µM ATP was used as agonist. pIC_{50} [14c] = 6.41 ± 0.07, n = 3. pIC_{50} [16c] = 6.17 ± 0.07, n = 3. Slopes were not significantly different from unity.

4.4.8 Competitiveness of compound 13c

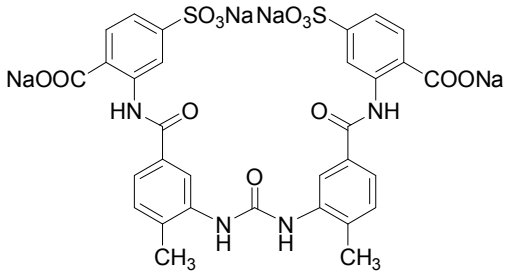

Figure 4.24. Structural formula of compound 13c, the most potent benzene sulfonic acid derivative and the most potent new compound in this work.

Compound 13c (Figure 4.24) was the first benzene sulfonic acid analogue, which showed activity slightly higher than NF157, and the most potent new compound found in this work. Therefore, the antagonistic character was further investigated. The concentration-response curves of ATP in the absence and the presence of increasing concentrations of 13c showed a rightward-shift with the same maximum effects and the same slopes (hill slopes were not significantly different from unity) (Figure 4.25).

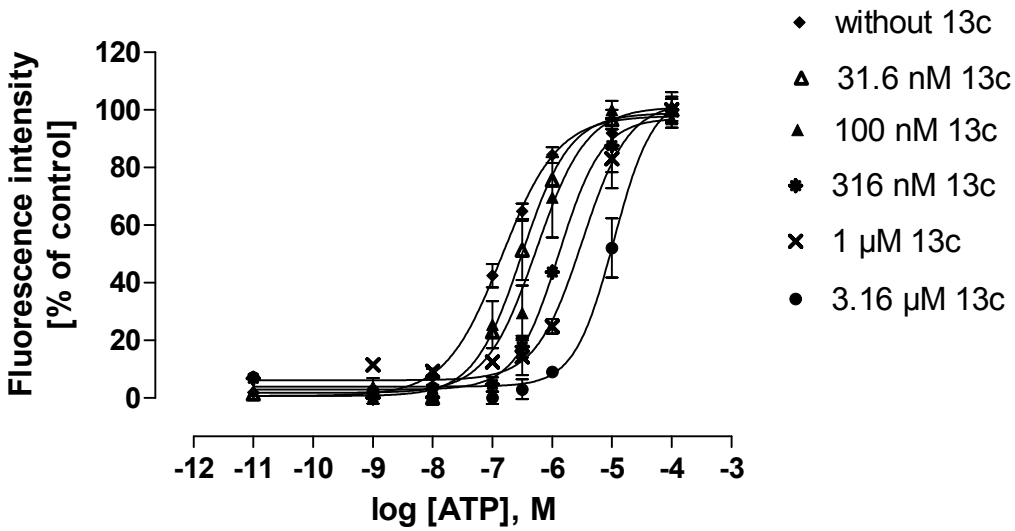

Figure 4.25. Concentration-response curves of ATP at $P2Y_{11}$ receptors using the calcium assay. ATP was tested in the absence and presence of increasing concentrations of compound 13c. n = 2. Each experiment was performed with 3 replicates. Hill coefficients were not significantly different from unity.

To investigate the nature of the antagonism of 13c and to obtain an estimate of its potency, a Schild analysis was performed. [102-104]

Schild analysis of compound 13c

The Schild plot of 13c is shown in Figure 4.26

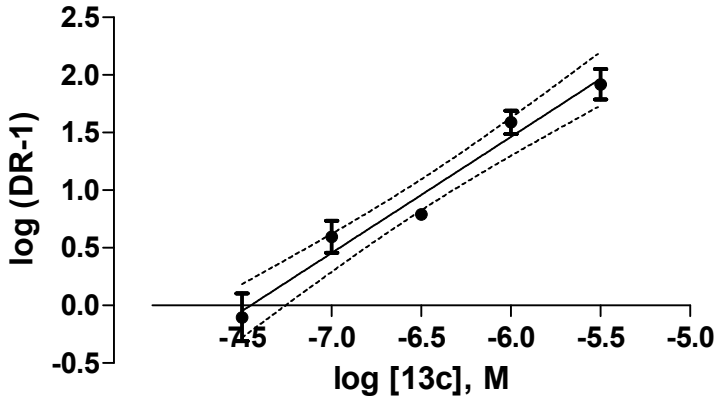

Figure 4.26. Schild plot of compound 13c. X intercept = 7.45, Hill coefficient = 1.007 ± 0.088, n = 2, each experiment was performed with 3 replicates.

The Schild plot showed a slope not significantly different from unity, hence a competitive antagonism between compound 13c at $P2Y_{11}$ receptors can be assumed.[105] The pA_2 value of compound 13c was estimated as 7.45.

Modified Clark Analysis of compound 13c

pEC_{50} values of ATP in the absence and presence of 13c were plotted against the concentration of 13c and analyzed by nonlinear regression (Figure 4.27).[106]

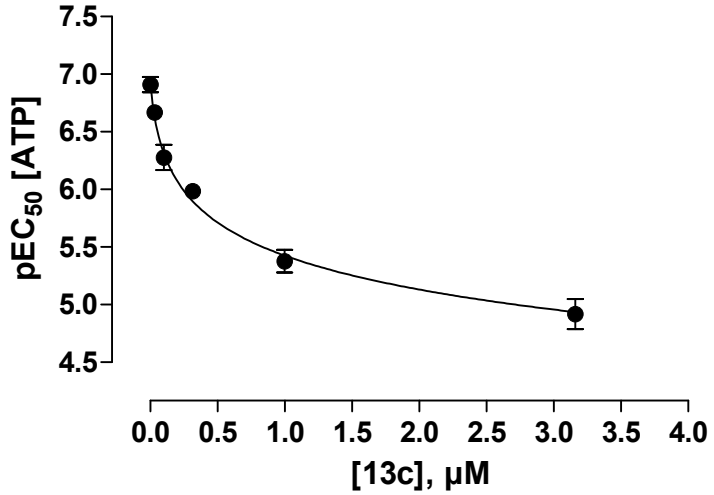

Figure 4.27. Effect of increasing concentrations of 13c on pEC_{50} ATP values. Slope = 1.003 ± 0.09

The pK_b value was obtained by nonlinear regression as 7.45 ± 0.12. This pK_b was equal to the pA_2 from Schild analysis (7.45). The corresponding Clark plot is shown in Figure 4.28. The slope was not significantly different from unity (1.003 ± 0.057).

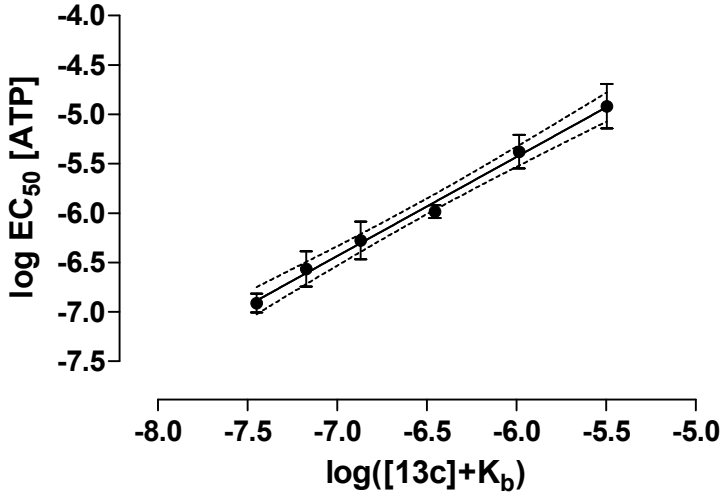

Figure 4.28. Clark plot displaying the effect of 13c on log EC_{50} ATP value. Slope = 1.003 ± 0.057.

The Clark plot shows the relationship between the experimental curve spacing and the prediction from a competitive interaction, along with the pK_b value obtained from the analysis.

4.4.9 Test for selectivity at $P2Y_{11}$ over other P2Y receptors

To evaluate the selectivity of test compounds, all compounds were screened at $P2Y_1$, $P2Y_2$ and $P2Y_4$ receptors recombinantly expressed in 1321N1 cells. None of the test compounds showed more than 40 % agonist response of the standard agonist at a concentration of 100 µM (Appendix A1-A4), except NF739 which showed 61.7 % response at $P2Y_4$ receptors. However, no response was detected at a concentration of 10 µM.

In antagonist screening, the % inhibition of all compounds screened at $P2Y_1$, $P2Y_2$ and $P2Y_4$ receptors is presented in Appendix A (A1-A4). None of the test compounds showed antagonistic activities at $P2Y_1$, $P2Y_2$ and $P2Y_4$ receptors, except NF771, 15c, NF722 and NF776. NF771 and 15c showed about 50 % inhibitory effects at $P2Y_1$ receptors at a concentration of 100 µM, but at a concentration of 10 µM, no activity was found. This phenomenon was also found for NF722 and NF776 at $P2Y_4$ receptors. Therefore, it could be concluded that none of

the compounds tested in this work shows interesting activity at $P2Y_1$, $P2Y_2$ and $P2Y_4$ receptors.

Moreover, this result allowed concluding that the most potent new antagonist 13c showed at least 2500-fold selectivity at $P2Y_{11}$ over $P2Y_1$, $P2Y_2$ and $P2Y_4$ receptors.

5 Conclusion

$P2Y_{11}$ receptors are receptors for extracellular ATP, which were found in different tissues and play roles in the immune system and are associated with an increased risk for acute myocardial infarction. However, the knowledge about this receptor subtype is limited. To evaluate and understand the pharmacological and physiological characteristics and functions of $P2Y_{11}$ receptors, potent and selective agonists and antagonists are required. Moreover, to further allow a rational design of new $P2Y_{11}$ receptor ligands, basic information about structural requirements of the compounds for activity are needed. In this study, NF340 derivatives were synthesized and studied for their activity at $P2Y_{11}$ receptors.

5.1 Synthesis of symmetrical and asymmetrical derivatives of NF340

2c (NF340) was resynthesized (originally synthesized by Prof. Nickel[73]) and its analytical data (so far not available) are presented. Five new symmetrical naphthalene- and eleven benzene-sulfonic acid derivatives of NF340 were synthesized via three step syntheses. Firstly, an aminonaphthalene or aminobenzene sulfonic acid was acylated with acid chloride at a constant pH of 4.0 – 4.5. Then, the nitro group was catalytically hydrogenated using 10 % Pd/C as a catalyst. Finally, urea formation was performed, using a solution of phosgene in toluene (20 %) at a constant pH of 3.7 – 5.5.

One *N*-monosubstituted urea was obtained from the reaction of the amine precursor of 2c (NF340) and potassium cyanate in acetic acid, whereas ten *N,N'*-asymmetrical urea/thiourea derivatives were synthesized via nucleophilic addition of amines to isocyanates/isothiocyanates. Triphosgene or phosgene was used to synthesize isocyanate intermediates.

The structure of all synthesized compounds was confirmed by nuclear magnetic resonance (^{1}H and ^{13}C NMR) spectroscopy, IR spectroscopy and mass spectrometry (MALDI-TOF or ESI). The purity of the compounds was checked by elemental analysis (C, H, N), Thin Layer Chromatography (TLC) and High Performance Liquid Chromatography (HPLC). All data are available in the Monographs section.

5.2 Biological evaluations and structure-activity relationships

Using measurement of ligand-induced changes in the intracellular calcium concentrations in 1321N1 astrocytoma cells recombinantly expressing $P2Y_{11}$ receptors, NF157, the standard $P2Y_{11}$ antagonist[65], gave an app. pK_i value of 7.35. The more potent antagonist 2c (NF340) previously identified by Meis[79] was confirmed to be 3-fold more potent than NF157 and used as a template for structure modifications.

13 Symmetrical urea derivatives of NF340 with variations in the numbers and positions of the sulfonic acid substitutions at the naphthalene ring were investigated for $P2Y_{11}$ receptor antagonistic activity. Their app. pK_i values were in the range of 4.57 – 7.80. Results are summarized as structure-activity relationships of naphthalene sulfonic acid urea derivatives of NF340 as follows (Figure 5.1):

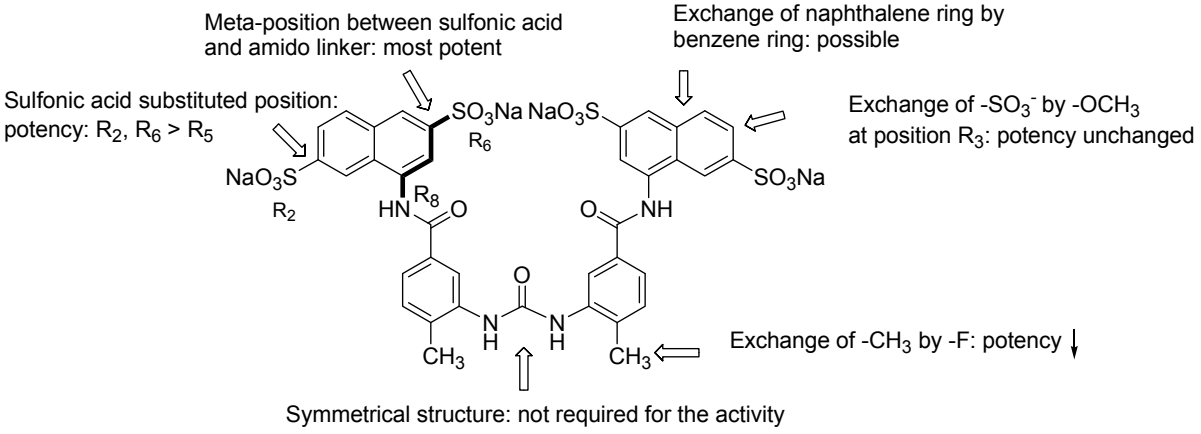

Figure 5.1. Summary of the structure-activity relationships of symmetrical derivatives of 2c (NF340) at $P2Y_{11}$ receptors derived from calcium assay. (↓ = decrease).

- Monosulfonic acid substituted naphthalene ureas showed weak antagonistic activities (see Table 4.6). Substitution of the sulfonic acid groups in R_2 or R_6 positions seems to be important for the activity and showed higher potency than the substitution in R_5 (para-) position. The combination of the substitution R_2 and R_6 resulted in the most potent $P2Y_{11}$ receptor antagonist 2c (NF340) (app. pK_i: 7.80).
- Substitution of the sulfonic acid group by a methoxy group in R_3 position or addition of a methoxy group in R_4 position showed no change in activity.

- Exchange of the 1-aminonaphthalene ring by a 2-aminonaphthalene ring retained antagonistic activity at $P2Y_{11}$ receptors (see Table 4.7). The most potent antagonist was NF294 (app. pK_i: 7.42); nevertheless, it was 2-fold less potent than the 1-aminonaphthalene sulfonic acid derivative 2c (NF340).
- The relative position at the naphthalene ring of the sulfonic acid group and the amido-linkage seems to be important for $P2Y_{11}$ receptor antagonistic potency (see Figure 4.13). Ureas with a substitution of the sulfonic acid moiety in meta-position to the amido-linkage showed high antagonistic potency in both naphthalene and benzene sulfonic acid derivatives (2c (NF340), NF294, 7c, 13c and 14c).
- The naphthalene ring could be substituted by a benzene ring. The benzene sulfonic acid ureas 13c and 14c were only slightly (2.4-fold and 3.6-fold) less potent then the naphthalene derivatives 2c (NF340).
- Exchange of the methyl group of the disulfonic acid derivative 2c (NF340) by fluorine reduced the potency by 23-fold which is in contrast to the result from Ullmann et al. for NF157 and suramin.[65]

The nitro- and amino-precursors of NF340 and derivatives were also screened for their activity and were reported as low potent $P2Y_{11}$ receptor antagonists. Eleven nitro- and six amino-derivatives showed weak to moderate antagonistic activity with app. pK_i values in the range of 4.35 – 6.24. This result indicated that the symmetry of the urea molecule is not required for $P2Y_{11}$ activity. Eleven asymmetrical urea derivatives of 2c (NF340) were thus synthesized and studied for their activity to further support this hypothesis. Although all asymmetrical ureas showed low to moderate potency at $P2Y_{11}$ receptors (app. pK_i: 5.89 – 6.89), 2g, 2h and 2j are relatively more potent than suramin (see Table 4.9). The structure-activity relationships of nitro-and amino derivatives and asymmetrical ureas are summarized as follows (Figure 5.2):

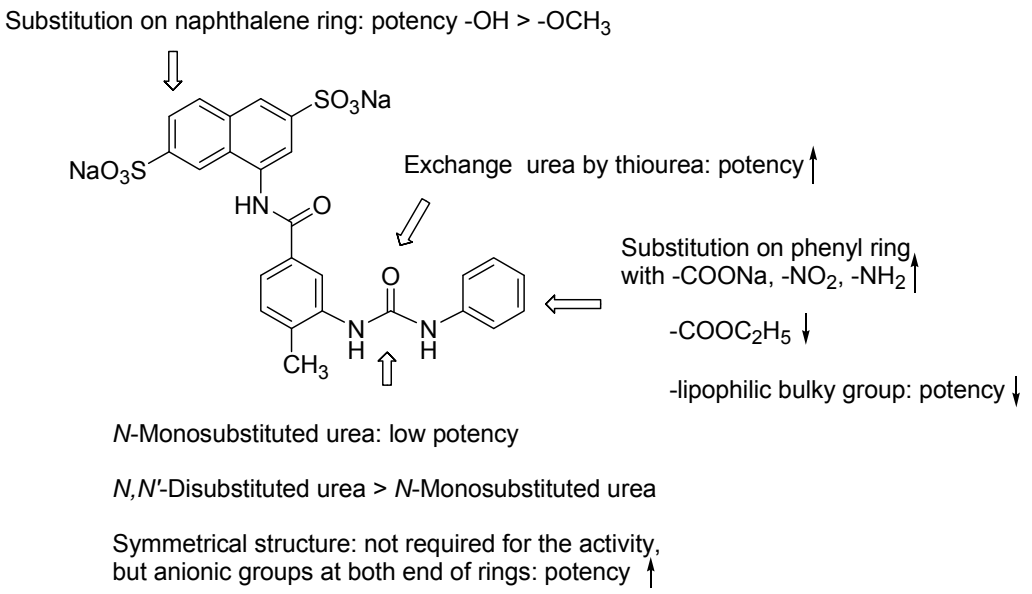

Figure 5.2. Summary of the structure-activity relationships of asymmetrical derivatives of 2c (NF340) at $P2Y_{11}$ receptors derived from calcium assay. (↑ = increase, ↓ = decrease)

- The *N*-monosubstituted urea (2d) showed similar potency to the amino precursor (2b) and lower potency than *N,N'*-disubstituted ureas (2e and 2c (NF340)).
- Substitution at the phenyl ring with $–NO_2$, $-NH_2$ or -COONa group increased the antagonistic activity at $P2Y_{11}$ receptors, whereas substitution with bulky or lipophilic groups decreased the potency.
- Exchange of urea to thiourea showed a 3-fold higher potency (2f in comparison with 2e).

The thiourea analogue 2f (Figure 5.3) showed the highest potency at $P2Y_{11}$ receptors among asymmetrical urea derivatives and was slightly (2-fold) more potent than suramin. Thiourea derivatives are suggested to be further studied.

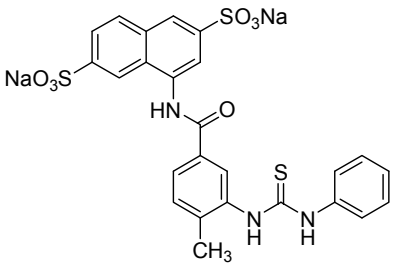

2f app. pK_i = 6.89 ± 0.26 (K_I = 129 nM)

Figure 5.3. Structural formula of thiourea 2f, the most potent asymmetrical urea confirmed that symmetrical structure was not required for $P2Y_{11}$ receptor antagonistic activity.

Eleven benzene sulfonic acid derivatives were synthesized and studied for their activity in order to investigate whether the naphthalene ring is required for $P2Y_{11}$ receptor antagonistic activity. 13 Benzene sulfonic acid urea derivatives and their nitro- and amino- precursors were investigated for their activity. The structure-activity relationships of benzene sulfonic acid derivatives are summarized as follows (Figure 5.4):

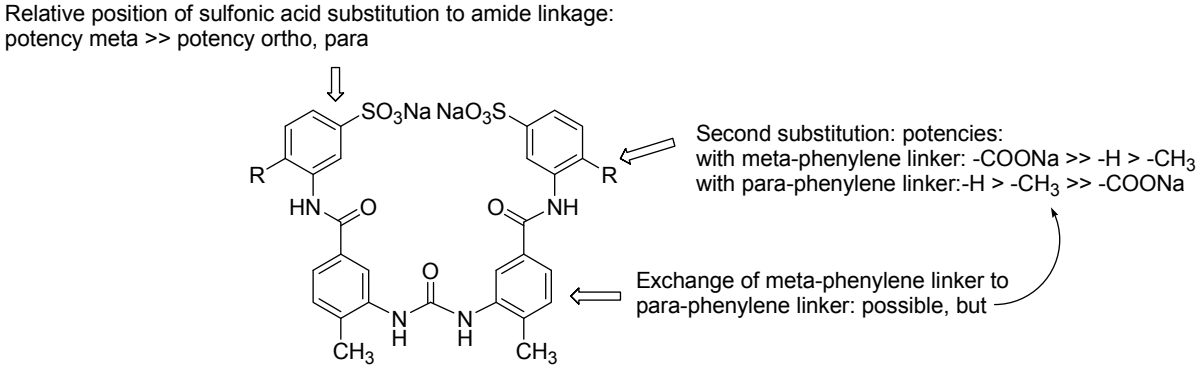

Figure 5.4 Summary of the structure-activity relationships of benzene sulfonic acid derivatives at $P2Y_{11}$ receptors derived from calcium assay.

- Relative position of a sulfonic acid group in meta-position to amido linkage showed the most potent antagonistic activity (13c and 14c, see Table 4.11 and Table 4.12).
- The second substitution at the benzene ring showed a different order of potency depending on the phenylene linker (see Figure 4.22).

  meta-phenylene linker series: -COONa >> -H > $-CH_3$

  para-phenylene linker series: H > $-CH_3$ >> -COONa
- The meta-phenylene linker in benzene sulfonic acid derivative could be substituted by a para-phenylene linker, but the rank of potency is connected with the change in the substitution pattern (see above).

13c: a new potent benzene sulfonic/carboxylic acid analogue

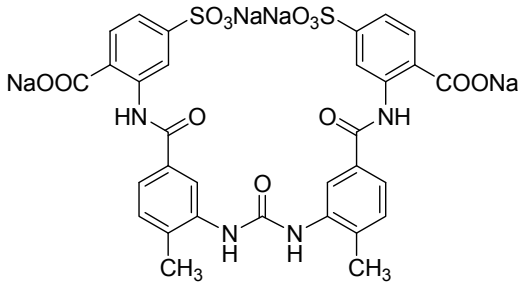

13c app. pK_i = 7.42 (K_i = 38.0 nM)

Figure 5.5. Structure formula of 13c, the most potent benzene sulfonic acid derivative with similar activity to the naphthalene sulfonic acid derivative NF294.

13c (Figure 5.5) showed a competitive antagonistic activity at recombinantly expressed $P2Y_{11}$ receptors with an app. pK_i value of 7.42 (calcium assay) and a pA_2 or pK_b value of 7.45 (Schild analysis and modified Clark analysis). 13c showed similarly potent as the standard $P2Y_{11}$ antagonist NF157 [65] and 2-fold less potent than the new standard antagonist NF340 [79]. Moreover, 13c showed at least 2500-fold selectivity for $P2Y_{11}$ over $P2Y_1$, $P2Y_2$ and $P2Y_4$ receptors.

From this result, benzene carboxylic acid derivatives are suggested to be used as templates for further investigated as $P2Y_{11}$ receptor antagonists.

6 Abstract

Because of their pharmacological role in the immune system and their discussed involvement in an increased risk for acute myocardial infarction, $P2Y_{11}$ receptors are one of the interesting pharmacological targets for drug development. In this study, NF340, the already known and so far most potent $P2Y_{11}$ receptor antagonist, and symmetrical and asymmetrical derivatives therefore were synthesized. All compounds were evaluated for their pharmacological activity by measurement of ligand-induced changes in the intracellular calcium concentration in 1321N1 astrocytoma cells recombinantly expressing $P2Y_{11}$ receptors. An app. pK_i value of 7.80 ± 0.15 of NF340 at $P2Y_{11}$ receptors was found which was in accordance with previously published data. Structure-activity relationships were analyzed: Firstly, monosulfonic acid substituted naphthalene derivatives exhibited weak antagonistic potency, whereas disulfonic acid substituted naphthalene compounds (2c (NF340) and NF294) showed the highest potency. Secondly, the symmetrical urea structure is not required for antagonistic activity at $P2Y_{11}$ receptors. However, negatively charged groups at both ends of the molecules as in 2c (NF340) increased the potency. Thirdly, compounds with meta-substitution of the sulfonic acid group and the amido-linkage showed higher antagonistic potency than ortho- or para-substitution. Fourthly, 2-aminonaphthalene sulfonic acid derivatives also exhibited potent antagonism such as compound NF294. Finally, the benzene sulfonic acid urea derivatives also showed antagonistic activity. The best benzene sulfonic acid urea (13c) showed an app. pK_i value of 7.42 ± 0.14. The rank order of potency of the most potent ligands at $P2Y_{11}$ receptors examined in this work was: 2c (NF340) > 13c = NF294 (naphthalene disulfonic acid urea) > NF157 > 2f (asymmetrical thiourea). Moreover, 13c showed also at least 2500-fold selectivity for $P2Y_{11}$ over $P2Y_1$, $P2Y_2$ and $P2Y_4$ receptors. The discovery of the activity of 13c, a benzene sulfonic/carboxylic acid urea derivative, led to the suggestion of the study of benzene carboxylic acid urea derivatives.

In conclusion, this work provided structure-activity relationships of symmetrical and asymmetrical NF340 derivatives, which will be helpful in the development of a pharmacophore model and further design of new $P2Y_{11}$ receptor ligands.

7 Zusammenfassung

Aufgrund der pharmakologischen Rolle im Immunsystem und als möglicher diskutierter Risikofaktor beim Myokardinfarkt ist der $P2Y_{11}$-Rezeptor ein interessantes pharmakologisches Target für die Arzneistoffentwicklung. Im Rahmen dieser Studie wurde NF340, der bereits bekannte und bisher potenteste $P2Y_{11}$-Rezeptor Antagonist, sowie symmetrische und unsymmetrische Derivate von NF340 synthetisiert. Diese Substanzen wurden durch Messung der Ligand-induzierten Änderung der intrazellulären Calcium-Konzentration an $P2Y_{11}$-Rezeptoren, die rekombinant in 1321N1 Astrocytoma-Zellen exprimiert wurden, auf ihre pharmakologische Aktivität hin untersucht. Der app. pK_i-Wert von NF340 betrug hierbei 7.80 ± 0.15, was in Übereinstimmung mit kürzlich publizierten Daten ist. Für die Substanzen mit ihren biologischen Aktivitäten wurden Struktur-Wirkungs-Beziehungen abgeleitet. Erstens, Naphthalinmonosulfonsäure-Derivate stellten sich als schwache Antagonisten heraus, während Naphthalindisulfonsäuren (2c (NF340) und NF294) die höchsten Potenzen zeigten. Zweitens ist die symmetrische Struktur der Harnstoffe für eine antagonistische Aktivität an $P2Y_{11}$-Rezeptoren nicht notwendig. Allerdings erhöhen negativ geladenen Gruppen an beiden Enden der Moleküle wie in 2c (NF340) die Potenz. Drittens zeigten die Verbindungen mit meta-Substitution der Sulfonsäuregruppe und der Amidgruppe höhere antagonistische Potenz als ortho- oder para-Substitution. Viertens wiesen 2-Aminonaphthalin-sulfonsäure-Derivate wie NF294 eine fast ebenbürtige antagonistische Potenz auf. Zuletzt wurden gezeigt, dass auch Benzensulfonsäure-Harnstoffe eine antagonistische Aktivität besitzen. Der beste Benzensulfonsäure-Harnstoff 13c besitzt einen app. pK_i-Wert von 7.42 ± 0.14. Die Rangfolge der potensten Liganden an $P2Y_{11}$-Rezeptoren, die in dieser Arbeit untersucht bzw. entdeckt wurden, ist: 2c (NF340) > 13c = NF294 (Naphthalindisulfonsäure-Harnstoff) > NF157 > 2f (unsymmetrischer Thioharnstoff). Außerdem ist 13c mindestens 2500-fach selektiv für den $P2Y_{11}$-Rezeptor gegenüber $P2Y_1$-, $P2Y_2$-, und $P2Y_4$-Rezeptoren. Die Entdeckung der hohen Aktivität von 13c, einem gemischten Benzensulfonsäure/carbon-säurederivat, führte zur Schlussfolgerung, dass die Entwicklung von weiteren Benzencarbonsäure-Harnstoff-Derivaten interessant ist. Zusammengefasst erstellte diese Arbeit Struktur-Aktivitäts-Beziehungen von symmetrischen und

unsymmetrischen Harnstoff-Derivaten von NF340. Diese sind für die Erstellung eines Pharmakophormodelles sowie für das weitere Design neuartiger $P2Y_{11}$-Rezeptor-Liganden sehr hilfreich.

8 Experimental Part: Chemistry

8.1 Equipments and methods

8.1.1 Melting point measurement

Mettler FP 61

Melting points were uncorrected. The melting points of naphthalene sulfonic acid derivatives were over 250°C, therefore the results were not shown in monograph.

8.1.2 Thin layer chromatography

TLC-Plate:	Silica gel 60 F254 (aluminium sheets), Merck; Art. Nr. 5554
Developing solvent:	see text
Detection:	UV-light at wavelength 254 nm and/or 366 nm.
Spraying agent:	Ehrlich's reagent (for detection of primary aromatic amine)
Ehrlich's reagent	1 g 4-dimethylaminobenzaldehyde
	2.5 ml glacial acetic acid
	7.5 ml methanol

8.1.3 High performance liquid chromatography (HPLC)

Computer:	HP9000 Series 300 model 310, Hardware: HP 9153C,
	Monitor: 35741B
Printer:	HP Think Jet Printer
Pump:	HP Series 1050, Manual Injection
Detector	Diode array detector HP 1040A
Column:	RP-8, MOS-Hypersil, 5 µM, 100 x 2.1 mm, HP
Precolumn:	RP-8, MOS-Hypersil, 5 µM, 20 x 2.1 mm, HP
Software:	HP79994A HPLC ChemStation
Flow rate:	0.6 ml/min
Injection volume:	10 µl
Detection:	UV 254, 299, 220 nm
Detection limit:	0.1 mAU

Mobile phase:

System 1

		% A	% B
0	min	20	80
8	min	46	54
9	min	80	20
11	min	20	80

System 2

		%A	%B
0	min	0	100
8	min	54	46
10	min	0	100

A = methanol

B = 400 ml TBAHS-phosphate buffer + 100 ml methanol

TBAHS-phosphate buffer pH 6.5

931 mg (7.76 mM)	NaH_2PO_4
1.738 g (12.24 mM)	Na_2HPO_4
2.122 g (6.25 mM)	TBAHS (Tetrabutylammonium hydrogensulfate)

931 mg NaH_2PO_4 and 1.738 mg Na_2HPO_4 was dissolved in 400 ml dist. water. 2.122 g TBAHS was added and dist. water was filled up to 1000 ml. The buffer was adjusted to pH 6.5 with *o*-phosphoric acid.

8.1.4 Sodium chloride measurement

20 mg substance was dissolved in 8 ml water and 2 ml glacial acetic acid and titrated with 0.1 M silver nitrate solution.

$$\%\,NaCl = \frac{58.44 \times V_{titrant} \times N_{titrant} \times 100}{m_{Substance}}$$

$V_{titrant:}$ Volume of 0.1 N silver nitrate (ml)
$N_{titrant}$: Normality of silver nitrate
$m_{Substance}$: weight of test compound (mg)

8.1.5 Elemental analysis

Elemental Analysensysteme GmbH VarioEL V2.4

Elemental analysis was done at Pharmaceutical Institute, University of Bonn. C/N-Ratio confirmed the purity by the comparison with the theoretical value. Most of % C and % H results showed a great deviation from calculation because of crystal water and sodium chloride. When calculation was performed considering amount of NaCl and water, all of results were in agreement with the calculation (deviation ≤ 0.4).

8.1.6 ^{1}H and ^{13}C NMR spectroscopy

Bruker DRX 500 MHz Spectrometer

DMSO-d_6 was used as a solvent for NMR measurement. D_2O exchange spectrum has been done to prove exchangeable protons. H-H COSY (Correlation Spectroscopy) and HSQC (Heteronuclear single quantum correlation) were done to prove the structure and position of 4-nitro-2,6-naphthalene disulfonic acid. HSQC was also done to prove the structure of 3c and 6c. The chemical shift is displayed as δ in ppm. Spectrum analysis was done by comparison with a calculated value from the “substituent increments” and also by comparison with other compounds in the series.

8.1.7 IR spectroscopy

Perkin-Elmer Paragon 1000FT-IR-Spectrometer

Software: Perkin-Elmer Report Manager 1.30

IR spectrum was done as KBr pellet. Results are presented as intensity (s = strong, m = medium, w = weak, br = broad).

8.1.8 UV spectroscopy

UV spectrum was obtained from HPLC-DAD.

8.1.9 Mass spectrometry

MALDI-TOF MS

Brucker Daltinics flexAnalysis

MALDI-TOF MS was done in the Chemistry Department, University of Düsseldorf. Dihydroxy benzoic acid (DHB) was used as a matrix.[107]

ESI-MS

Finnigan MAT 8200

ESI-MS was performed by Dr. Ebel and Ms. Julia Kjer from the department of Pharmaceutical Biology, University of Düsseldorf. The substances were dissolved in water and directly injected.

8.2 General procedures of synthesis

General procedure 1: Acylation of aromatic amine in aqueous solution

10 - 20 mmol Amino naphthalene/benzene sulfonic acid precursor was dissolved or suspended in 50-100 ml water. The pH of the solution was adjusted to 4.0-6.0 (see detail in Monographs). 4-Methyl-3-nitrobenzoyl chloride (or 4-nitrobenzoyl chloride) in toluene was slowly dropped into the aqueous solution under constant pH of 4.0 - 4.5 by automatic addition of 2 M Na_2CO_3 solution. The reaction was followed by TLC, in which the amine precursor was checked by spraying with Ehrlich's reagent. After the reaction was completed, the mixture was acidified to pH 2.0 with 2 N HCl and extracted four times with 100 ml diethyl ether. The aqueous phase was neutralized and evaporated by rotatory evaporator. The crude product was recrystallized in methanol.

General procedure 2: Catalytic hydrogenation of aromatic nitro derivatives

Each nitro-derivative was dissolved or suspended in water or aqueous methanol. 20 – 100 mg 10 % palladium/carbon was added to the solution and the nitro-derivative was hydrogenated under pressure (4 bars) in a Parr apparatus. After the reaction was completed, the Pd/C was filtrated out. The solution was neutralized and evaporated until dryness. The crude product was purified by stirring in methanol.

General procedure 3: Phosgenation

1 – 5 mmol Amine compound was dissolved in 30 - 100 ml water. A solution of 20 % phosgene in toluene was slowly dropped to the amine solution at a constant pH of 3.7 – 5.5 by automatic addition of 2 M Na_2CO_3 solution. After the reaction was completed, the water phase was separated, neutralized with 5 M NaOH and then evaporated until dryness. The crude product was stirred in 80 ml methanol for 24 h, filtrated and dried.

General procedure 3: Cation exchange chromatography

200 g Cation exchange (strong acid) were filled in a glass column. The column was washed with 200 ml 2 M HCl and followed by dist. water until pH 5.0. The sample, dissolved in 20 – 50 ml water, was loaded to the column and eluted with water. The eluate was collected until pH 5.0, neutralized with 1 M NaOH and evaporated until dryness. The crude product was stirred in methanol, filtrated and dried.

8.3 List of chemicals

	Company	Catalogue number.
Acetic acid	Riedel-de Haën	33015
1-Aminonaphthalene-3-monosulfonic acid	*	-
1-Aminonaphthalene-4-monosulfonic acid	Aldrich	250619
4-Aminonaphthalene-2,7-disulfonic acid	Sigma-Aldrich	S564028
7-Aminonaphthalene -1,3,5- trisulfonic acid, disodium salt	Wako	328-20712
8-Aminonaphthalene-2-monosulfonic acid	Sigma	A7782
6-Amino-m-toluenesulfonic acid	Acros	20400
Ammonia solution (25%)	Riedel-de Haën	05003
Aniline-2,4-disulfonic acid (4-aminobenzene-1,3-disulfonic acid)	Wako	328-43135
Aniline-2-sulfonic acid (2-aminobenzene sulfonic acid)	Fluka	75520
Aniline-3-sulfonic acid (3-aminobenzene sulfonic acid)	Fluka	06998
Aniline-4-sulfonic acid (Sulfanilic acid)	Fluka	86090
Cation exchange (strong acid)	Merck	15131
N,N-Dimethylformamide (DMF)	Fischer Scientific	D3841-15
4-(Dimethylamino)benzaldehyde	Merck	3085
Methyl-4-aminobenzoate	Acros	23528
Naphthyl-1-amine	Merck	6245
Naphthalene-2,6-disulfonic acid, disodium salt	Aldrich	N60-5
3-Nitrobenzoyl chloride	Fluka	73110
4-Nitrobenzoyl chloride	Aldrich	11220-8
5-Nitroisophthalic acid	Fluka	73450
3-Nitro-4-methylbenzoic acid	Fluka	68026
4-Nitrophenyl isocyanate	Acros	29670
10% Palladium/Carbon (Pd/C)	Merck	807104
Phenyl isocyanate	Acros	13069
Phenyl isothiocyanate	Acros	16097
Phosgene (20% in Toluene)	Fluka	79380
Potassium cyanate	Fluka	60160
Silica gel 60 for column chromatography, size 0.040 – 0.063	Merck	9385
Silver nitrate solution 0.1 N	Grüssing	23262
Sodium carbonate, dry	KMF Optichem	KM.04-005
Sodium dihydrogen phosphate water-free puriss	Fluka	71496
di-Sodium hydrogen phosphate water-free puriss	Fluka	71640

Sodium hydroxide	KMF lab	BAY02-4670500
4-Sulfoanthranilic acid	*	-
Tetrabutylammonium hydrogensulfate puriss	Fluka	86853
Thionyl chloride	Fluka	88952
p-Toluenesulfonic acid	Acros	42122
Triethylamine	Fluka	90335
Triphosgene	Acros	25895

* Gift from Bayer

9 Experimental Part: Pharmacology

9.1 Equipment and chemicals

Material and equipment

Novostar® Microplate-Reader	BMG LabTech, Offenburg, Germany
Cell culture flask	Cellstar® T175 and T75, Greiner Labortechnik, Frickenhausen
Incubator	CO_2 Water Jacket Incubator, Forma Scientific, Marjetta, USA
Centrifuge	AventiTM J25, Beckmann, California, USA Eppendorf 5417C, Hamburg
Shaker	MS1 Minishaker, IKA® Wilmington, USA
Measurement plate	Microplate, 96 wells, F-form, Greiner Labortechnik, Frickenhausen
Reagent plate	Microplate, 96 wells, U-Form Greiner Labortechnik, Frickenhausen

Cell culture medium

500 ml	Dulbecco's modified Eagle Medium (DMEM, Sigma)
10%	Fetal bovine serum FBS (Sigma)
5 mM	L-glutamine (Sigma)
100 U/ml	Pennicillin G (Sigma)
100 µg/ml	Streptomycin (Sigma)
200 µg/ml	G418 (Geneticinsulfate), Calbiochem-Navabiochem Corporation, San Diegeo, USA (concentation 100 mg/ml)

Fluorescence probe

Oregon green 488 BAPTA-1-AM® 1mM

50 µg Oregon green 488 BAPTA-1-AM were dissolved in 39.7 µl DMSO and aliquoted into 3 µl.

Pluronic F-127 solution 20 %

200 mg Pluronic F-127 were dissolved in 1 ml DMSO.

Krebs-HEPES-Buffer (KHB) stock solution (5x)

17.33 g	Sodium chloride
5.796 g	D-Glucose monohydrate
5.958 g	HEPES 4-(2-hydroxyethyl)-1-piperazineethanesulfonic acid
0.876 g	Potassium chloride
0.882 g	Sodium hydrogen carbonate
0.408 g	Potassium dihydrogenphosphate

The substances were dissolved in 450 ml dist. water in 500 ml volumetric flask. The buffer was adjusted to pH 7.4 with 1 N NaOH and then dist. water was filled up to 500 ml.

Calcium chloride (1 M) and Magnesium sulphate (1 M) stock solution

1.470 g	Calcium chloride dehydrated was dissolved in 10 ml dist. water.
2.465 g	Magnesium sulphate heptahydrate was dissolved in 10 ml dist. water

Krebs-HEPES-Buffer (KHB) solution (1x)
300 ml Water was added in 100 ml KHB stock solution (5x) in 500 ml volumetric flask. 650 µl 1 M $CaCl_2$ was added, following by adding of 600 µl 1 M $MgSO_4$. The dist. water was filled up to 500 ml.

9.2 1321N1 Cells

1321N1 astrocytoma cells, a human brain tumor cell line, were used for recombinant expression of $P2Y_1$, $P2Y_2$, $P2Y_4$, or $P2Y_{11}$ receptors, respectively. All recombinant cell lines were established by S. Meis.[79;108]
$P2Y_1$, $P2Y_2$, $P2Y_4$ and $P2Y_{11}$-receptors recombinantly expressed in 1321N1 in astrocytoma cells were cultured in Dulbecco's modified Eagle Medium, containing sodium pyruvate, glucose (4500 mg/L) 100 U/ml penicillin G, 100 µg/ml streptomycin, 10% fetal bovine serum, 5 mM L-Glutamine and 200 µg/ml G418. Cells were incubated at 37°C in 5% CO_2.

9.3 Measurements of intracellular calcium

1. Preparation of compounds

All compounds were dissolved in dist. water or in DMSO as a concentration of 10 mM and then diluted in KHB solution to a concentration of 10^{-9} – 10^{-4} M.

2. Preparation of cells

Cells were cultured in a T175 cell culture flask to 90% confluence, harvested by using 3 ml 0.05 % trypsin/0.02 % EDTA and rinsed with 10 ml cell culture medium. After centrifugation, pelleted cells were resuspended in new medium and incubated at 37°C in 5 % CO_2 for 30 min. The cells were washed two times with 800 µl KHB and then resuspended in 500 µl buffer. 3 µl Oregon Green G488® BAPTA-1AM and 3 µl pluronic F-127 were added and cell suspension was gently shaked for 60 min at room temperature. After rinsing three times with 800 µl KHB, the cell suspension was diluted and finally plated into 96 well plates at a density of 50,000 -100,000 cells/well.

3. Measurement of fluorescence intensities

For agonist activity, 20 µl of the test substances were directly injected into the cells. For antagonist activity, the test compounds were pre-incubated with the suspension cells at 37°C for 30 min, followed by injection of agonist (31.6 nM 2-Me-SADP for $P2Y_1$, 1 µM UTP for $P2Y_2$, 100 nM UTP for $P2Y_4$, or 1 µM ATP for $P2Y_{11}$ receptors). Excitation wavelength was 485 nm (bandwidth 12 nm). Fluorescence intensity was monitored at 520 nm (bandwidth 35 nm) for 30 second at 0.4 second intervals.

9.4 Data analysis

9.4.1 % Response and % inhibition

The fluorescence intensity (F) was obtained from the difference of the fluorescence intensity measuring before and after injection.

$$F = F_{Max} - F_{Min}$$

F: Fluorescence signal produced by a compound
F_{Max}: the maximum intensity after the injection of a compound (between 11.6 - 30 sec)
F_{Min} the minimal intensity before injection of the substance (between 0 - 11.5 sec)

A % response of test compounds was calculated from the comparison of the fluorescence intensity of the test compound, of buffer and of the standard agonist using the Excel® software.

The fluorescence intensity evoked by standard agonists was set as maximal stimulation (100 %), whereas the fluorescence intensity of buffer was set as control (0 %). Antagonistic activity of test compound was presented as % inhibition:

% Inhibition = 100 - % response.

All compounds were investigated for agonistic and antagonistic activities at a concentration of 100 µM as a primary screening with 3 replicates. % Response and % inhibition are shown in Appendix A as means ± SD.

9.4.2 EC_{50}, IC_{50} and pK_i values

IC_{50}: the molar concentration of an antagonist that reduces the response of an agonist by 50 %

EC_{50}: the molar concentration of an agonist that produces 50 % of the maximal possible effect of that agonist

A concentration-response curve or concentration-inhibition curve was constructed by plotting the fluorescence intensities (F) against log concentrations of test compound. An EC_{50} or IC_{50} was estimated, using nonlinear regression analysis by the software GraphPad Prism 4.00®. Fluorescence intensity was also presentes as % of control, in which the maximal fluorescence intensity of ATP was set as 100 %, whereas the fluorescence intensity of complete inhibition of 1 µM ATP by 100 µM NF157 was set as 0 %.

Apparent functional K_i values (app. pK_i = -log K_i) were calculated according to the equation of Cheng and Prusoff:[109]

$$K_i = \frac{IC_{50}}{1 + \frac{[L]}{EC_{50}}}$$

K_i: apparent functional K_I

IC_{50}: the molar concentration of a test compound that reduces the response to 1 µM ATP by 50 %

EC_{50}: the molar concentration of ATP that produces 50 % of the maximal possible effect of ATP

[L]: the molar concentration of the used agonist (1 µM ATP).

The app. pK_i value was presented as means ± SEM (n ≥ 3, each experiment was performed with 3 replicates).

9.4.3 Analysis of competitive character of compound 13c

Concentration-response curves of ATP in the absence and in the presence of 31.6 nM, 100 nM, 316 nM, 1 µM and 3.16 µM of compound 13c were monitored and an EC_{50} of each concentration was calculated. The obtained EC_{50} values were further used for analysis by linear regression method (Schild analysis[105,109]) and non-linear regression method (Clark analysis[106]).

Schild plot analysis

DR (Dose ratio) was calculated as follows:

$DR = EC_{50}^*/EC_{50}$

EC_{50}^*: The EC_{50} of ATP obtained in the presence of 13c.
EC_{50}: The EC_{50} of ATP obtained in the absence of 13c.

A plot of (DR-1) against log concentration of 13c was performed and analysed by linear regression, using the software GraphPad Prism 4.00®.
A pA_2 was calculated from an X-intercept of the plot.[110;111] If the slope was not significantly different from unity, a competitive character could be assumed and the pA_2 was allowed to refer as pK_d.

Modified Clark analysis

A plot of the pEC_{50} value of ATP against the concentrations of 13c was performed. If the slope is not significantly different from unity, a competitive character could be assumed and the pK_b can be directly estimated from the following equation.[106]

$$pEC_{50} = -\log([B] + 10^{\log(K_b)}) - \log(c)$$

EC_{50}: the molar concentration of ATP that produces 50 % of the maximal possible effect of ATP
[B]: concentration of antagonist (13c)
K_b: dissociation constant
c: constant

Further, log EC_{50} value of ATP were plotted against log ([13c]+K_b) (Clark plot).

10 Monographs

4-Nitronaphthalene-2,6-disulfonic acid disodium salt (1a)

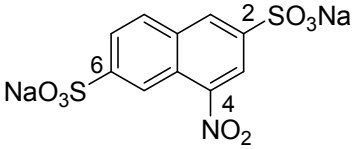

$C_{10}H_5NNa_2O_8S_2$ (377.3)

1.66 g (16.5 mmol) Potassium nitrate, dissolved in 10 ml conc. H_2SO_4, were slowly dropped into a cooled suspension of 5.00 g (15 mmol) naphthalene-2,6-disulfonic acid in 25 ml conc. H_2SO_4. The mixture was stirred for an hour at 0°C and then stirred overnight at room temperature. A cooled 10 ml 20 % NaCl aqueous solution was slowly dropped into the conc. H_2SO_4 reaction solution und the mixture was stirred at 0°C until a yellow product precipitated. The product was filtrated and washed with cooled 20 % NaCl aqueous solution and methanol. The product was recrystallized from methanol.

Yield: yellow powder, 4.73 g (83.6 %)
Purity: 88.4 % (HPLC: t_R = 5.03 min, system 2)
TLC: Rf = 0.34 (Isopr + NH_3 = 5 + 1)
NaCl: < 1 %
Water: 2 mol/mol
CHN analysis:

	% C	% H	% N	C/N
Calcd	31.84	1.34	3.71	8.58
Calcd (with NaCl/H_2O)	29.06	2.19	3.39	8.58
Found	29.23	2.46	3.45	8.46

500 MHz ^{1}H NMR Spectrum (DMSO-d_6): δ/ppm

ABX-A'X'-system

8.64	pt (H5; X)	8.53	pt (H1; X')
8.21	d (H8; B)	8.41	d (H3; A')
7.90	dd (H7; A)		
	$^3J_{AB}$ = 8.5 Hz	$^3J_{BA}$ = 8.5 Hz	
	$^4J_{AX}$ = 1.6 Hz	$^4J_{XA}$ = 1.6 Hz	
	$^4J_{A'X'}$ = 1.6 Hz		
	$^5J_{XX'}$ = 0.8 Hz		

125 MHz ^{13}C NMR Spectrum (DMSO-d_6): δ/ppm

C1	130.3	C4	146.2	C6	149.4	C8a	133.4
C2	145.1	C4a	123.4	C7	125.9		
C3	122.2	C5	118.7	C8	129.6		

IR Spectrum: cm^{-1}

3472 (s)	1628 (m)	1522 (s)	1348 (s)	1216 (s)	1153 (m)
1103 (s)	1044 (s)	896 (w)	812 (w)	686 (s)	640 (s)

UV Spectrum (phosphate buffer pH 6.5), λ_{max}: nm

222.5

ESI-MS negative mode (calcd/found): m/z
353.9/354.3 $[M-Na]^-$, 730.9/731.2 $[2M-Na]^-$

4-Aminonaphthalene-2,6-disulfonic acid disodium salt (1b)

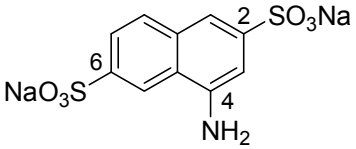

$C_{10}H_7NNa_2O_6S_2$ (347.3)

50 mg 10 % Pd/C were added to a solution of 5.32 g (13.88 mmol) 4-nitronaphthalene-2,6-disulfonic acid disodium salt (1a) in 150 ml water. The mixture was hydrogenated under pressure, according to general procedure 2. After the reaction was completed, the Pd/C was filtrated out and the solution was evaporated. The crude product was stirred in methanol and then filtrated.

Yield: brown powder, 4.82 g (98.4 %)
Purity: 93.5 % (HPLC: t_R = 2.66 min, system 2)
TLC: Rf = 0.15 (Isopr + NH_3 = 5 + 1)
NaCl: 12.5 %

500 MHz ^{1}H NMR Spectrum (DMSO-d_6): δ/ppm

ABX- A'X' system

8.26	pt (H5; X)	7.31	pt (H1; X')
7.67	d (H8; B)	6.98	d (H3; A')
7.60	dd (H7; A)		

$^3J_{AB}$ = 8.5 Hz $^3J_{BA}$ = 8.5 Hz
$^4J_{AX}$ = 1.6 Hz $^4J_{A'X'}$ = 1.6 Hz
$^5J_{XX'}$ = 0.8 Hz

$-NH_2$ 5.66 s (2H, exchangeable)

125 MHz ^{13}C NMR Spectrum (DMSO-d_6): δ/ppm

C1	112.3	C4	145.0	C6	144.2	C8a	133.2
C2	146.9	C4a	121.8	C7	123.9		
C3	106.3	C5	118.9	C8	128.0		

IR Spectrum: cm^{-1}

3406 (s)	1636 (m)	1586 (m)	1499 (w)	1458 (w)	1391 (m)
1295 (m)	1189 (s)	1130 (m)	1097 (s)	1036 (s)	860 (m)
648 (s)					

UV Spectrum (phosphate buffer pH 6.5), λ_{max}: nm
218.5, 244.5, 342.5

MALDI-TOF MS negative mode (calcd/found): m/z
692.9/692.8 $[2M-H]^-$, 714.9/714.8 $[2M+Na-2H]^-$

MALDI-TOF MS positive mode (calcd/found): m/z
348.0/347.7 $[M+H]^+$, 304.0/304.0$[M-2Na+3H]^+$

4-Methyl-3-nitrobenzoyl chloride (1c)

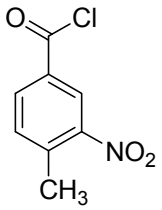

$C_8H_6ClNO_3$ (199.6)

8 ml (110 mmol) Thionyl chloride were added to 18.15 g (100 mmol) 3-nitro-4-methylbenzoic acid, suspended in 70 ml toluene and 1 ml DMF and then the mixture was heated at 60°C for 3 hrs. The excess thionyl chloride was removed by distillation. 4-Methyl-3-nitrobenzoyl chloride was not further purified and was stored in a closed bottle.

4-(4-Methyl-3-nitrobenzamido)naphthalene-2,6-disulfonic acid disodium salt (2a)

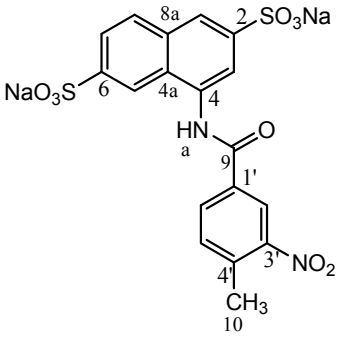

$C_{18}H_{12}N_2Na_2O_9S_2$ (510.4)

3.47 g (10 mmol) 4-Aminonaphthalene-2,6-disulfonic acid disodium salt (1b) were dissolved in 50 ml water and the pH was adjusted to 4.0. To this solution, 16 mmol 4-methyl-3-nitrobenzoyl chloride in 16 ml toluene were slowly dropped, under a constant pH of 4.0, according to general procedure 1. After completion of the reaction, the mixture was acidified to pH 2.0 with 2 N HCl and extracted four times with 75 ml diethyl ether. The water phase was neutralized and evaporated by rotatory evaporator. The crude product was stirred in methanol and then filtrated.

Yield: yellow powder, 3.55 g (69.6 %)
Purity: 97.7 % (HPLC: t_R = 2.01 min, system 1)
TLC: Rf = 0.51 (Isopr + NH_3 = 7.5 + 2.5)
NaCl: 2.09 %
Water: 1 mol/mol
CHN analysis:

	% C	% H	% N	C/N
Calcd	42.36	2.37	5.49	7.72
Calcd (with $NaCl/H_2O$)	40.06	2.62	5.19	7.72

Found	39.92	2.82	5.09	7.84

500 MHz ^{1}H NMR Spectrum (DMSO-d_6): δ/ppm

ABX- A'X'-System

8.19	pt (H5; X)	8.08	s (H1; X')
7.97	d (H8; B)	7.76	d (H3; A')
7.75	dd (H7; A)		
	$^{3}J_{AB}$ = 8.8 Hz	$^{3}J_{BA}$ = 8.8 Hz	
	$^{4}J_{AX}$ = 2.5 Hz	$^{4}J_{A'X'}$ = 1.6 Hz	

ABX-System

8.70	d (H2'; X)		
8.32	dd (H6'; B)		
7.73	d (H5'; A)		
	$^{3}J_{AB}$ = 8.0 Hz	$^{3}J_{BA}$ = 8.0 Hz	
	$^{4}J_{BX}$ = 1.7 Hz	$^{4}J_{XB}$ = 1.7 Hz	

-CONH-	10.79	s (1H, exchangeable)
-CH_3	2.63	s (3H)

125 MHz ^{13}C NMR Spectrum (DMSO-d_6): δ/ppm

C1	122.8	C5	119.7	C9	164.2	C4'	136.7
C2	146.2	C6	145.8	C10	19.8	C5'	132.3
C3	122.8	C7	124.7	C1'	132.9	C6'	133.4
C4	134.0	C8	128.6	C2'	123.9		
C4a	128.6	C8a	133.4	C3'	149.0		

IR Spectrum: cm^{-1}

3447 (m, br)	1653 (m)	1528 (s)	1350 (w)	1199 (s)	1098 (s)
1040 (s)	884 (w)	654 (s)	636 (s)		

UV Spectrum (phosphate buffer pH 6.5), λ_{max}: nm

234.5, 280.5

ESI-MS negative mode (calcd/found): m/z

509.0/509.4 [M-H]$^-$, 487.0/487.5 [M-Na]$^-$, 465.0/465.5 [M-2Na+H]$^-$, 997.0/997.5 [2M-Na]$^-$

4-(3-Amino-4-methylbenzamido)naphthalene-2,6-disulfonic acid disodium salt (2b)

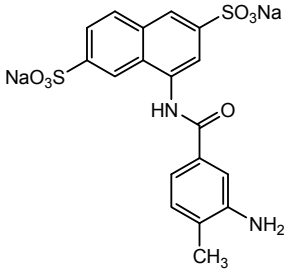

$C_{18}H_{14}N_2Na_2O_7S_2$ (480.4)

20 mg 10 % Pd/C were added to a solution of 1.81 g (3.55 mmol) 4-(4-methyl-3-nitrobenzamido)naphthalene-2,6-disulfonic acid disodium salt (2a) in 100 ml water. The mixture was hydrogenated overnight, according to the general procedure 2.

Yield: white powder, 2.50 g (80.7 %)
Purity: 90.9 % (HPLC: t_R = 1.11 min, system 1)
TLC: Rf = 0.51 (Isopr + NH_3 = 5 + 2)
NaCl: < 1 %
Water: 4 mol/mol
CHN analysis:

	% C	% H	% N	C/N
Calcd	45.00	2.94	5.83	7.72
Calcd (with $NaCl/H_2O$)	39.13	4.01	5.07	7.72
Found	39.07	4.10	5.12	7.63

500 MHz ^{1}H NMR Spectrum (DMSO-d_6): δ/ppm

ABX- A'X'-system

8.19	pt (H5; X)	8.05	pt (H1; X')
7.94	d (H8; B)	7.70	d (H3; A')
7.73	dd (H7; A)		
	$^3J_{AB}$ = 8.2 Hz	$^3J_{BA}$ = 8.2 Hz	
	$^4J_{AX}$ = 1.6 Hz	$^4J_{XA}$ = 1.6 Hz	
	$^4J_{A'X'}$ =1.6 Hz	$^5J_{XX'}$ = 0.8 Hz	

ABX-system

7.29	d (H2'; X)		
7.24	dd (H6'; B)		
7.08	d (H5'; A)		
	$^3J_{AB}$ = 8.0 Hz	$^3J_{BA}$ = 8.0 Hz	
	$^4J_{BX}$ = 1.7 Hz	$^4J_{XB}$ = 1.7 Hz	

-CONH-	10.20	s (1H, exchangeable)
$-NH_2$	5.03	s (2H, exchangeable)
$-CH_3$	2.14	s (3H)

125 MHz ^{13}C NMR Spectrum (DMSO-d_6): δ/ppm

C1	122.3	C5	119.9	C9	167.0	C4'	132.9
C2	145.9	C6	145.7	C10	17.6	C5'	129.8
C3	122.7	C7	124.5	C1'	125.1	C6'	115.3
C4	134.9	C8	128.4	C2'	113.6		
C4a	128.9	C8a	133.1	C3'	146.8		

IR Spectrum: cm^{-1}

3447 (s, br)	1635 (s)	1576 (w)	1533 (s)	1490 (m)	1387 (w)
1276 (m)	1192 (s)	1139 (w)	1098 (s)	1058 (m)	1035 (s)
889 (w)	656 (s)	639 (s)	571 (w)	548 (w)	

UV Spectrum (phosphate buffer pH 6.5), $\lambda_{max:}$: nm

232.5, 292.5

ESI-MS negative mode (calcd/found): m/z

479.0/479.3 $[M-H]^-$, 457.0/457.3 $[M-Na]^-$, 435.0/435.3 $[M-2Na+H]^-$, 937.0/937.3 $[2M-Na]^-$

4,4'-(Carbonylbis(imino-3,1-(4-methylphenylene)carbonyl imino))bis-(naphthalene-2,6-disulfonic acid) tetrasodium salt (2c, NF340)

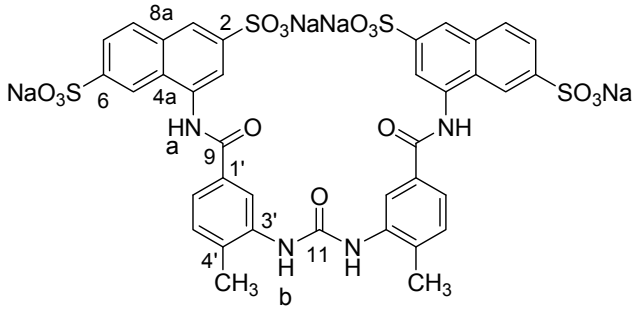

$C_{37}H_{26}N_4Na_4O_{15}S_4$ (986.8)

1.48 g (3.09 mmol) 4-(3-Amino-4-methylbenzamido)naphthalene-2,6-disulfonic acid disodium salt (2b) were dissolved in 35 ml water. To the solution, 6 ml (12 mmol) 20 % phosgene solution in toluene were dropwise added, under a constant pH of 3.7, according to general procedure 3. The crude product was stirred in 80 ml MeOH for 24 h, filtrated and dried.

Yield: pale pink powder, 1.44 g (94.3 %)
Purity: 95.9 % (HPLC: t_R = 3.48 min, system 1)
TLC: Rf = 0.45 (Isopr + NH_3 = 5 + 2)
NaCl: 1 %
Water: 9.5 mol/mol
CHN analysis:

	% C	% H	% N	C/N
Calcd	45.03	2.66	5.68	7.93
Calcd (with NaCl/H_2O)	37.99	3.88	4.79	7.93
Found	37.91	4.05	4.79	7.92

500 MHz ^{1}H NMR Spectrum (DMSO-d_6): δ/ppm

ABX- A'X'-System

8.21	pt (H5; X)	8.07	pt (H1; X')
7.97	d (H8; B)	7.76	d (H3; A')
7.77	dd (H7; A)		
	$^3J_{AB}$ = 8.3 Hz	$^3J_{BA}$ = 8.3 Hz	
	$^4J_{AX}$ = 1.6 Hz	$^4J_{A'X'}$ = 1.6 Hz	
	$^5J_{XX'}$ = 0.8 Hz		

ABX-System

8.42	d (H2'; X)
7.75	dd (H6'; B)

7.40	d (H5'; A)	
	$^3J_{AB}$ = 7.6 Hz	$^3J_{BA}$ = 7.6 Hz
	$^4J_{BX}$ = 1.4 Hz	$^4J_{XB}$ = 1.4 Hz

-CONH-	10.45	s (2H, exchangeable)
-NHCONH-	8.59	s (2H, exchangeable)
$-CH_3$	2.41	s (6H)

125 MHz ^{13}C NMR Spectrum (DMSO-d_6): δ/ppm

C1	122.5	C5	120.0	C9	166.2	C3'	137.8
C2	145.9	C6	145.6	C10	18.4	C4'	133.4
C3	122.8	C7	124.6	C11	153.2	C5'	130.3
C4	134.8	C8	128.5	C1'	132.7	C6'	122.6
C4a	128.9	C8a	132.9	C2'	122.3		

IR spectrum: cm^{-1}

3460 (s, br)	1647 (m)	1578 (m)	1526 (m)	1488 (m)	1450 (w)
1386 (w)	1300 (w)	1187 (s)	1096 (m)	1034 (s)	890 (w)
658 (m)	639 (m)	560 (w)			

UV Spectrum (phosphate buffer pH 6.5), λ_{max}: nm

234.5, 290.5

MALDI-TOF MS positive mode (calcd/found): m/z

1009.0/1009.1 $[M+Na]^+$, 987.0/987.1 $[M+H]^+$, 965.0/965.2 $[M-Na+2H]^+$, 943.0/943.2 $[M-2Na+3H]^+$, 921.0/921.2 $[M-3Na+4H]^+$

4-(4-Methyl-3-nitrobenzamido)naphthalene-2,7-disulfonic acid disodium salt (3a)

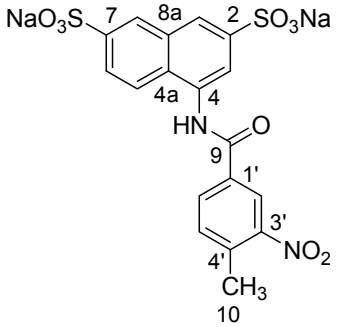

$C_{18}H_{12}N_2Na_2O_9S_2$ (510.4)

To a solution of 2.12 g (7 mmol) 4-aminonaphthalene-2,7-disulfonic acid in 50 ml water, a solution of 12 mmol 4-methyl 3-nitrobenzoyl chloride in 12 ml toluene was dropwise added under the constant pH of4.0. After the reaction was finished, the pH of the mixture was adjusted to 2. 250 ml Water were added and extracted three times with 100 ml diethyl ether. The aqueous phase was neutralized and evaporated by rotatory evaporator. The crude product was stirred with 30 ml methanol, filtrated and dried.

Yield: gray powder, 2.21 g (61.9 %)
Purity: 89.6 % (HPLC: t_R = 3.36 min, system 1)

TLC: Rf = 0.54 (Isopr + NH_3 = 5 + 2)
NaCl: 31.00 %
Water: 1.5 mol/mol
CHN analysis:

	% C	% H	% N	C/N
Calcd	42.36	2.37	5.49	7.72
Calcd (with $NaCl/H_2O$)	27.76	1.94	3.60	7.72
Found	27.79	2.23	3.60	7.72

500 MHz ^{1}H NMR Spectrum (DMSO-d_6): δ/ppm

ABX- A'X'-System

8.18	s (H8; X)	8.08	s (H1; X')
7.91	d (H5; B)	7.81	s (H3; A')
7.75	d (H6; A)		
	$^3J_{AB}$ = 8.5 Hz	$^3J_{BA}$ = 8.5 Hz	

ABX-System

8.68	s (H2'; X)		
8.34	d (H6'; B)		
7.71	d (H5'; A)		
	$^3J_{AB}$ = 7.7 Hz	$^3J_{BA}$ = 7.7 Hz	

-CONH-	10.76	s (1H, exchangeable)
$-CH_3$	2.62	s (3H)

125 MHz ^{13}C NMR Spectrum (DMSO-d_6): δ/ ppm

C1	123.3	C5	123.3	C9	164.2	C4'	133.5
C2	146.2	C6	123.9	C10	19.7	C5'	132.3
C3	122.5	C7	145.8	C1'	133.3	C6'	133.3
C4	136.4	C8	124.9	C2'	124.7		
C4a	128.8	C8a	132.4	C3'	149.0		

IR Spectrum: cm^{-1}

3430 (s)	3318 (s)	3099 (m)	1673 (m)	1619 (m)	1524 (s)
1500 (s)	1390 (m)	1342 (m)	1295 (w)	1254 (w)	1223 (w)
1182 (s)	1124 (m)	1055 (w)	1036 (m)	917 (m)	682 (w)

UV Spectrum (phosphate buffer pH 6.5), λ_{max}: nm

232.5

4-(3-Amino-4-methylbenzamido)naphthalene-2,7-disulfonic acid disodium salt (3b)

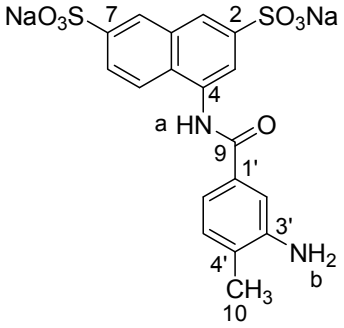

$C_{18}H_{14}N_2Na_2O_7S_2$ (480.4)

20 mg 10 % Pd/C were added to a solution of 1.81 g (3.55 mmol) nitro compound 3a in 50 ml water. The mixture was hydrogenated overnight, according to the general procedure 2. The crude product was stirred with 20 ml methanol, filtrated and dried.

Yield: purple powder, 1.70 g (99.7 %)
Purity: 96.1 % (HPLC: t_R = 1.30 minute, system 1)
TLC: Rf = 0.34 (Isopr + NH_3 = 5 + 2)
NaCl: 20.30 %
Water: 7.5 mol/mol
CHN analysis:

	% C	% H	% N	C/N
Calcd	45.00	2.94	5.83	7.72
Calcd (with NaCl/H_2O)	27.99	3.78	3.63	7.72
Found	27.61	3.39	3.61	7.65

500 MHz ^{1}H NMR Spectrum (DMSO-d_6): δ/ppm

ABX- A'X'-System

8.15	d (H8; X)	8.04	pt (H1; X')
7.85	d (H5; B)	7.79	d (H3; A')
7.72	dd (H6; A)		
	$^3J_{AB}$ = 8.8 Hz	$^3J_{BA}$ = 8.8 Hz	
	$^4J_{AX}$ = 1.7 Hz	$^4J_{XA}$ = 1.7 Hz	
	$^4J_{A'X'}$= 1.3 Hz		

ABX-System

7.29	d (H2'; X)		
7.23	dd (H6'; B)		
7.07	d (H5'; A)		
	$^3J_{AB}$ = 7.7 Hz	$^3J_{BA}$ = 7.7 Hz	
	$^4J_{BX}$ = 1.9 Hz	$^4J_{XB}$ = 1.9 Hz	

-CONH-	10.18	s (1H, exchangeable)
-NH_2	5.04	s (2H, exchangeable)
-CH_3	2.13	s (3H)

125 MHz ^{13}C NMR Spectrum (DMSO-d_6): δ/ppm

C1	122.8	C5	123.3	C9	167.0	C4'	133.1
C2	145.9	C6	124.4	C10	17.6	C5'	129.9
C3	122.2	C7	145.7	C1'	125.1	C6'	115.4
C4	134.1	C8	124.9	C2'	113.6		
C4a	129.1	C8a	132.2	C3'	146.8		

IR Spectrum: cm^{-1}

3437 (s, br)	1638 (s)	1577 (m)	1534 (s)	1490 (m)	1425 (w)
1188 (s)	1117 (s)	1052 (s)	912 (w)	750 (m)	692 (s)

UV Spectrum (phosphate buffer, pH 6.5), λ_{max}: nm

232.5, 294.5

4,4'-(Carbonylbis(imino-3,1-(4-methylphenylene)carbonylimino)) bis-(naphthalene-2,7-disulfonic acid) tetrasodium salt (3c)

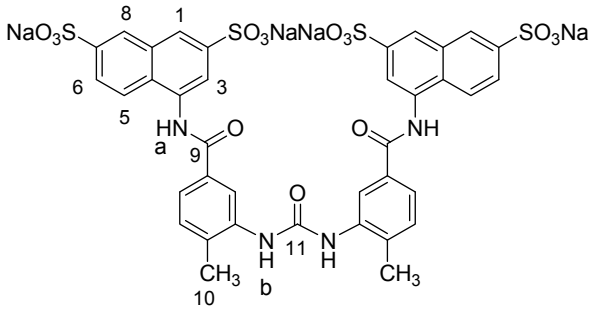

$C_{37}H_{26}N_4Na_4O_{15}S_4$ (986.8)

0.90 g (1.87 mmol) Amine 3b were dissolved in 50 ml water and pH adjusted to 4.0. To this solution, 2 ml (4 mmol) 20 % phosgene solution were slowly dropped under a constant pH of 4.0. The synthesis was performed according to the general method 3. The crude product was stirred in 20 ml methanol, filtrated and dried.

Yield: white powder, 0.88 g (93.7 %)
Purity: 94.7 % (HPLC: t_R = 3.58 min, system 1)
TLC: Rf = 0.30 (Isopr + NH_3 = 5 + 2)
NaCl: 1.28 %
Water: 8 mol/mol
CHN analysis:

	% C	% H	% N	C/N
Calcd	45.03	2.66	5.68	7.93
Calcd (with NaCl/H_2O)	38.79	3.69	4.89	7.93
Found	38.92	3.79	5.05	7.71

500 MHz ^{1}H NMR Spectrum (DMSO-d_6): δ/ppm

ABX- A'X'-System

8.15	d (H8; X)	8.05	pt (H1; X')
7.86	d (H5; B)	7.79	d (H3; A')
7.74	dd (H6; A)		
	$^3J_{AB}$ = 8.8 Hz	$^3J_{BA}$ = 8.8 Hz	

$^4J_{AX}$ = 1.6 Hz $^4J_{XA}$ = 1.6 Hz
$^4J_{A'X'}$ = 1.3 Hz

ABX-System
8.38 d (H2'; X)
7.76 dd (H6'; B)
7.38 d (H5'; A)
$^3J_{AB}$ = 8.0 Hz $^3J_{BA}$ = 8.0 Hz
$^4J_{BX}$ = 1.6 Hz $^4J_{XB}$ = 1.6 Hz

-CONH- 10.37 s (2H, exchangeable)
-NHCONH- 8.49 s (2H, exchangeable)
$-CH_3$ 2.39 s (6H)

125 MHz ^{13}C NMR Spectrum (DMSO-d_6): δ/ ppm

C1	123.0	C5	123.4	C9	166.2	C3'	137.7
C2	146.1	C6	124.5	C10	153.3	C4'	133.4
C3	122.4	C7	145.7	C11	18.3	C5'	130.3
C4	133.9	C8	124.9	C1'	132.7	C6'	122.7
C4a	129.1	C8a	132.3	C2'	122.3		

IR Spectrum: cm^{-1}

3466 (s, br)	1652 (s)	1575 (m)	1539 (s)	1489 (m)	1417 (w)
1307 (m)	1190 (s)	1125 (m)	1102 (m)	1036 (s)	915 (w)
852 (w)	821 (w)	751 (m)	692 (s)	613 (w)	580 (w)

UV Spectrum (phosphate buffer pH 6.5), λ_{max}: nm
232.5, 290.5

MALDI-TOF MS positive mode (calcd /found): m/z
1009.0/1009.1 $[M+Na]^+$, 987.0/987.1 $[M+H]^+$, 965.0/965.1 $[M+2H-Na]^+$, 943.0/943.1 $[M+3H-2Na]^+$, 921.0/921.2 $[M+4H-3Na]^+$

8-(4-Methyl-3-nitrobenzamido)naphthalene-2-sulfonic acid sodium salt (4a)

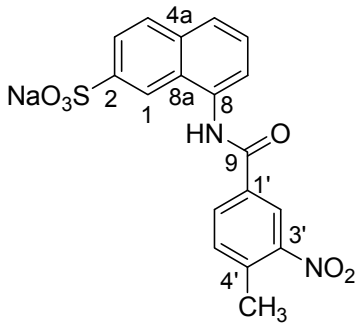

$C_{18}H_{13}N_2NaO_6S$ (408.4)

To a solution of 4.46 g (20 mmol) 8-aminonaphthalene-2-sulfonic acid dissolved in 100 ml water, 24 mmol 4-methyl-3-nitrobenzoyl chloride in 24 ml toluene were

slowly dropped under a constant pH of 4.5. The synthesis was performed according to the general procedure 1.

Yield: pale gray powder, 6.01 g (73.6 %)
Purity: 96.1 % (HPLC: t_R = 4.19 min, system 1)
TLC: Rf = 0.58 (Isopr + NH_3 = 5 + 2)
NaCl: < 1 %
Water: 1 mol/mol
CHN analysis:

	% C	% H	% N	C/N
Calcd	52.94	3.21	6.86	7.72
Calcd (with NaCl/H_2O)	50.70	3.55	6.57	7.72
Found	50.73	3.82	6.47	7.84

500 MHz ^{1}H NMR Spectrum (DMSO-d_6): δ/ppm

ABX-A'B'X'-System

8.25	pt (H1; X)	7.76	dd (H5; X')
7.93	d (H4; B)	7.58	d (H7; B')
7.86	dd (H3; A)	7.56	t (H6; A')
	$^3J_{AB}$ = 7.7 Hz		$^3J_{BA}$ = 7.7 Hz
	$^4J_{XA}$ = 2.2 Hz		$^4J_{AX}$ = 2.2 Hz
	$^3J_{A'B'}$ = 7.2 Hz		$^3J_{B'A'}$ = 7.2 Hz
	$^3J_{A'X'}$ = 7.8 Hz		$^3J_{X'A'}$ = 7.8 Hz
	$^4J_{X'B'}$ = 1.6 Hz		

ABX-System

8.70	d (H2'; X)		
8.32	dd (H6'; B)		
7.73	d (H5'; A)		
	$^3J_{AB}$ = 8.0 Hz		$^3J_{BA}$ = 8.0 Hz
	$^4J_{BX}$ = 1.7 Hz		$^4J_{XB}$ = 1.7 Hz

-CONH-	10.77	s (1H, exchangeable)
-CH_3	2.63	s (3H)

125 MHz ^{13}C NMR Spectrum (DMSO-d_6): δ/ppm

C1	123.9	C5	124.4	C9	164.2	C4'	134.3
C2	136.6	C6	127.9	C10	19.8	C5'	132.3
C3	126.5	C7	119.6	C1'	133.4	C6'	133.5
C4	128.7	C8	145.9	C2'	124.9		
C4a	133.7	C8a	126.1	C3'	149.0		

IR spectrum: cm^{-1}

3447 (s, br)	1652 (m)	1623 (m)	1524 (s)	1348 (m)	1296 (w)
1271 (w)	1187 (s)	1114 (m)	1073 (w)	1045 (m)	1029 (m)
831 (m)	748 (w)	680 (m)	597 (w)		

UV Spectrum (phosphate buffer pH 6.5), λ_{max}: nm

228.5

8-(3-Amino-4-methylbenzamido)naphthalene-2-sulfonic acid sodium salt (4b)

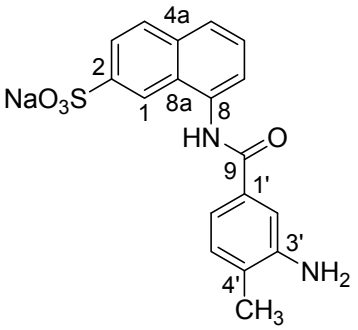

$C_{18}H_{15}N_2NaO_4S$ (378.4)

20 mg 10 % Pd/C were added to a solution of 2.92 g (7.15 mmol) nitro compound 4a in 200 ml water. The mixture was hydrogenated overnight, according to the general procedure 2.

Yield: gray powder, 2.68 g (99.0 %)
Purity: 96.4 % (HPLC: t_R = 1.76 min, system 3)
TLC: Rf = 0.72 (Isopr + NH_3 = 5 + 2)
NaCl: 1 %
Water: 2.5 mol/mol
CHN analysis:

	% C	% H	% N	C/N
Calcd	57.14	4.00	7.40	7.72
Calcd (with NaCl/H_2O)	50.55	4.71	6.55	7.72
Found	50.25	4.99	6.64	7.56

500 MHz ^{1}H NMR Spectrum (DMSO-d_6): δ/ppm

ABX-A'B'X'-System

8.25	pt (H1; X)	7.73	dd (H5; X')
7.89	d (H4; B)	7.53	t (H6; B')
7.81	d (H3; A)	7.49	dd (H7; A')
	$^3J_{AB}$ = 8.2 Hz		$^3J_{BA}$ = 8.2 Hz
	$^4J_{XA}$ = 1.6 Hz		$^5J_{XX'}$ = 0.8 Hz
	$^3J_{A'B'}$ = 7.4 Hz		$^3J_{B'A'}$ = 7.4 Hz
	$^3J_{X'B'}$= 8.0 Hz		$^3J_{B'X'}$ = 8.0 Hz
	$^4J_{A'X'}$ = 1.4 Hz		$^4J_{X'A'}$ = 1.4 Hz

ABX-System

7.28	d (H2'; X)	
7.23	dd (H6'; B)	
7.08	d (H5'; A)	
	$^3J_{AB}$ = 7.7 Hz	$^3J_{BA}$ = 7.7 Hz
	$^4J_{BX}$ = 1.9 Hz	$^4J_{XB}$ = 1.9 Hz

-CONH-	10.19	s (1H, exchangeable)
-NH_2	5.03	s (2H, exchangeable)
-CH_3	2.14	s (3H)

125 MHz ^{13}C NMR Spectrum (DMSO-d_6): δ/ppm

C1	124.2	C5	124.8	C9	167.0	C4'	133.1
C2	135.2	C6	127.7	C10	17.6	C5'	129.8
C3	126.1	C7	119.9	C1'	125.1	C6'	115.3
C4	129.1	C8	145.7	C2'	113.6		
C4a	133.7	C8a	125.9	C3'	146.8		

IR Spectrum: cm^{-1}

3381 (m, br)	1654 (m)	1577 (w)	1529 (s)	1491 (s)	1371 (w)
1331 (w)	1190 (s)	1129 (w)	1027 (m)	827 (m)	744 (w)
680 (s)	550 (m)				

UV Spectrum (phosphate buffer, pH 6.5) λ_{max}: nm

228.5, 292.5

8,8'-(Carbonylbis(imino-3,1-(4-methylphenylene)carbonyl imino))bis-(naphthalene-2-sulfonic acid) disodium salt (4c)

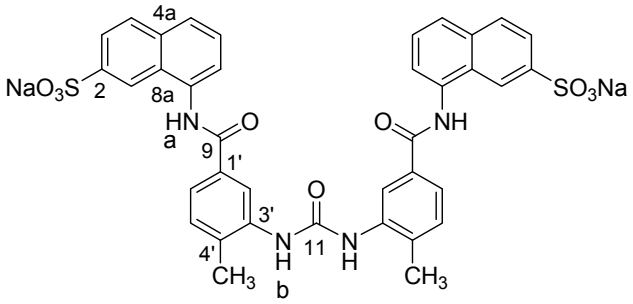

$C_{37}H_{28}N_4Na_2O_9S_2$ (782.7)

1.90 g (5.02 mmol) Amine 4b were dissolved in 40 ml water and the pH was adjusted to 4.0. 4 ml (8 mmol) phosgene solution in toluene (20 %) were slowly dropped to the solution under a constant pH of 4.0. The synthesis was performed according to the general procedure 3.

Yield: pale gray powder, 2.65 g (81.0 %)
Purity: 94.9 % (HPLC: t_R = 5.72, system 1)
TLC: Rf = 0.66 (Isopr + NH_3 = 5 + 2)
NaCl: 22.50 %
Water: 3 mol/mol
CHN analysis:

	%C	%H	%N	C/N
Calcd	56.77	3.61	7.16	7.93
Calcd (with NaCl/H_2O)	40.72	3.23	5.13	7.93
Found	40.57	3.58	5.06	8.02

500 MHz ^{1}H NMR Spectrum (DMSO-d_6): δ/ppm

ABX-A'B'X'-System

8.25	pt (H1; X)	7.70	dd (H5; X')
7.89	d (H4; B)	7.52	t (H6; B')

7.81	m (H3; A)	7.51 d (H7; A')
	$^3J_{AB}$ = 8.3 Hz	$^3J_{BA}$ = 8.3 Hz
	$^4J_{XA}$ = 1.6 Hz	$^5J_{XX'}$ = 0.9 Hz
	$^3J_{A'B'}$= 7.2 Hz	$^3J_{B'A'}$ = 7.2 Hz
	$^3J_{B'X'}$ = 7.7 Hz	$^3J_{X'B'}$ = 7.7 Hz
	$^4J_{A'X'}$ = 1.9 Hz	

ABX-System

8.46	d (H2'; X)	
7.72	dd (H6'; B)	
7.36	d (H5'; A)	
	$^3J_{AB}$ = 8.2 Hz	$^3J_{BA}$ = 8.2 Hz
	$^4J_{BX}$ = 1.7 Hz	$^4J_{XB}$ = 1.7 Hz

-CONH-	10.41	s (2H, exchangeable)
-NHCONH-	8.90	s (2H, exchangeable)
$-CH_3$	2.41	s (6H)

125 MHz ^{13}C NMR Spectrum (DMSO-d_6): δ/ppm

C1	124.2	C5	124.9	C9	166.4	C3'	137.9
C2	135.0	C6	127.7	C10	18.7	C4'	132.8
C3	126.1	C7	119.9	C11	153.3	C5'	130.2
C4	128.9	C8	145.5	C1'	132.7	C6'	122.3
C4a	133.7	C8a	126.0	C2'	121.9		

IR Spectrum: cm^{-1}

3391 (s, br)	1652 (s)	1575 (s)	1531 (s)	1486 (s)	1451 (m)
1371 (w)	1187 (s)	1123 (m)	1029 (s)	830 (w)	753 (w)
681 (s)	563 (w)				

UV Spectrum (phosphate buffer, pH 6.5) λ_{max}: nm

228.5, 288.5

MALDI-TOF MS positive mode (calcd/ found): m/z

805.1/805.2 $[M+Na]^+$, 783.1/783.2 $[M+H]^+$, 761.1/761.2 $[M-Na+2H]^+$

4-(4-Methyl-3-nitrobenzamido)naphthalene-2-sulfonic acid sodium salt (5a)

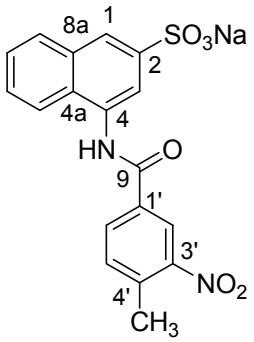

$C_{18}H_{13}N_2NaO_6S$ (408.4)

3.36 g (15 mmol) 4-Aminonaphthalene-2-sulfonic acid were dissolved in 100 ml water and adjusted pH to 4.5. To this solution, 20 mmol 4-methyl-3-nitrobenzoyl

chloride, dissolved in 20 ml toluene, were slowly dropped under a constant pH of 4.5. The synthesis was performed according to the general procedure 1.

Yield: brown powder, 4.32 g (70.4 %)
Purity: 95.9 % (HPLC: t_R = 4.93 min, system 1)
TLC: Rf = 0.79 (Isopr + NH_3 = 5 + 2)
NaCl: 9.22 %
Water: 1.5 mol/mol
CHN analysis:

	% C	% H	% N	C/N
Calcd	52.94	3.21	6.86	7.72
Calcd (with $NaCl/H_2O$)	45.08	3.36	5.84	7.72
Found	45.00	3.56	6.05	7.44

500 MHz ^{1}H NMR Spectrum (DMSO-d_6): δ/ppm

ABXY- A'X'-System

8.02	m (H5; Y)	8.10	s (H1; X')
7.93	m (H8; X)	7.80	d (H3; A')
7.56	m (H6; B)		
7.53	m (H7; A)		

$^3J_{AB}$ = 6.6 Hz $^3J_{BA}$ = 6.6 Hz
$^3J_{BY}$ = 8.1 Hz $^3J_{YB}$ = 8.1 Hz
$^3J_{AX}$ = 7.9 Hz $^3J_{XA}$ = 7.9 Hz
$^4J_{BX}$ = 2.0 Hz $^4J_{XB}$ = 2.0 Hz
$^4J_{AY}$ = 1.9 Hz $^4J_{YA}$ = 1.9 Hz
$^4J_{A'X'}$ = 1.6 Hz

ABX-System

8.68	d (H2'; X)
8.32	dd (H6'; B)
7.71	d (H5'; A)

$^3J_{AB}$ = 7.9 Hz $^3J_{BA}$ = 7.9 Hz
$^4J_{BX}$ = 1.9 Hz $^4J_{XB}$ = 1.9 Hz

-CONH- 10.70 s (1H, exchangeable)
$-CH_3$ 2.62 s (1H)

125 MHz ^{13}C NMR Spectrum (DMSO-d_6): δ/ppm

C1	122.0	C5	123.5	C9	164.2	C4'	133.6
C2	145.4	C6	126.6	C10	19.7	C5'	132.3
C3	122.9	C7	128.9	C1'	133.1	C6'	133.3
C4	136.4	C8	129.0	C2'	123.9		
C4a	126.6	C8a	133.3	C3'	149.0		

IR Spectrum: cm^{-1}

3437 (s, br)	1654 (s)	1622 (s)	1597 (m)	1523 (s)	1449 (m)
1395 (w)	1345 (m)	1301 (m)	1189 (s)	1104 (s)	1048 (s)
800 (m)	741 (m)	666 (m)	642 (m)		

UV Spectrum (phosphate buffer pH 6.5), λ_{max}: nm

228.5, 286.5

4-(3-Amino-4-methylbenzamido)naphthalene-2-sulfonic acid sodium salt (5b)

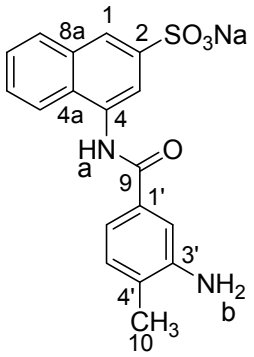

$C_{18}H_{15}N_2NaO_4S$ (378.4)

40 mg 10 % Pd/C were added to a solution of 2.28 g (5.58 mmol) nitro compound 5a in 150 ml 50 % aqueous methanol. The mixture was hydrogenated overnight, according to the general procedure 2.

Yield: brown powder, 2.04 g (96.8 %)
Purity: 96.4 % (HPLC: t_R = 2.65 min, system 1)
TLC: Rf = 0.65 (Isopr + NH_3 = 5 + 2)
NaCl: 9.18 %
Water: 2 mol/mol
CHN analysis:

	% C	% H	% N	C/N
Calcd	57.14	4.00	7.40	7.72
Calcd (with NaCl/H_2O)	47.38	4.20	6.14	7.72
Found	47.48	4.46	6.21	7.64

500 MHz ^{1}H NMR Spectrum (DMSO-d_6): δ/ppm

ABXY- A'X'-System

8.00	m (H5; Y)	8.06	s (H1; X')
7.88	m (H8; X)	7.77	d (H3; A')
7.54	m (H6; B)		
7.52	m (H7; A)		

$^3J_{AB}$ = 6.9 Hz $^3J_{BA}$ = 6.9 Hz
$^3J_{BY}$ = 8.0 Hz $^3J_{YB}$ = 8.0 Hz
$^3J_{AX}$ = 9.1 Hz $^3J_{XA}$ = 9.1 Hz
$^4J_{BX}$ = 1.9 Hz $^4J_{XB}$ = 1.9 Hz
$^4J_{AY}$ = 2.8 Hz $^4J_{YA}$ = 2.8 Hz
$^4J_{A'X'}$ = 1.3 Hz

ABX-System

7.29	d (H2'; X)
7.23	dd (H6'; B)
7.07	d (H5'; A)

$^3J_{AB}$ = 8.0 Hz $^3J_{BA}$ = 8.0 Hz
$^4J_{BX}$ = 1.9 Hz $^4J_{XB}$ = 1.9 Hz

-CONH- 10.14 s (1H, exchangeable)

$-NH_2$	5.04	s (2H, exchangeable)
$-CH_3$	2.14	s (3H)

125 MHz ^{13}C NMR Spectrum (DMSO-d_6): δ/ppm

C1	121.8	C5	123.5	C9	166.9	C4'	133.1
C2	145.4	C6	126.4	C10	17.6	C5'	129.8
C3	122.4	C7	128.9	C1'	125.0	C6'	115.4
C4	134.1	C8	129.3	C2'	113.5		
C4a	126.4	C8a	133.2	C3'	146.8		

IR Spectrum: cm^{-1}

3352 (s)	1683 (m)	1627 (m)	1575 (m)	1538 (s)	1495 (s)
1399 (m)	1224 (s)	1189 (s)	1104 (m)	1048 (s)	732 (m)
641 (m)					

UV Spectrum (phosphate buffer pH 6.5), λ_{max}: nm

226.5, 292.5

2,2'-(Carbonylbis(imino-3,1-(4-methylphenylene)carbonylimino)) bis-(naphthalene-1-sulfonic acid) disodium salt (5c)

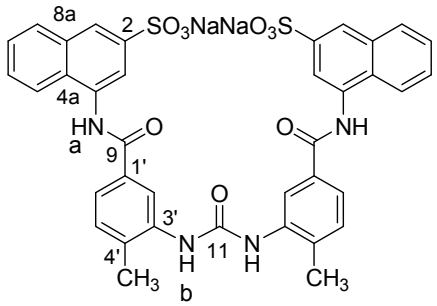

$C_{37}H_{28}N_4Na_2O_9S_2$ (782.7)

1.65 g (4.36 mmol) Amine 5b were dissolved in 50 ml water and the pH was adjusted to 4.0. To this solution, 4 ml (8 mmol) 20 % phosgene solutions were dropped under a constant pH of 4.0. The synthesis was performed according to the general procedure 3. The product was stirred in 20 ml methanol, filtrated and dried.

Yield: white powder, 1.06 g (62.4 %)
Purity: 97.3 % (HPLC: t_R = 6.32 min, system 1)
TLC: Rf = 0.58 (Isopr + NH_3 = 5 + 2)
NaCl: 1.81%
Water: 5.5 mol/mol
CHN analysis:

	% C	% H	% N	C/N
Calcd	56.77	3.61	7.16	7.93
Calcd (with $NaCl/H_2O$)	49.48	4.38	6.24	7.93
Found	49.52	4.41	6.27	7.89

500 MHz ^{1}H NMR Spectrum (DMSO-d_6): δ/ppm

ABXY- A'X'-System

7.99	m (H5; Y)	8.07	s (H1; X')
7.88	m (H8; X)	7.77	s (H3; A')
7.52	d (H6; B)		
7.50	d (H7; A)		
	$^3J_{AB}$ = 6.3 Hz	$^3J_{BA}$ = 6.3 Hz	
	$^3J_{BY}$ = 6.0 Hz	$^3J_{AX}$ = 6.0 Hz	
	$^4J_{AY}$ = 3.1 Hz	$^4J_{XB}$ = 3.1 Hz	

ABX-System

8.45	d (H2'; X)		
7.73	dd (H6'; B)		
7.37	d (H5'; A)		
	$^3J_{AB}$ = 7.9 Hz	$^3J_{BA}$ = 7.9 Hz	
	$^4J_{BX}$ = 1.6 Hz	$^4J_{XB}$ = 1.6 Hz	

-CONH-	10.35	s (2H, exchangeable)
-NHCONH-	8.52	s (2H, exchangeable)
-CH_3	2.39	s (6H)

125 MHz ^{13}C NMR Spectrum (DMSO-d_6): δ/ppm

C1	122.0	C5	123.5	C9	166.3	C3'	137.7
C2	145.4	C6	126.6	C10	18.3	C4'	132.9
C3	122.6	C7	128.9	C11	153.2	C5'	130.3
C4	133.9	C8	129.2	C1'	132.8	C6'	122.5
C4a	126.5	C8a	133.1	C2'	121.9		

IR Spectrum: cm^{-1}

3435 (s, br)	1652 (s)	1575 (s)	1538 (s)	1450 (s)	1394 (s)
1342 (m)	1186 (s)	1100 (s)	1045 (s)	858 (w)	745 (s)
667 (s)					

UV Spectrum (phosphate buffer pH 6.5), λ_{max}: nm

228.5, 290.5

MALDI-TOF MS positive mode (calcd/found): m/z

805.1/805.2 $[M+Na]^+$, 783.1/783.2 $[M+H]^+$, 761.1/761.2 $[M+2H-Na]^+$

4-(4-Methyl-3-nitrobenzamido)naphthalene-1-sulfonic acid sodium salt (6a)

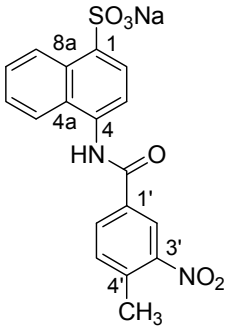

$C_{18}H_{13}N_2NaO_6S$ (408.4)

4.46 g (18.2 mmol) 8-Aminonaphthalene-2-sulfonic acid were dissolved in 100 ml water. A solution of 22.5 mmol 4-methyl-3-nitrobenzoyl chloride in 22.5 ml toluene was dropwisely added to the solution under a constant pH of 4.5. The synthesis was performed and purified according to the general procedure 1.

Yield: pale purple, 6.50 g (87.6 %)
Purity: 99.8 % (HPLC: t_R = 4.17 min, system 1)
TLC: Rf = 0.68 (Isopr + NH_3 = 5 + 2)
NaCl: < 1 %
CHN analysis:

	% C	% H	% N	C/N
Calcd	52.94	3.21	6.86	7.72
Found	52.69	3.37	6.66	7.91

500 MHz ^{1}H NMR Spectrum (DMSO-d_6): δ/ppm

ABXY-A'B'-System

8.92	dd (H8; Y)	7.99	d (H3; B')
7.98	dd (H5; X)	7.52	d (H2; A')
7.55	ddd (H7; B)		
7.50	dd (H6; A)		
	$^3J_{AB}$ = 6.6 Hz	$^3J_{BA}$ = 6.6 Hz	
	$^3J_{BY}$ = 7.9 Hz	$^3J_{YB}$ = 7.9 Hz	
	$^4J_{AY}$ = 1.7 Hz	$^4J_{YA}$ = 1.7 Hz	
	$^4J_{BX}$ = 1.7 Hz	$^4J_{XB}$ = 1.7 Hz	
	$^3J_{A'B'}$ = 7.6 Hz	$^3J_{B'A'}$ = 7.6 Hz	

ABX-System

8.68	d (H2'; X)		
8.32	dd (H6'; B)		
7.70	d (H5'; A)		
	$^3J_{AB}$ = 8.0 Hz	$^3J_{BA}$ = 8.0 Hz	
	$^4J_{BX}$ = 1.6 Hz	$^4J_{XB}$ = 1.6 Hz	

-CONH-	10.67	s (1H, exchangeable)
$-CH_3$	2.62	s (3H)

125 MHz ^{13}C NMR Spectrum (DMSO-d_6): δ/ppm

C1	142.8	C5	123.2	C9	164.2	C4'	134.5
C2	122.5	C6	124.3	C10	19.69	C5'	132.4
C3	123.9	C7	125.8	C1'	133.3	C6'	133.6
C4	136.4	C8	128.1	C2'	125.7		
C4a	129.5	C8a	129.9	C3'	149.0		

IR Spectrum: cm^{-1}

3459 (s, br)	3011 (w)	1658 (s)	1639 (s)	1529 (s)	1335 (m)
1211 (s)	1196 (s)	1163 (m)	1065 (s)	844 (m)	758 (m)
693 (m)					

UV Spectrum (phosphate buffer pH 6.5), λ_{max}: nm
224.5, 296.5

4-(3-Amino-4-methylbenzamido)naphthalene-1-sulfonic acid sodium salt (6b)

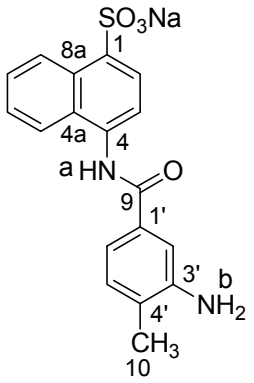

$C_{18}H_{15}N_2NaO_4S$ (378.4)

100 mg 10 % Pd/C were added to a solution of 3.52 g (8.62 mmol) nitro compound 6a in 200 ml 50 % aqueous methanol. The mixture was hydrogenated overnight, according to the general procedure 2.

Yield: brown powder, 3.22 g (98.7 %)
Purity: 95.2 % (HPLC: t_R = 2.52 min, system 1)
TLC: Rf = 0.65 (Isopr + NH_3 = 5 + 2)
NaCl: 1.05 %
Water: 2 mol/mol
CHN analysis:

	%C	%H	%N	C/N
Calcd	57.14	4.00	7.40	7.72
Calcd (with NaCl/H_2O)	51.62	4.57	6.69	7.72
Found	51.79	4.84	6.67	7.77

500 MHz ^{1}H NMR Spectrum (DMSO-d_6): δ/ppm

ABXY-A'B'-System

8.89	m (H8; Y)	7.96	d (H3; B')
7.94	dd (H5; X)	7.50	d (H2; A')
7.52	m (H7; B)		
7.48	dd (H6; A)		

$^3J_{AB}$ = 6.6 Hz	$^3J_{BA}$ = 6.6 Hz
$^3J_{XA}$ = 6.6 Hz	$^3J_{YB}$ = 7.9 Hz
$^4J_{BX}$ = 1.6 Hz	$^4J_{XB}$ = 1.6 Hz
$^4J_{AY}$ = 1.6 Hz	$^4J_{YA}$ = 1.6 Hz
$^3J_{A'B'}$ = 7.6 Hz	$^3J_{B'A'}$ = 7.6 Hz

ABX-System

7.30	d (H2'; X)
7.23	dd (H6'; B)
7.07	d (H5'; A)

	$^3J_{AB}$ = 7.9 Hz	$^3J_{BA}$ = 7.9 Hz	
	$^4J_{BX}$ = 1.9 Hz	$^4J_{XB}$ = 1.9 Hz	
-CONH-	10.14	s (1H, exchangeable)	
$-NH_2$	5.04	s (2H, exchangeable)	
$-CH_3$	2.14	s (3H)	

125 MHz ^{13}C NMR Spectrum (DMSO-d_6): δ/ppm

C1	142.2	C5	123.3	C9	166.9	C4'	133.1
C2	122.2	C6	125.5	C10	17.6	C5'	129.9
C3	124.3	C7	125.6	C1'	125.1	C6'	115.4
C4	135.4	C8	128.0	C2'	113.6		
C4a	129.7	C8a	129.9	C3'	146.8		

IR Spectrum: cm^{-1}

3386 (s, br)	1641 (s)	1572 (m)	1495 (s)	1456 (m)	1331 (m)
1286 (m)	1188 (s)	1055 (s)	763 (m)	691 (s)	644 (m)

UV Spectrum (phosphate buffer pH 6.5), λ_{max}: nm

228.5, 298.5

4,4'-(Carbonylbis(imino-3,1-(4-methylphenylene)carbonylimino)) bis-(naphthalene-1-sulfonic acid) disodium salt (6c)

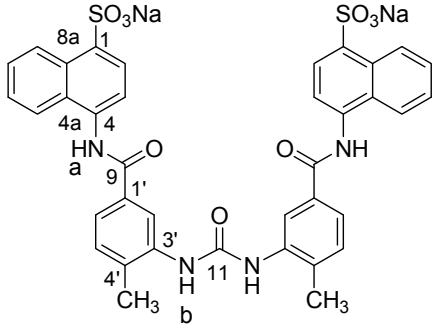

$C_{37}H_{28}N_4Na_2O_9S_2$ (782.7)

1.49 g (3.94 mmol) Amine 6b were dissolved in 50 ml water and pH adjusted to 4.0. 17 ml (34 mmol) 20 % phosgene solutions were slowly added under a constant pH of 4.0. The synthesis was performed and the product was purified according to the general procedure 3.

Yield: brown powder, 1.35 g (87.8 %)
Purity: 93.3 % (HPLC: t_R = 5.15 min, system 1)
TLC: Rf = 0.58 (Isopr + NH_3 = 5 + 2)
NaCl: 7.47 %
Water: 4 mol/mol
CHN analysis:

	%C	%H	%N	C/N
Calcd	56.77	3.61	7.16	7.93
Calcd (with NaCl/H_2O)	48.10	3.93	6.06	7.93
Found	48.01	4.30	6.01	7.99

500 MHz ^{1}H NMR Spectrum (DMSO-d_6); δ/ppm

ABXY-A'B'-System

8.90	dd (H8; Y)	7.97	d (H3; B')
7.95	dd (H5; X)	7.50	d (H2; A')
7.51	m (H7; B)		
7.51	m (H6; A)		
	$^{3}J_{YB}$ = 6.6 Hz	$^{3}J_{XA}$ = 6.3 Hz	
	$^{4}J_{XB}$ = 2.2 Hz	$^{4}J_{YA}$ = 2.5 Hz	
	$^{3}J_{A'B'}$ = 7.9 Hz	$^{3}J_{B'A'}$ = 7.9 Hz	

ABX-System

8.47	d (H2'; X)		
7.72	dd (H6'; B)		
7.36	d (H5'; A)		
	$^{3}J_{AB}$ = 7.9 Hz	$^{3}J_{BA}$ = 7.9 Hz	
	$^{4}J_{BX}$ = 1.5 Hz	$^{4}J_{XB}$ = 1.5 Hz	

-CONH-	10.34	s (1H, exchangeable)
-NHCONH-	8.85	s (1H, exchangeable)
-CH_3	2.41	s (3H)

125 MHz ^{13}C NMR Spectrum (DMSO-d_6): δ/ppm

C1	142.3	C5	123.3	C9	166.7	C3'	137.8
C2	122.4	C6	125.6	C10	153.4	C4'	132.8
C3	124.3	C7	125.7	C11	18.5	C5'	130.3
C4	135.2	C8	128.0	C1'	132.7	C6'	122.4
C4a	129.7	C8a	129.9	C2'	121.9		

IR Spectrum: cm^{-1}

3346 (s, br)	1654 (s)	1577 (s)	1551 (s)	1529 (s)	1497 (s)
1453 (m)	1408 (m)	1330 (m)	1187 (s)	1049 (s)	836 (w)
752 (m)	691 (s)	633 (m)			

UV Spectrum (phosphate buffer pH 6.5), λ_{max}: nm

226.5, 296.5

MALDI-TOF MS positive mode (calcd/found): m/z

805.1/805.1 $[M+Na]^+$, 783.1/783.1 $[M+H]^+$, 761.1/761.1 $[M-Na+2H]^+$, 1587.3 $[2M+Na]^+$, 2369.3 $[3M+Na]^+$

7-(4-Methyl-3-nitrobenzamido)naphthalene-1,3,5-trisulfonic acid trisodium salt (7a)

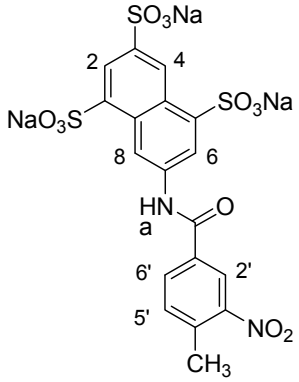

$C_{18}H_{11}N_2Na_3O_{12}S_3$ (612.4)

2.02 g (5 mmol) 7-Aminonaphthalene-1,3,5-trisulfonic acid were dissolved in 10 ml water and pH was adjusted to 4.0. To this solution, 10 mmol 4-methyl-3-nitrobenzoyl chloride, dissolved in 12 ml toluene, were dropwisely added, under a constant pH of 4.0. The synthesis was performed and the product was purified according to the general procedure 1.

Yield: pale orange powder, 1.65 g (91.9 %)
Purity: 98.8 % (HPLC: t_R = 3.88 min, system 1)
TLC: Rf = 0.30 (Isopr + NH_3 = 5 + 2)
NaCl: 1.14 %
Water: 5.5 mol/mol
CHN analysis:

	%C	%H	%N	C/N
Calcd	35.30	1.81	4.57	7.72
Calcd (with NaCl/H_2O)	30.04	3.08	3.89	7.72
Found	29.94	3.40	3.90	7.67

500 MHz ^{1}H NMR Spectrum (DMSO-d_6): δ/ppm

AX-A'X'-System

9.07	dd (H4; X)	9.14	dd (H8; X')
8.45	d (H2; A)	8.29	d (H6; A')
	$^4J_{AX}$ = 1.9 Hz		$^4J_{XA}$ = 1.9 Hz
	$^4J_{A'X'}$ = 2.5 Hz		$^4J_{X'A'}$ = 2.5 Hz
	$^5J_{X'X}$ = 0.6 Hz		$^5J_{XX'}$ = 0.6 Hz

ABX-System

8.67	d (H2'; X)		
8.30	dd (H6'; B)		
7.68	d (H5'; A)		
	$^3J_{AB}$ = 8.2 Hz		$^3J_{BA}$ = 8.2 Hz
	$^4J_{BX}$ = 1.9 Hz		$^4J_{XB}$ = 1.9 Hz

-CONH- 10.81 s (1H, exchangeable)
-CH_3 2.60 s (3H)

125 MHz ^{13}C NMR Spectrum (DMSO-d_6): δ/ppm

C1	142.7	C5	142.9	C9	163.4	C4'	136.4
C2	120.9	C6	123.5	C10	19.7	C5'	132.5
C3	134.9	C7	145.2	C1'	133.1	C6'	133.9
C4	119.5	C8	125.3	C2'	123.9		
C4a	126.6	C8a	130.2	C3'	148.9		

IR spectrum: cm^{-1}

3469 (s, br)	1673 (m)	1620 (m)	1580 (m)	1551 (m)	1529 (s)
1470 (w)	1353 (m)	1196 (s)	1112 (m)	1141 (s)	670 (m)
736 (w)	614 (s)				

UV Spectrum (phosphate buffer pH 6.5), λ_{max}: nm

230.5, 258.5, 310.5

7-(3-Amino-4-methylbenzamido)naphthalene-1,3,5-trisulfonic acid trisodium salt (7b)

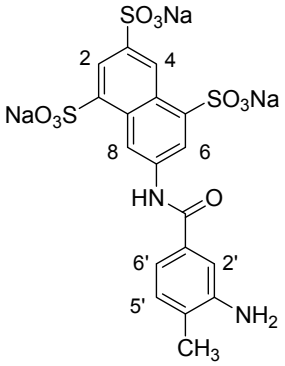

$C_{18}H_{13}N_2Na_3O_{10}S_3$ (582.5)

30 mg 10 % Pd/C were added to a solution of 1.00 g (1.62 mmol) nitro compound 7a in 50 ml water. The mixture was hydrogenated overnight and the product was purified, according to the general procedure 2.

Yield: white powder, 0.80 g (85.2 %)
Purity: 98.7 % (HPLC: t_R = 1.17 min, system 1)
TLC: Rf = 0.22 (Isopr + NH_3 = 5 + 2)
NaCl: 1.63 %
Water: 4.5 mol/mol
CHN analysis:

	%C	%H	%N	C/N
Calcd	37.12	2.25	4.81	7.72
Calcd (with NaCl/H_2O)	32.05	3.29	4.15	7.72
Found	32.25	3.31	4.21	7.66

500 MHz ^{1}H NMR Spectrum (DMSO-d_6): δ/ppm

AX-A'X'-System

8.96	dd (H4; X)	9.11	dd (H8; X')
8.38	d (H2; A)	8.26	d (H6; A')
	$^4J_{AX}$ = 1.9 Hz		$^4J_{XA}$ = 1.9 Hz

$^4J_{A'X'}$ = 2.0 Hz $^4J_{X'A'}$ = 2.0 Hz
$^5J_{X'X}$ = 0.7 Hz $^5J_{XX'}$ = 0.7 Hz

ABX-System
7.26 d (H2'; X)
7.19 dd (H6'; B)
7.02 d (H5'; A)
$^3J_{AB}$ = 7.9 Hz $^3J_{BA}$ = 7.9 Hz
$^4J_{BX}$ = 1.9 Hz $^4J_{XB}$ = 1.9 Hz

-CONH- 10.26 s (1H, exchangeable)
-NH_2 4.99 s (2H, exchangeable)
-CH_3 2.19 s (3H)

125 MHz ^{13}C NMR Spectrum (DMSO-d_6): δ/ppm

C1	142.4	C5	142.7	C9	166.3	C4'	133.4
C2	121.3	C6	123.4	C10	17.6	C5'	129.7
C3	135.6	C7	144.9	C1'	125.0	C6'	115.6
C4	119.3	C8	125.3	C2'	113.6		
C4a	126.3	C8a	130.2	C3'	146.5		

IR Spectrum: cm^{-1}

3400 (s)	1667 (m)	1634 (m)	1580 (m)	1546 (s)	1440 (m)
1362 (w)	1331 (m)	1195 (s)	1112 (m)	1043 (s)	794 (m)
671 (m)	618 (s)				

UV Spectrum (phosphate buffer pH 6.5), λ_{max}: nm
222.5, 260.5, 312.5

7,7'-(Carbonylbis(imino-3,1-(4-methylphenylene)carbonylimino)) bis-(naphthalene-1,3,5-trisulfonic acid) hexasodium salt (7c)

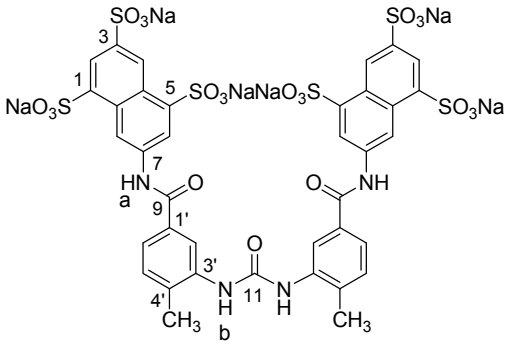

$C_{37}H_{24}N_4Na_6O_{21}S_6$ (1190.9)

0.54 g (0.9 mmol) Amine 7b were dissolved in 30 ml water and pH was adjusted to 4.0. To this solution, 4 ml (8 mmol) 20 % phosgene solution in toluene were added, under a constant pH of 4.0. The synthesis was performed and the product was purified according to the general procedure 3.

Yield: pale pink powder, 0.34 g (62.3 %)

Purity: 97.3 % (HPLC: t_R = 4.25 min, system 1)
TLC: Rf = 0.12 (Isopr + NH_3 = 5 + 2)
NaCl: 4.02 %
Water: 16.5 mol/mol
CHN analysis:

	%C	%H	%N	C/N
Calcd	37.32	2.03	4.70	7.94
Calcd (with NaCl/H_2O)	28.66	3.70	3.61	7.94
Found	28.70	3.86	3.66	7.85

500 MHz ^{1}H NMR Spectrum (DMSO-d_6): δ/ppm

AX-A'X'-System

9.06	dd (H4; X)	9.13	dd (H8; X')
8.36	d (H2; A)	8.28	d (H6; A')
	$^4J_{AX}$ = 1.6 Hz		$^4J_{XA}$ = 1.6 Hz
	$^4J_{A'X'}$ = 2.0 Hz		$^4J_{X'A'}$ = 2.0 Hz
	$^5J_{X'X}$ = 0.6 Hz		$^5J_{XX'}$ = 0.6 Hz

ABX-System

8.42	d (H2'; X)		
7.73	dd (H6'; B)		
7.34	d (H5'; A)		
	$^3J_{AB}$ = 8.0 Hz		$^3J_{BA}$ = 8.0 Hz
	$^4J_{BX}$ = 2.0 Hz		$^4J_{XB}$ = 2.0 Hz

-CONH-	10.51	s (2H, exchangeable)
-NHCONH-	8.58	s (2H, exchangeable)
$-CH_3$	2.38	s (6H)

125 MHz ^{13}C NMR Spectrum (DMSO-d_6): δ/ppm

C1	142.5	C5	142.7	C9	165.6	C3'	137.6
C2	122.4	C6	122.8	C10	18.4	C4'	133.4
C3	135.4	C7	144.9	C11	153.3	C5'	130.1
C4	119.2	C8	125.3	C1'	133.0	C6'	123.4
C4a	126.3	C8a	130.1	C2'	121.2		

IR Spectrum: cm^{-1}

3468 (s, br)	1638 (m)	1577 (m)	1540 (m)	1472 (w)	1441 (w)
1328 (w)	1193 (s)	1123 (m)	1042 (s)	669 (m)	613 (m)

UV Spectrum (Phosphate buffer, pH 6.5) λ_{max}: nm

226.5, 260.5, 312.5

ESI-MS positive mode (calcd/found): m/z

1168.9/1169.6 $[M-Na+2H]^+$, 1102.9/1103.0 $[M-4Na+5H]^+$

ESI-MS negative mode (calcd/found): m/z

1166.9/1167.4 $[M-Na]^-$

4-(4-Methyl-3-ureidobenzamido)naphthalene-2,6-disulfonic acid disodium salt (2d)

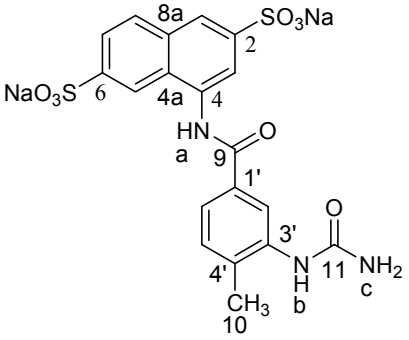

$C_{19}H_{15}N_3Na_2O_8S_2$ (523.4)

309 mg (0.64 mmol) Amine 2b were dissolved in 18 ml water and 3 ml acetic acid. To the solution, 360 mg (4.4 mmol) potassium cyanate were added in small portions. After the reaction was finished, the solution was adjusted to pH 6 with 5 M NaOH. The solution was evaporized until dryness. The crude product was stirred with 30 ml ethanol for 24 h and then filtrated. The product was further purified by stirring in methanol.

Yield: pale pink powder, 300 g (89.6 %)
Purity: 84.9 % (HPLC: t_R = 0.96 min, system 1)
TLC: Rf = 0.54 (Isopr + NH_3 = 5 + 2)
NaCl: 1.22 %
Water: 4.5 mol/mol
CHN analysis:

	%C	%H	%N	C/N
Calcd	43.60	2.89	8.03	5.43
Calcd (with NaCl/H_2O)	37.29	3.95	6.87	5.43
Found	37.52	4.04	6.76	5.55

500 MHz ^{1}H NMR Spectrum (DMSO-d_6): δ/ppm

ABX- A'X'-System

8.20	s (H5; X)	8.05	s (H1; X')
7.94	d (H8; B)	7.72	d (H3; A')
7.73	dd (H7; A)		
	$^3J_{AB}$ = 8.5 Hz	$^3J_{BA}$ = 8.5 Hz	
	$^4J_{AX}$ = 1.6 Hz	$^4J_{A'X'}$ = 1.6 Hz	

ABX-System

8.41	d (H2'; X)		
7.66	dd (H6'; B)		
7.30	d (H5'; A)		
	$^3J_{AB}$ = 7.8 Hz	$^3J_{BA}$ = 7.8 Hz	
	$^4J_{BX}$ = 1.9 Hz	$^4J_{XB}$ = 1.9 Hz	

-CONHa-	10.37	s (1H, exchangeable)
-CONHb-	7.96	s (1H, exchangeable)

$-NH_2$	6.10	s (2H, exchangeable)
$-CH_3$	2.28	s (3H)

125 MHz ^{13}C NMR Spectrum (DMSO-d_6): δ/ppm

C1	122.4	C5	119.9	C9	166.5	C3'	138.5
C2	146.0	C6	145.8	C10	18.2	C4'	132.6
C3	122.7	C7	124.5	C11	156.4	C5'	130.0
C4	134.7	C8	128.5	C1'	132.0	C6'	121.6
C4a	128.8	C8a	132.9	C2'	121.5		

IR Spectrum: cm^{-1}

3448 (m)	1665 (m)	1575 (w)	1532 (m)	1488 (w)	1450 (w)
1385 (w)	1272 (w)	1191 (s)	1097 (m)	1036 (s)	886 (w)
658 (m)	639 (m)				

UV Spectrum (phosphate buffer pH 6.5), λ_{max}: nm

234.5, 288.5

MALDI-TOF MS positive mode (calcd/found): m/z

546.0/545.9 $[M+Na]^+$, 524.0/523.9 $[M+H]^+$

4-(4-Methyl-3-(3-phenylureido)benzamido)naphthalene-2,6-disulfonic acid disodium salt (2e)

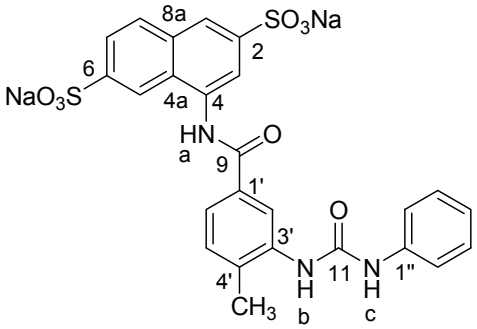

$C_{25}H_{19}N_3Na_2O_8S_2$ (599.5)

0.25 g (0.52 mmol) Amine 2b were dissolved in 20 ml water and 0.5 ml triethylamine. To this solution, 0.51 g (4.28 mmol) phenyl isocyanate were slowly dropped and stirred until finished. 50 ml Diethyl ether were added and the mixture was stirred for 2 hours. The aqueous phase was separated and extracted with two times 50 ml diethyl ether and then evaporated to dryness. The crude product was purified by cation exchange chromatography to get rid of triethylamine salt, according to general procedure 4.

Yield: pink powder, 276.8 mg (88.8 %)
Purity: 94.5 % (HPLC: t_R = 3.96 min, system 1)
TLC: Rf = 0.55 (Isopr + NH_3 = 5 + 2)
NaCl: 22.43 %
Water: 6.5 mol/mol

CHN analysis:

	% C	% H	% N	C/N
Calcd	50.08	3.19	7.01	7.14
Calcd (with $NaCl/H_2O$)	32.50	3.49	4.55	7.15
Found	32.59	3.80	4.62	7.05

500 MHz ^{1}H NMR Spectrum (DMSO-d_6): δ/ppm

ABX- A'X'-System

8.21	pt (H5; X)	8.06	s (H1; X')
7.96	d (H8; B)	7.73	d (H3; A')
7.75	dd (H7; A)		
	$^3J_{AB}$ = 8.5 Hz	$^3J_{BA}$ = 8.5 Hz	
	$^4J_{AX}$ = 1.6 Hz	$^3J_{XA}$ = 1.6 Hz	
	$^4J_{A'X'}$ = 1.6 Hz	$^5J_{XX'}$ = 0.8 Hz	

ABX-System

8.51	d (H2'; X)		
7.70	dd (H6; B)		
7.35	d (H5'; A)		
	$^3J_{AB}$ = 8.0 Hz	$^3J_{BA}$ = 8.0 Hz	
	$^4J_{BX}$ = 1.9 Hz	$^4J_{XB}$ = 1.9 Hz	

AA'XX'Y-System

7.52	dd (H2"H6"; AA')		
7.25	m (H3"H5"; XX')		
6.93	tt (H4"; Y)		
	$^3J_{AX} = {}^3J_{XA}$ = 8.0 Hz	$^3J_{A'X'} = {}^3J_{X'A'}$ = 8.0 Hz	
	$^3J_{XY} = {}^3J_{YX}$ = 7.3 Hz	$^3J_{X'Y} = {}^3J_{YX'}$ = 7.3 Hz	
	$^4J_{AY} = {}^4J_{YA}$ = 1.3 Hz	$^4J_{YA'} = {}^4J_{A'Y}$ = 1.3 Hz	
	$^4J_{XX'} = {}^4J_{X'X}$ = 1.3 Hz		

-CONHa-	10.41	s (1H, exchangeable)
-CONHb-	8.59	s (1H, exchangeable)
-CONHc-	9.83	s (1H, exchangeable)
$-CH_3$	2.38	s (3H)

125 MHz ^{13}C NMR Spectrum (DMSO-d_6): δ/ppm

C1	122.4	C6	145.7	C11	153.0	C6'	121.6
C2	146.0	C7	124.6	C1'	132.1	C1"	140.3
C3	122.8	C8	128.5	C2'	121.1	C4"	121.9
C4	134.8	C8a	132.9	C3'	138.0	C2"C6"	118.1
C4a	128.9	C9	166.4	C4'	132.7	C3"C5"	128.8
C5	120.0	C10	18.6	C5'	130.2		

IR Spectrum: cm^{-1}

3437 (m, br)	1654 (m)	1599 (w)	1551 (s)	1488 (s)	1443 (w)
1385 (w)	1297 (w)	1189 (s)	1094 (s)	1033 (s)	751 (w)
657 (m)	637 (m)				

UV Spectrum (phosphate buffer pH 6.5), λ_{max}: nm

234.5

MALDI-TOF MS positive mode (calcd/found): m/z
600.0/600.0 $[M+H]^+$, 622.0/622.0 $[M+Na]^+$, 578.1/578.0 $[M-Na+2H]^+$, 556.1/556.1 $[M-2Na+3H]^+$

MALDI-TOF MS negative mode (calcd/found): m/z
576.1/575.9 $[M-Na]^-$, 554.1/554.0 $[M-2Na+H]^-$

4-(4-Methyl-3-(3-phenylthioureido)benzamido)naphthalene-2,6-disulfonic acid disodium salt (2f)

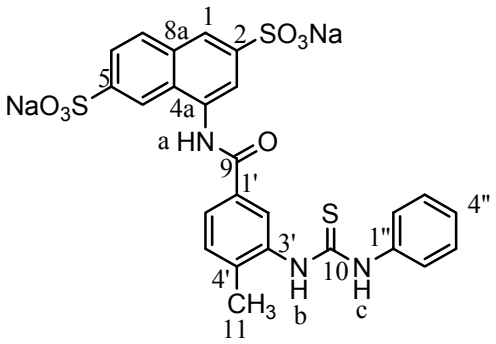

$C_{25}H_{19}N_3Na_2O_7S_3$ (615.6)

300 mg (0.62 mmol) Amine 2b were dissolved in 10 ml water and 0.5 ml triethylamine. 80 Drops phenyl isothiocyanate were slowly added to the solution and the reaction was stirred until it was finished. 70 ml Water was added to the mixture and extracted with three times 5o ml diethyl ether. The water phase was adjusted to pH of 7.0 and evaporated under vacuo. The product was purified by column chromatography (silica gel G60/Isopr + NH_3 = 5 + 1).

Yield: yellow powder, 190 mg (49.9 %)
Purity: 87.0 % (HPLC: t_R = 3.61 min, system 2)
TLC: Rf = 0.66 (Isopr + NH_3 = 5 + 2)
NaCl: 18.00 %
Water: 5.5 mol/mol
CHN analysis:

	% C	% H	% N	C/N
Calcd	48.78	3.11	6.83	7.14
Calcd (with $NaCl/H_2O$)	34.45	3.47	4.82	7.15
Found	34.44	3.64	4.97	6.93

500 MHz ^{1}H NMR Spectrum (DMSO-d_6): δ/ppm
ABX- A'X'-System

8.20	pt (H5; X)	8.06	s (H1; X')
7.95	d (H8; B)	7.72	d (H3; A')
7.74	dd (H7; A)		
	$^3J_{AB}$ = 8.5 Hz	$^3J_{BA}$ = 8.5 Hz	
	$^4J_{AX}$ = 1.6 Hz	$^4J_{XA}$ = 1.6 Hz	
	$^4J_{A'X'}$ = 1.3 Hz	$^5J_{XX'}$ = 0.8 Hz	

ABX-System

8.02 d (H2'; X)
7.94 dd (H6'; B)
7.43 d (H5'; A)
$^3J_{AB}$ = 8.3 Hz $^3J_{BA}$ = 8.3 Hz
$^4J_{BX}$= 1.7 Hz $^4J_{XB}$ = 1.7 Hz

AA'XX'Y-System

7.56 d (H2"H6"; AA')
7.31 m (H3"H5"; XX')
7.10 tt (H4"; Y)
$^3J_{AX}$ = $^3J_{XA}$= 7.6 Hz $^3J_{A'X'}$ = $^3J_{X'A'}$ = 7.6 Hz
$^3J_{XY}$ = $^3J_{YX}$ = 7.6 Hz $^3J_{X'Y}$ = $^3J_{YX'}$ = 7.6 Hz
$^4J_{YA'}$ = $^4J_{YA}$ = 1.3 Hz $^4J_{XX'}$ = $^4J_{X'X}$ = 2.2 Hz

-CONHa- 10.48 s (1H, exchangeable)
-CONHb- 9.80 s (1H, exchangeable)
-CONHc- 10.19 s (1H, exchangeable)
-CH_3 2.35 s (3H)

125 MHz ^{13}C NMR Spectrum (DMSO-d_6): δ/ppm

C1	122.5	C6	145.7	C11	180.8	C6'	125.9
C2	146.0	C7	124.6	C1'	132.3	C1"	139.8
C3	122.8	C8	128.5	C2'	123.8	C4"	127.9
C4	134.6	C8a	132.9	C3'	139.5	C2"C6"	124.4
C4a	128.9	C9	165.6	C4'	138.2	C3"C5"	128.5
C5	119.9	C10	18.2	C5'	130.5		

IR Spectrum: cm^{-1}

3437 (m, br)	1652 (m)	1531 (s)	1489 (m)	1447 (w)	1384 (w)
1191 (s)	1097 (m)	1035 (s)	886 (w)	657 (m)	639 (m)

UV Spectrum (phosphate buffer pH 6.5), λ_{max}: nm

234.5

MALDI-TOF MS positive mode (calcd/found): m/z

616.0/616.0[M+H]$^+$, 638.0/638.0 [M+Na]$^+$, 594.0/594.0 [M-Na+2H]$^+$, 572.1/572.0 [M-2Na+3H]$^+$

MALDI-TOF MS negative mode (calcd/found): m/z

614.0/613.9 [M-H]$^-$, 592.0/591.9 [M-Na]$^-$, 570.0/569.9 [M-2Na+H]$^-$

4-(4-Methyl-3-(3-(4-nitrophenyl)ureido)benzamido) naphthalene-2,6-disulfonic acid disodium salt (2g)

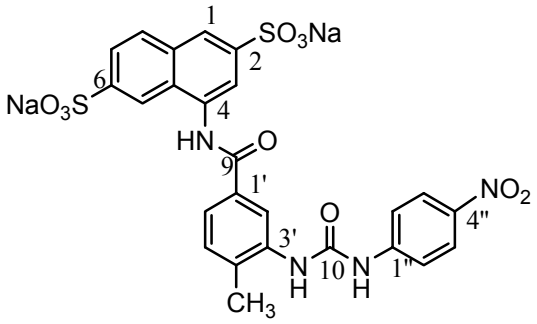

$C_{25}H_{18}N_4Na_2O_{10}S_2$ (644.5)

240 mg (0.5 mmol) Amine 2b were dissolved in 5 ml DMSO. A solution of 240 mg (6.09 mmol) 4-nitrophenyl isocyanate in 10 ml dichloroethane was slowly dropped to the amine. After the reaction was finished, 100 ml diethyl ether were added and the mixture was stirred for 3 hours. The yellow precipitate was filtrated and dried. The product was purified by column chromatography (siliga gel G60/Isopr + NH_3 = 5 + 1).

Yield: yellow powder, 244 mg (75.7 %)
Purity: 90.1 % (HPLC: t_R = 5.6 7 min, system 1)
TLC: Rf = 0.62 (Isopr + NH_3 = 5 + 2)
NaCl: 8.84 %
Water: 9.5 mol/mol

CHN analysis:

	%C	%H	%N	C/N
Calcd	46.59	2.81	8.69	5.36
Calcd (with NaCl/H_2O)	33.56	4.17	6.26	5.36
Found	33.75	4.41	6.18	5.46

500 MHz ^{1}H NMR Spektrum (DMSO-d_6): δ/ppm

ABX- A'X'-System

8.20 s (H5; X) 8.06 s (H1; X')
7.95 d (H8; B) 7.73 m (H3; A')
7.72 m (H7; A)
$^3J_{AB}$ = 8.2 Hz $^3J_{BA}$ = 8.2 Hz
$^4J_{AX}$ = 1.6 Hz

ABX-System

8.48 d (H2'; X-Part)
7.76 m (H6'; B-Part)
7.38 d (H5'; A-Part)
$^3J_{AB}$ = 8.2 Hz $^4J_{XB}$ = 1.6 Hz

AA'BB'-System

8.17 d (H3"H5"; BB'-Part)

	7.75	m (H2"H6"; AA'-Part) $^3J_{AB}$ = 9.5 Hz $^4J_{AA'}$ = 2.8 Hz $^4J_{BB'}$ = 2.2 Hz
-CONHa-	10.50	s (1H, exchangeable)
-CONHb-	8.77	s (1H, exchangeable)
-CONHc-	10.43	s (1H, exchangeable)
$-CH_3$	2.38	s (3H)

125 MHz ^{13}C NMR Spectrum (DMSO-d_6): δ/ppm

C1	122.5	C6	145.8	C11	152.5	C6'	122.8
C2	146.0	C7	124.6	C1'	133.0	C1"	141.0
C3	122.8	C8	128.5	C2'	121.8	C4"	146.9
C4	134.7	C8a	132.9	C3'	137.2	C2"C6"	117.4
C4a	128.9	C9	166.2	C4'	132.7	C3"C5"	125.3
C5	119.9	C10	18.3	C5'	130.3		

IR Spectrum: cm^{-1}

3425 (m, br) 1504 (m) 1331 (m) 1179 (s) 1031 (s)

UV Spectrum (phosphate buffer pH 6.5), λ_{max}: nm

234.5, 330.5

ESI-MS negative mode (calcd/found): m/z

643.0/643.3 $[M-H]^-$

4-(3-(3-(4-Aminophenyl)ureido)-4-methylbenzamido) naphthalene-2,6-disulfonic acid disodium salt (2h)

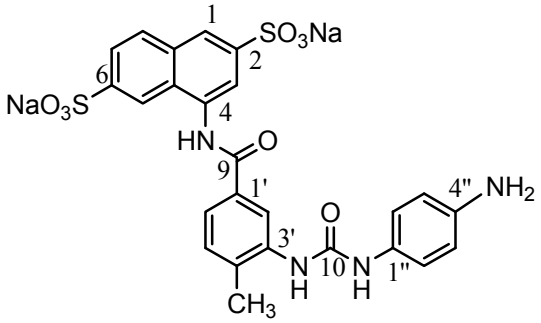

$C_{25}H_{20}N_4Na_2O_8S_2$ (614.6)

10 mg 10 % Pd/C were added to a solution of 130 mg (0.2 mmol) compound 2g in 20 ml water. The mixture was hydrogenated overnight and the product was purified according to the general procedure 2.

Yield: brown powder, 101 mg (80.0 %)
Purity: 91.9 % (HPLC: t_R = 6.49 min, system 2)
TLC: Rf = 0.57 (Isopr + NH_3 = 5 + 2)
NaCl: 1.90 %
Water: 6.5 mol/mol

CHN analysis:

	% C	% H	% N	C/N
Calcd	48.86	3.28	9.12	5.36
Calcd (with $NaCl/H_2O$)	40.26	4.46	7.51	5.36
Found	40.54	4.10	7.14	5.68

500 MHz ^{1}H NMR Spectrum (DMSO-d_6): δ/ppm

ABX- A'X'-System

8.19	pt (H5; X)	8.06	s (H1; X')
7.95	d (H8; B)	7.72	d (H3; A')
7.73	dd (H7; A)		
	$^3J_{AB}$ = 8.3 Hz	$^3J_{BA}$ = 8.3 Hz	
	$^4J_{AX}$= 1.7 Hz	$^4J_{XA}$ = 1.7 Hz	
	$^4J_{A'X'}$ = 1.6 Hz	$^5J_{XX'}$ = 0.7 Hz	

ABX-System

8.48	d (H2'; X)		
7.68	dd (H6'; B)		
7.33	d (H5'; A)		
	$^3J_{AB}$ = 7.9 Hz	$^3J_{BA}$ = 7.9 Hz	
	$^4J_{BX}$ = 1.9 Hz	$^4J_{XB}$ = 1.9 Hz	

AA'BB'-System

7.11	m (H2"H6"; BB')		
6.51	m (H3"H5"; AA')		
	$^3J_{AB}$ = 8.5 H z	$^3J_{A'B'}$ = 8.5 Hz	
	$^4J_{AA'}$ = 2.2 Hz	$^4J_{A'A}$ = 2.2 Hz	
	$^4J_{BB'}$ = 3.1 Hz	$^4J_{B'B}$ = 3.1 Hz	

-CONHa-	10.39	s (1H, ex)	
-CONHb-	8.55	s (1H, ex)	
-CONHc-	7.90	s (1H, ex)	
$-NH_2$	4.75	s (2H, ex)	
$-CH_3$	2.32	s (3H)	

125 MHz ^{13}C NMR Spectrum (DMSO-d_6): δ/ppm

C1	122.4	C6	145.8	C11	153.1	C6'	121.7
C2	146.0	C7	124.6	C1'	132.7	C1"	128.5
C3	122.8	C8	128.9	C2'	121.0	C4"	144.1
C4	134.7	C8a	132.9	C3'	138.2	C2"C6"	120.7
C4a	128.9	C9	166.4	C4'	131.8	C3"C5"	114.7
C5	119.9	C10	18.2	C5'	130.1		

IR Spectrum: cm^{-1}

3400 (s, br)	1641 (m)	1514 (s)	1450 (w)	1384 (w)	1191 (s)
1096 (m)	1033 (s)	655 (m)	637 (m)		

UV Spectrum (phosphate buffer pH 6.5), λ_{max}: nm

234.5

MALDI-TOF MS positive mode (calcd/found): m/z

615.1/615.0 $[M+H]^+$, 637.0/637.0 $[M+Na]^+$, 593.1/593.0 $[M-Na+2H]^+$, 571.1/571.0 $[M-2Na+3H]^+$

MALDI-TOF MS negative mode (calcd/found): m/z

591.1/591.0 $[M-Na]^-$, 569.1/569.0 $[M-2Na+H]^-$

4-(3-(3-(3-(Ethoxycarbonyl)phenyl)ureido)-4-methylbenzamido) naphthalene-2,6-disulfonic acid disodium salt (2i)

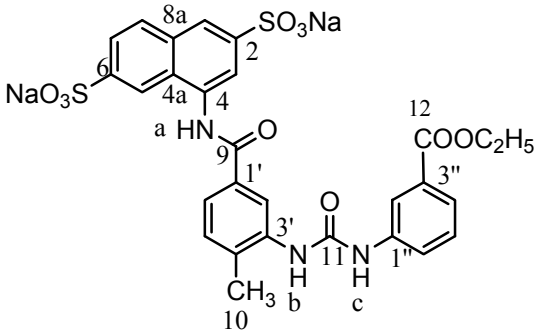

$C_{28}H_{23}N_3Na_2O_{10}S_2$ (671.6)

3.32 g (20 mmol) Ethyl 3- aminobenzoate, dissolved in 20 ml dichloroethane and 3 ml (21.56 mmol) triethylamine, were slowly dropped into a cooled (0°C) solution of 2.19 g (7.38 mmol) triphosgene, dissolved in 30 ml dichloroethane. The mixture was stirred for 5 hours. Triethylamine HCl precipitate was filtered out. The solution containing the isocyanate (checked by IR) was then added to 365 mg (0.76 mmol) amine 2b, dissolved in a mixture of 10 ml water and 0.1 ml triethylamine. The mixture was vigorously stirred until the reaction was finished. 50 ml water and 60 ml diethyl ether were added to the solution and stirred for an hour. The aqueous phase was separated and extracted again two times with 50 ml diethyl ether. The aqueous phase was separated, neutralized and evaporated to dryness. The product was purified by cation exchange column chromatography, according general procedure 4. The product was then stirred in methanol/water, filtrated and dried.

Yield: pale pink powder, 320 mg (63.0 %)
Purity: 91.9 % (HPLC: t_R = 4.78 min, system 1)
TLC: Rf = 0.64 (Isopr + NH_3 = 5 + 2)
NaCl: 24.39 %
Water: 5.5 mol/mol
CHN analysis:

	%C	%H	%N	C/N
Calcd	50.07	3.45	6.26	8.00
Calcd (with NaCl/H_2O)	32.99	3.36	4.12	8.00
Found	33.18	3.35	4.25	7.81

500 MHz ^{1}H NMR Spectrum (DMSO-d_6): δ/ppm

ABX- A'X'-System

8.20	pt (H5, X)	8.06	s (H1; X')
7.95	d (H8; B)	7.72	d (H3; A')

7.73 dd (H7; A)
$^3J_{AB}$ = 8.5 Hz $^3J_{BA}$ = 8.5 Hz
$^4J_{BX}$ = 1.6 Hz $^4J_{XB}$ = 1.6 Hz
$^5J_{XX'}$ = 0.7 Hz

ABX-System
8.49 d (H2'; X)
7.74 dd (H6'; B)
7.36 d (H5'; A)
$^3J_{AB}$ = 7.5 Hz $^3J_{BA}$ = 7.5 Hz
$^4J_{XB}$ = 1.6 Hz $^4J_{BX}$ = 1.6 Hz

ABCX-System
8.15 t (H2''; X)
7.76 ddd (H6''; C)
7.53 dt (H4''; A)
7.40 pt (H5''; B)
$^3J_{AB}$ = 7.6 Hz $^3J_{BA}$ = 7.6 Hz
$^3J_{BC}$ = 8.2 Hz $^3J_{CB}$ = 8.2 Hz
$^4J_{AX}$ = 1.6 Hz $^4J_{XA}$ = 1.6 Hz
$^4J_{CX}$ = 2.2 Hz $^4J_{XC}$ = 2.2 Hz
$^4J_{AC}$ = 1.3 Hz $^4J_{CA}$ = 1.3 Hz

A_3M_2-System
4.30 q (H13; M)
1.30 t (H14; A)
$^3J_{AM}$ = 7.1 Hz $^3J_{MA}$ = 7.1 Hz

-CONHa- 10.42 s (1H, exchangeable)
-CONHb- 8.57 s (1H, exchangeable)
-CONHc- 10.00 s (1H, exchangeable)
$-CH_3$ 2.38 s (3H)

125 MHz ^{13}C NMR Spectrum (DMSO-d_6): δ/ppm

C1	122.5	C7	124.6	C13	60.8	C6'	122.2
C2	146.0	C8	128.5	C14	14.3	C1''	140.6
C3	122.8	C8a	132.9	C1'	132.5	C2''	118.4
C4	134.7	C9	165.9	C2'	121.4	C3''	130.6
C4a	128.9	C10	18.5	C3'	137.7	C4''	122.4
C5	119.9	C11	152.9	C4'	132.7	C5''	129.3
C6	145.8	C12	166.3	C5'	130.2	C6''	122.3

IR spectrum: cm^{-1}

3445 (m, br)	1713 (m)	1652 (m)	1527 (s)	1486 (m)	1445 (w)
1387 (w)	1296 (s)	1187 (s)	1096 (m)	1033 (s)	887 (w)
750 (m)	657 (m)				

UV Spectrum (phosphate buffer pH 6.5), λ_{max}: nm
230.5, 312.5

MALDI-TOF MS positive mode (calcd/found): m/z
672.1/672.0 $[M+H]^+$, 694.1/694.0 $[M+Na]^+$, 650.1/650.0 $[M-Na+2H]^+$

MALDI-TOF MS negative mode (calcd/found): m/z
648.1/648.1 $[M-Na]^-$, 626.1/626.0 $[M-2Na+H]^-$

3-(3-(5-(3,7-Disulfonatonaphthalen-1-ylcarbamoyl)-2-methylphenyl) ureido) benzoic acid trisodium salt (2j)

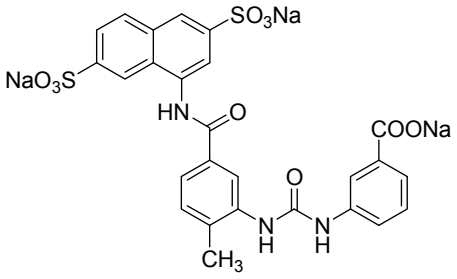

$C_{26}H_{19}N_3Na_2O_{10}S_2$ (643.6)

To a solution of 111 mg (0.16 mmol) 2i in 10 ml water, 1.0 ml 0.1 M. NaOH were added and stirred for an hour. After the reaction was completed, the mixture was purified by cation exchange chromatography according to general procedure 4. The product was stirred with 10 ml methanol, filtrated and dried.

Yield: white powder, 65 mg (63.0 %)
Purity: 89.9 % (HPLC: t_R = 2.25 min, system 1)
TLC: Rf = 0.43 (Isopr + NH_3 = 5 + 2)
NaCl: 34.52 %
Water: 10 mol/mol
CHN analysis:

	% C	% H	% N	C/N
Calcd	48.52	2.98	6.53	7.43
Calcd.(with NaCl/H_2O)	24.82	3.12	3.34	7.43
Found	24.86	3.18	3.31	7.52

500 MHz ^{1}H NMR Spectrum (DMSO-d_6): δ/ppm

ABX- A'X'-System

8.19	pt (H5; X)	8.06	s (H1; X')
7.95	d (H8; B)	7.71	d (H3; A')
7.74	dd (H7; A)		
	$^3J_{AB}$ = 8.5 Hz	$^3J_{BA}$ = 8.5 Hz	
	$^4J_{AX}$ = 1.6 Hz	$^4J_{XA}$ = 1.6 Hz	
	$^4J_{A'X'}$ = 1.3 Hz	$^5J_{XX'}$ = 0.6 Hz	

ABX-System

8.56	d (H2'; X)	
7.68	dd (H6'; B)	
7.33	d (H5'; A)	
	$^3J_{AB}$ = 7.9 Hz	$^3J_{BA}$ = 7.9 Hz

$^4J_{BX}$ = 1.6 Hz $^4J_{XB}$ = 1.6 Hz

ABCX-System

8.20	dd (H2''; X)	
7.53	ddd (H6''; A)	
7.50	ddd (H4''; C)	
7.23	t (H5''; B)	
	$^3J_{AB}$ = 7.6 Hz	$^3J_{BA}$ = 7.6 Hz
	$^3J_{BC}$ = 7.9 Hz	$^3J_{CB}$ = 7.9 Hz
	$^4J_{AC}$ = 1.3 Hz	$^4J_{AX}$ = 1.3 Hz
	$^4J_{CA}$ = 1.5 Hz	$^4J_{CX}$ = 1.5 Hz

-CONHa-	10.42	s (1H, exchangeable)
-CONHb-	8.91	s (1H, exchangeable)
-CONHc-	10.22	s (1H, exchangeable)
$-CH_3$	2.40	s (3H)

IR Spectrum: cm^{-1}

3413 (s, br)	1645 (m)	1564 (m)	1489 (w)	1440 (w)	1404 (w)
1312 (m)	1098 (m)	1037 (m)	658 (w)		

UV Spectrum (phosphate buffer pH 6.5), λ_{max}: nm

234

MALDI-TOF MS positive mode (calcd/found): m/z

644.0/644.0 $[M+H]^+$, 666.0/666.0 $[M+Na]^+$, 688.0/688.0 $[M+2Na-H]^+$

MALDI-TOF MS negative mode (calcd/found): m/z

642.0/642.0 $[MM-H]^-$, 620.0/620.0 $[M-Na]^-$, 598.1/598.0 $[M-2Na+H]^-$

4-(3-(3-(3,5-Bis(ethoxycarbonyl)phenyl)ureido)-4-methylbenzamido)- naphthalene-2,6-disulfonate disodium salt (2k)

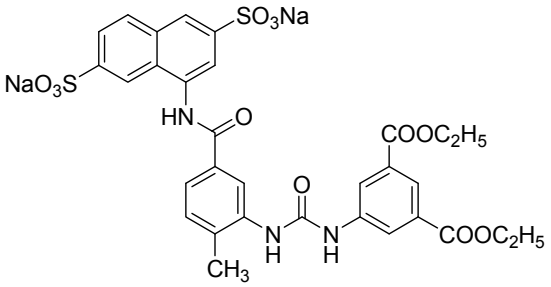

$C_{31}H_{27}N_3Na_2O_{12}S_2$ (743.7)

0.48 g (2 mmol) Diethyl 5-aminoIsoprhthalate, dissolved in 10 ml dichloromethane and 750 µl (4.2 mmol) triethylamine were slowly dropped into a cooled solution of 0.50 g (1.7 mmol) triphosgene, dissolved in 10 ml dichloroethane. The mixture was stirred for 5 hours. Triethylmine HCl precipitat was filtered out. The solvent was partially evaporated. The solution containing isocyanate (checked by IR) was slowly added into a solution of 240 mg (0.5 mmol) amine 2b, dissolved in 2 ml DMSO and 1 ml triethylamine. The mixture was vigorously stirred until the reaction

was finished. 50 ml Diethyl ether were added to the reaction mixture and stirred for 3 hours. The product was filtered and purified by column chromatography (siliga gel G60/Isopr + NH_3 = 5 + 1) and cation exchange chromatography according to general procedure 4.

Yield: white powder, 336 mg (90.4 %)
Purity: 96.1 % (HPLC: t_R = 6.48 min, system 1)
TLC: Rf = 0.73 (Isopr + NH_3 = 5 + 2)
NaCl: 30.98 %
Water: 3 mol/mol
CHN-analysis:

	% C	% H	% N	C/N
Calcd	50.07	3.66	5.65	8.86
Calcd (with NaCl/H_2O)	32.21	2.88	3.64	8.86
Found	32.06	2.68	3.70	8.66

500 MHz ^{1}H NMR Spectrum (DMSO-d_6): δ/ppm

ABX- A'X'-System

8.21	s (H5; X)	8.07 s (H1; Y')
7.96	d (H8; B)	7.74 d (H3; X')
7.76	dd (H7; A)	
	$^3J_{AB}$ = 8.5 Hz	$^3J_{BA}$ = 8.5 Hz
	$^4J_{AX}$ = 1.6 Hz	$^4J_{A'X'}$ = 1.6 Hz

ABX-System

8.51	d (H2'; X)	
7.73	dd (H6'; B)	
7.36	d (H5'; A)	
	$^3J_{AB}$ = 7.5 Hz	$^3J_{BA}$ = 7.5 Hz
	$^4J_{BX}$ = 1.7 Hz	$^4J_{XB}$ = 1.7 Hz

AB_2-System

8.39	d (H2''H6''; B)	
8.05	t (H4''; A)	
	$^4J_{AB}$ = 1.3 Hz	$^4J_{BA}$ = 1.3 Hz

A_3M_2-System-1

4.34	q (H13; M)	
1.32	t (H14; A)	
	$^3J_{AX}$ = 7.1 Hz	$^3J_{XA}$ = 7.1 Hz

A_3M_2-System-2

4.34	q (H13; M)	
1.32	t (H14; A)	
	$^3J_{AX}$ = 7.1 Hz	$^3J_{XA}$ = 7.1 Hz

-CONHa-	10.77	s (1H, exchangeable)
-CONHb-	8.94	s (1H, exchangeable)
-CONHc-	10.45	s (1H, exchangeable)
$-CH_3$	2.40	s (3H)

125 MHz ^{13}C NMR Spectrum (DMSO-d_6): δ/ppm

C1	122.5	C7	124.6	C13	61.3	C6'	122.3
C2	145.9	C8	128.5	C14	14.3	C1"	141.4
C3	122.8	C8a	132.9	C1'	132.5	C4"	122.5
C4	134.8	C9	166.3	C2'	121.3	C2"C6"	122.3
C4a	128.9	C10	18.7	C3'	137.6	C3"C5"	131.1
C5	120.0	C11	153.1	C4'	132.6		
C6	145.7	C12	165.2	C5'	130.3		

IR Spectrum: cm^{-1}

3463 (s, br)	3346 (s)	2984 (w)	1712 (s)	1672 (m)	1611 (w)
1561 (m)	1513 (m)	1485 (m)	1454 (w)	1375 (m)	1237 (s)
1211 (s)	1097 (m)	1037 (s)	753 (m)	655 (s)	637 (s)

UV Spectrum (phosphate buffer pH 6.5), λ_{max}: nm

233

ESI-MS negative mode (calcd/found): m/z

720.1/720.1 $[M-Na]^-$

5-(3-(5-(3,7-Disulfonatonaphthalen-1-ylcarbamoyl)-2-methylphenyl)ureido)-Isoprhthalate tetrasodium salt (2l)

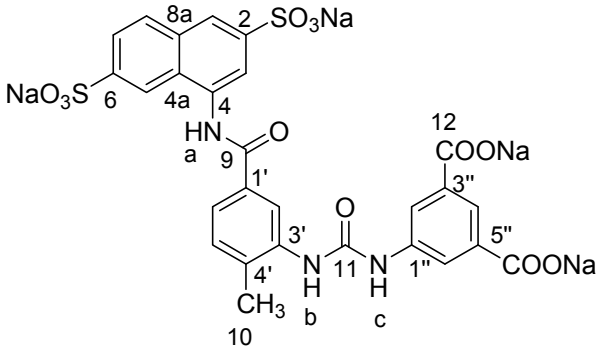

$C_{27}H_{17}N_3Na_4O_{12}S_2$ (731.5)

1 ml 0.1 M NaOH was added to a solution of 120 mg (0.16 mmol) ester 2k dissolved in 20 ml water. The mixture was stirred for an hour. The product was purified by stirring in 10 ml methanol.

Yield: white powder, 71.6 mg (61.2 %)
Purity: 96.2 % (HPLC: t_R = 1.14 min, system 1)
TLC: Rf = 0.34 (Isopr + NH_3 = 5 + 2)
NaCl: 22.13 %
Water: 7 mol/mol
CHN analysis:

	% C	% H	% N	C/N
Calcd	44.33	2.34	5.74	7.72
Calcd (with NaCl/H_2O)	29.14	2.90	3.78	7.72

Found	29.25	3.30	3.95	7.40

500 MHz ^{1}H NMR Spectrum (DMSO-d_6): δ/ppm

ABX- A'X'-System

8.21	s (H5; X)	8.09	s (H1; X')
7.96	d (H8; B)	7.73	d (H3; A')
7.75	dd (H7; A)		
	$^{3}J_{AB}$ = 8.5 Hz	$^{3}J_{BA}$ = 8.5 Hz	
	$^{4}J_{AX}$ = 1.6 Hz		
	$^{4}J_{A'X'}$ = 1.6 Hz		

ABX-System

8.43	d (H2'; X)		
7.74	dd (H6'; B)		
7.38	d (H5'; A)		
	$^{3}J_{AB}$ = 7.5 Hz	$^{3}J_{BA}$ = 7.5 Hz	
	$^{4}J_{BX}$ = 1.4 Hz	$^{4}J_{XB}$ = 1.4 Hz	

AB_2-System

8.24	s (H2"H6"; B)
8.06	s (H4"; A)

-CONHa-	10.44	s (1H, exchangeable)
-CONHb-	8.99	s (1H, exchangeable)
-CONHc-	9.88	s (1H, exchangeable)
-CH_3	2.39	s (3H)

125 MHz ^{13}C NMR Spectrum (DMSO-d_6): δ/ppm

C1	122.6	C6	145.7	C11	153.3	C5'	130.3
C2	145.9	C7	124.5	C12	166.3	C6'	122.7
C3	122.7	C8	128.5	C1'	132.5	C1"	140.1
C4	134.7	C8a	133.5	C2'	121.6	C4"	123.7
C4a	128.9	C9	168.5	C3'	137.8	C2"C6"	122.4
C5	119.9	C10	18.2	C4'	132.5	C3"C5"	132.9

IR Spectrum: cm^{-1}

3436 (s, br)	1701 (m)	1654 (m)	1629 (m)	1577 (s)	1529 (m)
1491 (w)	1412 (m)	1375 (m)	1303 (w)	1210 (s)	1095 (s)
1031 (s)	782 (w)	637 (s)			

UV Spectrum (phosphate buffer pH 6.5), λ_{max}: nm

233

ESI-MS negative mode (calcd/found): m/z

730.0/730.2 $[M-H]^-$, 708.0/708.2 $[M-Na]^-$, 686.0/686.2 $[M-2Na+H]^-$, 664.0/664.2 $[M-3Na+2H]^-$, 642.0/642.2 $[M-4Na+3H]^-$, 331.5/331.6 $[M-3Na+H]^{2-}$

ESI-MS positive mode (calcd/found): m/z

754.0/754.2 $[M+Na]^+$, 688.0/688.4 $[M-2Na+3H]^+$

4-(4-Methyl-3-(3-naphthalen-1-ylureido)benzamido)naphthalene-2,6-disulfonic acid disodium salt (2m)

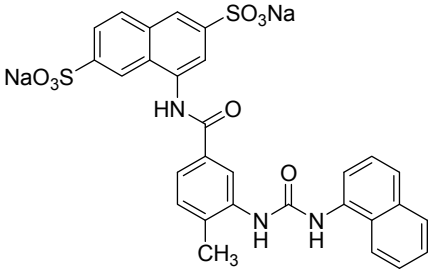

$C_{29}H_{21}N_3Na_2O_8S_2$ (649.6)

2.1 g (14.7 mmol) 1-Aminonaphthalene, dissolved in 70 ml diethyl ether, was dropped into a 10 ml cooled (0°C) (20 mmol) 20 % phosgene solution in toluene. The mixture was stirred at 0°C for 2 hours and then heated to reflux for 4 hours. The solid side product was filtered out and the brown solution was evaporated to dryness. The obtained isocyanate (checked by IR) was added to a solution of 264 mg (0.55 mmol) amine 2b in 20 ml water and 0.4 ml triethylamine. The mixture was vigorously stirred until the reaction was finished. 50 ml Diethyl ether were added to the reaction and the mixture was stirred for 3 hours. The product was filtered and purified by column chromatography (siliga gel G60/Isopr + NH_3 = 5 + 1), following by cation exchange chromatography according to general procedure 4.

Yield: white substance, 213 mg (59.6 %)
Purity: 98.4 % (HPLC: t_R = 6.8 min, system 1)
TLC: Rf = 0.70 (Isopr + NH_3 = 5 + 2)
NaCl: 9.57 %
Water: 4 mol/mol
CHN analysis:

	% C	% H	% N	C/N
Calcd	53.62	3.26	6.47	8.29
Calcd (with NaCl/H_2O)	43.65	3.66	5.26	8.29
Found	43.72	4.00	5.33	8.20

500 MHz ^{1}H NMR Spectrum (DMSO-d_6): δ/ppm

ABX- A'X'-System

8.20	pt (H5; X)	8.05	s (H1; X')
7.95	d (H8; B)	7.72	d (H3; A')
7.73	dd (H7; A)		
	$^3J_{AB}$ = 8.5 Hz	$^3J_{BA}$ = 8.5 Hz	
	$^4J_{XB}$ = 1.6 Hz	$^4J_{A'X'}$ = 2.2 Hz	
	$^5J_{XX'}$ = 0.9 Hz		

ABX-System

8.53	d (H2'; X)		
7.74	dd (H6'; B)		
7.39	d (H5'; A)		
	$^3J_{AB}$ = 8.3 Hz	$^3J_{BA}$ = 8.3 Hz	
	$^4J_{BX}$ = 1.7 Hz	$^4J_{XB}$ = 1.7 Hz	

ABX-A'B'X'Y'-System

8.34	d (H8''; Y')	7.91	dd (H4''; X)
8.07	dd (H5''; X')	7.61	d (H2''; B)
7.58	dt (H7''; B')	7.46	t (H3''; A)
7.53	dt (H6''; A')		

$^3J_{AB}$ = 8.1 Hz $^3J_{BA}$ = 8.1 Hz
$^3J_{AX}$ = 8.1 Hz $^3J_{XA}$ = 8.1 Hz
$^4J_{XB}$ = 1.3 Hz
$^3J_{A'B'}$ = 7.6 Hz $^3J_{B'A'}$ = 7.6 Hz
$^3J_{A'X'}$ = 8.0 Hz $^3J_{X'A'}$ = 8.0 Hz
$^3J_{B'Y'}$ = 8.0 Hz $^3J_{Y'B'}$ = 8.0 Hz
$^4J_{A'Y'}$ = 1.3 Hz
$^4J_{B'X'}$ = 1.1 Hz $^4J_{X'B'}$ = 1.1 Hz

-CONHa-	10.41	s (1H, exchangeable)
-CONHb-	8.84	s (1H, exchangeable)
-CONHc-	9.42	s (1H, exchangeable)
$-CH_3$	2.44	s (3H)

125 MHz ^{13}C NMR Spectrum (DMSO-d_6): δ/ppm

C1	122.4	C8	128.4	C4'	132.7	C5''	128.4
C2	146.0	C8a	132.9	C5'	130.2	C6''	126.0
C3	122.8	C9	166.3	C6'	122.1	C7''	125.9
C4	134.7	C10	18.5	C1''	134.7	C8''	122.9
C4a	128.9	C11	153.4	C2''	117.7	C8a''	125.7
C5	119.9	C1'	132.5	C3''	126.2		
C6	145.8	C2'	121.7	C4''	122.2		
C7	124.6	C3'	137.9	C4a''	133.9		

UV Spectrum (phosphate buffer pH 6.5), λ_{max}: nm

226.5, 290.5

IR Spectrum: cm^{-1}

3459 (s, br)	1652 (m)	1532 (s)	1488 (m)	1402 (w)	1189 (s)
1096 (m)	1034 (s)	887 (w)	783 (w)	658 (s)	638 (m)

MALDI-TOF MS positive mode (calcd/found): m/z

650.1/650.1 $[M+H]^+$, 628.1/628.1 $[M-Na+2H]^+$

MALDI-TOF MS negative mode (calcd/found): m/z

626.1/626.0 $[M-Na]^-$, 604.1/604.0 $[M-2Na+H]^-$

4-(4-Methyl-3-(3-(3-(naphthalen-1-ylcarbamoyl)phenyl)ureido) benzamido)naphthalene-2,6-disulfonic acid disodium salt (2n)

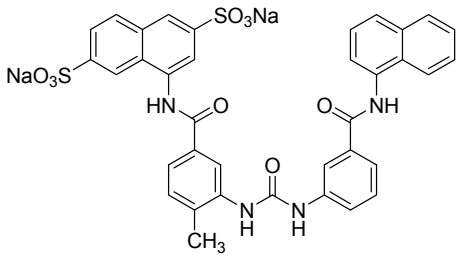

$C_{36}H_{26}N_4Na_2O_9S_2$ (768.7)

To a stirred solution of 0.53 g (2.02 mmol) 3-amino-*N*-naphthalen-1-yl-benzamide (synthesized and confirmed the structure according to Wehner[(55)]) and 610 µl (4.4 mmol) triethylamine in 75 ml dichloroethane in an ice-cooled flask, 0.31 g (1.04 mmol) triphosgene in 5 ml dichloroethane were slowly dropped and stirred for 3 hours.The obtained isocyanate checked by IR was slowly dropped into 200 mg (0.4 mmol) amine 2b, dissolved in 3 ml DMSO and 0.5 ml triethylamine. The mixture was stirred at room temperature for 48 hours. After the reaction was completed, the solid side product was filtered out. 100 ml Water were added to the reaction mixture and extracted three times with 100 ml diethyl ether. The water phase was neutralized and evaporated until dryness. The substance was purified by column chromatography (siliga gel G60/Isopr + NH_3 = 5 + 1) and cation exchange chromatography according to general procedure 4.

Yield: brown powder, 124 mg (40.3 %)
Purity: 94.4 % (HPLC: t_R = 7.40 min, system 1)
TLC: Rf = 0.58 (Isopr + NH_3 = 5 + 2)
NaCl: 23.40 %
Water: 8 mol/mol
CHN analysis:

	%C	%H	%N	C/N
Calcd	56.25	3.41	7.29	7.72
Calcd (with NaCl/H_2O)	36.28	3.55	4.70	7.72
Found	35.97	3.18	4.46	8.06

500 MHz ^{1}H NMR Spectrum (DMSO-d_6): δ/ppm

ABX- A'X'-System

8.17	pt (H5, X)	8.03	s (H1; X')
7.94	d (H8; B)	7.70	d (H3; A')
7.75	dd (H7; A)		
	$^3J_{AB}$ = 8.4 Hz	$^3J_{BA}$ = 8.4 Hz	
	$^4J_{AX}$ = 1.6 Hz	$^4J_{A'X'}$ = 1.6 Hz	
	$^5J_{XX'}$ = 0.9 Hz		

ABX-System

8.47	d (H2'; X)		
7.72	dd (H6'; B)		
7.38	d (H5'; A)		
	$^3J_{AB}$ = 8.3 Hz	$^3J_{BA}$ = 8.3 Hz	

$^4J_{XB}$ = 1.6 Hz $^4J_{BX}$ = 1.6 Hz

ABCX-System

8.05 t (H2''; X)
7.97 m (H6''; C)
7.94 m (H5''; B)
7.85 m (H4''; A)

$^3J_{AB}$ = 8.2 Hz $^3J_{BA}$ = 8.8 Hz
$^3J_{BC}$ = 8.8 Hz $^3J_{CB}$ = 9.7 Hz
$^4J_{AX}$ = 1.6 Hz $^4J_{XA}$ = 1.9 Hz
$^4J_{CX}$ = 1.6 Hz $^4J_{XC}$ = 1.9 Hz
$^4J_{AC}$ = 1.6 Hz $^4J_{CA}$ = 2.5 Hz

ABX-A'B'X'Y'-System

7.84 dt (H8'''; Y') 7.60 dd (H4'''; X)
7.67 dt (H5'''; X') 7.53 d (H2'''; B)
7.54 t (H7'''; B') 7.46 t (H3'''; A)
7.54 t (H6'''; A')

$^3J_{AB}$ = 7.2 Hz $^3J_{BA}$ = 7.2 Hz
$^3J_{AX}$ = 7.6 Hz $^3J_{XA}$ = 7.6 Hz
$^4J_{XB}$ = 1.7 Hz
$^3J_{A'B'}$ = 8.2 Hz $^3J_{B'A'}$ = 8.2 Hz
$^3J_{A'X'}$ = 7.6 Hz $^3J_{X'A'}$ = 7.6 Hz
$^3J_{B'Y'}$ = 7.9 Hz $^3J_{Y'B'}$ = 7.9 Hz
$^4J_{Y'A'}$ = 1.3 Hz $^4J_{X'B'}$ = 1.3 Hz

-CONHa- 10.40 s (1H, exchangeable)
-CONHb- 8.26 s (1H, exchangeable)
-CONHc- 9.44 s (1H, exchangeable)
-CONHd- 10.40 s (1H, exchangeable)
-CH_3 2.36 s (3H)

IR spectrum: cm^{-1}

3448 (s, br) 1735 (m) 1654 (s) 1560 (s) 1540 (s) 1099 (s)

UV Spectrum (phosphate buffer pH 6.5), λ_{max}: nm

222.5, 232.5, 280.5

MALDI-TOF MS positive mode (calcd/found): m/z

769.1/769.1 $[M+H]^+$, 791.1/791.1 $[M+Na]^+$, 747.1/747.1 $[M-Na+2H]^+$, 725.1/725.2 $[M-2Na+3H]^+$

MALDI-TOF MS negative mode (calcd/found): m/z

745.1/745.1 $[M-Na]^-$, 723.1/723.1 $[M-2Na+H]^-$

2-(4-Methyl-3-nitrobenzamido)benzenesulfonic acid sodium salt (8a)

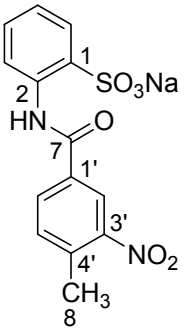

$C_{14}H_{11}N_2NaO_6S$ (358.3)

To a solution of 1.73 g (10 mmol) 2-aminobenzene sulfonic acid dissolved in 50 ml water, 13 mmol 4-methyl-3-nitrobenzoyl chloride, dissolved in 13 ml toluene, were dropwisely added under a constant pH of 4.0 and stirred until the reaction was finished (according to the general procedure 1). Crude product was stirred in 20 ml methanol, filtrated and dried.

Yield: white powder, 3.23 g (90.1 %)
Purity: 97.9 % (HPLC: t_R = 5.14 min, system 1)
TLC: Rf = 0.74 (Isopr + NH_3 = 5 + 2)
NaCl: 17.59 %
Water: 2 mol/mol
CHN analysis:

	%C	%H	%N	C/N
Calcd	46.93	3.09	7.82	6.00
Calcd (with NaCl/H_2O)	35.14	3.16	5.85	6.00
Found	35.09	3.52	5.89	5.96

500 MHz ^{1}H NMR Spectrum (DMSO-d_6): δ/ppm

ABXY-System

7.39	ddd (H5; B)	8.44	dd (H6; Y)
7.11	dt (H4; A)	7.72	dd (H3; X)
	$^3J_{AB}$ = 7.5 Hz		$^3J_{BA}$ = 7.5 Hz
	$^3J_{AX}$ = 7.7 Hz		$^3J_{XA}$ = 7.7 Hz
	$^3J_{BY}$ = 8.1 Hz		$^3J_{YB}$ = 8.1 Hz
	$^4J_{AY}$ = 1.1 Hz		$^4J_{YA}$ = 1.1 Hz
	$^4J_{BX}$ = 1.6 Hz		$^4J_{XB}$ = 1.6 Hz

ABX-System

8.47	d (H2'; X)		
8.11	dd (H6'; B)		
7.73	d (H5'; A)		
	$^3J_{AB}$ = 8.2 Hz		$^3J_{BA}$ = 7.9 Hz
	$^4J_{BX}$ = 1.9 Hz		$^4J_{XB}$ = 1.9 Hz

-CONH- 11.66 s (1H, exchangeable)
-CH_3 2.60 s (3H)

125 MHz ^{13}C NMR Spectrum (DMSO-d_6): δ/ppm

C1	135.8	C5	123.3	C1'	133.8	C5'	130.9
C2	134.8	C6	127.2	C2'	123.3	C6'	133.9
C3	119.9	C7	161.9	C3'	149.3		
C4	130.0	C8	19.7	C4'	136.8		

IR Spectrum: cm^{-1}

3493 (s)	3260 (m)	1686 (s)	1624 (s)	1591 (s)	1532 (s)
1439 (m)	1328 (s)	1257 (s)	1224 (s)	1184 (s)	1128 (m)
1070 (m)	1019 (s)	927 (w)	760 (s)	734 (s)	613 (m)

UV Spectrum (phosphate buffer pH 6.5), λ_{max}: nm

220, 262

2-(3-Amino-4-methylbenzamido)benzenesulfonic acid sodium salt (8b)

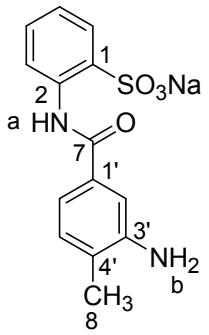

$C_{14}H_{13}N_2NaO_4S$ (328.3)

40 mg 10 % Pd/C were added to a solution of 2.50 g (6.98 mmol) compound 8a in 100 ml water. The mixture was hydrogenated overnight and purified, according to the general procedure 2.

Yield: orange powder, 2.05 g (89.4 %)
Purity: 90.1 % (HPLC: t_R = 2.79 min, system 1)
TLC: Rf = 0.82 (Isopr + NH_3 = 5 + 2)
NaCl: 14.75 %
Water: 1.5 mol/mol
CHN analysis:

	%C	%H	%N	C/N
Calcd	51.22	3.99	8.53	6.00
Calcd (with NaCl/H_2O)	40.34	3.87	6.72	6.00
Found	40.17	3.73	6.76	5.95

500 MHz ^{1}H NMR Spectrum (DMSO-d_6): δ/ppm

ABXY-System

7.34	ddd (H5; B)	8.47	dd (H6; Y)
7.04	m (H4; A)	7.70	dd (H3; X)
	$^3J_{AB}$ = 7.7 Hz		$^3J_{BA}$ = 7.7 Hz
	$^3J_{AX}$ = 7.7 Hz		$^3J_{XA}$ = 7.7 Hz
	$^3J_{BY}$ = 8.0 Hz		$^3J_{YB}$ = 8.0 Hz
	$^4J_{BX}$ = 1.6 Hz		$^4J_{XB}$ = 1.6 Hz

$^4J_{AY}$ = 0.9 Hz $^4J_{YA}$ = 0.9 Hz

ABX-System

7.21	d (H2'; X)	
7.05	d (H5'; A)	
7.03	dd (H6'; B)	
	$^3J_{AB}$ = 7.6 Hz	$^3J_{BA}$ = 7.6 Hz
	$^4J_{BX}$ = 1.3 Hz	$^4J_{XB}$ = 1.3 Hz

-CONH-	11.16	s (1H, exchangeable)
$-NH_2$	5.07	s (2H, exchangeable)
$-CH_3$	2.11	s (3H)

125 MHz ^{13}C NMR Spectrum (DMSO-d_6): δ/ppm

C1	135.6	C5	122.3	C1'	125.3	C5'	129.7
C2	135.5	C6	127.1	C2'	113.0	C6'	114.2
C3	119.8	C7	164.9	C3'	147.1		
C4	130.1	C8	17.6	C4'	133.4		

IR Spectrum: cm^{-1}

3338 (m, br)	1664 (m)	1588 (s)	1541 (s)	1510 (m)	1437 (s)
1319 (s)	1181 (s)	1140 (w)	1088 (m)	1019 (s)	869 (w)
761 (m)	713 (m)	616 (s)	565 (w)		

UV Spectrum (phosphate buffer pH 6.5), λ_{max}: nm

219, 266

2,2'-(Carbonylbis(imino-3,1-(4-methylphenylene)carbonylimino))-bis(benzensulfonic acid) disodium salt (8c)

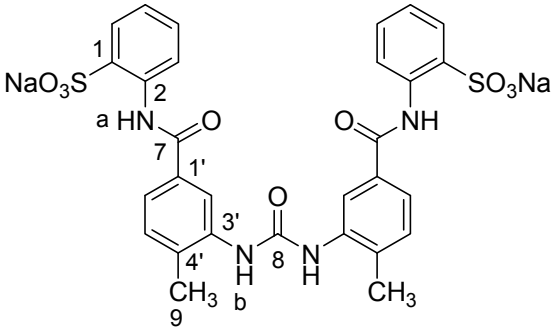

$C_{29}H_{24}N_4Na_2O_9S_2$ (682.6)

0.68 g (2.0 mmol) Amine 8b were suspended in 30 ml water and the pH was adjusted to 5.5. 6 ml (12 mmol) 20 % phosgene solution in toluene was dropwisely added to the solution under a constant pH of 5.0, according to the general procedure 3. After reaction was completed, the crude product was stirred in 30 ml methanol, filtrated and dried.

Yield: white powder, 0.48 g (67.9 %)
Purity: 99.6 % (HPLC: t_R = 6.03 min, system 1)
TLC: Rf = 0.59 (Isopr + NH_3 = 5 + 2)
NaCl: 4.25 %

Water: 6 mol/mol

CHN analysis:

	%C	%H	%N	C/N
Calcd	51.02	3.54	8.21	6.22
Calcd (with $NaCl/H_2O$)	42.18	4.39	6.78	6.22
Found	42.34	4.43	6.91	6.12

500 MHz ^{1}H NMR Spectrum (DMSO-d_6): δ/ppm

ABXY-System

7.38	dt (H5; B)	8.49	dd (H6; Y)
7.07	dt (H4; A)	7.71	dd (H3; X)

$^3J_{AB}$ = 7.4 Hz	$^3J_{BA}$ = 7.4 Hz
$^3J_{BY}$ = 8.3 Hz	$^3J_{YB}$ = 8.3 Hz
$^3J_{AX}$ = 7.7 Hz	$^3J_{XA}$ =7.7 Hz
$^4J_{AY}$ = 1.3 Hz	$^4J_{YA}$ = 1.3 Hz
$^4J_{BX}$ = 1.7 Hz	$^4J_{XB}$ = 1.7 Hz

ABX-System

8.41	d (H2'; X)
7.53	dd (H6'; B)
7.36	d (H5'; A)

$^3J_{AB}$ = 8.0 Hz	$^3J_{BA}$ = 8.0 Hz
$^4J_{BX}$ = 1.9 Hz	$^4J_{XB}$ = 1.9 Hz

-CONH-	11.32	s (2H, exchangeable)
-NHCONH-	8.66	s (2H, exchangeable)
$-CH_3$	2.38	s (6H)

125 MHz ^{13}C NMR Spectrum (DMSO-d_6): δ/ppm

C1	135.5	C5	122.6	C9	153.1	C4'	133.1
C2	135.5	C6	127.1	C1'	132.7	C5'	130.6
C3	119.9	C7	164.2	C2'	120.8	C6'	121.4
C4	129.9	C8	18.4	C3'	138.2		

IR Spectrum: cm^{-1}

3340 (s, br)	1706 (m)	1666 (m)	1578 (s)	1536 (s)	1438 (s)
1322 (s)	1179 (s)	1084 (m)	1018 (m)	759 (m)	617 (m)

UV Spectrum (phosphate buffer pH 6.5), λ_{max}: nm

260.5

ESI-MS positive mode (calcd/found): m/z

683.1/683.5 $[M+H]^+$, 705.1/705.6 $[M+Na]^+$, 1387.1/1387.3 $[2M+Na]^+$

ESI-MS negative mode (calcd/found]: m/z

659.1/659.3 $[M-Na]^-$, 681.1/681.1 $[M-H]^-$, 1342.2/1341.1 $[2M-Na]^-$

4-(4-Methyl-3-nitrobenzamido)benzenesulfonic acid sodium salt (9a)

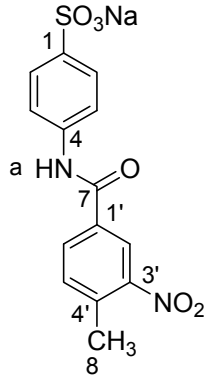

$C_{14}H_{11}N_2NaO_6S$ (358.3)

2.69 g (15.55 mmol) Sulfanilic acid were dissolved in 50 ml water. To this solution, 20 mmol 4-methyl-3-nitrobenzoyl chloride, dissolved in 20 ml toluene, was slowly dropped under a constant pH of 4.0 and stirred until the reaction was finished, according to the general procedure 1. The crude product was stirred in 30 ml methanol, filtrated and dried.

Yield: white powder, 4.58 g (82.2 %)
Purity: 98.8 % (HPLC: t_R = 3.10 min, system 1)
TLC: Rf = 0.51 (Isopr + NH_3 = 5 + 2)
NaCl: 19.09 %
Water: 1 mol/mol
CHN analysis:

	%C	%H	%N	C/N
Calcd	46.93	3.09	7.82	6.00
Calcd (with NaCl/H_2O)	36.15	2.82	6.02	6.00
Found	36.49	3.13	6.21	5.88

500 MHz ^{1}H NMR Spectrum (DMSO-d_6): δ/ppm

AA'BB'-System
7.74 m (H3H5; BB')
7.58 m (H2H6; AA')
$^3J_{AB}$ = 8.8 Hz $^3J_{A'B'}$ = 8.8 Hz
$^3J_{BA}$ = 8.8 Hz $^3J_{B'A'}$ = 8.8 Hz
$^4J_{BB'}$ = 2.0 Hz $^4J_{AB'}$ = 2.0 Hz

ABX-System
8.58 d (H2'; X)
8.25 dd (H6'; B)
7.66 d (H5'; A)
$^3J_{AB}$ = 8.2 Hz $^3J_{BA}$ = 8.2 Hz
$^4J_{BX}$ = 1.6 Hz $^4J_{XB}$ = 1.6 Hz

-CONH- 10.61 s (1H, exchangeable)
-CH_3 2.58 s (3H)

125 MHz ^{13}C NMR Spectrum (DMSO-d_6): δ/ppm

C1	144.1	C4	138.9	C1'	133.2	C4'	136.4
C2C6	126.2	C7	163.3	C2'	123.8	C5'	132.4
C3C5	119.7	C8	19.6	C3'	148.9	C6'	133.8

IR Spectrum: cm^{-1}

3314 (s)	2989 (m)	2934 (w)	1660 (s)	1623 (s)	1596 (s)
1560 (w)	1527 (s)	1449 (w)	1402 (s)	1342 (s)	1323 (s)
1260 (m)	1190 (s)	1134 (s)	1075 (w)	1039 (s)	1014 (s)
937 (w)	911 (w)	831 (s)	794 (w)	767 (w)	724 (m)
703 (s)	685 (m)	642 (s)	630 (m)	606 (s)	571 (s)

UV Spectrum (phosphate buffer pH 6.5), λ_{max}: nm

222, 261

4-(3-Amino-4-methylbenzamido)benzenesulfonic acid sodium salt (9b)

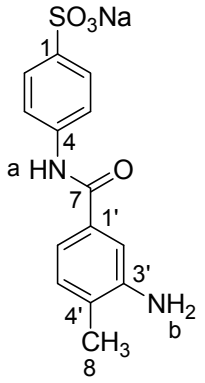

$C_{14}H_{13}N_2NaO_4S$ (328.3)

40 mg 10 % Pd/C were added to a solution of 3.24 g (9.03 mmol) compound 9a in a mixture of 100 ml water and 20 ml methanol. The mixture was hydrogenated overnight according to the general procedure 2. The crude product was stirred in 20 ml methanol, filtrated and dried.

Yield: white powder, 2.60 g (87.7 %)
Purity: 98.1 % (HPLC: t_R = 4.27 min, system 2)
TLC: Rf = 0.47 (Isopr + NH_3 = 5 + 2)
NaCl: < 1 %
Water: 1.5 mol/mol
CHN analysis:

	%C	%H	%N	C/N
Calcd	51.22	3.99	8.53	6.00
Calcd (with NaCl/H_2O)	47.08	4.52	7.84	6.00
Found	47.41	4.61	7.68	6.17

500 MHz ^{1}H NMR Spectrum (DMSO-d_6): δ/ppm

AA'BB'-System

7.69 m (H3H5; BB')
7.54 m (H2H6; AA')
$^3J_{AB} = {}^3J_{BA} = 8.8$ Hz $^3J_{A'B'} = {}^3J_{B'A'} = 8.5$ Hz
$^4J_{AA'} = {}^4J_{A'A} = 2.5$ Hz $^4J_{BB'} = {}^4J_{B'B} = 2.2$ Hz
$^4J_{AB'} = {}^4J_{B'A} = 1.9$ Hz $^4J_{A'B} = {}^4J_{BA'} = 1.9$ Hz

ABX-System
7.17 d (H2'; X)
7.07 dd (H6'; B)
7.02 d (H5'; A)
$^3J_{AB} = 7.7$ Hz $^3J_{BA} = 7.7$ Hz
$^4J_{BX} = 1.9$ Hz $^4J_{XB} = 1.9$ Hz

-CONH- 10.02 s (1H, exchangeable)
$-NH_2$ 5.02 s (2H, exchangeable)
$-CH_3$ 2.11 s (3H)

125 MHz ^{13}C NMR Spectrum (DMSO-d_6): δ/ppm

C1	143.5	C4	139.6	C1'	125.1	C4'	133.5
C2C6	126.1	C7	166.3	C2'	113.3	C5'	129.8
C3C5	119.2	C8	17.6	C3'	146.7	C6'	115.3

IR Spectrum: cm^{-1}

3351 (m)	1658 (s)	1625 (m)	1592 (m)	1524 (s)	1397 (m)
1323 (m)	1197 (s)	1132 (s)	1042 (m)	1013 (m)	886 (w)
833 (m)	745 (w)	706 (m)	641 (m)	573 (m)	

UV Spectrum (phosphate buffer pH 6.5), λ_{max}: nm
268.5

4,4'-(Carbonylbis(imino-3,1-(4-methylphenylene)carbonylimino))-bis(benzensulfonic acid) disodium salt (9c)

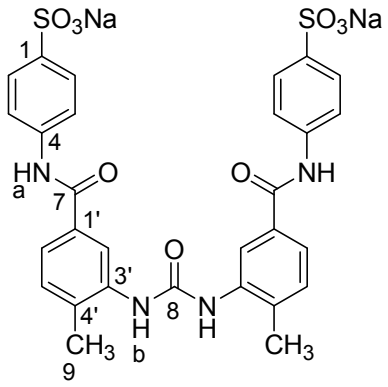

$C_{29}H_{24}N_4Na_2O_9S_2$ (682.6)

To a solution of 1.00 g (3.05 mmol) amine 9b in 50 ml water, 6 ml (12 mmol) 20 % phosgene solution in toluene was added under a constant pH of 5.0. The reaction was performed according to the general procedure 3. The crude product was stirred in 30 ml methanol, filtrated and dried.

Yield: white powder, 932 mg (89.2 %)
Purity: 99.0 % (HPLC: t_R = 3.23 min, system 1)
TLC: Rf = 0.38 (Isopr + NH_3 = 5 + 2)
NaCl: 11.47 %
Water: 3.5 mol/mol
CHN analysis:

	%C	%H	%N	C/N
Calcd	51.02	3.54	8.21	6.22
Calcd (with $NaCl/H_2O$)	41.35	3.71	6.65	6.22
Found	41.31	3.97	6.61	6.25

500 MHz ^{1}H NMR Spectrum (DMSO-d_6): δ/ppm

AA'BB'-System

7.71 m (H3H5; BB')
7.56 m (H2H6; AA')
$^3J_{AB} = {}^3J_{BA}$ = 8.8 Hz $^3J_{A'B'} = {}^3J_{B'A'}$ = 8.8 Hz
$^4J_{AA'} = {}^4J_{A'A}$ = 2.2 Hz $^4J_{BB'} = {}^4J_{BB'}$ = 2.2 Hz
$^4J_{AB'} = {}^4J_{B'A}$ = 1.9 Hz $^4J_{A'B} = {}^4J_{BA'}$ = 1.9 Hz

ABX-System

8.35 d (H2'; X)
7.58 dd (H6'; B)
7.31 d (H5'; A)
$^3J_{AB}$ = 7.9 Hz $^3J_{BA}$ = 7.9 Hz
$^4J_{BX}$ = 1.9 Hz $^4J_{XB}$ = 1.9 Hz

-CONH- 10.20 s (2H, exchangeable)
-NHCONH- 8.92 s (2H, exchangeable)
-CH_3 2.38 s (6H)

125 MHz ^{13}C NMR Spectrum (DMSO-d_6): δ/ppm

C1	143.5	C1'	132.6	C5'	130.2	C9	153.4
C2C6	126.1	C2'	121.6	C6'	122.2		
C3C5	119.4	C3'	137.8	C7	165.7		
C4	139.5	C4'	133.1	C8	18.5		

IR Spectrum: cm^{-1}

3350 (s)	1709 (m)	1665 (m)	1594 (s)	1575 (s)	1525 (s)
1400 (m)	1324 (m)	1258 (m)	1189 (s)	1130 (s)	1037 (s)
1011 (m)	834 (m)	754 (w)	708 (m)	569 (m)	

UV Spectrum (phosphate buffer pH 6.5), λ_{max}: nm

264.5

ESI-MS positive mode (calcd/found): m/z

683.1/683.4 $[M+H]^+$, 705.1/705.4 $[M+Na]^+$, 661.1/661.4 $[M-Na+2H]^+$, 639.1/639.3 $[M-2Na+3H]^+$

ESI-MS negative mode (calcd/found): m/z

681.1/681.5 $[M-H]^-$, 659.1/659.6 $[M-Na]^-$, 637.1/637.7 $[M-2Na+H]^-$

4-(4-Methyl-3-nitrobenzamido)benzene-1,3-disulfonic acid disodium salt (10a)

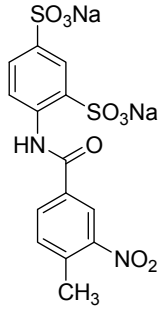

$C_{14}H_{10}N_2Na_2O_9S_2$ (460.4)

To a solution of 2.56 g (10.10 mmol) 4-aminobenzene-1,3-disulfonic acid in 30 ml water, 12 mmol 4-methyl-3-nitrobenzoyl chloride, dissolved in 12 ml toluene, was slowly added under a constant pH of 4.0. The reaction was performed according to the general procedure 1. The crude product was stirred in 30 ml methanol, filtrated and dried.

Yield: pale yellow powder, 3.73 g (80.2 %)
Purity: 98.2 % (HPLC: t_R = 4.31 min, system 1)
TLC: Rf = 0.40 (Isopr + NH_3 = 5 + 2)
NaCl: 13.28 %
Water: 2.5 mol/mol
CHN analysis:

	%C	%H	%N	C/N
Calcd	36.53	2.19	6.09	6.00
Calcd (with NaCl/H_2O)	28.85	2.59	4.81	6.00
Found	28.81	2.78	4.92	5.86

500 MHz ^{1}H NMR Spectrum (DMSO-d_6): δ/ppm

ABX-System
8.41 d (H5; B)
8.04 d (H2; X)
7.62 dd (H6; A)
$^3J_{AB}$ = 8.3 Hz $^3J_{BA}$ = 8.3 Hz
$^4J_{AX}$ = 2.2 Hz $^4J_{XA}$ = 2.2 Hz

ABX-System
8.47 d (H2'; X)
8.11 dd (H6'; B)
7.74 d (H5'; A)
$^3J_{AB}$ = 8.2 Hz $^3J_{BA}$ = 8.2 Hz
$^4J_{BX}$ = 1.9 Hz $^4J_{XB}$ = 1.9 Hz

-CONH 11.72 s (1H, exchangeable)
-CH_3 2.60 s (3H)

125 MHz ^{13}C NMR Spectrum (DMSO-d_6): δ/ppm

C1	142.9	C5	125.0	C1'	134.8	C5'	130.9
C2	118.9	C6	127.2	C2'	123.4	C6'	133.8
C3	134.8	C7	161.9	C3'	149.3		
C4	133.9	C8	19.7	C4'	136.9		

IR Spectrum: cm^{-1}

3502 (s, br)	1685 (m)	1623 (m)	1590 (m)	1530 (s)	1393 (m)
1329 (m)	1192 (s)	1079 (m)	1039 (s)	835 (w)	733 (m)
693 (m)	625 (m)	550 (m)			

UV Spectrum (phosphate buffer pH 6.5), λ_{max}: nm

218.5, 268.5

4-(3-Amino-4-methylbenzamido)benzene-1,3-disulfonic acid disodium salt (10b)

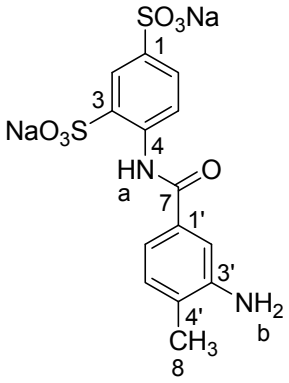

$C_{14}H_{12}N_2Na_2O_7S_2$ (430.4)

40 mg 10 % Pd/C were added to a solution of 3.24 g (7.04 mmol) compound 10a in 100 ml water. The mixture was hydrogenated overnight, according to the general procedure 2. The crude product was stirred in 20 ml methanol, filtrated and dried.

Yield: pale pink powder, 2.44 g (80.5 %)
Purity: 97.5 % (HPLC: t_R = 2.33 min, system 1)
TLC: Rf = 0.38 (Isopr + NH_3 = 5 + 2)
NaCl: < 1 %
CHN analysis:

	%C	%H	%N	C/N
Calcd	39.07	2.81	6.51	6.00
Calcd (with NaCl/H_2O)	34.08	3.88	5.68	6.00
Found	34.35	3.96	5.76	5.96

500 MHz ^{1}H NMR Spectrum (DMSO-d_6): δ/ppm

ABX-System
8.43 d (H5; B)
8.02 d (H2; X)

7.56 dd (H6; A)
$^3J_{AB}$ = 8.3 Hz $^3J_{BA}$ = 8.3 Hz
$^4J_{AX}$ = 1.9 Hz $^4J_{XA}$ = 1.9 Hz

ABX-System
7.21 d (H2'; X)
7.05 d (H5'; B)
7.03 dd (H6'; A)
$^3J_{AB}$ = 7.9 Hz $^3J_{BA}$ = 7.9 Hz
$^4J_{AX}$ = 1.6 Hz $^4J_{XA}$ = 1.6 Hz

-CONH- 11.22 s (1H, exchangeable)
-NH_2 5.08 s (2H, exchangeable)
-CH_3 2.11 s (3H)

125 MHz ^{13}C NMR Spectrum (DMSO-d_6): δ/ppm

C1	142.1	C5	124.9	C1'	125.4	C5'	130.1
C2	118.7	C6	126.9	C2'	113.0	C6'	114.3
C3	134.5	C7	164.9	C3'	147.1		
C4	133.3	C8	17.6	C4'	135.6		

IR Spectrum: cm^{-1}

3515 (s, br)	1586 (s)	1535 (m)	1512 (m)	1422 (w)	1391 (m)
1333 (m)	1211 (s)	1138 (m)	1084 (w)	1032 (s)	842 (w)
741 (m)	692 (s)	626 (m)			

UV Spectrum (phosphate buffer pH 6.5), λ_{max}: nm
218.5, 276.5

4,4'-(Carbonylbis(imino-3,1-(4-methylphenylene)carbonylimino))-bis(benzene-1,3-disulfonic acid) tetrasodium salt (10c)

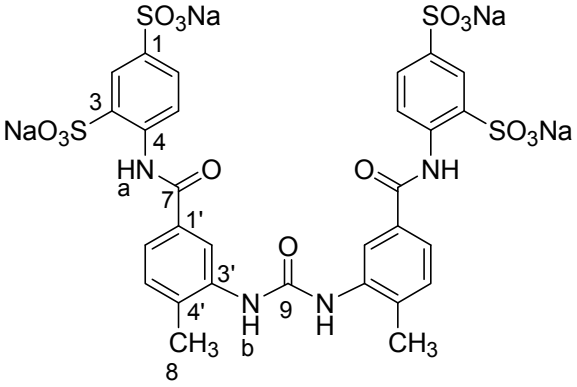

$C_{29}H_{22}N_4Na_4O_{15}S_4$ (886.7)

To a solution of 0.50 g (1.16 mmol) amine 10b in 20 ml water, 3 ml (6 mmol) 20 % phosgene solution in toluene was slowly dropped under a constant pH of 4.0. The reaction was performed according to the general procedure 3. The crude product was stirred in 20 ml methanol, filtrated and dried.

Yield: pink powder, 488 mg (94.8 %)
Purity: 98.3 % (HPLC: t_R = 4.83 min, system 1)
TLC: Rf = 0.19 (Isopr + NH_3 = 5 + 2)
NaCl: 2.09 %
Water: 7.5 mol/mol
CHN analysis:

	%C	%H	%N	C/N
Calcd	39.28	2.50	6.32	6.22
Calcd (with $NaCl/H_2O$)	33.37	3.57	5.37	6.22
Found	33.36	3.88	5.38	6.20

500 MHz ^{1}H NMR Spectrum (DMSO-d_6): δ/ppm

ABX-System
8.45 d (H5; B)
8.03 d (H2; X)
7.53 dd (H6; A)
$^3J_{AB}$ = 8.3 Hz $^3J_{BA}$ = 8.3 Hz
$^4J_{AX}$ = 1.9 Hz $^4J_{XA}$ = 1.9 Hz

ABX-System
8.38 d (H2'; X)
7.58 dd (H6'; B)
7.37 d (H5'; A)
$^3J_{AB}$ = 8.0 Hz $^3J_{BA}$ = 8.0 Hz
$^4J_{BX}$ = 1.7 Hz $^4J_{XB}$ = 1.7 Hz

-CONH- 11.39 s (2H, exchangeable)
-NHCONH- 8.54 s (2 H, exchangeable)
$-CH_3$ 2.37 s (6H)

125 MHz ^{13}C NMR Spectrum (DMSO-d_6): δ/ppm

C1	142.4	C5	124.9	C9	153.0	C4'	133.0
C2	118.8	C6	127.0	C1'	135.5	C5'	130.6
C3	134.6	C7	164.2	C2'	120.9	C6'	121.5
C4	133.0	C8	18.3	C3'	138.1		

IR Spectrum: cm^{-1}

3467 (s, br)	1684 (m)	1577 (s)	1533 (s)	1393 (m)	1325 (s)
1187 (s)	1079 (w)	1041 (s)	759 (w)	695 (m)	623 (m)

UV Spectrum (phosphate buffer pH 6.5), λ_{max}: nm
270.5

MALDI-TOF MS positive mode (calcd/found): m/z
887.0/887.1 $[M+H]^+$, 908.9/909.1 $[M+Na]^+$. 865.0/865.1 $[M-Na+2H]^+$, 843.0/843.1 $[M-2Na+3H]^+$

3-Methyl-4-(4-methyl-3-nitrobenzamido)benzenesulfonic acid sodium salt (11a)

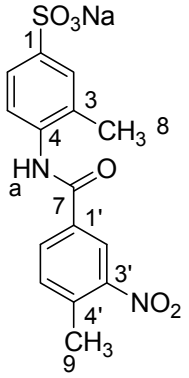

$C_{15}H_{13}N_2NaO_6S$ (372.3)

17 mmol 4-methyl-3-nitrobenzoyl chloride, dissolved in 17 ml toluene, were dropwisely added into a solution of 1.87 g (10 mmol) 4-amino-3-methylbenzene sulfonic acid in 60 ml water under a constant pH of 4.0. The reaction was performed according to the general procedure 1. The crude product was stirred in 20 ml methanol, filtrated and dried.

Yield: white powder, 2.91 g (78.2 %)
Purity: 98.5 % (HPLC: t_R = 2.77 min, system 1)
TLC: Rf = 0.59 (Isopr + NH_3 = 5 + 2)
NaCl: < 1%
Water: 1 mol/mol
CHN analysis:

	%C	%H	%N	C/N
Calcd	48.39	3.52	7.52	6.43
Calcd (with NaCl/H_2O)	46.16	3.87	7.18	6.43
Found	45.98	4.10	7.05	6.52

500 MHz ^{1}H NMR Spectrum (DMSO-d_6): δ/ppm

ABX-System
7.51 d (H2; X)
7.44 dd (H6; B)
7.27 d (H5; A)
$^3J_{AB}$ = 8.2 Hz $^3J_{BA}$ = 8.2 Hz
$^4J_{BX}$ = 1.6 Hz $^4J_{XB}$ = 1.6 Hz

ABX-System
8.56 d (H2'; X)
8.21 dd (H6'; B)
7.67 d (H5'; A)
$^3J_{AB}$ = 8.0 Hz $^3J_{BA}$ = 8.0 Hz
$^4J_{BX}$ = 1.7 Hz $^4J_{XB}$ = 1.7 Hz

-CONH- 10.14 s (1H, exchangeable)
-CH_3 2.59 s (3H)
-CH_3 2.22 s (3H)

125 MHz ^{13}C NMR Spectrum (DMSO-d_6): δ/ppm

C1	146.3	C5	123.7	C9	19.9	C4'	136.4
C2	127.8	C6	125.9	C1'	133.1	C5'	132.2
C3	133.3	C7	18.0	C2'	123.6	C6'	133.6
C4	136.1	C8	163.3	C3'	148.9		

IR Spectrum: cm^{-1}

3584 (s)	3512 (m)	3286 (s)	1655 (s)	1624 (m)	1589 (m)
1526 (s)	1446 (w)	1342 (m)	1319 (m)	1282 (w)	1210 (m)
1146 (m)	1056 (s)	830 (m)	711 (m)		

UV Spectrum (phosphate buffer pH 6.5), λ_{max}: nm

224

4-(3-Amino-4-methylbenzamido)-3-methylbenzenesulfonic acid sodium salt (11b)

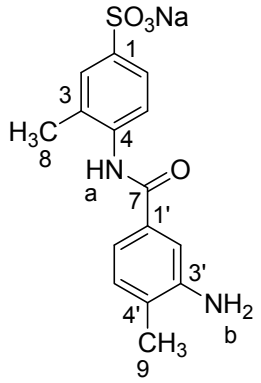

$C_{15}H_{15}N_2NaO_4S$ (342.4)

20 mg 10 % Pd/C were added to a solution of 1.38 g (3.70 mmol) compound 11a in a mixture of 100 ml water and 50 ml methanol. The mixture was hydrogenated overnight, according to the general procedure 2. The crude product was stirred in 30 ml methanol, filtrated and dried.

Yield: white powder, 1.18 g (93.3 %)
Purity: 96.7 % (HPLC: t_R = 1.14 min, system 1)
TLC: Rf = 0.53 (Isopr + NH_3 = 5 + 2)
NaCl: < 1 %
Water: 1.5 mol/mol
CHN analysis:

	%C	%H	%N	C/N
Calcd	52.63	4.42	8.18	6.43
Calcd (with NaCl /H_2O)	48.78	5.19	7.58	6.43
Found	49.01	5.18	7.50	6.53

500 MHz ^{1}H NMR Spectrum (DMSO-d_6): δ/ppm

ABX-System

7.48 d (H2; X)

7.41 dd (H6; B)
7.28 d (H5; A)
$^3J_{AB}$ = 8.2 Hz $^3J_{BA}$ = 8.2 Hz
$^4J_{BX}$ = 1.6 Hz $^4J_{XB}$ = 1.6 Hz

ABX-System
7.20 d (H2'; X)
7.10 dd (H6'; B)
7.02 d (H5'; A)
$^3J_{AB}$ = 7.9 Hz $^3J_{BA}$ = 7.9 Hz
$^4J_{BX}$ = 1.6 Hz $^4J_{XB}$ = 1.6 Hz

-CONH- 9.54 s (1H, exchangeable)
$-NH_2$ 5.01 s (2H, exchangeable)
$-CH_3$ 2.21 s (3H)
$-CH_3$ 2.11 s (3H)

125 MHz ^{13}C NMR Spectrum (DMSO-d_6): δ/ppm

C1	145.6	C5	123.4	C9	17.6	C4'	132.6
C2	125.5	C6	124.9	C1'	129.8	C5'	127.6
C3	133.2	C7	166.1	C2'	113.4	C6'	115.2
C4	136.9	C8	18.1	C3'	146.7		

IR Spectrum: cm^{-1}

3436 (s, br)	1642 (m)	1573 (m)	1512 (m)	1450 (w)	1315 (w)
1191 (s)	1042 (m)	824 (w)	764 (w)	701 (m)	641 (w)

UV Spectrum (phosphate buffer pH 6.5), λ_{max}: nm
210

4,4'-(Carbonylbis(imino-3,1-(4-methylphenylene)carbonylimino))-bis(3-methylbenzenesulfonic acid) disodium salt (11c)

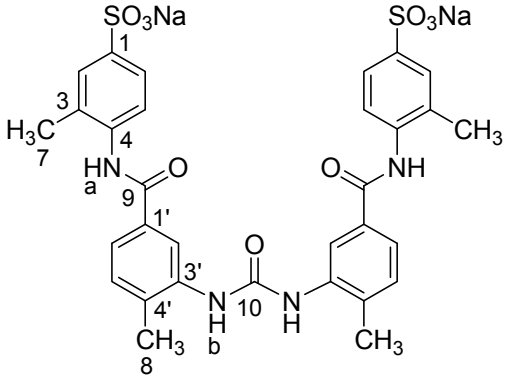

$C_{31}H_{28}N_4Na_2O_9S_2$ (710.7)

To a solution of 0.86 g (2.5 mmol) amine 11b in 30 ml water, 4 ml (8 mmol) 20 % phosgene solution in toluene were added under a constant pH to 4.5 until finished. The purification was done according to the general procedure 3.

Yield: white powder, 0.80 g (89.2 %)

Purity: 99.9 % (HPLC: t_R = 4.03 min, system 1)
TLC: Rf = 0.32 (Isopr + NH_3 = 5 + 2)
NaCl: 16.59 %
Water: 5.5 mol/mol
CHN analysis:

	%C	%H	%N	C/N
Calcd	52.39	3.97	7.88	6.65
Calcd (with NaCl/H_2O)	38.35	4.05	5.77	6.65
Found	38.44	4.34	5.73	6.71

500 MHz ^{1}H NMR Spectrum (DMSO-d_6): δ/ppm

ABX-System
7.48 d (H2; X)
7.42 dd (H6; B)
7.27 d (H5, A)
$^3J_{AB}$ = 8.0 Hz $^3J_{BA}$ = 8.0 Hz
$^4J_{BX}$ = 1.3 Hz $^4J_{XB}$ = 1.3 Hz

ABX-System
8.37 d (H2'; X)
7.58 dd (H6'; B)
7.30 d (H5'; A)
$^3J_{AB}$ = 7.9 Hz $^3J_{BA}$ = 7.9 Hz
$^4J_{BX}$ = 1.3 Hz $^4J_{XB}$ = 1.3 Hz

-CONH- 9.78 s (2H, exchangeable)
-NHCONH- 9.08 s (2H, exchangeable)
$-CH_3$ 2.39 s (6H)
$-CH_3$ 2.21 s (6H)

125 MHz ^{13}C NMR Spectrum (DMSO-d_6): δ/ppm

C1	145.6	C5	123.4	C9	18.6	C3'	137.9
C2	127.7	C6	125.7	C10	153.4	C4'	132.9
C3	132.6	C7	18.1	C1'	132.7	C5'	130.2
C4	136.9	C8	165.5	C2'	121.6	C6'	122.1

IR Spectrum: cm^{-1}

3436 (s, br)	1659 (s)	1578 (s)	1549 (s)	1513 (s)	1446 (m)
1408 (m)	1314 (m)	1192 (s)	1135 (m)	1117 (m)	1097 (w)
1042 (s)	895 (w)	826 (w)	752 (m)	699 (s)	637 (m)

UV Spectrum (phosphate buffer pH 6.5), λ_{max}: nm
248.5

ESI-MS positive mode (calcd/found): m/z
733.1/733.4 $[M+Na]^+$, 711.1/711.5 $[M+H]^+$, 689.1/689.5 $[M-Na+2H]^+$, 1443.2/1443.2 $[2M+Na]^+$

ESI-MS negative mode (calcd/found): m/z
687.1/687.3 $[M-Na]^-$, 709.1/709.2 $[M-H]^-$

4-Methyl-3-nitrobenzenesulfonic acid sodium salt (1d)

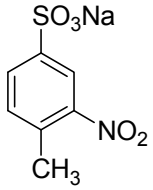

$C_7H_6NNaO_5S$ (239.2)

32.00 g (316 mmol) Potassium nitrate, dissolved in 50 ml conc. H_2SO_4, were slowly dropped into a cooled 57.0 g (300 mmol) 4-methylphenyl sulfonic acid monohydrate, dissolved in 50 ml conc. H_2SO_4. The mixture was stirred for an hour at 0˚C and then overnight at room temperature. 50 ml Cooled 20 % NaCl solution were slowly dropped into the clear solution and the mixture was stirred at 0˚C until white product precipitated. The product was filtrated and washed with cooled NaCl solution and methanol.

Yield: white powder, 44.45 g (68.2 %)
Purity: 94.6 % (HPLC: t_R = 1.68 min, system 1)
TLC: Rf = 0.66 (Isopr + NH_3 = 5 + 2)
NaCl: 3 %
Water: 0.5 mol/mol
CHN analysis:

	%C	%H	%N	C/N
Calcd	35.15	2.53	5.86	6.00
Calcd (with $NaCl/H_2O$)	32.86	2.76	5.47	6.00
Found	32.76	2.44	5.65	5.80

500 MHz ^{1}H NMR Spectrum (DMSO-d_6): δ/ppm

ABX-System

7.60 d (H2; X)
7.30 dd (H6; B)
6.98 d (H5; A)
$^3J_{AB}$ = 7.9 Hz $^3J_{BA}$ = 7.9 Hz
$^4J_{BX}$ = 1.7 Hz $^4J_{XB}$ = 1.7 Hz

$-CH_3$ 2.02 s (3H)

125 MHz ^{13}C NMR Spectrum (DMSO-d_6): δ/ppm

C1	147.8	C3	148.2	C5	130.3	C7	19.5
C2	121.4	C4	133.1	C6	132.7		

IR Spectrum: cm^{-1}

1612 (w)	1533 (s)	1453 (w)	1387 (w)	1336 (s)	1298 (w)
1236 (s)	1194 (s)	1137 (m)	1073 (w)	1050 (s)	1046 (s)
892 (m)	836 (m)	377 (m)	603 (s)		

UV Spectrum (phosphate buffer pH 6.5), λ_{max}: nm

212, 256

ESI-MS negative mode (calcd/found): m/z

216.2/216.2 $[M-Na]^-$, 455.4/455.0 $[2M-Na]^-$

3-Amino-4-methylbenzenesulfonic acid sodium salt (1e)

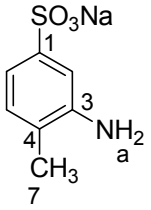

$C_7H_8NNaO_3S$ (209.2)

200 mg 10 % Pd/C were added to a suspension of 16.70 g (76.90 mmol) compound 1c in a mixture of 250 ml water and 100 ml methanol. The mixture was hydrogenated overnight, according to the general procedure 2.

Yield: pale brown powder, 14.29 g (88.9 %)
Purity: 90.2 % (HPLC: t_R = 1.80 min, system 2)
TLC: Rf = 0.50 (Isopr + NH_3 = 5 + 2)
NaCl: 2.96 %
Water: 1.5 mol/mol
CHN analysis:

	%C	%H	%N	C/N
Calcd	40.19	3.85	6.70	6.00
Calcd (with $NaCl/H_2O$)	34.54	4.56	5.75	6.00
Found	34.16	4.17	5.79	5.90

500 MHz ^{1}H NMR Spectrum (DMSO-d_6): δ/ppm

ABX-System

6.93 d (H2; X)
6.82 d (H5; B)
6.73 dd (H6; A)
$^3J_{AB}$ = 7.7 Hz $^3J_{BA}$ = 7.7 Hz
$^4J_{AX}$ = 1.6 Hz $^4J_{XA}$ = 1.6 Hz

$-NH_2$ 4.78 s (2H, exchangeable)
$-CH_3$ 2.02 s (3H)

125 MHz ^{13}C NMR Spectrum (DMSO-d_6): δ/ppm

C1	145.8	C3	146.8	C5	121.3	C7	17.4
C2	111.8	C4	128.9	C6	113.7		

IR Spectrum: cm^{-1}

3450 (s)	3397 (s)	3325 (s)	1625 (m)	1578 (m)	1497 (m)
1443 (w)	1415 (m)	1315 (w)	1265 (m)	1191 (s)	1117 (s)
1080 (m)	1039 (s)	1006 (m)	883 (m)	817 (s)	695 (s)

UV Spectrum (phosphate buffer pH 6.5), λ_{max}: nm

210

4-Methyl-3-(4-methyl-3-nitrobenzamido)benzenesulfonic acid sodium salt (12a)

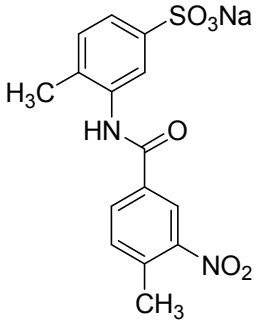

$C_{15}H_{13}N_2NaO_6S$ (372.3)

To a solution of 2.14 g (10.25 mmol) 3-amino-4-methylbenzene sulfonic acid sodium salt in 50 ml water, 14 mmol 4-methyl-3-nitrobenzoyl chloride, dissolved in 14 ml toluene were dropwisely added under a constant pH of 4.5, according to the general procedure 1. The crude product was stirred in 30 ml methanol, filtrated and dried.

Yield: pale pink powder, 3.26 g (85.4 %)
Purity: 99.0 % (HPLC: t_R = 3.58 min, system 1)
TLC: Rf = 0.66 (Isopr + NH_3 = 5 + 2)
NaCl: 22.80 %
Water: 1 mol/mol
CHN analysis:

	%C	%H	%N	C/N
Calcd	48.39	3.52	7.52	6.43
Calcd (with NaCl/H_2O)	35.63	2.99	5.54	6.43
Found	35.33	3.06	5.74	6.16

500 MHz ^{1}H NMR Spectrum (DMSO-d_6): δ/ppm

ABX-System
7.55 d (H2; X)
7.41 dd (H6; B)
7.21 d (H5; A)
$^3J_{AB}$ = 7.9 Hz $^3J_{BA}$ = 7.9 Hz
$^4J_{BX}$ = 1.9 Hz $^4J_{XB}$ = 1.9 Hz

ABX-System
8.57 d (H2'; X)
8.23 dd (H6'; B)
7.67 d (H5'; A)
$^3J_{AB}$ = 8.0 Hz $^3J_{BA}$ = 8.0 Hz
$^4J_{BX}$ = 1.9 Hz $^4J_{XB}$ = 1.9 Hz

-CONH- 10.24 s (1H, exchangeable)
-CH_3 2.59 s (3H)
-CH_3 2.21 s (3H)

125 MHz ^{13}C NMR Spectrum (DMSO-d_6): δ/ppm

C1	146.6	C5	129.7	C9	19.7	C4'	136.3
C2	123.6	C6	124.1	C1'	133.2	C5'	132.2
C3	134.4	C7	17.9	C2'	123.7	C6'	133.6
C4	135.3	C8	163.2	C3'	148.9		

IR Spectrum: cm^{-1}

3447 (m, br)	3250 (m)	1645 (m)	1623 (w)	1531 (s)	1484 (w)
1451 (w)	1406 (w)	1347 (s)	1312 (w)	1245 (m)	1190 (s)
1094 (m)	1049 (s)	801 (m)	688 (m)		

UV Spectrum (phosphate buffer pH 6.5), λ_{max}: nm

222.5

3-(3-Amino-4-methylbenzamido)-4-methylbenzenesulfonic acid sodium salt (12b)

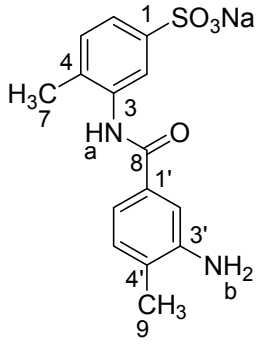

$C_{15}H_{15}N_2NaO_4S$ (342.4)

40 mg 10 % Pd/C were added to a solution of 1.16 g (3.12 mmol) compound 12a in 50 ml water. The mixture was hydrogenated overnight, according to the general procedure 2. The crude product was stirred in 20 ml methanol, filtrated and dried.

Yield: pale orange powder, 1.03 g (96.5 %)
Purity: 91.0 % (HPLC: t_R = 1.39 min, system 1)
TLC: Rf = 0.57 (Isopr + NH_3 = 5 + 2)
NaCl: 13.35 %
Water: 1.5 mol/mol
CHN analysis:

	%C	%H	%N	C/N
Calcd	52.63	4.42	8.18	6.43
Calcd (with NaCl /H_2O)	42.26	4.26	6.57	6.43
Found	42.01	4.34	6.34	6.63

500 MHz ^{1}H NMR Spectrum (DMSO-d_6): δ/ppm

ABX-System

7.56 d (H2; X)
7.36 dd (H6; B)
7.18 d (H5; A)

$^3J_{AB}$ = 8.0 Hz $^3J_{BA}$ = 8.0 Hz
$^4J_{BX}$ = 1.7 Hz $^4J_{XB}$ = 1.7 Hz

ABX-System

7.20	d (H2'; X)	
7.10	dd (H6'; B)	
7.02	d (H5'; A)	
	$^3J_{AB}$ = 7.9 Hz	$^3J_{BA}$ = 7.9 Hz
	$^4J_{BX}$ = 1.9 Hz	$^4J_{XB}$ = 1.9 Hz

-CONH-	9.61	s (1H, exchangeable)
$-NH_2$	5.01	s (2H, exchangeable)
$-CH_3$	2.19	s (3H)
$-CH_3$	2.10	s (3H)

125 MHz ^{13}C NMR Spectrum (DMSO-d_6): δ/ppm

C1	146.4	C5	129.5	C9	17.6	C4'	133.2
C2	123.0	C6	123.9	C1'	124.9	C5'	129.8
C3	134.1	C7	17.9	C2'	113.4	C6'	115.2
C4	136.1	C8	166.1	C3'	146.7		

IR Spectrum: cm^{-1}

3435 (s, br)	1643 (m)	1575 (m)	1530 (m)	1504 (m)	1405 (w)
1311 (w)	1195 (s)	1138 (w)	1095 (w)	1041 (s)	999 (w)
821 (w)	759 (w)	693 (m)	598 (w)	556 (w)	

UV Spectrum (phosphate buffer pH 6.5), λ_{max}: nm

220.5

3,3'-(Carbonylbis(imino-3,1-(4-methylphenylene)carbonylimino))-bis(4-methylbenzenesulfonic acid) disodium salt (12c)

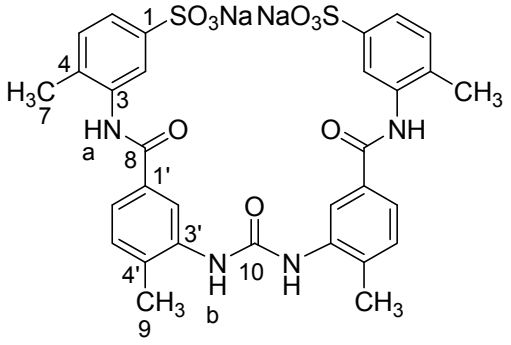

$C_{31}H_{28}N_4Na_2O_9S_2$ (710.68)

To a solution of 0.53 g (1.54 mmol) amine 12b in 20 ml water, 2 ml (4 mmol) 20 % phosgene solution in toluene were added under a constant pH of 4.5. The synthesis was performed according to the general procedure 3. The crude product was stirred in 15 ml methanol, filtrated and dried.

Yield: white powder, 0.19 g (34.2 %)
Purity: 96.1 % (HPLC: t_R = 4.60 min, system 1)
TLC: Rf = 0.40 (Isopr + NH_3 = 5 + 2)
NaCl: 3.51 %

Water: 9 mol/mol

CHN analysis:

	%C	%H	%N	C/N
Calcd	52.39	3.97	7.88	6.65
Calcd (with $NaCl/H_2O$)	41.16	4.85	6.19	6.65
Found	41.32	5.13	6.20	6.66

500 MHz ^{1}H NMR Spectrum (DMSO-d_6): δ/ppm

ABX-System

7.55 d (H2; X)
7.38 dd (H6; B)
7.19 d (H5; A)
$^3J_{AB}$ = 7.9 Hz $^3J_{BA}$ = 7.9 Hz
$^4J_{BX}$ = 1.6 Hz $^4J_{XB}$ = 1.6 Hz

ABX-System

8.35 d (H2'; X)
7.60 dd (H6'; B)
7.32 d (H5'; A)
$^3J_{AB}$ = 7.9 Hz $^3J_{BA}$ = 7.9 Hz
$^4J_{BX}$ = 1.6 Hz $^4J_{XB}$ = 1.6 Hz

-CONH-	9.83	s (2H, exchangeable)
-NHCONH-	8.62	s (2H, exchangeable)
$-CH_3$	2.36	s (6H)
$-CH_3$	2.19	s (6H)

125 MHz ^{13}C NMR Spectrum (DMSO-d_6): δ/ppm

C1	146.4	C5	129.6	C9	18.3	C3'	137.7
C2	123.2	C6	124.1	C10	153.3	C4'	132.8
C3	134.4	C7	17.9	C1'	132.6	C5'	130.2
C4	135.9	C8	165.4	C2'	121.7	C6'	122.3

IR Spectrum: cm^{-1}

3460 (s, br)	1657 (s)	1475 (s)	1526 (s)	1485 (m)	1447 (m)
1409 (m)	1312 (m)	1190 (s)	1140 (w)	1041 (s)	823 (w)
753 (w)	694 (s)				

UV Spectrum (phosphate buffer pH 6.5), λ_{max}: nm

224

ESI-MS negative mode (calcd/found): m/z

709.1/709.3 $[M-H]^-$, 689.1/687.4 $[M-Na]^-$, 665.1/665.4 $[M-2Na+H]^-$

2-(4-Methyl-3-nitrobenzamido)-4-sulfonatobenzoic acid disodium salt (13a)

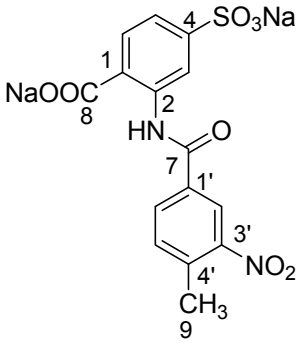

$C_{15}H_{10}N_2Na_2O_8S$ (424.3)

To a solution of 2.49 g (10.41 mmol) 4-sulfoanthranilic acid in 50 ml water, 15 mmol 4-methyl-3-nitrobenzoyl chloride, dissolved in 15 ml toluene, were slowly dropped under a constant pH of 4.0. The reaction was performed according to the general procedure 1. Crude product was stirred in 40 ml methanol, filtrated and dried.

Yield: brown powder, 3.51 g (79.4 %)
Purity: 96.2 % (HPLC: t_R = 3.45 min, system 1)
TLC: Rf = 0.55 (Isopr + NH_3 = 5 + 2)
NaCl: 14.60 %
Water: 2 mol/mol

CHN analysis:

	%C	%H	%N	C/N
Calcd	42.46	2.38	6.60	6.43
Calcd (with NaCl/H_2O)	33.42	2.62	5.20	6.43
Found	33.20	2.57	5.14	6.46

500 MHz ^{1}H NMR Spectrum (DMSO-d_6): δ/ppm

ABX-System
8.92 s (H3; X)
7.98 d (H6; B)
7.27 d (H5; A)
$^3J_{AB}$ = 8.0 Hz $^3J_{BA}$ = 8.0 Hz

ABX-System
8.53 s (H2'; X)
8.22 d (H6'; B)
7.68 d (H5'; A)
$^3J_{AB}$ = 7.9 Hz $^3J_{BA}$ = 7.9 Hz

-CONH- 15.85 s (1H, exchangeable)
$-CH_3$ 2.59 s (3H)

125 MHz ^{13}C NMR Spectrum (DMSO-d_6): δ/ppm

C1	130.7	C5	119.4	C9	19.7	C4'	136.2
C2	140.2	C6	124.9	C1'	134.9	C5'	131.2
C3	116.2	C7	170.1	C2'	123.3	C6'	133.5
C4	150.0	C8	161.7	C3'	149.3		

IR Spectrum: cm^{-1}

3436 (m, br)	1659 (m)	1620 (s)	1582 (s)	1510 (s)	1438 (s)
1367 (m)	1313 (w)	1249 (m)	1188 (m)	1127 (s)	1046 (s)
937 (w)	804 (w)	738 (m)	635 (m)		

UV Spectrum (phosphate buffer pH 6.5), λ_{max}: nm

232.5, 268.5

2-(3-Amino-4-methylbenzamido)-4-sulfonatobenzoic acid disodium salt (13b)

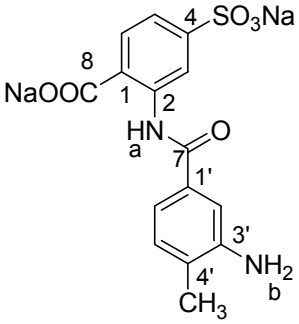

$C_{15}H_{12}N_2Na_2O_6S$ (394.3)

40 mg 10 % Pd/C were added to a solution of 2.14 g (5.04 mmol) compound 13a in 100 ml water. The mixture was hydrogenated overnight, according to the general procedure 2.

Yield: brown powder, 1.91 g (96.2 %)
Purity: 96.1 % (HPLC: t_R = 1.66 min, system 1)
TLC: Rf = 0.52 (Isopr + NH_3 = 5 + 2)
Water: 0.5 mol/mol
NaCl: < 1%

CHN analysis:	%C	%H	%N	C/N
Calcd	45.69	3.07	7.10	6.44
Calcd (with NaCl/H_2O)	44.67	3.42	6.95	6.43
Found	44.28	3.26	6.71	6.60

500 MHz ^{1}H NMR Spectrum (DMSO-d_6): δ/ppm

ABX-System
- 8.94 s (H3; X)
- 7.96 d (H6; B)
- 7.22 d (H5; A)
  - $^3J_{AB}$ = 7.0 Hz $^3J_{BA}$ = 7.0 Hz

ABX-System
- 7.29 s (H2'; X)
- 7.17 d (H6'; B)
- 7.01 d (H5'; A)

$^3J_{AB}$ = 6.7 Hz $^3J_{BA}$ = 6.7 Hz

-CONH-	14.81	s (1H, exchangeable)
-NH_2	5.02	s (2H, exchangeable)
-CH_3	2.11	s (3H)

125 MHz ^{13}C NMR Spectrum (DMSO-d_6): δ/ppm

C1	130.7	C5	118.6	C9	17.6	C4'	134.3
C2	140.6	C6	124.8	C1'	124.8	C5'	129.9
C3	116.2	C7	170.5	C2'	113.3	C6'	114.8
C4	149.8	C8	164.9	C3'	146.8		

IR Spectrum: cm^{-1}

3409 (m)	3360 (m)	3112 (m)	1665 (m)	1630 (m)	1581 (s)
1498 (s)	1426 (s)	1371 (m)	1311 (w)	1274 (w)	1241 (s)
1194 (s)	1125 (m)	1049 (s)	800 (m)	746 (m)	626 (m)

UV Spectrum (phosphate buffer pH 6.5), λ_{max}: nm

226.5, 275.5, 306.5

2,2'-(Carbonylbis(imino-3,1-(4-methylphenylene)carbonyl imino))bis-(4-sulfonatobenzoate) tetrasodium salt (13c)

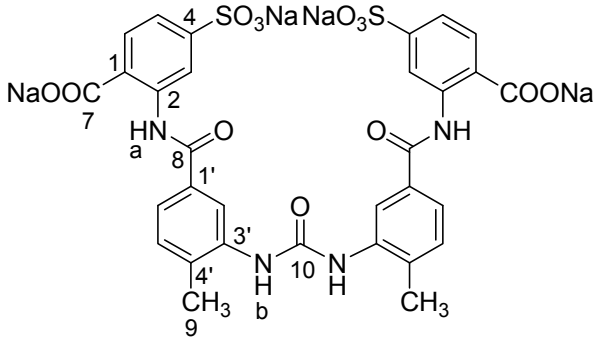

$C_{31}H_{22}N_4Na_4O_{13}S_2$ (814.6)

To a solution of 0.70 g (1.8 mmol) amine 13b in 30 ml water, 3 ml (6 mmol) 20 % phosgene solution in toluene were added under a constant pH of 4.0. The synthesis was performed according to the general procedure 3. The crude product was stirred in 30 ml methanol, filtrated and dried.

Yield: brown powder, 552 mg (75.3 %)
Purity: 97.8 % (HPLC: t_R = 6.13 min, system 1)
TLC: Rf = 0.40 (Isopr + NH_3 = 5 + 2)
NaCl: 23.35 %
Water: 5 mol/mol
CHN analysis:

	%C	%H	%N	C/N
Calcd	45.71	2.72	6.88	6.64
Calcd (with NaCl/H_2O)	31.55	2.73	4.75	6.65
Found	31.56	3.02	4.76	6.63

500 MHz ^{1}H NMR Spectrum (DMSO-d_6): δ/ppm

ABX-System

8.92	d (H3; X)	
7.97	d (H6; B)	
7.23	dd (H5; A)	
	$^3J_{AB}$ = 8.0 Hz	$^3J_{BA}$ = 8.0 Hz
	$^4J_{AX}$ = 1.3 Hz	$^4J_{XA}$ = 1.3 Hz

ABX-System

8.29	s (H2'; X)	
7.63	dd (H6'; B)	
7.33	d (H5'; A)	
	$^3J_{AB}$ = 8.2 Hz	$^3J_{BA}$ = 8.2 Hz
	$^4J_{BX}$ = 0.9 Hz	

-CONH-	14.82	s (2H, exchangeable)
-NHCONH-	8.84	s (2H, exchangeable)
-CH_3	2.38	s (6H)

125 MHz ^{13}C NMR Spectrum (DMSO-d_6): δ/ppm

C1	130.8	C5	118.9	C9	18.7	C3'	137.8
C2	140.3	C6	124.5	C10	153.8	C4'	134.0
C3	116.4	C7	170.9	C1'	132.7	C5'	130.6
C4	149.9	C8	164.5	C2'	120.3	C6'	122.4

IR Spectrum: cm^{-1}

3423 (s, br)	1581 (s)	1507 (s)	1442 (s)	1371 (m)	1304 (w)
1196 (m)	1126 (w)	1047 (m)	800 (w)	749 (m)	636 (m)

UV Spectrum (phosphate buffer pH 6.5), λ_{max}: nm

236

ESI-MS positive mode (calcd/found): m/z

815.0/815.5 $[M+H]^+$, 837.0/837.4 $[M+Na]^+$, 793.0/ 793.5 $[M-Na+2H]^+$

ESI-MS negative mode (calcd/found): m/z

791.0/791.1 $[M-Na]^-$, 813.0/813.2 $[M-H]^-$

3-(4-Nitrobenzamido)benzenesulfonate sodium salt (14a)

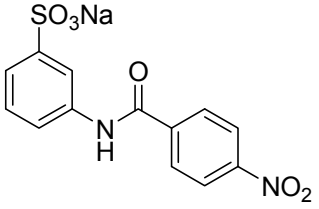

$C_{13}H_9N_2NaO_6S$ (344.3)

To a solution of 1.73 g (10 mmol) 3-aminobenzene sulfonic acid in 50 ml water, 2.30 g (12.4 mmol) 4-nitrobenzoyl chloride, dissolved in 20 ml toluene, were dropwisely added under a constant pH of 4.0, according to the general procedure 1. The crude product was stirred in 30 ml methanol, filtrated and dried.

Yield: yellow powder, 3.35 g (97.3 %)
Purity: 98.8 % (HPLC: t_R = 1.99 min, system 1)
TLC: Rf = 0.71 (Isopr + NH_3 = 5 + 2)
NaCl: 2.99 %
Water: 0.5 mol/mol
CHN analysis:

	%C	%H	%N	C/N
Calcd	45.35	2.63	8.14	5.57
Calcd (with $NaCl/H_2O$)	42.88	2.77	7.69	5.57
Found	42.50	3.02	7.75	5.48

500 MHz ^{1}H NMR Spectrum (DMSO-d_6): δ/ppm

ABCX-system

8.05 t (H2; X)
7.82 ddd (H4; C)
7.38 dt (H6; A)
7.32 t (H5; B)

$^3J_{AB}$ = 7.9 Hz $^3J_{BA}$ = 7.9 Hz
$^3J_{BC}$ = 7.9 Hz $^3J_{CB}$ = 7.9 Hz
$^4J_{AC}$ = 1.7 Hz $^4J_{CA}$ = 1.7 Hz
$^4J_{AX}$ = 1.7 Hz $^4J_{XA}$ = 1.7 Hz
$^4J_{CX}$ = 1.9 Hz $^4J_{XC}$ = 1.9 Hz

AA'BB'-system

8.35 m (H3'H5'; BB')
8.22 m (H2'H6'; AA')

$^3J_{AB}$ = 8.9 Hz $^3J_{BA}$ = 8.9 Hz
$^3J_{A'B'}$ = 8.9 Hz $^3J_{B'A'}$ = 8.9 Hz
$^4J_{AA'}$ = 2.2 Hz $^4J_{BB'}$ = 2.2 Hz

-CONH- 10.60 s (1H, exchangeable)

125 MHz ^{13}C NMR Spectrum (DMSO-d_6): δ/ppm

C1	148.9	C4	121.5	C7	163.9	C2'C6'129.4
C2	118.2	C5	128.1	C1'	140.6	C3'C5'123.6
C3	138.3	C6	120.6	C4'	149.3	

IR Spectrum: cm^{-1}

3410 (m)	3338 (m)	3073 (m)	1683 (s)	1603 (s)	1554 (s)
1521 (s)	1483 (s)	1429 (m)	1354 (s)	1320 (s)	1289 (w)
1214 (s)	1177 (s)	1125 (m)	1099 (m)	1040 (s)	996 (m)
852 (m)	791 (m)	709 (s)	622 (s)		

UV Spectrum (phosphate buffer pH 6.5), λ_{max}: nm

240, 274

3-(4-Aminobenzamido)benzenesulfonate sodium salt (14b)

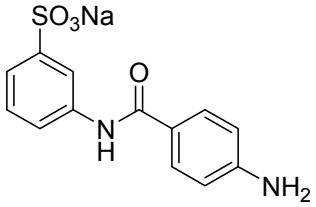

$C_{13}H_{11}N_2NaO_4S$ (314.3)

40 mg 10 % Pd/C were added to a solution of 1.97 g (5.14 mmol) compound 14a in a mixture of 100 ml water and 50 ml methanol. The mixture was hydrogenated overnight, according to the general procedure 2. The crude product was stirred in 30 ml methanol, filtrated and dried.

Yield: white powder, 1.44 g (89.1 %)
Purity: 99.0 % (HPLC: t_R = 0.84 min, system 1)
TLC: Rf = 0.63 (Isopr + NH_3 = 5 + 2)
NaCl: < 1%
Water: 0.5 mol/mol
CHN analysis:

	%C	%H	%N	C/N
Calcd	49.68	3.53	8.91	5.57
Calcd (with NaCl/H_2O)	48.30	3.94	8.43	5.57
Found	48.26	3.94	8.51	5.67

500 MHz ^{1}H NMR Spectrum (DMSO-d_6): δ/ppm

ABCX-System

8.00 t (H2; X)
7.78 ddd (H4; C)
7.28 dt (H6; A)
7.23 t (H5; B)

$^3J_{AB}$ = 7.9 Hz $^3J_{BA}$ = 7.9 Hz
$^3J_{BC}$ = 7.9 Hz $^3J_{CB}$ = 7.9 Hz
$^4J_{AC}$ = 1.3 Hz $^4J_{CA}$ = 1.3 Hz
$^4J_{AX}$ = 1.6 Hz $^4J_{XA}$ = 1.6 Hz
$^4J_{CX}$ = 2.0 Hz $^4J_{XC}$ = 2.0 Hz

AA'BB'-system

7.73 m (H2'H6'; BB')
6.58 m (H3'H5'; AA')

$^3J_{AB}$ = 9.5 Hz $^3J_{BA}$ = 9.5 Hz
$^4J_{AA'}$ = 2.2 Hz $^4J_{BB'}$ = 2.2 Hz

-CONH- 9.78 s (1H, exchangeable)
-NH_2 5.70 s (2H, exchangeable)

125 MHz ^{13}C NMR Spectrum (DMSO-d_6): δ/ppm

C1	148.7	C4	121.2	C7	165.3	C2'C6'129.5
C2	117.8	C5	127.7	C1'	120.3	C3'C5'112.7

C3	139.3	C6	120.3	C4'	152.2

IR Spectrum: cm^{-1}

3413 (w)	3307 (w)	1667 (s)	1606 (s)	1544 (s)	1514 (s)
1478 (s)	1409 (w)	1321 (s)	1285 (m)	1267 (s)	1127 (s)
1193 (s)	1127 (m)	1045 (s)	847 (m)	719 (s)	

UV Spectrum (phosphate buffer pH 6.5), λ_{max}: nm

294

3,3'-(Carbonylbis(imino-4,1-phenylenecarbonylimino))bis-(benzenesulfonic acid) disodium salt (14c)

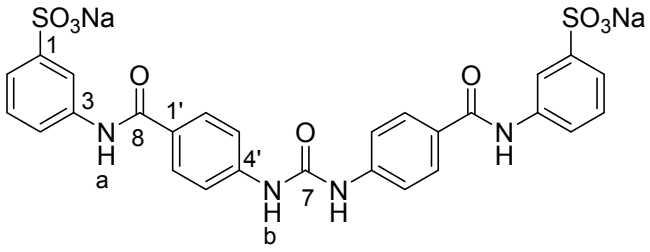

$C_{27}H_{20}N_4Na_2O_9S_2$ (654.6)

To a solution of 0.74 g (2.36 mmol) amine 14b in 50 ml water, 3 ml (6 mmol) 20 % phosgene solution were added undera constant pHof 4.0. The synthesis was performed according to the general procedure 3. The crude product was stirred in 20 ml methanol, filtrated and dried.

Yield: white powder, 683 mg (88.4 %)
Purity: 96.5 % (HPLC: t_R = 1.46 min, system 1)
TLC: Rf = 0.50 (Isopr + NH_3 = 5 + 2)
NaCl: 1.15 %
Water: 6.5 mol/mol
CHN analysis:

	%C	%H	%N	C/N
Calcd	49.54	3.08	8.56	5.79
Calcd (with $NaCl/H_2O$)	41.54	4.26	7.18	5.79
Found	41.78	4.49	7.06	5.92

500 MHz ^{1}H NMR Spectrum (DMSO-d_6): δ/ppm

ABCX-System

8.05 pt (H2; X)
7.82 dt (H4; C)
7.34 dt (H6; A)
7.28 t (H5; B)

$^3J_{AB}$ = 7.9 Hz	$^3J_{BA}$ = 7.9 Hz
$^3J_{BC}$ = 7.7 Hz	$^3J_{CB}$ = 7.7 Hz
$^4J_{AC}$ = 1.3 Hz	$^4J_{CA}$ = 1.3 Hz
$^4J_{AX}$ = 1.7 Hz	$^4J_{XA}$ = 1.7 Hz
$^4J_{CX}$ = 1.5 Hz	$^4J_{XC}$ = 1.5 Hz

AA'BB'-System
7.96 m (H3'H5'; BB')
7.62 m (H2'H6'; AA')
$^3J_{AB}$ = 8.8 Hz $^3J_{A'B'}$ = 8.8 Hz
$^4J_{AA'}$ = 1.9 Hz $^4J_{BB'}$ = 1.9 Hz

-CONH- 10.13 s (2H, exchangeable)
-NHCONH- 9.20 s (2H, exchangeable)

125 MHz ^{13}C NMR Spectrum (DMSO-d_6): δ/ppm

C1	148.7	C4	120.8	C7	164.9	C4'	142.8
C2	118.0	C5	128.0	C8	152.2	C2'C6'	128.9
C3	138.9	C6	120.5	C1'	127.9	C3'C5'	117.5

IR Spectrum: cm^{-1}

3468 (s, br)	3318 (s)	1704 (m)	1666 (s)	1637 (s)	1595 (s)
1537 (s)	1507 (s)	1482 (m)	1418 (s)	1313 (s)	1182 (s)
1128 (m)	1045 (s)	994 (w)	923 (w)	843 (w)	794 (w)
722 (m)	623 (s)	526 (m)			

UV Spectrum (phosphate buffer pH 6.5), λ_{max}: nm
302.5

ESI-MS negative mode (calcd/found): m/z
631.1/631.2 $[M-Na]^-$, 653.0/653.0 $[M-H]^-$

2-(4-Nitrobenzamido)-4-sulfonatobenzoate disodium salt (15a)

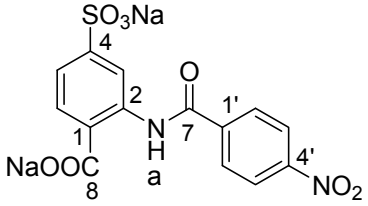

$C_{14}H_8N_2Na_2O_8S$ (410.3)

2.39 g (10.00 mmol) 4-Sulfoanthranilic acid, dissolved in 50 ml water, was acylated with 2.00 g (10.78 mmol) 4-nitrobenzoyl chloride, dissolved in 20 ml toluene, under a constant pH of 4.0. The synthesis was performed according to the general procedure 1. The crude product was stirred in 30 ml methanol, filtrated and dried.

Yield: yellow powder, 3.22 g (80.2 %)
Purity: 95.0 % (HPLC: t_R = 2.54 min, system 1)
TLC: Rf = 0.56 (Isopr + NH_3 = 5 + 2)
NaCl: 20.98 %
Water: 2 mol/mol
CHN analysis:

	%C	%H	%N	C/N
Calcd	40.99	1.97	6.83	6.00
Calcd (with NaCl/H_2O)	29.77	2.14	4.96	6.00

Found	29.99	2.09	4.97	6.04

500 MHz ^{1}H NMR Spectrum (DMSO-d_6): δ/ppm

ABX-System

8.92 s (H2; X)
7.97 d (H5; B)
7.26 d (H6; A)
$^3J_{AB}$ = 7.9 Hz $^3J_{BA}$ = 7.9 Hz

AA'BB'-System

8.36 d (H3'H5'; BB')
8.24 d (H2'H6'; AA')
$^3J_{AB}$ = 8.2 Hz $^3J_{BA}$ = 8.2 Hz

-CONH- 16.06 s (1H, exchangeable)

125 MHz ^{13}C NMR Spektrum (DMSO-d_6): δ/ppm

C1	130.7	C4	150.1	C7	170.1	C4'	149.2
C2	141.4	C5	119.6	C8	162.2	C2'C6'	128.7
C3	116.3	C6	124.9	C1'	140.1	C3'C5'	124.0

IR Spectrum: cm^{-1}

3569 (m)	3468 (m, br)	1668 (m)	1601 (s)	1581 (s)	1515 (s)
1441 (s)	1420 (s)	1352 (s)	1308 (w)	1191 (s)	1125 (m)
1044 (s)	855 (w)	714 (m)	637 (m)	488 (w)	

UV Spectrum (phosphate buffer pH 6.5), λ_{max}: nm

224, 248, 308

2-(4-Aminobenzamido)-4-sulfonatobenzoate disodium salt (15b)

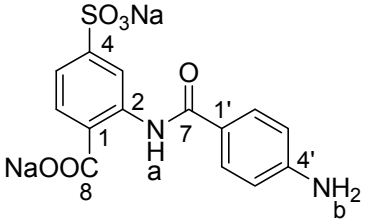

$C_{14}H_{10}N_2Na_2O_6S$ (380.3)

20 mg 10 % Pd/C were added to a solution of 2.21 g (5.82 mmol) compound 15a in 150 ml water. The mixture was hydrogenated overnight, according to the general procedure 2.

Yield: white powder, 2.17 g (98.1 %)
Purity: 97.6 % (HPLC: t_R = 4.80 min, system 2)
TLC: Rf = 0.50 (Isopr + NH_3 = 5 + 2)
Water: 2 mol/mol
NaCl: 22.02 %
CHN analysis:

	%C	%H	%N	C/N
Calcd	44.22	2.65	7.37	6.00

Calcd (with $NaCl/H_2O$)	31.50	2.64	5.24	6.00
Found	31.36	2.87	5.24	5.98

500 MHz ^{1}H NMR Spectrum (DMSO-d_6): δ/ppm

ABX-System

8.95 s (H3; X)
7.95 d (H6; B)
7.18 d (H5; A)
$^3J_{AB}$ = 6.9 Hz $^3J_{BA}$ = 6.9 Hz

AA'BB'-System

7.73 d (H2'H6'; BB')
6.60 d (H3'H5'; AA')
$^3J_{AB}$ = 7.3 Hz $^3J_{A'B'}$ = 7.3 Hz

-CONH- 14.59 s (1H, exchangeable)
$-NH_2$ 5.72 s (2H, exchangeable)

125 MHz ^{13}C NMR Spectrum (DMSO-d_6): δ/ppm

C1	130.7	C4	152.1	C7	170.8	C4'	149.8
C2	141.0	C5	118.2	C8	164.4	C2'C6'	128.9
C3	116.1	C6	124.2	C1'	122.2	C3'C5'	112.9

IR Spectrum: cm^{-1}

3413 (s)	3323 (m)	3103 (w)	1656 (m)	1609 (s)	1581 (s)
1502 (s)	1428 (s)	1381 (w)	1367 (m)	1279 (m)	1227 (m)
1187 (s)	1124 (m)	1040 (s)	802 (m)	761 (m)	691 (m)

UV Spectrum (phosphate buffer pH 6.5), λ_{max}: nm

218.5, 298.5

2,2'-(Carbonylbis(imino-4,1-phenylenecarbonylimino))bis-(4-sulfonatobenzoate) tetrasodium salt (15c)

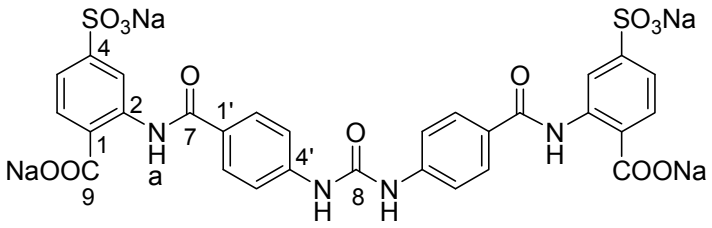

$C_{29}H_{18}N_4Na_4O_{13}S_2$ (786.6)

To a solution of 0.60 g (1.57 mmol) amine 15b in 50 ml water, 2 ml (4 mmol) 20 % phosgene solution in toluene were added under a constant pH of 4.0. The synthesis was performed according to the general procedure 3. The crude product was stirred in 30 ml methanol, filtrated and dried.

Yield: white powder, 403 mg (65.4 %)
Purity: 90.1 % (HPLC: t_R = 3.25 min, system 1)
TLC: Rf = 0.20 (Isopr + NH_3 = 5 + 2)
NaCl: 27.65 %

Water: 7.5 mol/mol

CHN analysis:

	%C	%H	%N	C/N
Calcd	44.28	2.31	7.12	6.22
Calcd(with $NaCl/H_2O$)	27.34	2.61	4.40	6.22
Found	27.32	2.41	4.30	6.36

500 MHz ^{1}H NMR Spectrum (DMSO-d_6): δ/ppm

ABX-System

8.99 s (H3; X)
8.09 d (H6; B)
7.28 d (H5; A)
$^3J_{AB}$ = 7.2 Hz $^3J_{BA}$ = 7.2 Hz

AA'BB'-System

8.01 d (H3'H5'; BB')
7.86 d (H2'H6'; AA')
$^3J_{AB}$ = 7.9 Hz $^3J_{BA}$ = 7.9 Hz

-CONH- 14.54 s (2H, exchangeable)
-NHCONH- 11.63 s (2H, exchangeable)

IR Spectrum: cm^{-1}

3435 (s, br)	1706 (m)	1583 (s)	1499 (s)	1438 (s)	1373 (s)
1323 (s)	1278 (m)	1186 (w)	1126 (s)	1074 (m)	1046 (s)
929 (w)	850 (w)	803 (m)	760 (m)	691 (m)	

UV Spectrum (phosphate buffer pH 6.5), λ_{max}: nm

316

ESI-MS positive mode (calcd/found): m/z

809.0/809.2 $[M+Na]^+$, 765.0/765.3 $[M-Na+2H]^+$

ESI-MS negative mode (calcd/found): m/z

763.0/763.3 $[M-Na]^-$, 719.0/719.3 $[M-3Na+2H]^-$

4-Methyl-3-(4-nitrobenzamido)benzenesulfonate sodium salt (16a)

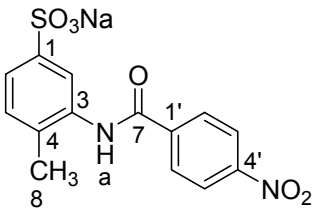

$C_{14}H_{11}N_2NaO_6S$ (358.3)

To a solution of 2.09 g (10 mmol) amine 1e in 50 ml water, 2.78 g (15 mmol) 4-nitrobenzoyl chloride, dissolved in 20 ml toluene, were slowly dropped under a constant pH of 4.0. The synthesis was performed according to the general procedure 1.

Yield: yellow powder, 3.24 g (90.4 %)
Purity: 95.2 % (HPLC: t_R = 2.24 min, system 1)
TLC: Rf = 0.66 (Isopr + NH_3 = 7.5 + 2.5)
NaCl: 23.04 %
Water: 1.5 mol/mol
CHN analysis:

	%C	%H	%N	C/N
Calcd	46.93	3.09	7.82	6.00
Calcd (with NaCl/H_2O)	33.58	2.82	5.60	6.00
Found	33.40	3.07	5.61	5.96

500 MHz ^{1}H NMR Spectrum (DMSO-d_6): δ/ppm

ABX-System
7.58 d (H2; X)
7.43 dd (H6; B)
7.24 d (H5; A)
$^3J_{AB}$ = 7.9 Hz $^3J_{BA}$ = 7.9 Hz
$^4J_{BX}$ = 1.6 Hz $^4J_{XB}$ = 1.6 Hz

AA'BB'-System
8.34 m (H3'H5'; BB')
8.20 d (H2'H6'; AA')
$^3J_{AB}$ = 8.6 Hz $^3J_{A'B'}$ = 8.6 Hz
$^4J_{BB'}$ = 1.9 Hz

-CONH- 10.28 s (1H, exchangeable)
-CH_3 2.22 s (3H)

125 MHz ^{13}C NMR-Spectrum (DMSO-d_6): δ/ppm

C1	146.6	C4	135.3	C7	17.9	C4'	149.3
C2	124.1	C5	129.7	C8	163.9	C2'C6'	129.3
C3	134.3	C6	129.7	C1'	140.4	C3'C5'	123.7

IR Spectrum: cm^{-1}

3448 (m, br)	3109 (w)	1663 (m)	1602 (m)	1525 (s)	1486 (m)
1448 (w)	1406 (w)	1348 (s)	1306 (m)	1286 (m)	1193 (s)
1089 (m)	1013 (w)	867 (w)	851 (m)	691 (s)	

UV Spectrum (phosphate buffer pH 6.5), λ_{max}: nm
269

3-(4-Aminobenzamido)-4-methylbenzenesulfonate sodium salt (16b)

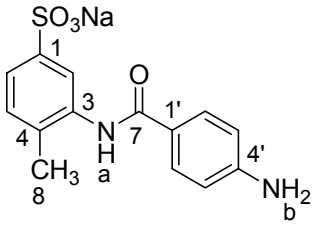

$C_{14}H_{13}N_2NaO_4S$ (328.3)

20 mg 10 % Pd/C were added to a solution of 2.03 g (6.45 mmol) compound 16a in 100 ml water. The mixture was hydrogenated overnight, according to the general procedure 2. The crude product was stirred in 20 ml methanol, filtrated and dried.

Yield: pale brown powder, 1.99 g (93.9 %)
Purity: 98.6 % (HPLC: t_R = 1.09 min, system 1)
TLC: Rf = 0.60 (Isopr + NH_3 = 7.5 + 2.5)
NaCl: 24.39 %
Water: 3 mol/mol
CHN analysis:

	%C	%H	%N	C/N
Calcd	51.22	3.99	8.53	6.00
Calcd (with NaCl/H_2O)	34.89	3.56	8.81	6.00
Found	34.51	3.17	5.79	5.88

500 MHz ^{1}H NMR Spectrum (DMSO-d_6): δ/ppm

ABX-System
7.55 d (H2; X)
7.35 dd (H6; B)
7.16 d (H5; A)
$^3J_{AB}$ = 8.0 Hz $^3J_{BA}$ = 8.0 Hz
$^4J_{BX}$ = 1.6 Hz $^4J_{XB}$ = 1.6 Hz

AA'BB'-System
7.70 m (H2'H6'; BB')
6.59 m (H3'H5'; AA')
$^3J_{AB}$ = 8.6 Hz $^3J_{BA}$ = 8.6 Hz
$^4J_{AA'}$ = 2.2 Hz $^4J_{BB'}$ = 2.2 Hz
$^4J_{A'A}$ = 2.2 Hz

-CONH- 9.41 s (1H, exchangeable)
-NH_2 5.67 s (2H, exchangeable)
-CH_3 2.18 s (3H)

125 MHz ^{13}C NMR Spectrum (DMSO-d_6): δ/ppm

C1	146.4	C4	136.5	C7	18.0	C4'	152.2
C2	122.8	C5	123.9	C8	165.3	C2'C6'	129.4

C3	134.0	C6	123.9	C1'	121.1	C3'	C5'	112.7			

IR Spectrum: cm^{-1}

3330 (s, br)	1640 (s)	1600 (s)	1510 (s)	1312 (m)	1271 (m)
1185 (s)	1120 (m)	1049 (s)	841 (m)	763 (m)	699 (s)
631 (s)					

UV Spectrum (phosphate buffer pH 6.5), λ_{max}: nm

214, 286

3,3'-(Carbonylbis(imino-4,1-phenylenecarbonylimino))bis-(4-methylbenzenesulfonic acid) disodium salt (16c)

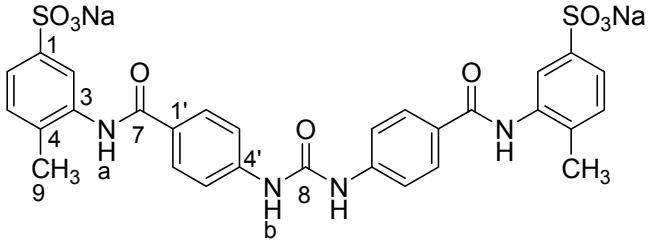

$C_{29}H_{24}N_4Na_2O_9S_2$ (682.6)

To a solution of 0.77 g (2.34 mmol) amine 16b in 50 ml water, 2 ml (4 mmol) 20 % phosgene solution in toluene were slowly dropped under a constant pH of 4.0. The synthesis was performed according to the general procedure 3. The crude product was stirred in 30 ml methanol, filtrated and dried.

Yield: white powder, 667 mg (83.5 %)
Purity: 95.3 % (HPLC: t_R = 3.74 min, system 1)
TLC: Rf = 0.40 (Isopr + NH_3 = 7 + 2)
NaCl: 20.23 %
Water: 4 mol/mol
CHN analysis:

	%C	%H	%N	C/N
Calcd	51.02	3.54	8.21	6.22
Calcd (with $NaCl/H_2O$)	36.82	3.41	5.92	6.22
Found	37.08	3.57	5.92	6.27

500 MHz ^{1}H NMR Spectrum (DMSO-d_6): δ/ppm

ABX-System

7.57 d (H2; X)
7.39 dd (H6; B)
7.20 d (H5; A)
$^3J_{AB}$ = 8.0 Hz $^3J_{BA}$ = 8.0 Hz
$^4J_{BX}$ = 1.7 Hz $^4J_{XB}$ = 1.7 Hz

AA'BB'-System

7.95 d (H3'H5'; BB')
7.61 d (H2'H6'; AA')
$^3J_{AB}$ = 8.8 Hz $^3J_{A'B'}$ = 8.8 Hz

-CONH-	10.06	s (2H, exchangeable)
-NHCONH-	9.79	s (2H, exchangeable)
$-CH_3$	2.21	s (6H)

125 MHz ^{13}C NMR-Spectrum (DMSO-d_6): δ/ppm

C1	146.3	C5	129.6	C9	152.6	C2'C6'	128.9
C2	123.2	C6	124.1	C1'	127.6	C3'C5'	117.1
C3	134.3	C7	18.0	C4'	142.9		
C4	136.1	C8	164.9				

IR Spectrum: cm^{-1}

3468 (m)	3364 (m)	1707 (m)	1666 (m)	1629 (m)	1597 (m)
1537 (s)	1502 (s)	1141 (w)	1406 (w)	1302 (m)	1231 (s)
1203 (s)	1182 (s)	1124 (w)	1034 (m)	848 (w)	690 (m)

UV Spectrum (phosphate buffer pH 6.5), λ_{max}: nm

298

ESI-MS negative mode (calcd/found): m/z

681.1/681.2 $[M-H]^-$, 659.1/659.3 $[M-Na]^-$, 637.1/637.2 $[M-2Na+H]^-$

3-Methyl-4-(4-nitrobenzamido)benzenesulfonate sodium salt (17a)

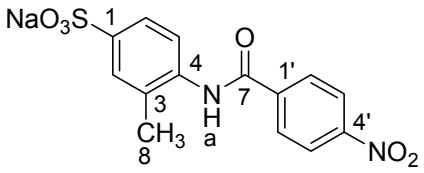

$C_{14}H_{11}N_2NaO_6S$ (358.3)

To a solution of 1.87 g (10.0 mmol) 4-amino-3-methylbenzenesulfonic acid in 50 ml water, 2.27 g (12.2 mmol) 4-nitrobenzoyl chloride, dissolved in 30 ml toluene and 20 ml diethyl ether were slowly added under a constant pH of 4.2. The synthesis was performed according to the general procedure 1. The crude product was stirred in 30 ml methanol, filtrated and dried.

Yield: pink powder, 3.42 g (95.5 %)
Purity: 99.2 % (HPLC: t_R = 1.81 min, system 1)
TLC: Rf = 0.62 (Isopr + NH_3 = 7.5 + 2.5)
NaCl: 2.21 %
Water: 1 mol/mol
CHN analysis:

	% C	% H	% N	C/N
Calcd	46.93	3.09	7.82	6.00
Calcd (with $NaCl/H_2O$)	43.69	3.40	7.28	6.00
Found	43.81	3.51	7.23	6.06

500 MHz ^{1}H NMR Spectrum (DMSO-d_6): δ/ppm

ABX-System

7.52 s (H2; X)
7.45 dd (H6; B)
7.30 d (H5; A)
$^3J_{AB}$ = 8.0 Hz $^3J_{BA}$ = 8.0 Hz
$^4J_{BX}$ = 1.3 Hz

AA'BB'-System

8.35 d (H3'H5'; BB')
8.21 d (H2'H6'; AA')
$^3J_{AB}$ = 8.7 Hz $^3J_{A'B'}$ = 8.7 Hz

-CONH- 10.22 s (1H, exchangeable)
-CH_3 2.24 s (3H)

125 MHz ^{13}C NMR Spectrum (DMSO-d_6): δ/ppm

C1	146.3	C4	136.1	C7	18.0	C4'	149.3
C2	127.8	C5	123.6	C8	163.9	C2'C6'	129.3
C3	133.0	C6	125.8	C1'	140.3	C3'C5'	123.7

IR Spectrum: cm^{-1}

3584 (m)	3477 (s)	3353 (s)	1655 (s)	1605 (s)	1584 (m)
1534 (s)	1446 (w)	1401 (m)	1351 (s)	1301 (m)	1184 (s)
1121 (s)	1041 (s)	870 (m)	855 (m)	808 (m)	695 (s)

UV Spectrum (phosphate buffer pH 6.5), λ_{max}: nm

236, 268

4-(4-Aminobenzamido)-3-methylbenzenesulfonate sodium salt (17b)

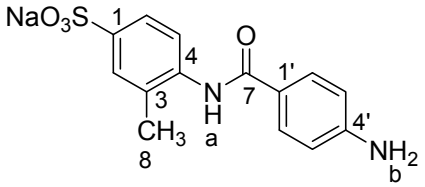

$C_{14}H_{13}N_2NaO_4S$ (328.3)

50 mg 10 % Pd/C were added to a solution of 1.53 g (4.27 mmol) compound 17a in 120 ml 20 % aqueous methanol. The mixture was hydrogenated overnight, according to the general procedure 2.

Yield: pink powder, 1.38 g (98.4 %)
Purity: 99.3 % (HPLC: t_R = 2.58 min, system 2)
TLC: Rf = 0.59 (Isopr + NH_3 = 5 + 2)
Water: 1.5 mol/mol
NaCl: 24.55 %
CHN analysis:

	%C	%H	%N	C/N
Calcd	51.22	3.99	8.53	6.00

Calcd (with $NaCl/H_2O$)	35.70	3.42	5.95	6.00
Found	35.67	3.47	5.90	6.05

500 MHz ^{1}H NMR Spectrum (DMSO-d_6): δ/ppm

ABX-System

7.46 d (H2; X)
7.40 dd (H6; B)
7.27 d (H5; A)
$^3J_{AB}$ = 8.2 Hz $^3J_{BA}$ = 8.2 Hz
$^4J_{BX}$ = 1.7 Hz $^4J_{XB}$ = 1.7 Hz

AA'BB'-System

7.70 d (H2'H6'; BB')
6.59 d (H3'H5'; AA')
$^3J_{AB}$ = 8.6 Hz $^3J_{A'B'}$ = 8.6 Hz

-CONH- 9.36 s (1H, exchangeable)
$-NH_2$ 5.69 s (2H, exchangeable)
$-CH_3$ 2.20 s (3H)

125 MHz ^{13}C NMR Spectrum (DMSO-d_6): δ/ppm

C1	145.2	C4	137.3	C7	18.1	C4'	152.2
C2	127.6	C5	123.3	C8	165.3	C2'C6'	129.4
C3	132.5	C6	125.5	C1'	120.9	C3'C5'	112.7

IR Spectrum: cm^{-1}

3339 (s, br)	1641 (s)	1608 (s)	1509 (s)	1445 (w)	1397 (w)
1313 (m)	1269 (m)	1186 (s)	1123 (m)	1099 (w)	1049 (s)
841 (m)	763 (m)	699 (s)	631 (s)		

UV Spectrum (phosphate buffer pH 6.5), λ_{max}: nm

286.5

4,4'-(Carbonylbis(imino-4,1-phenylenecarbonylimino))bis-(3-methylbenzenesulfonic acid) disodium salt (17c)

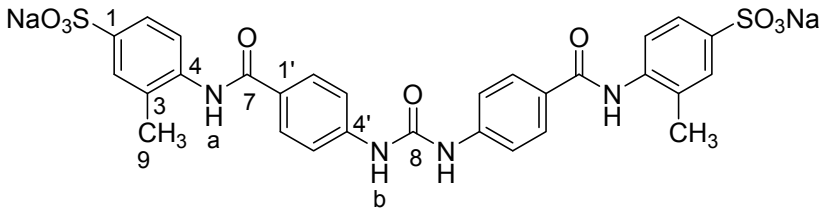

$C_{29}H_{24}N_4Na_2O_9S_2$ (682.6)

To a solution of 0.65 g (2.0 mmol) amine 17b was dissolved in 50 ml water and adjusted pH to 4.0, 3 ml (6 mmol) 20 % phosgene solution in toluene was dropwisely added under a constant pHof 4.0. The synthesis was performed according to the general procedure 3.

Yield: white powder, 0.60 g (87.3 %)

Purity: 95.2 % (HPLC: t_R = 2.58 min, system 1)
TLC: 0.20 (Isopr + NH_3 = 5 + 2)
NaCl: 2.30 %
Water: 1.5 mol/mol
CHN analysis:

	% C	% H	% N	C/N
Calcd	51.02	3.54	8.21	6.22
Calcd (with NaCl/H_2O)	47.95	3.75	7.71	6.22
Found	48.04	3.81	7.45	6.45

500 MHz ^{1}H NMR Spectrum (DMSO-d_6): δ/ppm

ABX-System
7.52 d (H2; X)
7.45 dd (H6; B)
7.31 d (H5; A)
$^3J_{AB}$ = 8.3 Hz $^3J_{BA}$ = 8.3 Hz
$^4J_{BX}$ = 1.9 Hz $^4J_{XB}$ = 1.9 Hz

AA'BB'-System
7.95 d (H3'H5'; BB')
7.62 d (H2'H6'; AA')
$^3J_{AB}$ = 8.8 Hz $^3J_{BB'}$ = 8.8 Hz

-CONH- 9.72 s (1H, exchangeable)
-NHCONH- 9.38 s (1H, exchangeable)
-CH_3 2.24 s (3H)

125 MHz ^{13}C NMR Spectrum (DMSO-d_6): δ/ppm

C1	145.5	C5	123.4	C9	152.3	C2'C6'128.9
C2	127.7	C6	125.7	C1'	127.7	C3'C5'117.5
C3	132.9	C7	18.1	C4'	142.9	
C4	136.9	C8	164.9			

IR Spectrum: cm^{-1}

3334 (m)	3255 (m)	1654 (s)	1591 (m)	1554 (w)	1526 (m)
1507 (m)	1444 (w)	1400 (w)	1320 (m)	1227 (m)	1201 (m)
1177 (m)	1129 (m)	1100 (w)	1056 (m)	696 (m)	625 (m)

UV Spectrum (phosphate buffer pH 6.5), λ_{max}: nm
299

ESI-MS negative mode (calcd/found): m/z
681.1/681.2 $[M-H]^-$, 659.1/659.4 $[M-Na]^-$, 637.1/637.4 $[M-2Na+H]^-$, 1341.2/1341.2 $[2M-Na]^-$

ESI-MS positive mode (calcd/found): m/z
683.1/683.3 $[M+H]^+$, 639.1/639.3 $[M-2Na+3H]^+$, 705.1/705.4 $[M+Na]^+$

5-Methyl-2-(4-nitrobenzamido)benzenesulfonate sodium salt (18a)

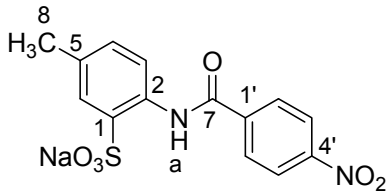

$C_{14}H_{11}N_2NaO_6S$ (358.3)

To a solution of 1.87 g (10 mmol) 2-amino-5-methylbenzenesulfonic acid in 50 ml water, 2.22 g (12.0 mmol) 4-nitrobenzoyl chloride, dissolved in 30 ml toluene and 20 ml diethyl ether were dropwisely added under a constant pH of 4.0. The synthesis was performed according to the general procedure 1.

Yield: yellow powder, 2.71 g (75.6 %)
Purity: 99.4 % (HPLC: t_R = 5.84 min, system 1)
TLC: Rf = 0.81 (Isopr + NH_3 = 5 + 2)
NaCl: < 1 %
Water: 1 mol/mol
CHN analysis:

	% C	% H	% N	C/N
Calcd	46.93	3.09	7.82	6.00
Calcd (with NaCl/H_2O)	44.68	3.48	7.44	6.00
Found	45.00	3.87	7.39	6.09

500 MHz ^{1}H NMR Spectrum (DMSO-d_6): δ/ppm

ABX-System
8.34 d (H3; B)
7.55 d (H6; X)
7.21 dd (H4; A)
$^3J_{AB}$ = 8.2 Hz $^3J_{BA}$ = 8.2 Hz
$^4J_{AX}$ = 1.9 Hz $^4J_{XA}$ = 1.9 Hz

AA'BB'-System
8.40 m (H3'H5'; BB')
8.14 m (H2'H6'; AA')
$^3J_{AB}$ = 8.8 Hz $^3J_{A'B'}$ = 8.8 Hz
$^4J_{AA'}$ = 2.5 Hz $^4J_{BB'}$ = 2.5 Hz
$^4J_{A'A}$ = 1.9 Hz $^4J_{B'B}$ = 1.9 Hz

-CONH- 11.62 s (1H, exchangeable)
-CH_3 2.29 s (3H)

125 MHz ^{13}C NMR Spectrum (DMSO-d_6): δ/ppm

C1	135.8	C4	132.3	C7	20.6	C4'	149.5
C2	130.3	C5	132.5	C8	162.2	C2'C6'	128.5
C3	119.9	C6	127.5	C1'	140.5	C3'C5'	124.2

IR Spectrum: cm^{-1}

3433 (m)	3245 (m)	3117 (w)	1675 (s)	1601 (s)	1513 (s)
1396 (m)	1351 (s)	1313 (s)	1246 (s)	1181 (s)	1081 (m)
1027 (s)	858 (m)	827 (w)	714 (s)	699 (s)	621 (s)

UV Spectrum (phosphate buffer pH 6.5), λ_{max}: nm

247

2-(4-Aminobenzamido)-5-methylbenzenesulfonate sodium salt (18b)

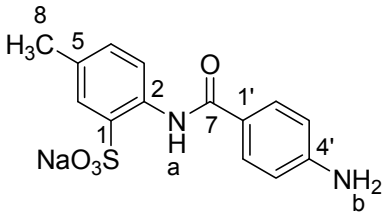

$C_{14}H_{13}N_2NaO_4S$ (328.3)

40 mg 10 % Pd/C were added to a solution of 1.77 g (4.94 mmol) compound 18a in a mixture of 100 ml water and 50 ml methanol. The mixture was hydrogenated overnight, according to the general procedure 2.

Yield: white powder, 1.54 g (94.8 %)
Purity: 99.0 % (HPLC: t_R = 6.44 min, system 1)
TLC: Rf = 0.67 (Isopr + NH_3 = 5 + 2)
NaCl: 26.33 %
Water: 2 mol/mol
CHN analysis:

	% C	% H	% N	C/N
Calcd	51.22	3.99	8.53	6.00
Calcd (with NaCl/H_2O)	34.00	3.46	5.66	6.00
Found	33.62	3.06	5.68	5.99

500 MHz ^{1}H NMR Spectrum (DMSO-d_6): δ/ppm

ABX-System

8.37 d (H3; B)
7.50 d (H6; X)
7.12 dd (H4; A)
$^3J_{AB}$ = 8.5 Hz $^3J_{BA}$ = 8.5 Hz
$^4J_{AX}$ = 2.0 Hz $^4J_{XA}$ = 2.0 Hz

AA'BB'-System

7.62 m (H2'H6'; BB')
6.61 d (H3'H5'; AA')
$^3J_{AB}$ = 8.8 Hz $^3J_{A'B'}$ = 8.8 Hz

-CONH- 10.98 s (1H, exchangeable)
-NH_2 5.75 s (2H, exchangeable)
-CH_3 2.26 s (3H)

125 MHz ^{13}C NMR Spectrum (DMSO-d_6): δ/ppm

C1	134.9	C4	130.6	C7	20.5	C4'	152.4
C2	130.1	C5	133.6	C8	164.2	C2'C6'	128.8
C3	119.5	C6	127.4	C1'	121.4	C3'C5'	113.0

IR Spectrum: cm^{-1}

3408 (m)	3334 (m)	1661 (m)	1601 (s)	1538 (s)	1515 (s)
1397 (m)	1313 (s)	1264 (m)	1213 (s)	1173 (s)	1120 (m)
1082 (m)	1022 (m)	822 (m)	703 (m)	619 (m)	

UV Spectrum (phosphate buffer pH 6.5), λ_{max}: nm

307.5

2,2'-(Carbonylbis(imino-4,1-phenylenecarbonylimino))bis-(5-methylbenzenesulfonic acid) disodium salt (18c)

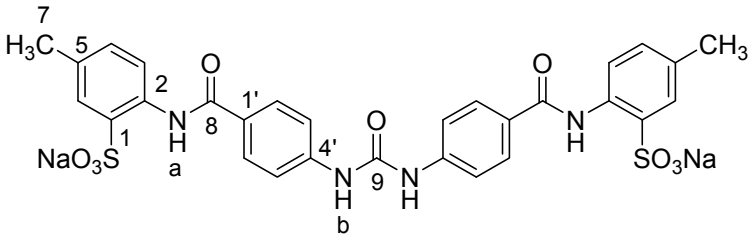

$C_{29}H_{24}N_4Na_2O_9S_2$ (682.6)

To a solution of 0.59 g (1.8 mmol) amine 18b in 70 ml water, 4 ml (8 mmol) 20 % phosgene solution in toluene were slowly added under a constant pH of 5.5. The synthesis was performed according to the general procedure 3. The crude product was stirred in 30 ml methanol, filtrated and dried.

Yield: white powder, 0.55 g (90.0 %)
Purity: 97.7 % (HPLC: t_R = 7.07 min, system 1)
TLC: Rf = 0.77 (Isopr + NH_3 = 5 + 2)
NaCl: < 1 %
Water: 3 mol/mol
CHN analysis:

	% C	% H	% N	C/N
Calcd	51.02	3.54	8.21	6.22
Calcd (with NaCl/ H_2O)	46.81	4.06	7.53	6.22
Found	46.92	4.11	7.64	6.14

500 MHz ^{1}H NMR Spectrum (DMSO-d_6): δ/ppm

ABX-System

8.38 d (H3; B)
7.54 d (H6; X)
7.17 dd (H4; A)
$^3J_{AB}$ = 8.3 Hz $^3J_{BA}$ = 8.3 Hz
$^4J_{AX}$ = 1.9 Hz $^4J_{XA}$ = 1.9 Hz

AA'BB'-System

7.88 d (H3'H5'; BB')

	7.64	d (H2'H6'; AA') $^3J_{AB}$ = 8.8 Hz $^3J_{A'B'}$ = 8.8 Hz
-CONH-	11.26	s (2H, exchangeable)
-NHCONH-	9.21	s (2H, exchangeable)
$-CH_3$	2.29	s (6H)

125 MHz ^{13}C NMR Spectrum (DMSO-d_6): δ/ppm

C1	135.6	C5	133.4	C9	152.5	C2'C6'	128.5
C2	130.5	C6	128.5	C1'	127.7	C3'C5'	118.2
C3	120.0	C7	20.9	C4'	143.2		
C4	131.7	C8	163.9				

IR Spectrum: cm^{-1}

3350 (s, br)	1704 (m)	1670 (m)	1594 (s)	1529 (s)	1507 (s)
1397 (m)	1313 (s)	1239 (s)	1212 (s)	1183 (s)	1086 (m)
1027 (m)	903 (w)	760 (w)	703 (m)	625 (m)	

UV Spectrum (phosphate buffer pH 6.5), λ_{max}: nm

308.5

ESI-MS positive mode (calcd/found): m/z

705.1/705.4 $[M+Na]^+$, 1387.2/1387.1 $[2M+Na]^+$

ESI-MS negative mode (calcd/found): m/z

659.4/659.4 $[M-Na]^-$

11 Abbreviations

ADP	Adenosine 5′-diphosphate
ADP-β-S	Adenosine 5′-O-(2-thio-diphosphate)
ATP	Adenosine 5′-triphosphate
C/N	ratio of % carbon to % nitrogen
Calcd	calculated
Conc.	Concentrated
Cpd	compound
d	doublet
dd	doublet of doublet
ddd	doublet of doublet of doublet
dist.	distilled
DMSO	Dimethyl sulfoxide
DMSO-d_6	Deuterated dimethyl sulfoxide
ESI	Electron spray ionization
H-H COSY	H-H Correlation Spectroscopy
HMBC	Heteronuclear multiple bond correlations
HPLC	High performance liquid chromatography
HSQC	Heteronuclear single quantum correlation
Hz	Hertz
IP_3	inositol trisphosphate
IR	Infrared
Isopr	Isopropanol
J	coupling constant
M	Molar
MALDI	Matrix-associated laser desorption ionization
MeOH	Methanol
2-MeSADP	2-Methylthioadenosine 5′-diphosphate
m	multiplet
MS	Mass Spectrometry
nm	nanometer
nM	nanomolar
NMR	Nuclear magnetic resonance

Pd/C	Palladium/Carbon
ppm	Part per million
pt	pseudotriplet
Rf	retention factor
RT	room temperature
s	singlet
sec.	second
t	triplet
t_R	Retention time
tt	triplet of triplet
TLC	Thin layer chromatography
TOF	Time-of-flight
UTP	Uridine 5-triphosphate
UV	Ultraviolet

12 References

(1) Jacobson KA, Jarvis MF, Williams M. Purine and pyrimidine (P2) receptors as drug targets. J Med Chem 2002; 45(19):4057-4093.

(2) Burnstock G. Purinergic signalling. Br J Pharmacol 2006; 147 Suppl 1:S172-S181.

(3) Fredholm BB, Abbracchio MP, Burnstock G, Daly JW, Harden TK, Jacobson KA et al. Nomenclature and classification of purinoceptors. Pharmacol Rev 1994; 46(2):143-156.

(4) Ralevic V, Burnstock G. Receptors for purines and pyrimidines. Pharmacol Rev 1998; 50(3):413-492.

(5) Khakh BS, Burnstock G, Kennedy C, King BF, North RA, Seguela P et al. International union of pharmacology. XXIV. Current status of the nomenclature and properties of P2X receptors and their subunits. Pharmacol Rev 2001; 53(1):107-118.

(6) Roberts JA, Vial C, Digby HR, Agboh KC, Wen H, Atterbury-Thomas A et al. Molecular properties of P2X receptors. Pflugers Arch 2006; 452(5):486-500.

(7) Vial C, Roberts JA, Evans RJ. Molecular properties of ATP-gated P2X receptor ion channels. Trends Pharmacol Sci 2004; 25(9):487-493.

(8) Migita K, Haines WR, Voigt MM, Egan TM. Polar residues of the second transmembrane domain influence cation permeability of the ATP-gated P2X(2) receptor. J Biol Chem 2001; 276(33):30934-30941.

(9) Chizh BA, Illes P. P2X receptors and nociception. Pharmacol Rev 2001; 53(4):553-568.

(10) Guo C, Masin M, Qureshi OS, Murrell-Lagnado RD. Evidence for functional P2X4/P2X7 heteromeric receptors. Mol Pharmacol 2007; 72(6):1447-1456.

(11) Shen JB, Shutt R, Pappano A, Liang BT. Characterization and mechanism of P2X receptor-mediated increase in cardiac myocyte contractility. Am J Physiol Heart Circ Physiol 2007; 293(5):H3056-H3062.

(12) Abbracchio MP, Burnstock G, Boeynaems JM, Barnard EA, Boyer JL, Kennedy C et al. International Union of Pharmacology LVIII: update on the P2Y G protein-coupled nucleotide receptors: from molecular mechanisms and pathophysiology to therapy. Pharmacol Rev 2006; 58(3):281-341.

(13) Abbracchio MP, Burnstock G, Boeynaems JM, Barnard EA, Boyer JL, Kennedy C et al. The recently deorphanized GPR80 (GPR99) proposed to be the P2Y15 receptor is not a genuine P2Y receptor. Trends Pharmacol Sci 2005; 26(1):8-9.

(14) Fumagalli M, Trincavelli L, Lecca D, Martini C, Ciana P, Abbracchio MP. Cloning, pharmacological characterisation and distribution of the rat G-protein-coupled P2Y(13) receptor. Biochem Pharmacol 2004; 68(1):113-124.

(15) Abbracchio MP, Boeynaems JM, Barnard EA, Boyer JL, Kennedy C, Miras-Portugal MT et al. Characterization of the UDP-glucose receptor (re-named here the P2Y14 receptor) adds diversity to the P2Y receptor family. Trends Pharmacol Sci 2003; 24(2):52-55.

(16) von Kugelgen I. Pharmacological profiles of cloned mammalian P2Y-receptor subtypes. Pharmacol Ther 2006; 110(3):415-432.

(17) Gachet C. Regulation of platelet functions by P2 receptors. Annu Rev Pharmacol Toxicol 2006; 46:277-300.

(18) Kahner BN, Shankar H, Murugappan S, Prasad GL, Kunapuli SP. Nucleotide receptor signaling in platelets. J Thromb Haemost 2006; 4(11):2317-2326.

(19) Müller CE. P2-pyrimidinergic receptors and their ligands. Curr Pharm Des 2002; 8(26):2353-2369.

(20) Fields RD, Burnstock G. Purinergic signalling in neuron-glia interactions. Nat Rev Neurosci 2006; 7(6):423-436.

(21) Michelson AD. P2Y12 antagonism: promises and challenges. Arterioscler Thromb Vasc Biol 2008; 28(3):s33-s38.

(22) Sugidachi A, Asai F, Yoneda K, Iwamura R, Ogawa T, Otsuguro K et al. Antiplatelet action of R-99224, an active metabolite of a novel thienopyridine-type G(i)-linked P2T antagonist, CS-747. Br J Pharmacol 2001; 132(1):47-54.

(23) Asai F, Jakubowski JA, Naganuma H, Brandt JT, Matsushima N, Hirota T et al. Platelet inhibitory activity and pharmacokinetics of prasugrel (CS-747) a novel thienopyridine P2Y12 inhibitor: a single ascending dose study in healthy humans. Platelets 2006; 17(4):209-217.

(24) Hasegawa M, Sugidachi A, Ogawa T, Isobe T, Jakubowski JA, Asai F. Stereoselective inhibition of human platelet aggregation by R-138727, the active metabolite of CS-747 (prasugrel, LY640315), a novel P2Y12 receptor inhibitor. Thromb Haemost 2005; 94(3):593-598.

(25) Springthorpe B, Bailey A, Barton P, Birkinshaw TN, Bonnert RV, Brown RC et al. From ATP to AZD6140: the discovery of an orally active reversible P2Y12 receptor antagonist for the prevention of thrombosis. Bioorg Med Chem Lett 2007; 17(21):6013-6018.

(26) Storey RF, Husted S, Harrington RA, Heptinstall S, Wilcox RG, Peters G et al. Inhibition of platelet aggregation by AZD6140, a reversible oral

P2Y12 receptor antagonist, compared with clopidogrel in patients with acute coronary syndromes. J Am Coll Cardiol 2007; 50(19):1852-1856.

(27) Cannon CP, Husted S, Harrington RA, Scirica BM, Emanuelsson H, Peters G et al. Safety, tolerability and initial efficacy of AZD6140, the first reversible oral adenosine diphosphate receptor antagonist, compared with clopidogrel, in patients with non-ST-segment elevation acute coronary syndrome: primary results of the DISPERSE-2 trial. J Am Coll Cardiol 2007; 50(19):1844-1851.

(28) Deterding R, Retsch-Bogart G, Milgram L, Gibson R, Daines C, Zeitlin PL et al. Safety and tolerability of denufosol tetrasodium inhalation solution, a novel P2Y2 receptor agonist: results of a phase 1/phase 2 multicenter study in mild to moderate cystic fibrosis. Pediatr Pulmonol 2005; 39(4):339-348.

(29) Tauber J, Davitt WF, Bokosky JE, Nichols KK, Yerxa BR, Schaberg AE et al. Double-masked, placebo-controlled safety and efficacy trial of diquafosol tetrasodium (INS365) ophthalmic solution for the treatment of dry eye. Cornea 2004; 23(8):784-792.

(30) Yerxa BR, Sabater JR, Davis CW, Stutts MJ, Lang-Furr M, Picher M et al. Pharmacology of INS37217 [P(1)-(uridine 5')-P(4)- (2'-deoxycytidine 5')tetraphosphate, tetrasodium salt], a next-generation P2Y(2) receptor agonist for the treatment of cystic fibrosis. J Pharmacol Exp Ther 2002; 302(3):871-880.

(31) Suh BC, Kim TD, Lee IS, Kim KT. Differential regulation of P2Y(11) receptor-mediated signalling to phospholipase C and adenylyl cyclase by protein kinase C in HL-60 promyelocytes. Br J Pharmacol 2000; 131(3):489-497.

(32) Communi D, Robaye B, Boeynaems JM. Pharmacological characterization of the human P2Y11 receptor. Br J Pharmacol 1999; 128(6):1199-1206.

(33) Berchtold S, Ogilvie AL, Bogdan C, Muhl-Zurbes P, Ogilvie A, Schuler G et al. Human monocyte derived dendritic cells express functional P2X and P2Y receptors as well as ecto-nucleotidases. FEBS Lett 1999; 458(3):424-428.

(34) Swennen EL, Bast A, Dagnelie PC. Purinergic receptors involved in the immunomodulatory effects of ATP in human blood. Biochem Biophys Res Commun 2006; 348(3):1194-1199.

(35) Wilkin F, Duhant X, Bruyns C, Suarez-Huerta N, Boeynaems JM, Robaye B. The P2Y11 receptor mediates the ATP-induced maturation of human monocyte-derived dendritic cells. J Immunol 2001; 166(12):7172-7177.

(36) Schnurr M, Toy T, Stoitzner P, Cameron P, Shin A, Beecroft T et al. ATP gradients inhibit the migratory capacity of specific human dendritic cell

types: implications for P2Y11 receptor signaling. Blood 2003; 102(2):613-620.

(37) Balogh J, Wihlborg AK, Isackson H, Joshi BV, Jacobson KA, Arner A et al. Phospholipase C and cAMP-dependent positive inotropic effects of ATP in mouse cardiomyocytes via P2Y11-like receptors. J Mol Cell Cardiol 2005; 39(2):223-230.

(38) Amisten S, Melander O, Wihlborg AK, Berglund G, Erlinge D. Increased risk of acute myocardial infarction and elevated levels of C-reactive protein in carriers of the Thr-87 variant of the ATP receptor P2Y11. Eur Heart J 2007; 28(1):13-18.

(39) Vaughan KR, Stokes L, Prince LR, Marriott HM, Meis S, Kassack MU et al. Inhibition of neutrophil apoptosis by ATP is mediated by the P2Y11 receptor. J Immunol 2007; 179(12):8544-8553.

(40) Moreschi I, Bruzzone S, Nicholas RA, Fruscione F, Sturla L, Benvenuto F et al. Extracellular NAD+ is an agonist of the human P2Y11 purinergic receptor in human granulocytes. J Biol Chem 2006; 281(42):31419-31429.

(41) Moreschi I, Bruzzone S, Bodrato N, Usai C, Guida L, Nicholas RA et al. NAADP(+) is an agonist of the human P2Y(11) purinergic receptor. Cell Calcium 2007.

(42) Greve H, Meis S, Kassack MU, Kehraus S, Krick A, Wright AD et al. New iantherans from the marine sponge Ianthella quadrangulata: novel agonists of the P2Y(11) receptor. J Med Chem 2007; 50(23):5600-5607.

(43) Glanzel M, Bultmann R, Starke K, Frahm AW. Structure-activity relationships of novel P2-receptor antagonists structurally related to Reactive Blue 2. Eur J Med Chem 2005; 40(12):1262-1276.

(44) Tuluc F, Bultmann R, Glanzel M, Frahm AW, Starke K. P2-receptor antagonists: IV. Blockade of P2-receptor subtypes and ecto-nucleotidases by compounds related to reactive blue 2. Naunyn Schmiedebergs Arch Pharmacol 1998; 357(2):111-120.

(45) Phillips MA, Stanley SL, Jr. Chemotherapy of parasitic infections. In: Brunton LL, Lazo JS, Parker KL, editors. Goodman & Gilman's The Pharmacological Basis of Therapeutics. McGraw-Hill, 2006: 1067-1069.

(46) Oesterle R, Jurkiewicz E, Luke W, Nickel P, Hunsmann G, Jentsch KD. Chemical modifications of aminonaphthalenesulfonic acid derivatives increase effectivity and specificity of reverse transcriptase inhibition and change mode of action of reverse transcriptase and DNA polymerase alpha inhibition. Antiviral Res 1993; 22(2-3):107-119.

(47) Jentsch KD, Hunsmann G, Hartmann H, Nickel P. Inhibition of human immunodeficiency virus type I reverse transcriptase by suramin-related compounds. J Gen Virol 1987; 68 (Pt 8):2183-2192.

(48) Firsching-Hauck A, Nickel P, Yahya C, Wandt C, Kulik R, Simon N et al. Angiostatic effects of suramin analogs in vitro. Anticancer Drugs 2000; 11(2):69-77.

(49) Kreimeyer A, Muller G, Kassack M, Nickel P, Gagliardi AR. Suramin analogues with a 2-phenylbenzimidazole moiety as partial structure; potential anti HIV- and angiostatic drugs, 2: Sulfanilic acid-, benzenedisulfonic acid- and naphthalenetrisulfonic acid analogues. Arch Pharm (Weinheim) 1998; 331(3):97-103.

(50) Nickel P, Haack HJ, Widjaja H, Ardanuy U, Gurgel C, Duwel D et al. [Potential filaricides. Suramin analogs]. Arzneimittelforschung 1986; 36(8):1153-1157.

(51) Dhar S, Gullbo J, Csoka K, Eriksson E, Nilsson K, Nickel P et al. Antitumour activity of suramin analogues in human tumour cell lines and primary cultures of tumour cells from patients. Eur J Cancer 2000; 36(6):803-809.

(52) Gagliardi AR, Kassack M, Kreimeyer A, Muller G, Nickel P, Collins DC. Antiangiogenic and antiproliferative activity of suramin analogues. Cancer Chemother Pharmacol 1998; 41(2):117-124.

(53) Junker M. Synthese von suraminanalogen Verbindungen mit Methoxynaphthalinsulfonsäure-Teilstruktur - Potentielle Virustatika und Zytostatika. Dissertation. Rheinische Friedrich-Wilhelms-Universität Bonn, 1999.

(54) Müller G. Synthese von Suramin-analogen Verbindungen - Variationen der Struktur von NF279, einem hochselektiven P2-Rezeptor Antagonisten. Dissertation. Rheinische Friedrich-Wilhelms-Universität Bonn, 1999.

(55) Wehner K. Synthese von suraminanalogen Verbindungen mit N-Methylbenzimidazol als Teilstuktur und von nicht sulfonierten Suramin-Analogen - Potentielle Virustatika und Zytostatika sowie GRK2-Inhibitioren. Dissertation. Rheinische Friedrich-Wilhelms-Universität Bonn, 2001.

(56) Haack H-J. Synthese von Suraminanalogen mit potentieller Wirksamkeit gegen Onchocercose, Variation der Methylgruppen. Freie Universität Berlin, 1984.

(57) Böing B. Synthese von Methylen-Homologen und Methylen-Analogen des Suramins Potentielle Hemmstoffe von HIV-Viren. Dissertation. Rheinische Friedrich-Wilhelms-Universität Bonn, 1990.

(58) Dunn PM, Blakeley AG. Suramin: a reversible P2-purinoceptor antagonist in the mouse vas deferens. Br J Pharmacol 1988; 93(2):243-245.

(59) Lambrecht G, Braun K, Damer M, Ganso M, Hildebrandt C, Ullmann H et al. Structure-activity relationships of suramin and pyridoxal-5'-phosphate

derivatives as P2 receptor antagonists. Curr Pharm Des 2002; 8(26):2371-2399.

(60) Rettinger J, Schmalzing G, Damer S, Muller G, Nickel P, Lambrecht G. The suramin analogue NF279 is a novel and potent antagonist selective for the P2X(1) receptor. Neuropharmacology 2000; 39(11):2044-2053.

(61) Klapperstuck M, Buttner C, Nickel P, Schmalzing G, Lambrecht G, Markwardt F. Antagonism by the suramin analogue NF279 on human P2X(1) and P2X(7) receptors. Eur J Pharmacol 2000; 387(3):245-252.

(62) Damer S, Niebel B, Czeche S, Nickel P, Ardanuy U, Schmalzing G et al. NF279: a novel potent and selective antagonist of P2X receptor-mediated responses. Eur J Pharmacol 1998; 350(1):R5-R6.

(63) Hulsmann M, Nickel P, Kassack M, Schmalzing G, Lambrecht G, Markwardt F. NF449, a novel picomolar potency antagonist at human P2X1 receptors. Eur J Pharmacol 2003; 470(1-2):1-7.

(64) Hausmann R, Rettinger J, Gerevich Z, Meis S, Kassack MU, Illes P et al. The suramin analog 4,4',4'',4'''-(carbonylbis(imino-5,1,3-benzenetriylbis (carbonylimino)))tetra-kis-benzenesulfonic acid (NF110) potently blocks P2X3 receptors: subtype selectivity is determined by location of sulfonic acid groups. Mol Pharmacol 2006; 69(6):2058-2067.

(65) Ullmann H, Meis S, Hongwiset D, Marzian C, Wiese M, Nickel P et al. Synthesis and structure-activity relationships of suramin-derived P2Y11 receptor antagonists with nanomolar potency. J Med Chem 2005; 48(22):7040-7048.

(66) Meis S, Hongwiset D, Kassack MU. Discovery of new potent, non-nucleotide ligands at human P2Y11-receptors results in NF546, the first non-nucleotide P2Y receptor agonist, and NF340, the so far most potnet and selective P2Y11 antagonist. Purinergic Signalling 2006; 2(2):177.

(67) Qi AD, Zambon AC, Insel PA, Nicholas RA. An arginine/glutamine difference at the juxtaposition of transmembrane domain 6 and the third extracellular loop contributes to the markedly different nucleotide selectivities of human and canine P2Y11 receptors. Mol Pharmacol 2001; 60(6):1375-1382.

(68) Torres B, Zambon AC, Insel PA. P2Y11 receptors activate adenylyl cyclase and contribute to nucleotide-promoted cAMP formation in MDCK-D(1) cells. A mechanism for nucleotide-mediated autocrine-paracrine regulation. J Biol Chem 2002; 277(10):7761-7765.

(69) Qi AD, Kennedy C, Harden TK, Nicholas RA. Differential coupling of the human P2Y(11) receptor to phospholipase C and adenylyl cyclase. Br J Pharmacol 2001; 132(1):318-326.

(70) Lee H, Jun DJ, Suh BC, Choi BH, Lee JH, Do MS et al. Dual roles of P2 purinergic receptors in insulin-stimulated leptin production and lipolysis in

differentiated rat white adipocytes. J Biol Chem 2005; 280(31):28556-28563.

(71) Kassack MU. Quantitative comparison of functional screening by measuring intracellular Ca2+ with radioligand binding at recombinant human dopamine receptors. AAPS PharmSci 2002; 4(4):E31.

(72) Kassack MU, Hofgen B, Lehmann J, Eckstein N, Quillan JM, Sadee W. Functional screening of G protein-coupled receptors by measuring intracellular calcium with a fluorescence microplate reader. J Biomol Screen 2002; 7(3):233-246.

(73) Gurgel C. Labor Journal N30. 1983. [Unpublished Work]

(74) Farbenfabriken Bayer AG. 1-Nitronaphthalene-3,6-(or 3,7-)disulfonic acid. Patent GB 801870. 1958 1958.

(75) Friebolin H. Basic One- and Two-dimensional NMR Spectroscopy. 4 ed. Weinheim: Wiley-VCH Verlag GmbH, 2005.

(76) Hesse M, Meier H, Zeeh B. Spektroskopische Methoden in der Organischen Chemie. 7 ed. Stuttgart: Thieme, 2005.

(77) Brückner R. Reaktionsmechanismen. 3 ed. Barcelona: Elsevier GmbH, 2004.

(78) Petersen U. Offenkettige Organoharnstoffe aus Phosgen mit Aminen bzw. Iminen, Methoden der Organischen Chemie. 4 ed. Stuttgart: Georg Thieme Verlag, 1983.

(79) Meis S. Molekulare und funktionelle Charakterisierung des P2Y11-Rezeptoren sowie die Pharmakologische Evaluierung neuer Agonisten und Antagonisten. Dissertation. Heinrich-Heine-Universität Düsseldorf. 2008.

(80) Petersen U. Offenkettige Organoharnstoffe aus Alkalimetallcyanaten, Methoden der Organischen Chemie. 4 ed. Stuttgart: Georg Thieme Verlag, 1983.

(81) Furniss BS, Hannaford NJ, Smith PWG, Tatchell AR. Vogel's Textbook of Practical Organic Chemistry. 5 ed. The Bath Press, 1991.

(82) Walid F, Pazdera P. The synthesis of new *N*3-aryl-*N*1-(2-phenylquinazolin-4-yl)thioureas. ARKIVOC 2002; (i):7-11.

(83) Breitmaier E, Voelter W. 13C NMR Spectroscopy of Organic Compounds. Carbon-13 NMR Spectroscopy. Weinheim: VCH, 1987: 233-235.

(84) Bruzuad S, Mingotaud A-F, Soum A. Multinucleus NMR characterization of new silylamines and their corresponding lithium silylamides. Journal of Organometallic Chemisty 1998; 561:77-84.

(85) Ozaki S. Recent Advances in Isocynate Chemistry. Chemical Reviews 1972; 72(5):457-496.

(86) Majer P, Randad RS. A Safe and Efficient Method for Preparation of N,N'-Unsymmetrically Disubstituted Ureas Utilizing Triphosgene. J Org Chem 1994; 59:1937-1938.

(87) Norwick JS, Powell NA, Nguyen TM, Noronha G. An Improved Method for the Synthesis of Enantiomerically Pure Amino Acid Ester Isocyanates. J Org Chem 1992; 57:7364-7366.

(88) Cotarca L, Delogu P, Nardelli A, Sunjic V. Bis(trichloromethyl) Carbonate in Organic Synthesis. Synthesis 1996;(05):553-576.

(89) Pasquato L, Modena G, Cotarca L, Delogu P, Mantovani S. Conversion of bis(trichloromethyl) carbonate to phosgene and reactivity of triphosgene, diphosgene, and phosgene with methanol(1). J Org Chem 2000; 65(24):8224-8228.

(90) Igarashi Y, Yanagisawa E, Ohshima T, Takeda S, Aburada M, Miyamoto K. Synthesis and evaluation of carbamate prodrugs of a phenolic compound. Chem Pharm Bull 2007; 55(2):328-333.

(91) Janin YL, Croisy A, Riou JF, Bisagni E. Synthesis and evaluation of new 6-amino-substituted benzo[c]phenanthridine derivatives. J Med Chem 1993; 36(23):3686-3692.

(92) Lemoucheux L, Rouden J, Ibazizene M, Sobrio F, Lasne MC. Debenzylation of tertiary amines using phosgene or triphosgene: an efficient and rapid procedure for the preparation of carbamoyl chlorides and unsymmetrical ureas. Application in carbon-11 chemistry. J Org Chem 2003; 68(19):7289-7297.

(93) Nichols AC, Yielding KL. Anticonvulsant activity of 4-urea-5,7-dichlorokynurenic acid derivatives that are antagonists at the NMDA-associated glycine binding site. Mol Chem Neuropathol 1998; 35(1-3):1-12.

(94) Zhang D, Xing X, Cuny GD. Synthesis of hydantoins from enantiomerically pure alpha-amino amides without epimerization. J Org Chem 2006; 71(4):1750-1753.

(95) Boileau S, Bouteiller L, Laupretre F, Lortie F. Soluble supramolecular polymers based on urea compounds. New J Chem 2000; 24:845-848.

(96) Petersen U. b) Isocynate, Methoden der Organischen Chemie. 4 ed. Stuttgart: Georg Thieme Verlag, 1983.

(97) Niebauer RT, Gao ZG, Li B, Wess J, Jacobson KA. Signaling of the Human P2Y(1) Receptor Measured by a Yeast Growth Assay with Comparisons to Assays of Phospholipase C and Calcium Mobilization in 1321N1 Human Astrocytoma Cells. Purinergic Signal 2005; 1(3):241-247.

(98) Zylberg J, Ecke D, Fischer B, Reiser G. Structure and ligand-binding site characteristics of the human P2Y11 nucleotide receptor deduced from computational modelling and mutational analysis. Biochem J 2007; 405(2):277-286.

(99) Meis S. NF156. 2008. [Unpublished Work]

(100) Bultmann R, Wittenburg H, Pause B, Kurz G, Nickel P, Starke K. P2-purinoceptor antagonists: III. Blockade of P2-purinoceptor subtypes and ecto-nucleotidases by compounds related to suramin. Naunyn Schmiedebergs Arch Pharmacol 1996; 354(4):498-504.

(101) Kassack MU, Braun K, Ganso M, Ullmann H, Nickel P, Boing B et al. Structure-activity relationships of analogues of NF449 confirm NF449 as the most potent and selective known P2X1 receptor antagonist. Eur J Med Chem 2004; 39(4):345-357.

(102) Calderone V, Baragatti B, Breschi MC, Martinotti E. Experimental and theoretical comparisons between the classical Schild analysis and a new alternative method to evaluate the pA2 of competitive antagonists. Naunyn Schmiedebergs Arch Pharmacol 1999; 360(5):477-487.

(103) Cheng HC. The influence of cooperativity on the determination of dissociation constants: examination of the Cheng-Prusoff equation, the Scatchard analysis, the Schild analysis and related power equations. Pharmacol Res 2004; 50(1):21-40.

(104) Arunlakshana O, Schild HO. Some quantitative uses of drug antagonists. Br J Pharmacol Chemother 1959; 14(1):48-58.

(105) Poch G, Brunner F, Kuhberger E. Construction of antagonist dose-response curves for estimation of pA2-values by Schild-plot analysis and detection of allosteric interactions. Br J Pharmacol 1992; 106(3):710-716.

(106) Lew MJ, Angus JA. Analysis of competitive agonist-antagonist interactions by nonlinear regression. Trends Pharmacol Sci 1995; 16(10):328-337.

(107) Gross.J.H. Mass Spectrometry. Heidelberg: Springer-Verlag, 2004.

(108) Patel K, Barnes A, Camacho J, Paterson C, Boughtflower R, Cousens D et al. Activity of diadenosine polyphosphates at P2Y receptors stably expressed in 1321N1 cells. Eur J Pharmacol 2001; 430(2-3):203-210.

(109) Cheng Y, Prusoff WH. Relationship between the inhibition constant (K_i) and the concentration of inhibitor which causes 50 per cent inhibition (IC_{50}) of an enzymatic reaction. Biochem Pharmacol 1973; 22(23):3099-3108.

(110) Lazareno S, Birdsall NJ. Estimation of competitive antagonist affinity from functional inhibition curves using the Gaddum, Schild and Cheng-Prusoff equations. Br J Pharmacol 1993; 109(4):1110-1119.

(111) Neubig RR, Spedding M, Kenakin T, Christopoulos A. International Union of Pharmacology Committee on Receptor Nomenclature and Drug Classification. XXXVIII. Update on terms and symbols in quantitative pharmacology. Pharmacol Rev 2003; 55(4):597-606.

13 Publications

Publications

Ullmann H, Meis S, Hongwiset D, Marzian C, Wiese M, Nickel P, Communi D, Boeynaems JM, and Kassack MU. Synthesis and structure-activity relationships of suramin-derived P2Y11 receptor antagonists with nanomolar potency. *J Med Chem*. 2005; 8(22):7040-8.

Trapp J, Meier R, Hongwiset D, Kassack MU, Sippl W, Jung M. Structure activity studies on suramin analogues as inhibitors of NAD+-dependent histone diacetylases (sirtuins). *ChemMedChem*. 2007; 2(10):1419-31.

Meis S, Hongwiset D, Bles N, Communi D, Boeynaems JM, and Kassack MU. Characterisation of a novel, selective non-nucleotide agonist and antagonist at human $P2Y_{11}$-receptors in recombinant and dendritic cells, in preparation.

Patent

Patent WO200817586/DE102006037920; Special carbonyl-bis imino compounds for treating immune diseases; Kassack MU; Meis S, Hongwiset D (14.02.2008)

Oral presentation

Hongwiset D, Meis S, Kassack MU. Synthesis and biological activity of asymmetric NF157-derivatives at $P2Y_{11}$-receptors. First Joint Italian-German Purine Club Meeting, Chieti, Italy, Sep, 2005

Posters

Meis S, Hongwiset D and Kassack MU. Functional comparison of different $P2Y_{11}$-Receptor variants. Minisymposium des GRK677, Bonn, 2006

Meis S, Hongwiset D and Kassack MU. Discovery of new potent, nucleotide ligands at human $P2Y_{11}$-receptors results in NF546, the first non-nuclotide P2Y receptor agonist, and NF340, the so far most potent and selective P2Y11 antagonist, 8^{th} International Adenosine and Adenine Nucleotides Symposium, Ferrara, Italy, 2006 (Abstract was published in Purinergic Signal, 2006, 2, 177)

Meis S, Hongwiset D and Kassack MU. An allosteric mechanism at $P2Y_{11}$-receptor? Internationales Symposium des GRK677, Bonn, Germany, 2006.

Damayanti S., Hongwiset D. and Kassack M.U. G protein-coupled receptors: new ligands at $P2Y_{11}$ receptors-synthesis and biological testing. Second Joint Italian-German Purine Club Meeting, Leipzig, Germany, 2007.

14 Appendix

Appendix A1 % Response and inhibition by 100 μM naphthalene derivatives of agonist induced calcium mobilization at P2Y receptors recombinantly expressed in 1321N1 astrocytoma cells. Structures (Str.) are shown in Appendix B.

Compound	Str.	$P2Y_1$		$P2Y_2$		$P2Y_4$		$P2Y_{11}$	
		% response	% inhibition	% response	% inhibition	% response	% inhibition	% response	% inhibition
4a (MK083)	B1	0 ± 23.6	27.2 ± 10.9	11.8 ± 15.7	22.7 ± 8.5	0 ± 8.9	18.6 ± 4.9	0 ± 9.1	10.8 ± 5.0
4b (MK084)	B1	0 ± 5.4	0 ± 20.6	0 ± 9.1	23.7 ± 19.9	7.2 ± 5.0	0 ± 10.1	2.9 ± 7.8	9.5 ± 5.3
4c (MK085)	B1	0 ± 32.1	0 ± 2.1	13.9 ± 17.1	21.9 ± 5.4	24.5 ± 5.2	12.5 ± 7.0	2.3 ± 7.6	92.6 ± 9.4
6a (MK089)	B1	6.4 ± 17.1	0 ± 6.7	0 ± 18.2	3.5 ± 16.7	6.2 ± 6.9	0 ± 9.2	5.3 ± 8.2	1.5 ± 8.2
6b (MK090)	B1	0 ± 24.0	0 ± 11.1	0 ± 17.9	28.4 ± 10.6	11.4 ± 5.7	31.6 ± 9.9	5.3 ± 10.3	18.7 ± 13.0
6c (MK091)	B1	0 ± 33.1	32.4 ± 11.7	0 ± 13.6	19.7 ± 6.5	11.3 ± 8.1	8.8 ± 11.6	0 ± 13.9	35.5 ± 3.0
5a (MK086)	B1	20.7 ± 8.6	3.8 ± 17.2	0 ± 8.01	12.2 ± 8.9	0 ± 19.7	7.3 ± 9.5	15.3 ± 10.9	22.4 ± 6.7
5b (MK087)	B1	4.4 ± 14.2	14.6 ± 12.5	0 ± 39.6	15.6 ± 19.5	0 ± 10.7	33.7 ± 6.7	0 ± 3.9	19.5 ± 3.2
5c (MK088)	B1	37.8 ± 67.3	25.1 ± 28.3	0 ± 14.1	16.0 ± 12.0	6.2 ± 9.2	13.3 ± 7.2	0 ± 5.7	95.7 ± 29.1
MK095	B2	0 ± 9.1	44.8 ± 4.1	1.1 ± 10.7	9.9 ± 10.3	8.9 ± 7.9	10.6 ± 13.9	7.9 ± 2.4	12.4 ± 3.4
MK096	B2	24.1 ± 41.5	24.0 ± 9.2	0 ± 10.1	20.8 ± 1.7	14.6 ± 15.7	18.4 ± 14.3	6.5 ± 5.2	25.1 ± 20.7
NF290	B3	0 ± 4.7	18.0 ± 3.4	0 ± 17.0	0 ± 26.2	13.8 ± 7.9	18.0 ± 3.4	23.2 ± 7.1	100 ± 6.8
2a (MK063)	B2	0 ± 4.6	29.3 ± 40.2	3.1 ± 17.3	9.4 ± 7.5	0 ± 6.8	21.3 ± 4.7	20.9 ± 7.0	88.4 ± 1.9
2b (MK064)	B2	0 ± 17.4	17.4 ± 6.7	9.9 ± 15.7	8.1 ± 7.2	0.3 ± 5.0	15.1 ± 3.0	25.4 ± 9.9	97.9 ± 2.9
2c (NF340)	B2	0 ± 0.61	14.5 ± 20.6	19.3 ± 9.6	27.9 ± 6.6	30.6 ± 2.9	25.2 ± 4.9	3.9 ± 5.9	98.6 ± 4.9
3a (MK080)	B1	17.7 ± 3.3	0 ± 10.8	0.1 ± 25.5	26.0 ± 6.9	8.3 ± 3.6	25.1 ± 19.3	33.4 ± 17.6	10.2 ± 13.2
3b (MK081)	B1	14.4 ± 6.5	10.1 ± 10.6	0 ± 14.8	0.4 ± 15.1	3.6 ± 3.2	6.7 ± 5.9	15.1 ± 6.5	7.3 ± 11.3
3c (MK082)	B1	28.8 ± 59.9	20.1 ± 10.8	4.9 ± 15.2	12.4 ± 0.5	21.4 ± 3.8	6.9 ± 9.6	0 ± 5.9	95.0 ± 3.6
MK097	B2	6.1 ± 7.42	18.3 ± 3.7	10.3 ± 17.7	8.0 ± 3.3	10.8 ± 7.3	9.6 ± 7.3	28.5 ± 5.7	2.3 ± 19.2
MK098	B2	0 ± 34.9	34.8 ± 32.2	0 ± 7.3	3.0 ± 13.5	0 ± 6.7	8.6 ± 10.5	12.4 ± 1.3	4.8 ± 16.9
NF298	B3	17.5 ± 9.7	9.8 ± 11.0	0 ± 13.2	14.5 ± 14.3	7.4 ± 10.8	9.8 ± 11.0	24.3 ± 16.7	50.7 ± 11.8
NF006	B2	0 ± 35.5	6.9 ± 13.2	0 ± 2.9	11.9 ± 4.9	0 ± 5.9	19.8 ± 12.7	13.4 ± 11.8	28.2 ± 8.8
MK099	B2	0 ± 2.5	7.3 ± 5.7	3.4 ± 10.7	0 ± 3.6	0 ± 13.3	14.2 ± 1.5	0 ± 7.6	41.9 ± 16.4
NF248	B3	0 ± 13.5	3.4 ± 9.7	0 ± 14.9	31.9 ± 10.6	0 ± 4.8	8.9 ± 3.6	20.2 ± 4.1	100 ± 2.3
NF757	B3	1.2 ± 11.2	14.8 ± 8.6	10.4 ± 1.2	0 ± 12.8	0 ± 12.2	22.4 ± 18.5	0 ± 2.1	100 ± 8.6
NF758	B3	0 ± 24.7	13.7 ± 29.6	6.9 ± 8.1	4.8 ± 8.73	2.8 ± 9.8	10.5 ± 14.8	13.1 ± 23.1	14.4 ± 28.7
NF759	B3	0 ± 9.6	27.1 ± 0.2	0 ± 4.3	10.1 ± 8.0	0 ± 4.5	23.4 ± 10.8	0 ± 4.4	29.3 ± 18.7
NF762	B3	0 ± 6.7	0.8 ± 29.3	0 ± 11.3	23.3 ± 8.7	4.5 ± 5.5	32.1 ± 7.3	0 ± 2.9	100 ± 12.9
NF722	B3	0 ± 24.4	0 ± 12.4	0 ± 4.5	23.3 ± 6.1	0 ± 1.7	39.4 ± 5.9 (0 ± 5.1)*	0 ± 5.9	100 ± 1.72

Appendix A1 (cont.)

Compound	Str.	$P2Y_1$		$P2Y_2$		$P2Y_4$		$P2Y_{11}$	
		% response	% inhibition	% response	% inhibition	% response	% inhibition	% response	%inhibition
NF729	B3	0 ± 12.9	27.3 ± 1.7	7.4 ± 0.6	8.1 ± 2.6	0 ± 4.9	28.8 ± 1.6	4.8 ± 3.0	72.2 ± 12.6
NF730	B3	0 ± 11.8	0 ± 9.8	20.5 ± 2.1	5.3 ± 1.3	1.8 ± 19.2	25.8 ± 5.0	2.1 ± 15.7	35.1 ± 21.2
NF739	B3	23.3 ± 11.7	3.67 ± 1 4.2	23.5 ± 1.4	21.2 ± 4.0	61.7 ± 7.5 (0.5 ± 4.8)*	27.7 ± 8.9	24.8 ± 5.7	92.7 ± 22.3
NF750	B3	0 ± 5.4	2.3 ± 19.6	2.1 ± 0.2	33.5 ± 11.8	2.1 ± 0.2	16.3 ± 6.6	27.0 ± 1.1	40.0 ± 9.1
NF751	B3	10.6 ± 14.2	0 ± 24.7	3.6 ± 0.4	16.1 ± 2.9	10.4 ± 14.4	4.8 ± 2.6	34.7 ± 11.3	26.2 ± 4.8
NF752	B3	2.1 ± 9.3	0 ± 15.8	3.8 ± 0.5	9.0 ± 18.0	13.4 ± 3.4	3.5 ± 1.4	0 ± 19.6	36.4 ± 9.7
NF755	B3	26.3 ± 14.9	0 ± 14.5	4.1 ± 0.8	16.7 ± 2.3	16.5 ± 10.9	3.7 ± 1.8	29.0 ± 10.4	85.0 ± 5.4
NF743	B3	0 ± 4.7	7.1 ± 41.3	0 ± 6.1	18.3 ± 6.7	0 ± 11.2	14.4 ± 1.5	0 ± 6.6	63.4 ± 4.6
NF744	B3	0 ± 5.9	0 ± 18.9	0 ± 5.4	4.8 ± 5.6	0 ± 1.2	22.1 ± 2.2	9.7 ± 18.5	44.7 ± 4.8
NF745	B3	0 ± 17.4	0 ± 15.8	8.1 ± 1.2	2.0 ± 4.9	0 ± 5.9	27.0 ± 10.3	0 ± 9.6	40.0 ± 11.6
NF748	B3	6.7 ± 2.6	19.0 ± 8.9	0 ± 3.1	0 ± 9.7	31.7 ± 7.9	3.7 ± 15.3	19.1 ± 18.6	91.6 ± 6.5
NF764	B3	0 ± 4.8	0 ± 14.5	3.1 ± 0.7	15.5 ± 2.8	3.0 ± 0.7	14.8 ± 8.5	23.3 ± 14.9	20.2 ± 11.1
NF765	B3	0 ± 18.2	23.0 ± 5.9	2.5 ± 0.3	9.0 ± 1.0	2.6 ± 0.3	35.9 ± 4.3	0 ± 4.9	35.6 ± 6.9
NF766	B3	0 ± 15.2	0 ± 21.7	2.3 ± 1.3	35.7 ± 4.9	2.3 ± 1.3	27.1 ± 7.7	0 ± 5.2	14.3 ± 7.8
NF769	B3	0 ± 12.2	0 ± 37.1	0.4 ± 0.3	30.7 ± 7.5	0.4 ± 0.3	37.6 ± 3.2	14.9 ± 10.7	72.4 ± 9.6
7a (MK092)	B1	5.1 ± 46.3	33.9 ± 19.7	14.9 ± 8.8	27.1 ± 8.7	23.2 ± 6.2	9.7 ± 8.4	5.5 ± 3.8	57.2 ± 7.8
7b (MK093)	B1	0 ± 15.0	31.5 ± 6.7	23.5 ± 6.2	0 ± 6.9	6.0 ± 5.3	1.0 ± 7.5	6.6 ± 22.3	51.4 ± 2.9
7c (MK094)	B1	9.8 ± 6.4	11.8 ± 8.2	13.9 ± 9.70	18.9 ± 17.6	4.5 ± 6.4	13.4 ± 11.9	14.0 ± 5.0	89.6 ± 8.1
MK100	B2	0 ± 11.0	11.5 ± 2.2	1.6 ± 10.8	18.9 ± 4.3	8.1 ± 1.3	0 ± 3.6	0 ± 5.4	64.3 ± 9.7
MK101	B2	0 ± 11.4	19.9 ± 5.2	25.6 ± 11.8	0 ± 17.9	8.6 ± 1.3	2.1 ± 5.6	11.6 ± 16.0	54.7 ± 3.7
NF294	B2	0 ± 6.4	5.6 ± 2.8	22.1 ± 1.7	29.1 ± 3.7	11.4 ± 1.4	7.5 ± 2.5	10.5 ± 8.7	98.6 ± 1.7
NF771	B3	0.13 ± 38.3	52.8 ± 2.3 (0 ± 5.2)*	1.7 ± 1.2	31.6 ± 7.2	1.7 ± 1.2	16.9 ± 14.5	1.3 ± 18.5	54.1 ± 32.3
NF772	B3	0 ± 6.8	31.1 ± 17.6	1.3 ± 0.8	26.4 ± 6.4	1.3 ± 0.8	18.0 ± 13.8	9.4 ± 25.1	21.6 ± 3.7
NF773	B3	8.5 ± 9.5	0 ± 24.4	3.8 ± 0.3	22.5 ± 2.0	3.8 ± 0.3	10.3 ± 8.2	0 ± 3.2	17.3 ± 6.7
NF776	B3	0 ± 13.3	21.6 ± 20.5	3.5 ± 2.0	25.9 ± 8.5	3.5 ± 2.0	54.1 ± 14.5 (32.8 ± 15.1)*	11.2 ± 20.5	91.9 ± 20.0
NF252	B3	10.2 ± 20.2	11.8 ± 13.1	0 ± 5.4	30.3 ± 10.8	33.2 ± 9.7	13.7 ± 8.9	36.0 ± 5.8	79.9 ± 3.0

* at concentration of 10 μM test compound

Appendix A2 % Response and inhibition by 100 μM *N,N'*-asymmetrical urea derivatives of agonist induced calcium mobilization at P2Y receptors recombinantly expressed in 1321N1 astrocytoma cells. Structures (Str.) are shown in Appendix B.

Compound	Str.	$P2Y_1$		$P2Y_2$		$P2Y_{4\ \%}$		$P2Y_{11}$	
		% response	% inhibition	% response	% inhibition	% response	% inhibition	% response	% inhibition
2d (MK065)	B1	0 ± 4.6	24.8 ± 1.6	7.0 ± 14.9	9.8 ± 3.9	31.5 ± 3.1	11.8 ± 1.6	0 ± 10.1	93.9 ± 21.9
2e (MK066)	B1	0 ± 9.4	1.5 ± 8.5	14.2 ± 1.3	4.8 ± 12.8	9.0 ± 1.2	10.9 ± 11.4	29.6 ± 5.1	97.0 ± 6.2
2f (MK067)	B1	0 ± 17.9	21.7 ± 9.5	6.1 ± 6.7	0.3 ± 9.6	11.8 ± 4.6	5.5 ± 2.1	0 ± 0.8	94.1 ± 20.8
2g (MK068)	B1	0 ± 9.2	29.9 ± 5.7	5.4 ± 16.9	23.2 ± 24.2	21.0 ± 10.6	13.7 ± 3.0	5.1 ± 7.7	99.7 ± 16.9
2h (MK069)	B1	0 ± 6.5	6.6 ± 19.6	9.5 ± 7.6	0.8 ± 1.6	12.9 ± 7.1	8.4 ± 8.9	5.0 ± 2.8	91.3 ± 26.7
2i (MK070)	B1	0 ± 5.3	30.7 ± 18.9	0.8 ± 2.3	10.6 ± 2.1	1.3 ± 2.1	22.6 ± 6.8	25.6 ± 2.7	81.1 ± 8.9
2j (MK071)	B1	21.1 ± 16.9	5.9 ± 13.8	27.2 ± 12.8	7.4 ± 4.0	1.1 ± 1.7	14.7 ± 6.0	2.0 ± 3.7	91.2 ± 12.1
2k (MK072)	B1	11.8 ± 20.3	1.3 ± 9.3	13.1 ± 4.7	9.6 ± 3.6	7.2 ± 3.3	8.3 ± 0.5	4.9 ± 8.5	88.4 ± 10.4
2l (MK073)	B1	10.7 ± 11.8	11.6 ± 9.9	26.2 ± 1.5	8.4 ± 15.4	6.8 ± 2.2	0 ± 7.0	0 ± 2.5	88.9 ± 1.7
2m (MK074)	B1	0 ± 11.3	5.2 ± 2.0	5.5 ± 5.3	1.5 ± 7.2	5.4 ± 6.7	5.1 ± 1.4	10.6 ± 3.8	92.5 ± 4.6
2n (MK075)	B1	0 ± 6.4	30.7 ± 2.9	23.5 ± 2.3	29.5 ± 15.6	6.4 ± 4.1	5.8 ± 13.9	30.4 ± 7.7	96.3 ± 9.5

Appendix A3 % Response and inhibition by 100 μM benzene sulfonic acid derivatives with meta-pheneylene linker of agonist induced calcium mobilization at P2Y receptors recombinantly expressed in 1321N1 astrocytoma cells. Structures (Str.) are in Appendix B.

Compound	Str.	$P2Y_1$		$P2Y_2$		$P2Y_4$		$P2Y_{11}$	
		% response	% inhibition	% response	% inhibition	% response	% inhibition	% response	% inhibition
8a (MK102)	B1	4.1 ± 5.9	0 ± 14.5	0 ± 11.9	28.1 ± 5.9	17.8 ± 21.3	0 ± 7.1	0 ± 9.0	1.4 ± 20.5
8b (MK103)	B1	3.6 ± 18.3	0 ± 11.2	0 ± 6.7	16.1 ± 16.0	0 ± 3.4	0 ± 10.6	0 ± 1.5	16.6 ± 25.2
8c (MK104)	B1	0 ± 11.4	0 ± 9.0	17.5 ± 3.1	20.8 ± 3.7	9.8 ± 15.3	35.3 ± 12.1	0 ± 9.9	30.5 ± 2.6
MK120	B2	0 ± 31.4	24.6 ± 12.9	10.9 ± 11.2	0 ± 12.7	23.6 ± 7.7	27.5 ± 5.5	0 ± 6.2	16.2 ± 11.8
MK121	B2	0 ± 19.2	3.7 ± 19.9	6.2 ± 13.2	26.3 ± 6.8	8.8 ± 2.4	0.7 ± 10.9	0 ± 9.5	17.1 ± 10.2
NF250	B3	0 ± 14.4	15.6 ± 17.9	6.7 ± 12.6	10.7 ± 11.4	27.5 ± 4.1	16.8 ± 3.3	0 ± 0.7	82.0 ± 2.7
9c (MK105)	B1	0 ± 1.5	25.2 ± 14.8	8.8 ± 21.0	19.2 ± 10.6	11.2 ± 2.4	0.9 ± 5.5	13.4 ± 5.0	0 ± 2.1
9b (MK106)	B1	0 ± 35.4	0 ± 45.9	12.3 ± 16.6	11.4 ± 12.7	7.7 ± 9.4	0 ± 18.7	6.2 ± 18.8	0 ± 7.2
9c (MK107)	B1	18.8 ± 4.8	0 ± 15.3	16.1 ± 7.9	20.8 ± 17.7	0 ± 16.5	18.6 ± 13.5	19.2 ± 15.9	8.7 ± 9.9
10a (MK108)	B1	3.8 ± 9.3	0 ± 2.7	14.2 ± 13.1	21.2 ± 12.8	0 ± 8.8	29.1 ± 2.9	1.1 ± 9.7	16.2 ± 2.5
10b (MK109)	B1	0 ± 34.5	19.7 ± 27.7	10.3 ± 6.3	30.0 ± 9.5	9.1 ± 10.8	14.8 ± 13.8	20.2 ± 22.7	26.0 ± 18.4
10c (MK110)	B1	0 ± 9.5	0 ± 9.2	1.6 ± 13.3	10.0 ± 9.3	0 ± 10.5	14.9 ± 6.2	26.8 ± 16.1	96.7 ± 18.6
MK122	B2	0 ± 41.2	0 ± 16.8	9.6 ± 18.3	28.8 ± 12.3	25.3 ± 2.1	1.1 ± 17.9	0 ± 0.9	31.4 ± 17.5
MK123	B2	0 ± 18.4	0 ± 8.2	23.7 ± 3.5	9.0 ± 1.9	13.3 ± 1.6	0.5 ± 6.7	7.0 ± 5.8	55.8 ± 11.2
NF251	B3	0 ± 7.8	0 ± 15.9	0 ± 15.0	6.9 ± 6.8	0 ± 7.4	17.0 ± 5.7	20.9 ± 12.3	94.7 ± 21.8
11a (MK111)	B1	24.7 ± 7.7	0 ± 7.1	0 ± 6.0	5.3 ± 3.8	15.1 ± 6.7	27.9 ± 1.2	36.2 ± 3.4	6.7 ± 4.3
11b (MK112)	B1	2.4 ± 4.1	7.5 ± 6.1	2.5 ± 3.9	10.4 ± 12.3	18.0 ± 19.4	24.4 ± 14.2	1.0 ± 10.4	12.4 ± 11.6
11c (MK113)	B1	0 ± 18.8	0 ± 14.9	12.9 ± 2.0	6.5 ± 12.8	18.0 ± 12.1	31.5 ± 7.3	20.0 ± 2.6	0 ± 14.4
12a (MK114)	B1	0 ± 2.1	0 ± 21.6	25.4 ± 2.2	0 ± 4.1	17.9 ± 5.5	15.8 ± 17.9	0.4 ± 3.3	0 ± 5.0
12b (MK115)	B1	0 ± 14.0	0 ± 23.3	10.3 ± 8.6	0 ± 1.5	16.2 ± 4.5	0 ± 12.7	0.7 ± 2.1	0 ± 18.6
12c (MK116)	B1	0 ± 10.3	0 ± 13.8	3.3 ± 5.2	0 ± 5.1	9.4 ± 1.4	0 ± 3.1	20.1 ± 11.9	47.8 ± 6.7
13a (MK117)	B1	0 ± 11.2	27.2 ± 3.8	12.4 ± 2.1	27.4 ± 6.9	0 ± 2.6	0 ± 1.3	0.4 ± 5.3	73.0 ± 16.2
13b (MK118)	B1	0 ± 17.8	0 ± 15.9	6.2 ± 6.5	19.6 ± 12.6	18.0 ± 7.3	0 ± 3.8	2.1 ± 2.3	61.8 ± 4.7
13c (MK119)	B1	0 ± 26.6	21.4 ± 9.1	6.9 ± 3.7	14.6 ± 2.6	0 ± 9.3	6.9 ± 4.1	0 ± 4.6	97.4 ± 4.8

Appendix A4 % Response and inhibition by 100 μM benzene sulfonic acid derivatives with para-phenylene linker of agonist induced calcium mobilization at P2Y receptors recombinantly expressed in 1321N1 astrocytoma cells. Structures (Str.) are shown in Appendix B.

Compound	Str.	$P2Y_1$		$P2Y_2$		$P2Y_4$		$P2Y_{11}$	
		% response	% inhibition	% response	% inhibition	% response	% inhibition	% response	% inhibition
14a (MK124)	B1	0 ± 5.8	11.9 ± 10.4	0 ± 7.5	9.1 ± 10.4	4.2 ± 8.4	16.1 ± 14.3	0 ± 6.6	5.9 ± 4.9
14b (MK125)	B1	8.5 ± 4.0	0 ± 18.5	0 ± 0.9	6.9 ± 9.4	9.8 ± 9.2	8.9 ± 7.5	6.0 ± 2.5	0 ± 8.9
14c (MK126)	B1	0 ± 21.1	1.9 ± 9.9	13.3 ± 9.3	9.1 ± 3.3	22.2 ± 4.9	7.7 ± 12.6	0 ± 4.6	95.8 ± 4.0
15a (MK127)	B1	0 ± 5.5	34.5 ± 4.5	8.1 ± 4.6	0 ± 18.5	21.2 ± 3.8	4.8 ± 4.7	0 ± 1.5	5.1 ± 0.9
15b (MK128)	B1	0 ± 4.5	14.4 ± 6.9	3.8 ± 5.7	28.9 ± 9.5	7.2 ± 9.5	36.5 ± 16.6	10.0 ± 5.7	25.5 ± 7.8
15c (MK129)	B1	0 ± 21.6	55.8 ± 13.4 (23.7 ± 15.4)*	19.5 ± 9.6	18.5 ± 7.0	30.4 ± 4.7	29.6 ± 4.1	0 ± 7.9	77.9 ± 18.2
16a (MK130)	B1	3.7 ± 6.1	0 ± 2.8	2.1 ± 11.5	0 ± 5.4	0 ± 8.5	38.8 ± 5.2	5.1 ± 5.4	0 ± 16.2
16b (MK131)	B1	0 ± 7.6	0 ± 18.5	3.3 ± 11.5	2.0 ± 9.8	8.8 ± 6.0	25.9 ± 3.9	6.2 ± 22.7	22.8 ± 2.7
16c (MK132)	B1	0 ± 18.9	19.4 ± 46.1	0 ± 15.3	5.9 ± 10.6	0 ± 4.1	3.5 ± 12.9	0 ± 8.0	98.9 ± 3.2
17a (MK133)	B1	0 ± 12.1	17.7 ± 9.0	0 ± 12.8	17.9 ± 7.8	10.6 ± 3.8	3.6 ± 4.2	3.9 ± 2.8	15.8 ± 10.5
17b (MK134)	B1	35.2 ± 16.8	27.9 ± 11.7	0 ± 5.9	19.2 ± 6.8	6.0 ± 6.2	28.3 ± 10.5	21.6 ± 4.4	0 ± 3.8
17c (MK135)	B1	0 ± 5.1	0 ± 22.1	12.4 ± 8.1	7.7 ± 5.7	12.7 ± 9.5	23.4 ± 8.8	0 ± 16.4	39.2 ± 5.5
18a (MK136)	B1	3.1 ± 4.7	0 ± 21.1	4.8 ± 1.8	0 ± 7.7	9.3 ± 5.0	34.4 ± 7.5	26.3 ± 7.5	0 ± 5.9
18b (MK137)	B1	34.1 ± 15.4	8.3 ± 21.6	5.8 ± 5.8	0.2 ± 4.4	21.8 ± 8.5	15.0 ± 16.4	30.1 ± 11.9	4.9 ± 3.8
18c (MK138)	B1	21.5 ± 53.9	27.9 ± 0.6	2.5 ± 13.4	36.8 ± 8.4	27.6 ± 43.3	47.3 ± 27.8	25.3 ± 5.0	78.7 ± 34.0

* at concentation of 10 μM test compound

Appendix B1: Newly synthesized compounds with MK-number

MK065 (2d)

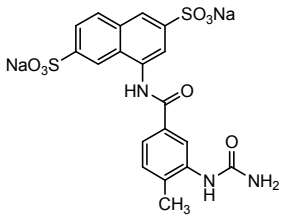

MK066 (2e)

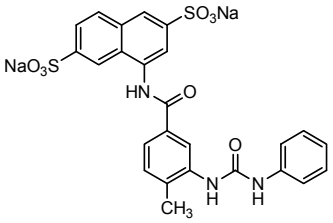

MK067 (2f)

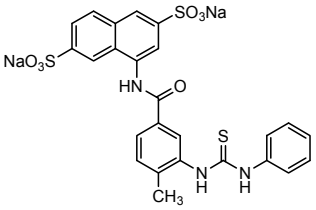

MK068 (2g)

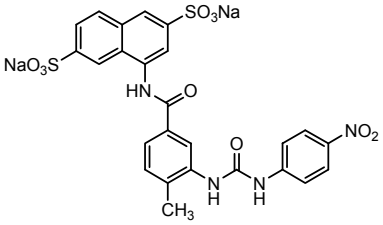

MK069 (2h)

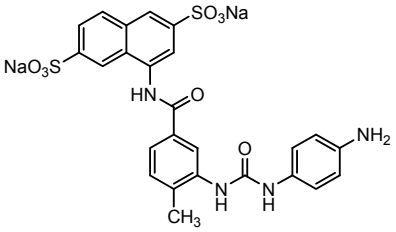

MK070 (2i)

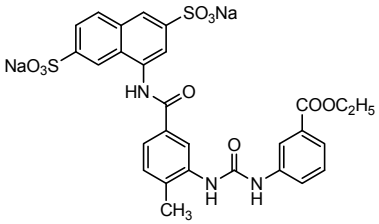

MK071 (2j)

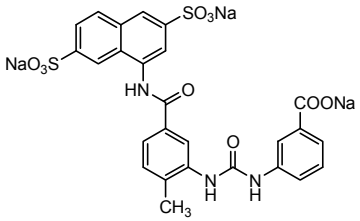

MK072 (2k)

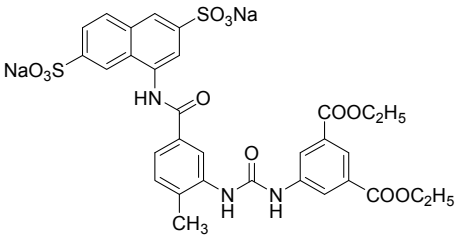

MK073 (2l)

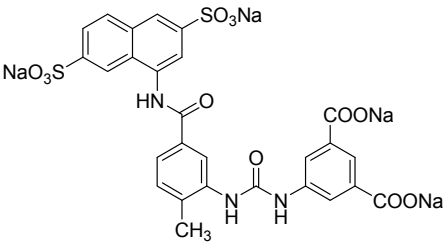

MK074 (2m)

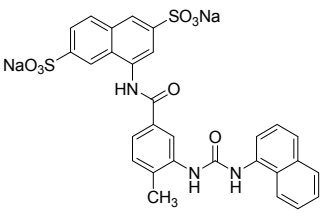

MK075 (2n)

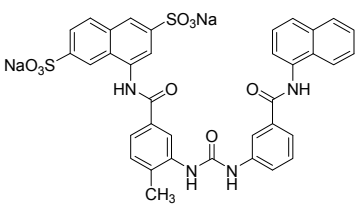

MK080 (3a)

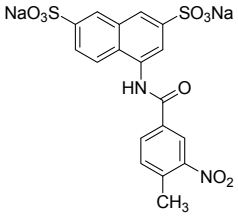

MK081 (3b)

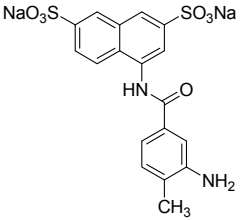

MK082 (3c)

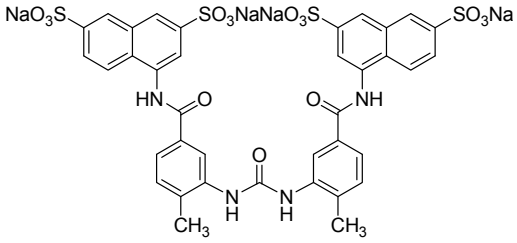

MK083 (4a)

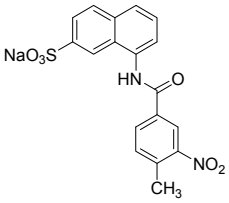

MK084 (4b)

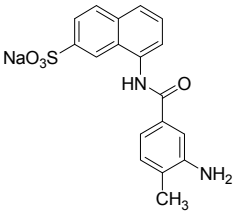

MK085 (4c)

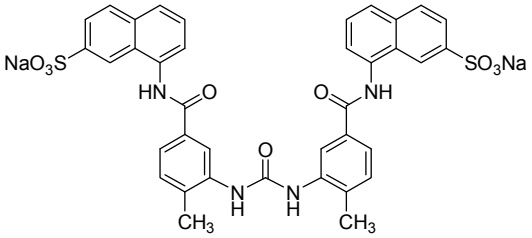

MK086 (5a)

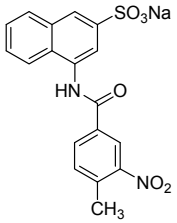

MK087 (5b)

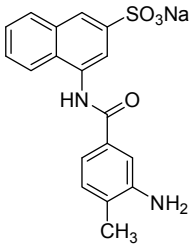

MK088 (5c)

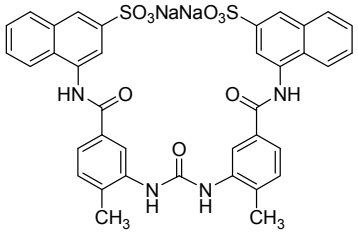

MK089 (6a)

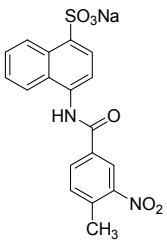

MK090 (6b)

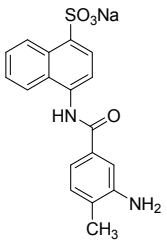

MK091 (6c)

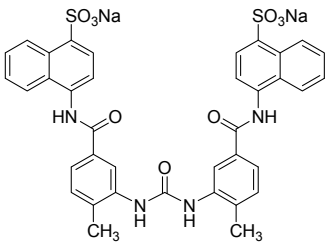

MK092 (7a)

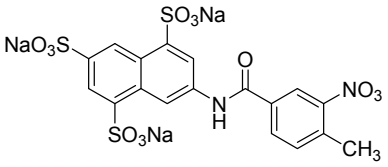

MK093 (7b)

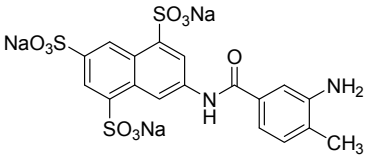

MK094 (7c)

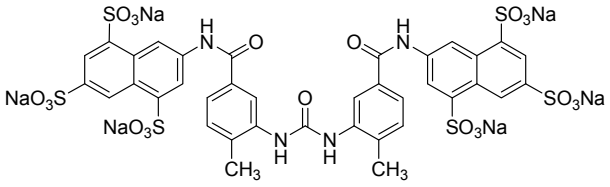

MK102 (8a)

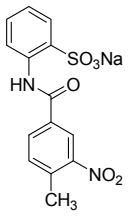

MK103 (8b)

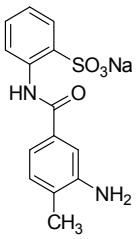

MK104 (8c)

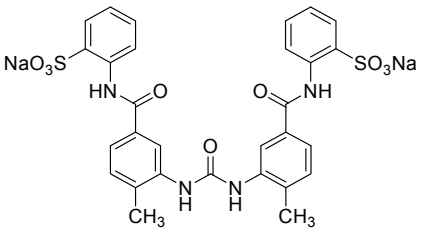

MK105 (9a)

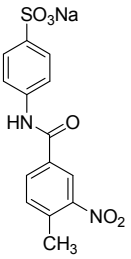

MK106 (9b)

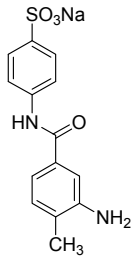

MK107 (9c)

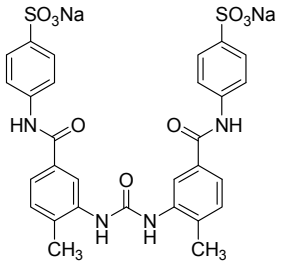

MK108 (10a)

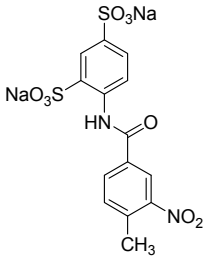

MK109 (10b)

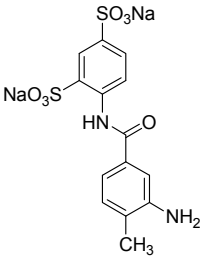

MK110 (10c)

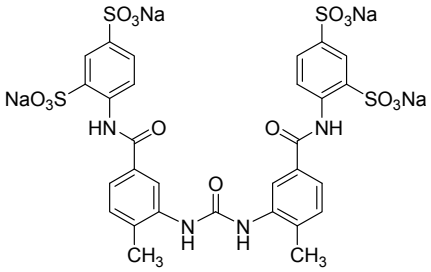

MK111 (11a)

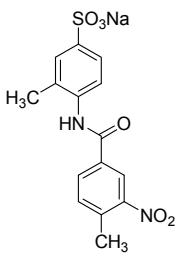

MK112 (11b)

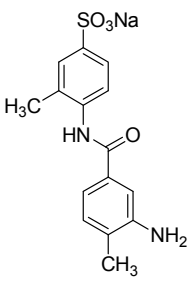

MK113 (11c)

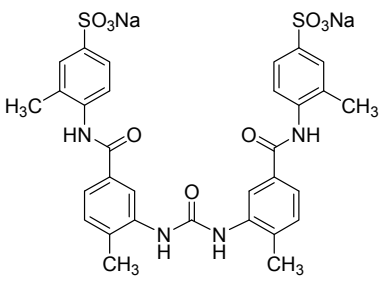

MK114 (12a)

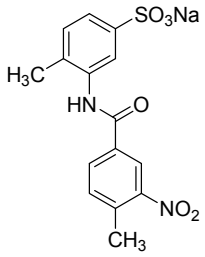

MK115 (12b)

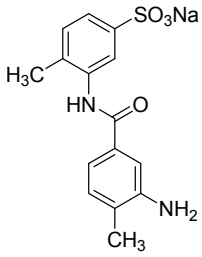

MK116 (12c)

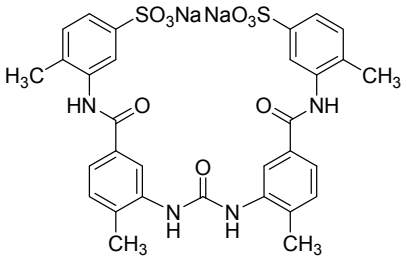

MK117 (13a)

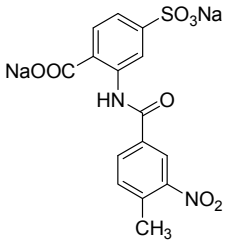

MK118 (13b)

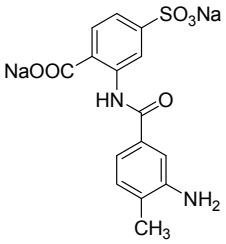

MK119 (13c)

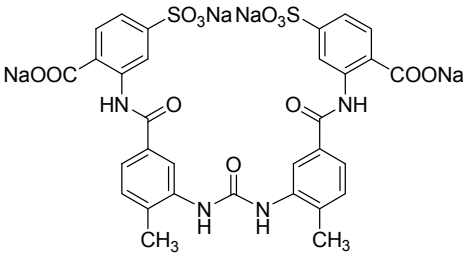

MK124 (14a)

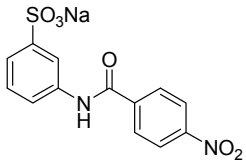

MK125 (14b)

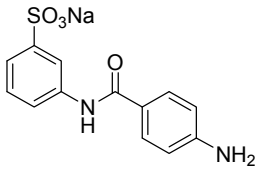

MK126 (14c)

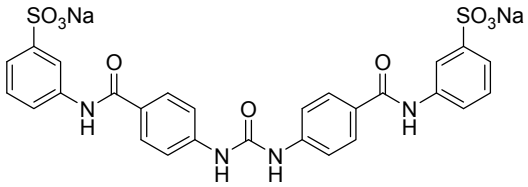

MK127 (15a)

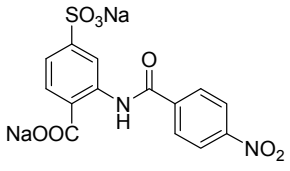

MK128 (15b)

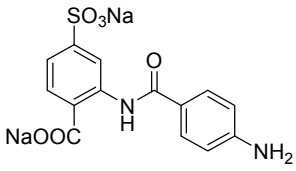

MK129 (15c)

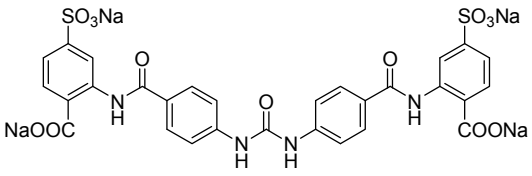

MK130 (16a)

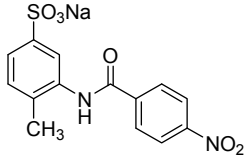

MK131 (16b)

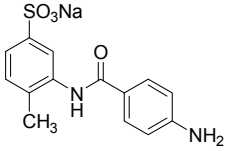

MK132 (16c)

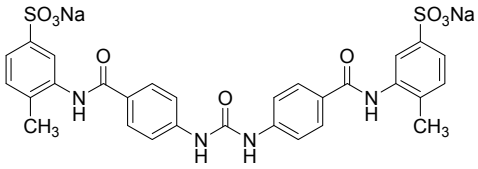

MK133 (17a)

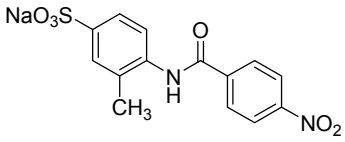

MK134 (18b)

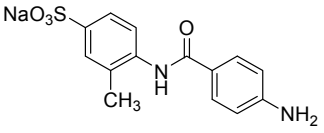

MK135 (18c)

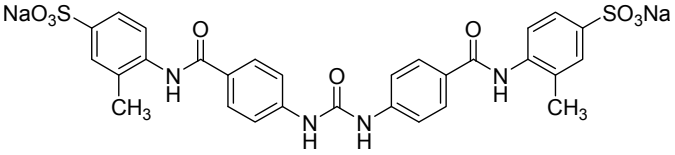

MK136 (18a)

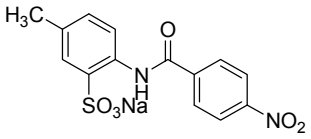

MK137 (18b)

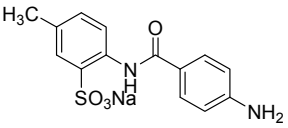

MK138 (18c)

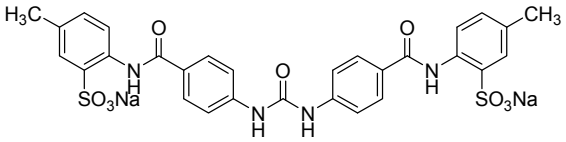

Appendix B2: Resynthesized compounds with MK-number

MK034 (1e) 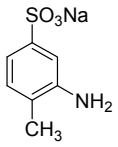	MK060 (1a) 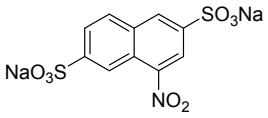	MK061 (1b) 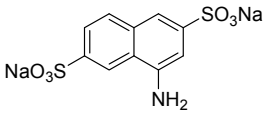
MK062 (1d) 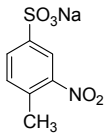	MK063 (2a) 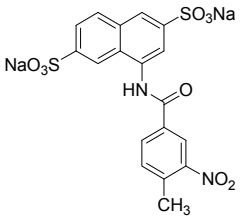	MK064 (2b) 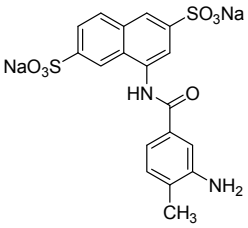
MK095 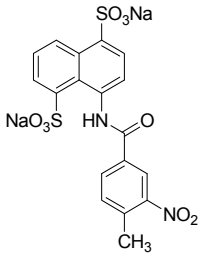	MK096 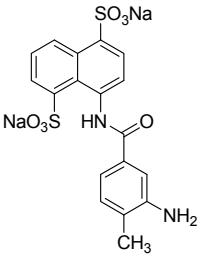	MK097 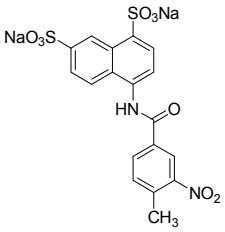
MK098 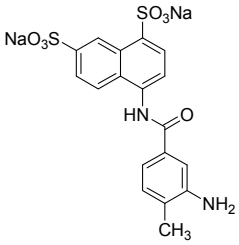	MK099 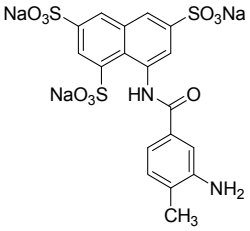	MK100 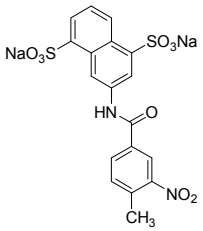
MK101 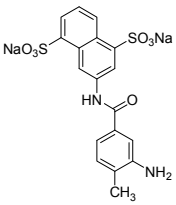	MK120 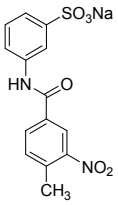	MK121 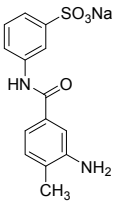
MK122 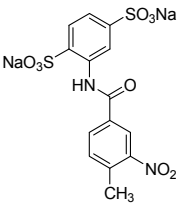		
MK123 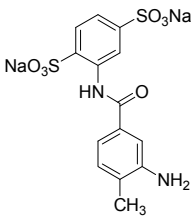	NF006 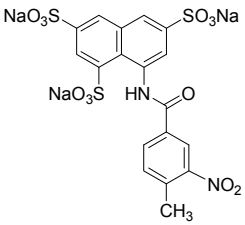	NF340 (2c) 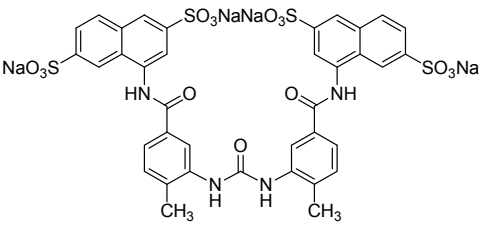

Appendix B3: NF-compounds from the library of Prof. Nickel.

NF248

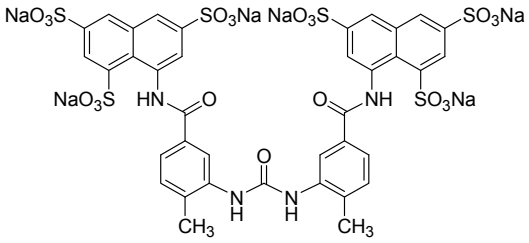

NF250

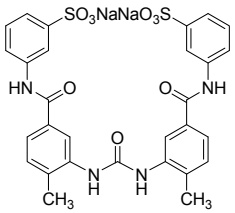

NF251

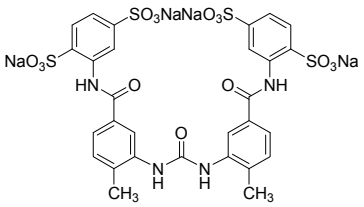

NF252

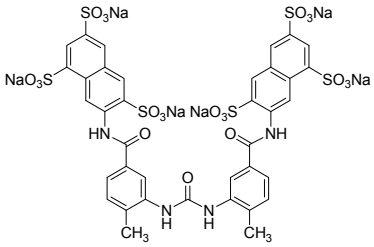

NF294

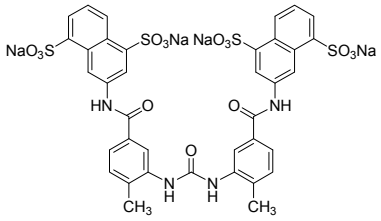

NF290

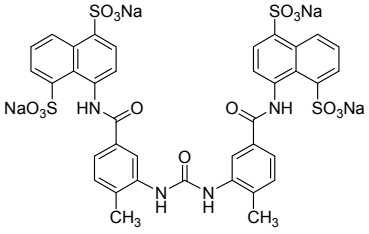

NF298

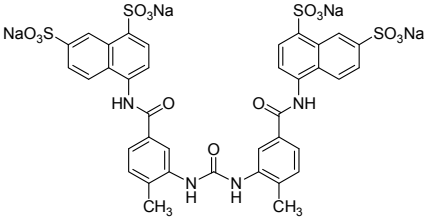

NF722

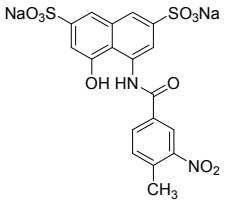

NF729

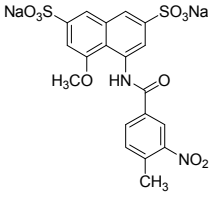

NF730

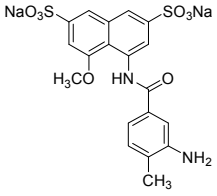

NF739

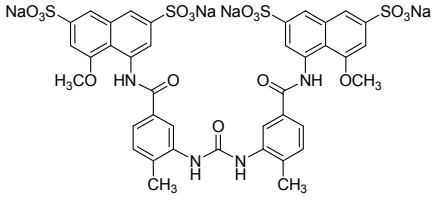

NF743 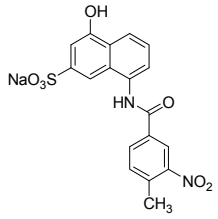	NF744 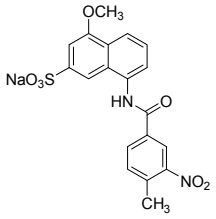
NF745 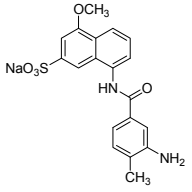	NF748 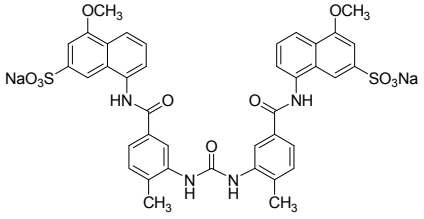
NF750 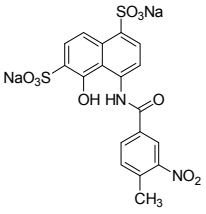	NF751 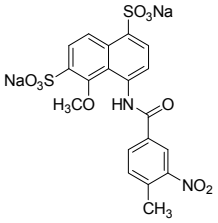
NF752 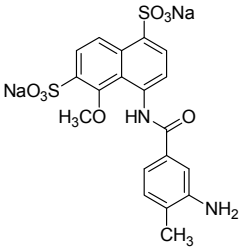	NF755 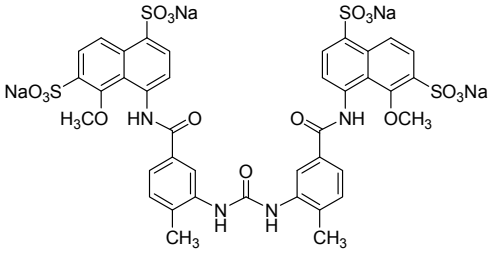
NF757 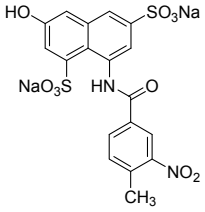	NF758 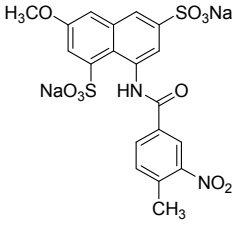
NF759 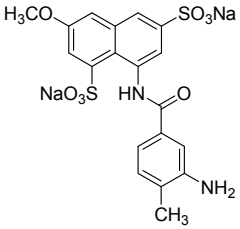	NF762 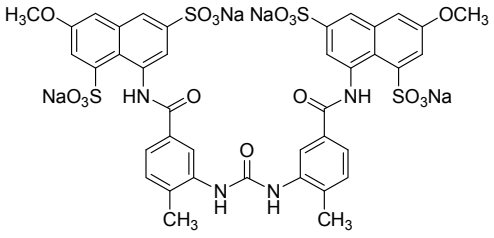

NF764 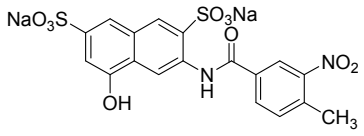	NF765 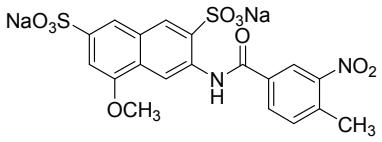
NF766 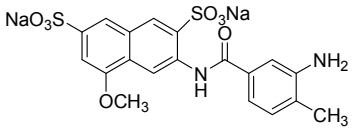	NF769 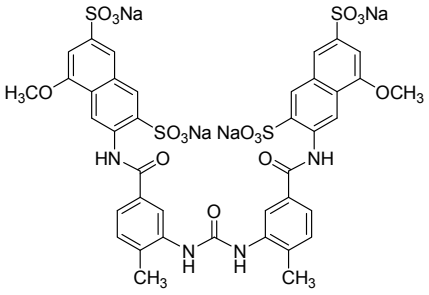
NF771 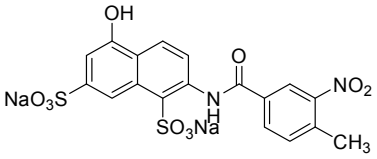	NF772 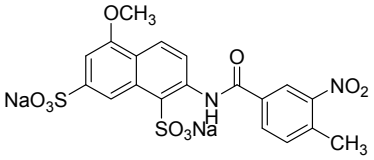
NF773 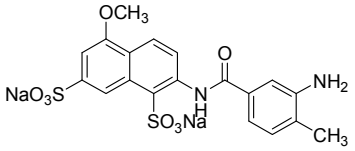	NF776